NTNU
Norwegian University of
Science and Technology

Feasibility of Deep-Sea Mining Operation Within Norwegian Jurisdiction

Erik Kristian Thon Frimanslund

Marine Technology
Submission date: June 2016
Supervisor: Martin Ludvigsen, IMT
Co-supervisor: Steinar Løve Ellefmo, IGB

Norwegian University of Science and Technology
Department of Marine Technology

Abstract

Numerous hydrothermal vent sites are discovered along the Arctic Mid-Ocean Ridge (AMOR), stretching some 1,050 km from Jan Mayen to Svalbard, mostly within Norway's economically exclusive zone (EEZ). Associated with these are seafloor massive sulfide (SMS) deposits; ore containing valuable metals, such as copper, zinc, gold, and silver. Loki's Castle is one of the most promising sites along the AMOR, with a 20-30 m thick and 200 m wide SMS deposit. It is located within Norwegian jurisdiction at a water depth of 2,400 m. Based on a combined geotechnical and economic analysis in which metal grade distributions are modelled separately, 51,100 t copper, 55,600 t zinc, 1.72 t gold, and 86 t silver are found to be recoverable. A production system concept is proposed for a deep-sea mining operation at Loki's Castle, and is based on the system developed for Nautilus Minerals' Solwara 1 project for the calm waters offshore Papua New Guinea. A combined bulk carrier and supply vessel handles transportation of ore, supplies and personnel. The production system design consists of: three remotely operated mining crawlers (Seafloor Production Tools, SPTs); a rigid riser system (Riser and Lifting System, RALS) with a suspended positive displacement pump (Subsea Slurry Lift Pump, SSLP); and a surface vessel (Production Support Vessel, PSV), at which the ore is dewatered and stored before being shipped to shore for further processing. Despite being the SSLP being limited to an H_s of 4-5 m and face design issues with respect to structural integrity in the harsh environment, the overall concept is regarded feasible. As the only relevant operational experience is De Beers' shallow-water diamond mining off the coast of South Africa and Namibia, most of the environmental criteria used are taken from offshore drilling. With respect to flow restrictions, the production capacity is limited by the SSLP at 8,202 t/day (for 3.3 SG ore, 12 % ore-water slurry). Based on the net operating time, and accounting for scheduled maintenance and waiting-on-weather time, an annual average production rate of 3,591 t/day and an annual production volume of 1,309,917 t are found. Significant downtime is excepted in January and July due to periodic maintenance of the SSLP; a criticality for the production system's performance. At full production rate, the cargo holds of the PSV has a capacity of 8.2 days of ore (12 %), which governs the maximum round-trip time for the bulk/supply vessel, including handling times and contingencies.

Significant uncertainties are associated with the early phases of projects. Probabilistic cost estimates allow dealing quantitatively with uncertainties by giving input variables as probability distributions. A particular normal or lognormal distribution is established by assuming P_{10} and P_{90} values from which mean and standard deviation are calculated. Monte Carlo simulations are run for different sets of random variables, and outputs are given as distributions. The mean total development cost is 444.754 M USD; SPTs and RALS being one-third each. Operating costs at 643,049 USD/day are mainly driven by PSV time charter rate and operating costs. Uncertainties in the latter are mainly related to fuel and repair costs, in addition to ROV charter rates. At 50 % thrust utilization, the average fuel consumption is 103.6 m^3/day. The project cash flow is only modelled for the recoverable copper equivalent; a weighted sum of the individual metals that are present in a deposit, when converted to copper value. After adjusting the production profile that is generated in GeoX (i.e., accumulating all tail production in the second year of production), a mean production period of 1.3 years is found. A typical SMS deposit is exploited in about 2-3 years. Three price scenarios for copper are defined based on forecasts towards 2025; low, mean, and high. When evaluating the expected free cash flow for both Norwegian ordinary corporate tax and the Norwegian petroleum tax scheme, positive net present value (NPV) is only obtained for the mean and high price scenarios for the petroleum tax scheme. The combined effect of CAPEX-heavy first years of cash flows and a 5-15-year lifetime of the production system are compensated for by a resale of the production system is included as a positive cash flow at the end of the production period.

Sammendrag

Tallrike hydrotermale skorsteiner er oppdaget langs den midtatlantiske ryggen, nordøst for Jan Mayen og vest-sørvest for Svalbard, som i store deler er innenfor norsk jurisdiksjon. Forbundet med disse er store forekomster av metalliske sulfider med innehold av verdifulle metaller, som kobber, sink, gull og sølv. Lokeslottet er en av de mest lovende området langs den midtatlantiske ryggen, med en 20-30 m tykk og 200 m bred forekomst på et vanndyp på 2400 m. Basert på en kombinert geoteknisk og økonomisk analyse, der sannsynlighetsfordelinger av de ulike metallenes gehalt er modellert separat, gir utvinnbare ressurser på 51.100 t kobber, 55.600 t sink, 1,72 t gull, og 86 t sølv. Et foreslått konsept for et produksjonssystem for undervannsgruvedrift på Lokeslottet er basert på et systemet som er utviklet for Nautilus Minerals' Solwara 1-prosjekt i rolige farvann utenfor Papua Ny-Guinea. Et kombinert bulk- og forsyningsskip transporterer malm, forsyninger og personell. Produksjonssystemet design består av tre fjernstyrte undervannsgravemaskiner (Seafloor Production Tools, SPTs); et stigerørssystem (Riser and Lifting System, RALS) med fortrengningspumpe (Subsea Slurry Lift Pump, SSLP); og et produksjonsfartøy (Production Support Vessel, PSV) der malmen avvannes og lagret før den fraktes til land for videre bearbeiding. Til tross for at SSLP-en er begrenset til en H_s på 4-5 m., og at stigerøret ikke er dimensjonert til værforholdene ved Lokeslottet, anses konseptet som gjennomførbart total sett. Den eneste relevante operasjonell erfaringen er fra De Beers' diamantutvinning på grunt vann utenfor kysten av Sør-Afrika og Namibia. Derfor er det meste av værkriterier hentet fra offshore boring. På grunn av strømningsrestriksjoner, er produksjonskapasiteten begrenses av SSLP-ens på 8202 t/dag (for 3,3 SG malm, 12 % malm-vann-slurry). Basert på netto driftstiden og ved å ta høyde for fastsatt vedlikehold og venting på vær, er en årlig gjennomsnittlig produksjonsrate på 3.591 t/dag og en årlig produksjonsvolum på 1,3 mill. t funnet. Det er betydelig nedetid i januar og juli på grunn av periodisk vedlikehold av SSLP-en, som er kritisk for produksjonssystemets ytelse. Ved full produksjonsrate er lastekapasiteten til PSV-en tidssvarende 8,2 dager (for 12% slurry), noe som styrer den maksimale tidsbruken for bulk- og forsyningsskipet per rundtur, inkludert lastetider og situasjoner.

Betydelig usikkerhet er knyttet til de tidlige fasene av et prosjekt. Ved å gi inndata som sannsynlighetsfordelinger i kostnadsestimater, er det mulig å kvantitativt ta høyde for usikkerhet. En normal- eller lognormalfordeling er etablert ved å anta P_{10}- og P_{90}-verdier, og deretter beregne gjennomsnitt og standardavvik. Monte Carlo-simuleringer kjøres for ulike sett av tilfeldige variabler, og resultater gitt som sannsynlighetsfordelinger. Gjennomsnittlig total utbyggingskostnad er 444,754 M USD, der SPT-er og RALS utgjør en tredjedel hver. Driftskostnadene på 643.049 USD/dag drives hovedsakelig av charterrate og driftskostnader på PSV-en. Usikkerhet i sistnevnte er i hovedsak knyttet til drivstoff- og reparasjonskostnader, i tillegg til ROV-rater. Ved 50 % utnyttelse av installert propelleffekt er gjennomsnittlige drivstofforbruk 103,6 m^3/dag. Prosjektets kontantstrøm er kun modellert for utvinnbar kobberekvivalent; en vektet sum av de enkelte metaller som er til stede i en forekomst, konvertert til kobberverdi. Etter justering av produksjonsprofilen som genereret i GeoX (der all haleproduksjon samles i det andre produksjonsåret), er en gjennomsnittlig produksjonsperiode funnet til 1,3 år. En typisk sulfidforekomst utvinnes i rundt 2-3 år. Tre prisscenarier for kobber er definert basert på prognoser frem mot 2025; lavt, middels, og høyt. Ved vurdering av den forventede kontantstrømmen, der både ordinær bedriftsbeskatning og petroleumsbeskatningen er beregnet, er positiv netto nåverdi kun nådd for middels og høyt prisscenario for petroleumsskatt. Det kompsenseres for de investeringstunge første årene av kontantstrømmene og en antatt 5-15 års levetid på produksjonssystemet ved at et videresalg av produksjonssystemet inngår som en positiv kontantstrøm på slutten av produksjonsperioden (altså i produksjonsår to).

NTNU
Norwegian University of
Science and Technology

Master's Thesis in Marine Subsea Engineering
for
Stud. tech. Erik Kristian Thon Frimanslund
Spring 2016

Feasibility of Deep-Sea Mining Operation Within Norwegian Jurisdiction

Background
Mineral resources on the seafloor is not yet considerably exploited despite the reducing availability of terrestrial minerals. A trade-off between exploitation technology cost and mineral prices form the basis for considering whether or not to develop deep-sea mining projects. This is a complex issue with large technological, geological, environmental and financial uncertainties.

Work Description
The objective of this thesis is to address the above issues and establish a measure of both financial and technological feasibility of a deep-sea mining operation within Norwegian jurisdiction. An operational scenario needs to be conceptualized for a specific site along the Atlantic Mid-Ocean Ridge on the extended Norwegian continental shelf. The work needs to identify, address and enumerate uncertain parameters associated with both selecting and evaluating a concept.

Considering published production system concepts for deep-sea mining, and utilizing experience and technology from the offshore oil and gas industry, an assessment of technological and economic feasibility will be performed. Due to the scarcity of publically available information on various concepts, the basis for this work is Nautilus Minerals' system architecture – the first commercial subsea mining system for deep waters. The production system concept as a whole should be outlined, as well as implemented and assessed in the decision support software GeoX, which is custom-made for oil and gas play analysis and early-phase field development.

Scope of Work
A detailed problem breakdown is as follows:

1. Present and evaluate different technical concepts for deep-sea mining of seafloor massive sulfides (SMS) deposits, including the system designed for Nautilus Minerals' Solwara 1 project.
2. Select a suitable concept, and define an operational scenario for an operation at the hydrothermal vent site Loki's Castle on the Arctic Mid-Ocean Ridge (AMOR).
3. Estimate the production profile/rate and the costs (both for development and operation) of the production.
4. From an operational and economical perspective, implement and assess the selected concept by use of the decision support software GeoX.

The report shall be written in English and edited as a research report, including literature survey, descriptions of mathematical models, descriptions of control algorithms, simulation results, model test results, discussion and a conclusion, including a proposal for further work. This includes a short assessment of the suitability of GeoX for deep-sea mining applications. Source code should be provided on a memory stick or similar. It is supposed that the Department of Marine Technology, NTNU, can use the results freely in its research work, unless otherwise agreed upon, by referring to the student's work. The thesis should be submitted within June 10, 2016.

Co-supervisor: Associate professor Steinar Ellefmo, IGB, NTNU

Professor Martin Ludvigsen
Supervisor

Preface

This thesis is the concluding part of my Master of Science degree in Marine Subsea Engineering at the Department of Marine Technology (IMT) at the Norwegian University of Science and Technology (NTNU) in Trondheim, Norway. The work has been entirely written at NTNU during the spring semester of 2016, and the workload corresponds to 30 ECTS.

The Master's thesis builds on the project thesis that was written in the fall semester of 2015. It resembled a workload of a 7.5 ECTS and was a scoping study on the potential of deep-sea mining on the Norwegian continental shelf. Being focused on literature study, it gave an overview of current state-of-the-art technical solutions and system concepts for deep-sea mining, in addition to technical challenges associated with such operations. Some topics covered in this thesis was in-part written as a part of the specialization module Safe Marine Systems and Integrated Operations, with focus on estimating the breakdown rate of remotely operated vehicles and related operational costs. Furthermore, a summary of various system architectures for deep-sea mining was written as part of a paper presented at "Fjellsprengningskonferansen 2015" by Associate Professor Steinar Løve Ellefmo in Oslo, Norway on November 26-27, 2015.

Starting to work with the subject of subsea mining in the fall of 2015, I had little knowledge of seafloor deposits and technical solutions for subsea mining. Working on this thesis has been challenging and very time demanding, especially with respect to literature review and the extent and complexity of dealing with an entire production system. Furthermore, figuring out how to apply GeoX for a mining case, as well as troubleshooting and understanding how parameters affect the analyses has been challenging due to GeoX not being especially transparent in many of its features.

Trondheim, June 10, 2016

Erik Kristian Thon Frimanslund

Acknowledgements

First, I would like to thank Professor Martin Ludvigsen and Associate Professor Steinar Løve Ellefmo for answering questions, providing contact information, and giving literature propositions and guidance throughout the work on this thesis. Richard Sinding-Larsen also deserves to be thanked for taking his time to review my models. Furthermore, Assistant Professor Svein Aanond Aanondsen has given valuable information through the work of his student's in the course TMR4254 Marine Systems Design. Moreover, I would like to thank Adjunct Professor Per Olaf Brett and Adjunct Professor Arne Ulrik Bindingsbø for providing information and sharing their thoughts on various operational concepts.

Johann Rongau at Technip should be acknowledged for his feedback on my calculations of both production profile and costs. Together with Julien Denegre and Thomas Parenteau at Technip, he has provided valuable answers to technical and operational questions on Technip's work on deep-sea mining in general and Nautilus Mineral's system architecture in particular.

With respect to other inputs from the industry, I would like to thank Sam Asplund and Peter F. Smits at Statoil for giving valuable information on operational practices in offshore drilling. Also, Tore M. Botne at Statoil has given much appreciated insight into how cost estimations in early-phase project development are done in the industry. Furthermore, Asbjørn S. Olsen, Pål A. Svensen and Jan Fredrik Dale at Transocean in Stavanger have given useful data with respect to power consumption onboard their semi-submersibles. Related to the section on operations schedules for seafloor production tools and parallels to other subsea tools, I would like to thank Rune Rosnes at Oceaneering and Bjørn Ladegård at Nexans for providing data, operational experience and system knowledge with ROV and trenching operations, as well as subsea operations in general. Also, Jens Laugesen at DNV GL should be thanked for sharing his insight into the environmental aspects of deep-sea mining, and I am grateful to Rolf Birger Pedersen at the University of Bergen for providing me information on Loki's Castle.

Additionally, the technical discussions with my close friends and office buddies, Kristoffer Bjerkelund, Kristian Mollestad and Brindu Muwage, have been invaluable, in additional to the motivational speeches from Emil Smilden. Last, but not least, I would like to thank my mother, Aud Karin Thon, for always being supportive and having my back.

Contents

List of Figures

List of Tables

Nomenclature

Periodic Metals

Ag	Silver
As	Arsenic
Au	Gold
Cd	Cadmium
Co	Cobalt
Cu	Copper
Fe	Iron
Mn	Manganese
Mo	Molybdenum
Ni	Nickel
Pb	Lead
Pt	Platinum
V	Vanadium
Zn	Zinc

Abbreviations

AC	Auxiliary Cutter
AMOR	Arctic Mid-Ocean Ridge
AUV	Autonomous Underwater Vehicle
AVR	Axial Valley Ridge
BC	Bulk Cutter
BOP	Blowout Preventer
CAPEX	Capital Expenditures
CM	Collecting Machine
DCF	Discounted Cash Flow
DG	Decision Gates
DGD	Dual Gradient Drilling
DP	Dynamic Positioning
DPS	Dynamic Positioning System
DWP	Dewatering Plant

EDP	Emergency Disconnect Package
EEZ	Exclusive Economic Zone
EHS	Enhanced System
EPCM	Engineering, Procurement, and Construction Management
E&P	Exploration and Production
FCF	Free Cash Flow
FEED	Front-End Engineering and Design
FPSO	Floating Production, Storage and Offloading
FSFR	Free Standing Flexible Riser
FSHR	Free-Standing Hybrid Riser
GDP	Gross Domestic Product
HXT	Horizontal XMT
HPU	Hydraulic Power Unit
ID	Internal Diameter
IMR	Intervention, Maintenance and Repair
IRR	Internal Rate of Return
ISA	International Seabed Authority
ISOPE	International Society of Offshore and Polar Engineers
KPI	Key Performance Indicator
LARS	Launch and Recovery System
LDD	Large Diameter Drill
LMRP	Lower Marine Riser Package
MAC	Marine Assets Corporation
MAR	Mid-Atlantic Ridge
MODU	Mobile Offshore Drilling Unit
MOR	Mid-Ocean Ridge
NCS	Norwegian Continental Shelf
NPV	Net Present Value
NTNU	Norwegian University of Science and Technology
OPEX	Operational Expenditures
O&G	Oil and Gas
PD	Positive Displacement
PNG	Papua New Guinea
PSV	Production Support Vessel
RALS	Riser and Lifting System
RAMEX	Reliability, Availability and Maintainability Costs
REE	Rare Earth Elements

ROT	Remotely Operated Tool
ROV	Remotely Operated Vehicle
RTP	Riser Transfer Pipe
R&D	Research and Development
SCFU	Subsea Crushing and Feeding Unit
SG	Specific Gravity
SMD	Soil Machine Dynamics
SMS	Seafloor Massive Sulfide
SPT	Seafloor Production Tool
SS	Seabed System
SSLP	Subsea Slurry Lift Pump
SWL	Safe Working Load
TAPM	Thruster Assisted Position Mooring
TS	Topside System
UCS	Unconfined Compressive Strength
UiB	University of Bergen
UN	United Nations
UNCLOS	United Nations Convention on the Law of the Sea
UTS	Underwater Transport System
VIV	Vortex Induced Vibrations
VXT	Vertical XMT
XMT	X-Mas Tree

CHAPTER 1
Introduction

1.1 Introduction to Subsea Mining

The oceans comprise more than 70 % of the Earth's surface, and are to a large extent unexplored. The seafloor sediments, reflecting the geological history of the ocean basins, are at many locations likely to contain mineral deposits. Marine minerals are not a recent discovery, and already in the late 1800s mineral deposits in the form of manganese-rich lumps of sediments (so-called manganese nodules) were found (SPC, 2013, p. 8). Other types of marine minerals are diamonds, iron sands, phosphorite nodules, manganese nodules, and cobalt-rich ferromanganese crusts.

The type that is of most relevance for Norwegian waters is seafloor massive sulfide (SMS) deposits. These metalliferous formations, together with its surrounding sediments, originate from hydrothermal vents typically located at mid-ocean ridges at 1,500-5,000 m water depth, which are actively formed by heated water emerging from the seafloor. In 1977, the first vent sites were discovered at the Galapagos Rift, west of Ecuador in the Pacific Ocean (SPC, 2013, p. 5). Numerous hydrothermal vent sites are discovered along the Arctic Mid-Ocean Ridge (AMOR), stretching some 1,050 km from Jan Mayen to Svalbard (Pedersen, et al., 2013), located mostly within Norway's economically exclusive zone (EEZ). The sites at the AMOR consist of both active and extinct smokers, as well as sulfide deposits, at 500-2,600 m depth. Generally, the depth increases going north along the Mohns Ridge. Loki's Castle is regarded as one of the most promising sites, and is located where the Mohns Ridge meets the Knipovich Ridge at a water depth of 2,400 m.

1.2 Definitions

In the literature, a vast range of terms are used inconsistently for underwater mining operations. These include subsea mining, seafloor mining, seabed mining, deep-sea mining, ocean mining, offshore mining, and marine mining. The following differentiation is applied in this work: *subsea mining* determines both shallow-water and deepwater operations; and *deep-sea mining* defines only mining in deep waters. Using the terminology for subsea field developments in offshore oil and gas (O&G), sites with water depths less than 200 m are regarded as shallow-water, depths ranging 200-1,500 m as deepwater, and depths greater than 1,500 m as ultra-deepwater (Bai & Bai, 2012, p. 29).

1.3 Objectives

As stated in the enclosed work description, the objectives of this thesis can be summarized as follows:

1. Present and evaluate different technical concepts for deep-sea mining of seafloor massive sulfides (SMS) deposits, including the system designed for Nautilus Minerals' Solwara 1 project.
2. Select a suitable concept, and define an operational scenario for an operation at the hydrothermal vent site Loki's Castle on the Arctic Mid-Ocean Ridge (AMOR).
3. Estimate the production profile/rate and the costs (both for development and operation) of the production.
4. From an operational and economical perspective, implement and assess the selected concept by use of the decision support software GeoX.

1.4 Limitations

As defined by the enclosed work description, this Master's thesis studies the feasibility of a specific deep-sea mining production system for a given site on the extended Norwegian continental shelf (NCS) – both with respect to operational and economical (project decision-making) aspects. The scope is delimited to cover only the mineral extraction and handling process performed by the production system; from commencing mining operation on the seafloor deposit with transportation of processed ore to shore to abandonment of the site. Hence, any upstream and downstream activities are excluded, including exploration and mapping of the seafloor, determining deposit characteristics, and onshore processing of ore (after sales to a third party). Environmental considerations related to the excavation process is indisputably important, and currently there is little knowledge regarding consequences for the biological environment at and around such a mining site. However, this will not be considered in the following. From this point and onwards, only aspects related to deep-sea mining will be covered, as this is the relevant case for an NCS operation. Any costs associated with abandonment of the mining site and restoration of the site to its original state are not covered in this thesis.

1.5 Approach

In the analysis, the hydrothermal vent site considered is Loki's Castle (see Chapter 2.6), and a production system similar to that of Nautilus Minerals' Solwara 1 project is applied (see Chapter 3.6). To determine whether or not to develop the project, the cash flow over the project's lifetime is evaluated. Typically, a site of SMS deposits is fully exploited in about 2-3 years. A cash flow model requires establishing both the costs and the revenue of the project. Costs are any initial investments, in addition to daily fixed and variable operational costs associated with running the production system and related sub-operations. The production volume is found by combining two parameters: a geological model of the mineral deposits to be exploited; and a production profile of the production system. Estimating the revenue of a mining project is done by multiplying this production volume with metal price scenarios (i.e., constant low, mean, and high of price forecasts for the production period). In the case of subsea mining, the production profile is governed by the design volumetric flow rates of its various components.

GeoX, a decision support system custom made for early-phase development of oil and gas (O&G) fields, allows combining a geological model of the deposit with a model of the production system. It outputs the cash flow of the modelled project from which a project development decision can be made. A resource estimate (i.e., a series of probability distribution of metal grades provided by NTNU) is entered into a geological analysis in GeoX, a so-called "Segment Analysis", together with an assumed ore tonnage distribution (based on previous exploration done by the University in Bergen). It outputs a resource diagram that is a probability distribution of recoverable resources (i.e., pure metals). Then, the resource diagram is risked, which means that it is multiplied with the assumed probability for the resource estimate to be present at the particular site considered. This is because the resource estimate is performed for the AMOR as a whole, and the geological analysis is being performed for Loki's Castle isolated (play level and segment level in geological terms, respectively).

The production system is broken down into key sub-systems and modelled in the "Full Cycle Analysis" in GeoX. Distributions for production capacity and costs associated with each sub-system, as well as for the general system, are defined and entered into the model. The cost distributions are established by using the same approach as O&G industry practice on probabilistic cost estimates. A lower bound for the estimate is based on numbers from various sources (e.g., books, speaker presentations, papers, and both consultant and annual reports) on costs in shipping and offshore. Contingency and allowances, in addition to assumed price volatilities and average cost-overruns, are the basis for the estimate's upper bound. The "Full Cycle Analysis" outputs the project's production profile and cash flow over time, as well as project evaluation parameters, such as net present value (NPV) and internal rate of return (IRR).

Due to lack of operational experience and data in the industry, most of the environmental restrictions on operations and time usage are taken from parallels in offshore drilling. Assuming a constant ore density range with depth, flow restrictions on the various components of the production system, as well as hindcast data for the site, give the effective availability and capacity for the overall system, considering both waiting-on-weather and scheduled maintenance downtime. These estimates are performed in Excel, and the result serves as input for the "Full Cycle Analysis" in GeoX.

1.6 Structure of the Report

The rest of the thesis is organized as follows:

- Chapter 2 gives a background for the field of subsea mining by providing a brief overview of forces that drive and restrict subsea mining as an industry, in addition to the legal framework and relevant definitions. Furthermore, types of marine minerals of commercial interest are presented with emphasis on seafloor massive sulfide deposits. Also, hydrothermal vent sites of interest along the Arctic Mid-Ocean Ridge are shown, including Loki's Castle.
- Chapter 3 provides a literature review of historic prices, volatility and characteristics of the metal market, as well as relevant aspects from terrestrial mining are reviewed. Moreover, an overview is given of former projects and the development within the field of subsea mining until today, including concepts for production system architecture with emphasis on those of Technip. Most importantly, a detailed description of the entire production system and operational concept of Nautilus Minerals' Solwara 1 project is included.
- Chapter 4 summarizes essential theory on project development and cost estimates for exploration and production ventures. Furthermore, the concept of probabilistic cost estimation through Monte Carlo simulations is described, in addition to breakdown structures for operational costs in shipping, offshore oil and gas, and terrestrial mining.
- Chapter 5 gives an outline of the operational scenario for deep-sea mining of SMS deposits at the hydrothermal vent site Loki's Castle, including logistics and emergency preparedness. Also, general assumptions regarding the production systems are elaborated on.
- Chapter 6 presents the methodology applied in the spreadsheet models of production rate, development costs, and operational costs, in addition to a stepwise description of input parameters and the modelling procedure for GeoX. Both the geological modelling of the seafloor deposit, as well as the operational/economical modelling of the production system (with respect to production rate and costs) are presented. Moreover, the fiscal (tax) regime and economical scenarios (i.e., forecasted low, mean, and high metals prices for the production period) are presented. The concept of copper equivalent is presented, ref. calculation in Appendix N. Moreover, methods applied for probabilistic costs estimates for offshore oil and gas applications are presented.
- Chapter 7 gives all the results from the spreadsheet model (i.e., production rates and costs serving as input for GeoX), as well as the output from each of the modelling cases in GeoX.
- Chapter 8 provides a discussion, synthesizing on the aforementioned material and a critical assessment of the proposed framework and results.
- Chapter 9 presents the conclusions of the thesis and recommendations for further work.

CHAPTER 2
Background

2.1 Drivers of the Deep-Sea Mining Industry

Driving and restricting forces for developing subsea mining as an industry are summarized in Table 2-1. In an economic perspective, the interest of subsea mining is predominantly driven by the metals market, which is outlined in Chapter 3.1. Currently, a key driving force is the increase in metal prices due to inadequate supply that is caused by the following factors (SPC, 2013, pp. 28-33):

- Decreasing metal grades
- Increasing metal demand
- Improved mining efficiency

Since the mid-1900s there has been a steadily decrease in metal grades in terrestrial mineral deposits. Thus, terrestrial mining activities require increasingly larger land areas, as more soil must be mined to generate the same amount of metal. This increases the environmental footprint of the activities, and a high amount of waste rock lowers the overall mining efficiency. Marine mineral deposits are significantly more mineral-rich (i.e., have much higher metal gradients) than terrestrial deposits, having a smaller footprint (Earney, 1990). An increased demand for metal in the global market has resulted in an increase in metal prices. Together with an expected increase in world population and gross domestic product (GDP) per capita, an increased metals consumption due to a growing production of consumer good (mostly electronics and other metal-intensive products) serves as the market logic behind developing the industry of deep-sea mining. Furthermore, a peak in copper production is forecasted at around 2040. Another important political driver is the countries' desire to be self-sufficient. Subsea mining is attractive for countries short of natural resources, such as China, as an opportunity to secure future supply of minerals.

Advantages of subsea mining compared to terrestrial mining are, as listed by Earney (1990): utilizing cheap transportation by sea (with respect to distribution); already existing port facilities for establishing supply hubs and unloading mineral products; and performing onshore processing at preferable locations with respect to processing costs or closeness to market.

Table 2-1 – Drivers and restoring forces for marine mineral mining (SPC, 2013, p. 27).

	Society	Industry
Primary Drivers	• Global economic growth • States securing access to resources, hence increases its independence with respect to mineral supply	• Innovative and risk tolerant actors • Increasing difficulty and complexity of terrestrial mining
Secondary Drivers	• Increased focus on, and support of environmental and social sustainability • Emerging appliances and markets	• Technological improvements and scalable applicability
Restricting Forces	• Price volatility • Uncertainty regarding environmental impact	• Availability of finance • Financial uncertainty • Regulatory uncertainties • Obligations to share knowledge

2.2 Seabed Legislation and Jurisdiction

Seabed legislation and jurisdiction constitute the operational framework. All activities on the ocean floor are authorized by the United Nations (UN) through international institutions and agreements, as described by Trujillo & Thurman (2014, pp. 320-321). In 1958, the first UN Conference on the Law of the Sea defined the international seabed as the common heritage of mankind, and stated that minerals on the continental shelf was controlled by the country that owned the nearest land. The continental shelf is the seafloor extending from the coastline to where the slope of the seabed significantly increases, thus subject to interpretation. An altered treaty was adopted in 1973-1982, leading to its ratification by the required 60 nations in 1991. In 1994, the convention was c to eliminate production control on subsea mining, scale back the organizational structure administering subsea mining, and ensure the United States a permanent seat and political say on subsea mining amendments, among other modifications.

The four main components of the United Nations Convention on the Law of the Sea (UNCLOS) are summarized below (Trujillo & Thurman, 2014, p. 321), with reference to Figure 2-1:

1) **Costal nations jurisdiction** – A uniform 12-nmi (19 km) territorial sea and 200-nmi (370-km) exclusive economic zone (EEZ) from all land within a nation, including islands. If the continental shelf exceeds the EEZ, the EEZ is extended to 350 nmi (648 km). A state can apply for an extension beyond 350 nmi under certain conditions (Fouquet & Lacroix, 2014, p. 26). Within the EEZ, the coastal state exerts jurisdiction over all resources (Cronan, 1992, p. 1).
2) **Ship passage** – Free passage for all vessels on the high seas is preserved, as well as within territorial seas and through straits for international navigation.
3) **Seafloor mineral resources** – Private exploration of seafloor resources are regulated by the International Seabed Authority (ISA), which was established in 1994 to organize and control all mineral-related activities on the international seabed.
4) **Arbitration of disputes** – A tribunal arbitrates any disputes in the treaty, or concerning ownership rights (i.e., settle maritime boundary disputes).

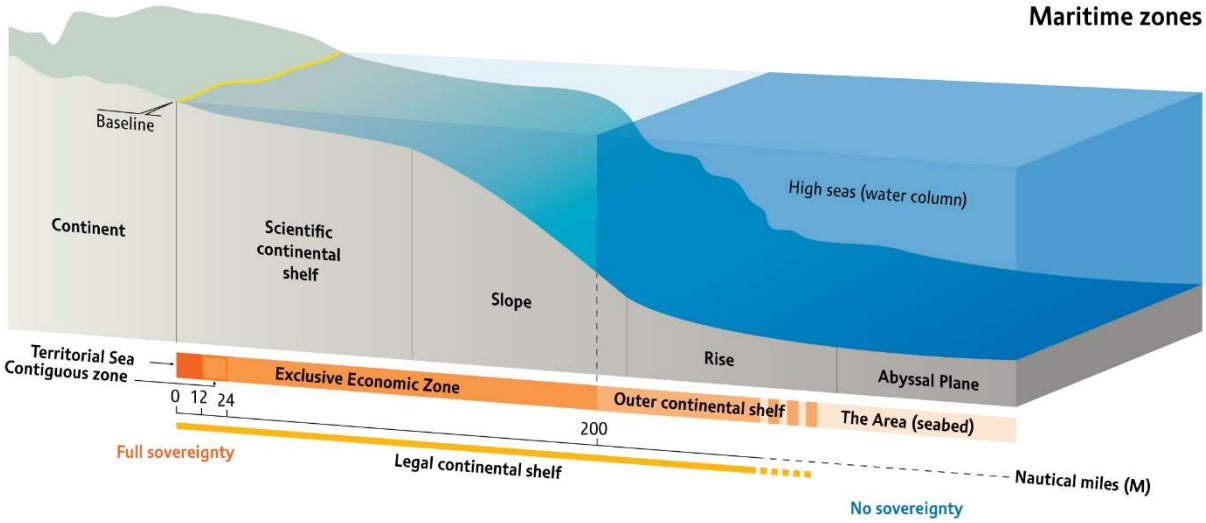

Figure 2-1 – Zones of maritime jurisdiction (UNEP/GRID-Arendal, 2011, p. 9).

As of 2014, 162 nations have ratified the UNCLOS (which also entails being an ISA member), putting 42 % of the world's oceans under the control of coastal nations. These nations have a legal right to extend its maritime claim and hold a seat on the commission that reviews subsea mining plans. The United States has not ratified the UNCLOS, and holds an observer status. In practice, the EEZ is recognized by most states. Companies interested in exploiting marine resources are required to obtain a license prior to initiating its operation, and the application is required to be sponsored or partnered by a country under the UNCLOS. In international waters outside countries' 200-nmi EEZ, the ISA issues exploration and mining licenses. Currently, the ISA has issued 26 deep sea exploration licenses for international waters covering seabed area of 1.2 million km^2, and national governments have granted licenses or received applications for a total of 25 explorations and mining campaigns located within their EEZ (ECORYS, 2014, pp. 9-14). While the legal framework for mineral exploration is in place, the overall regulatory regime for the international seabed does not include seabed exploitation. This will take between two to three years to complete, and is aimed to be finalized by 2016 (Wikborg Rein, 2015). According to (Fouquet & Lacroix, 2014, pp. 27-28), the area to be explored is divided into two parts of equal estimated value, enabling the designation of a reserved area for the ISA's commercial entity, the Enterprise. Thus, the ISA is able to develop its reserves without conducting any exploration or prospecting. The contract is valid for a fifteen-year period and may be extended. For sulfide contracts, fees must be paid when submitting an application. The applicant can either pay a fixed fee of 500,000 USD, or a fixed fee of 50,000 USD and an annual fee based on a revenue-sharing provision for the Enterprise as a joint-venture partner. The contractor's rights are guaranteed, as well as exclusivity for exploration.

2.3 Marine Minerals

Considering deep-sea mining, there are mainly three types of marine minerals of commercial interest. Their characteristics are described below, based on Figoni & Chand (2014), and listed in Table 2-2:

- **Seafloor massive sulfides** (SMS) originate from active and extinct hydrothermal vents at mid-ocean ridges, intra-plate hotspots, and at plate boundaries including volcanic/island arcs and back arc basins located at depths of 1,500-5,000 m (Cronan, 1992, p. 12);
- **Polymetallic nodules** are rich in rare earth elements (REE), and are found on the seafloor at 4,000-6,000 m water depth;
- **Cobalt-rich ferromanganese crusts** are present at seamounts and around flanks of volcanic islands at 400-4,000 m water depth.

Table 2-2 – Overview of marine minerals (Laugesen, et al., 2014).

Marine Mineral	Typical Depth [m]	Characteristic Metals[1]
Seafloor massive sulfides (SMS)	1,400-3,700	Cu, Pb, Zn; some Au and Ag
Polymetallic nodules	4,000-6,000	Cu, Co, Mn, and Ni
Cobalt-rich ferromanganese crusts	800-2,400	Mainly Co; some V, Mo, and Pt

2.4 Seafloor Massive Sulfide Deposits

2.4.1 Hydrothermal Vents and Associated Deposits

Mid-Ocean Ridges

The basic geological features allowing the formation of SMS deposits are described by Trujillo & Thurman (2014, pp. 86-92). There are three types of plate boundaries: transform; convergent; and divergent (Earney, 1990). Divergent plate boundaries are two tectonic plates that continuously are being pulled apart, and occur along the crest of mid-ocean ridges. The rate at which the seafloor spreads apart varies along the mid-ocean ridge. For the northern part of the Mid-Atlantic Ridge (MAR) the rate is about 2 cm/year. Such slow-spreading areas of a mid-ocean ridge is called oceanic ridges, and are characterized by a prominent rift valley (i.e., a central down-dropped linear depression) and steep, rugged slopes. Different spreading rates at different segments of a mid-ocean ridge, and spreading of a linear ridge system on spherical Earth, cause spreading zones to be offset by numerous transform faults perpendicular to the ridge. In the central rift valley of the mid-ocean ridge, there are tall volcanoes called seamounts, as well as pillow lavas, which are smooth, rounded lobes of rock formed from recent underwater lava flows. Numerous small earthquakes occur along the central rift valley due to magma that is injected into the seafloor or rifting along faults.

[1] Chemical elements: Ag – silver; Au – gold; Cu – copper; Co – cobalt; Mn – manganese; Mo – molybdenum; Ni – nickel; Pb – lead; Pt – platinum; V – vanadium, and Zn – zinc.

Hydrothermal Vents

Hot springs known as hydrothermal vents are found on the seafloor, as seen in Figure 2-2. The chimney-shaped features result from cold seawater entering the upper part of the oceanic crust through cracks and features in the seafloor, reaching several kilometers below to the mantle, which is the earth layer directly below the earth's crust. The water is heated by an underground magma chamber and leaches out metals from the surrounding rock before rising to the seafloor. The dissolved metal particles precipitate as a hydrothermal plume with subsequent particle fallout when the hot water mixes with cold seawater (at around 2°C), giving metalliferous sediments about the vent.

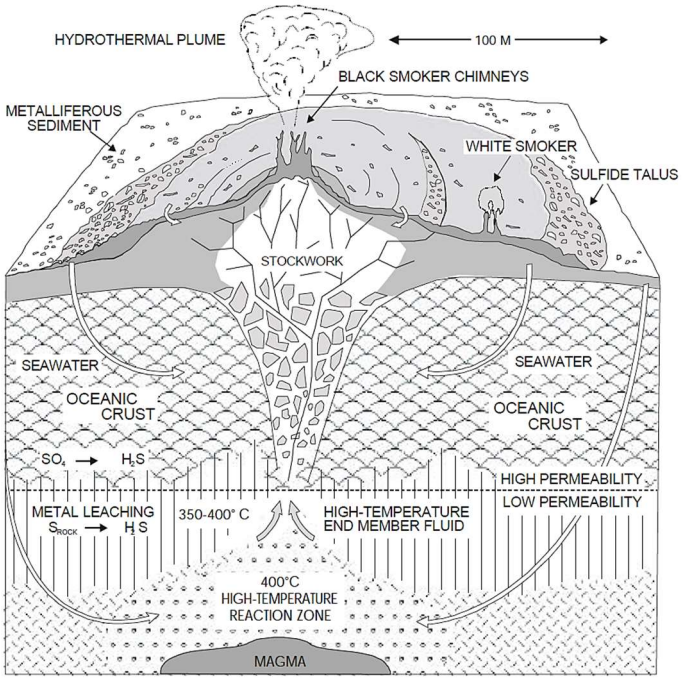

Figure 2-2 – Hydrothermal vent (International Seabed Authority, 2002).

Deposit Formation

Both active and collapsed hydrothermal vents (sulfide talus), together with the metalliferous sediments in the surrounding area, make up a more than 10 m thick layer of sulfide-rich material, called seafloor massive sulfide (SMS) deposits, that can be exploited in a marine mining operation. SMS deposits are similar to volcanogenic mineral deposits on land, and has significantly higher grades of metals, such as copper (Cu), zinc (Zn), gold (Au) and silver (Ag), than typically found on land. Most hydrothermal vents also emit heavy metals, like cadmium (Cd), arsenic (As), and lead (Pb), and an acidic flow of pH ranging 3-4. Hydrothermal vents show a great diversity in physical and geotechnical characteristics, as well as metal content. Based on SRK Consulting (2012, p. 49), the growth of SMS deposits takes place in the following way, with reference to Figure 2-3 (a)-(d):

a) Initiation of hydrothermal discharge and chimney growth
b) Collapse of old chimney and growth of new chimneys
c) Growth of mineral sulfide mound (black) by accumulation of chimney talus and defocusing of hydrothermal discharge
d) Decrease of mound permeability and intramound sulfide precipitation, replacement and remobilization

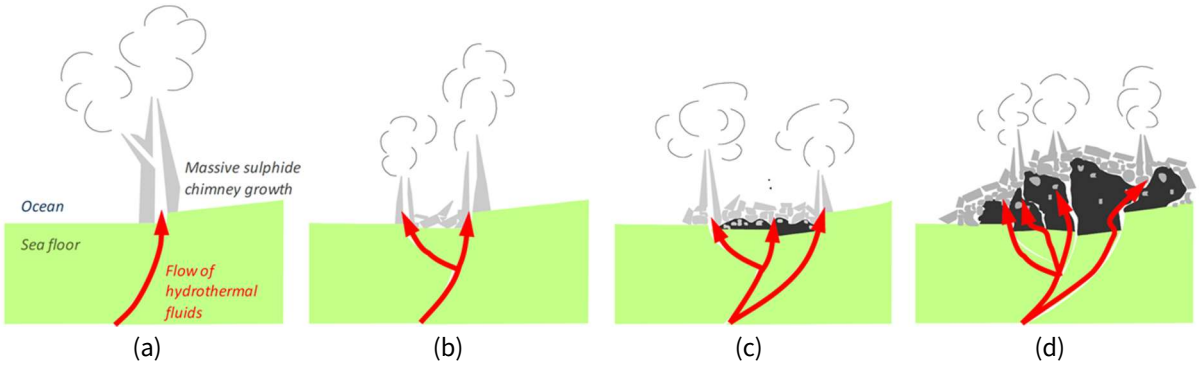

Figure 2-3 – Growth stages of SMS deposits (SRK Consulting, 2012, p. 49).

The appearance of the hydrothermal vent depends on the temperature of its water discharge (Trujillo & Thurman, 2014, pp. 90-91, 481):

- **Warm-water vents** emit clear water with a temperature below 30°C
- **White smokers** have white water at 30-350°C due to presence of light-colored compounds, such as barium sulfide (BaS)
- **Black smokers** emit black water at above 350°C due to presence of dark-colored metal sulfides, such as iron (Fe), nickel (Ni), copper (Cu), and zinc (Zn). The faster the spreading center is diverging, the greater the chance of having a black smoker (Earney, 1990). The black smokers are chimney-shaped structures that can be up to 60 m tall.

In 1962, the first SMS deposit was observed in the Red Sea, and today about 150 hydrothermal sites are discovered (Fouquet & Lacroix, 2014, p. 10). The global distribution of discovered vent sites, as well as their status of activity and the tectonic setting at which they are present, are shown in Figure 2-4.

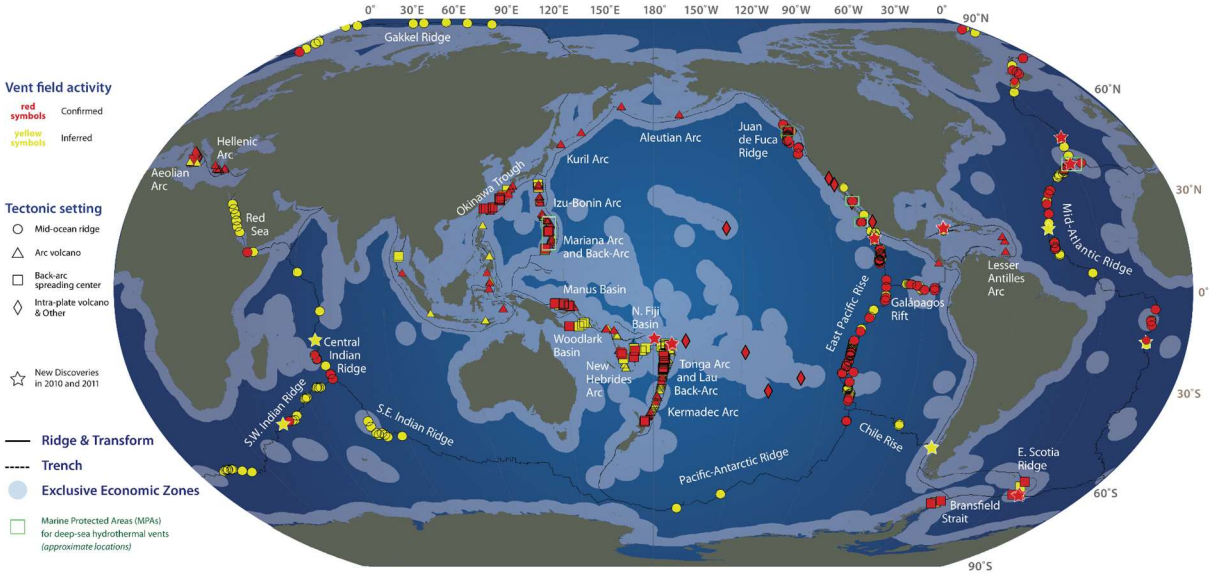

Figure 2-4 – Global distribution of hydrothermal vent fields (Woods Hole Oceanographic Institution[2]).

2.4.2 Mechanical Properties

As with terrestrial mining, the mechanical properties of the ore determine both the production rate and energy consumption of the miners. Two key factors affecting the properties of SMS deposits are:

- Maturation threshold
- High hydrostatic pressures

Maturation Threshold

Waquet & Fouquet (2010) examine the interrelation between maturation and geotechnical properties of SMS deposits. Hydrothermal mound is built up as the chimney-shaped hydrothermal vents collapse due to earthquakes. As debris accumulate, hydrothermal fluid flows through the masses and deposits metals. Hence, as the deepest mound are more exposed to hydrothermal fluids, the metal grade increases with depth below the seafloor. Deep-lying layers get continuously more compressed as new

[2] http://www.whoi.edu/home/pdf/ventmap_2011.pdf, accessed May 31, 2016.

layers of debris accumulate on top, becoming less porous and more mature. Thus, there is a vertical gradient of both porosity and maturation – both total and connected porosity decreases with depth, as these are linearly dependent. As seen from Figure 2-5, there is a linear relation between the uniaxial compressive strength (UCS) and porosity for deposits with porosities higher than 0.2, and all UCS values are lower than 20 MPa. However, an exponential increase in UCS is seen for lower porosities, hence a connected porosity of 0.2 is a maturation threshold. The typical porosity of SMS deposits is above the threshold at 0.3-0.5 (Chen, et al., 2014). Deposits with a higher UCS are more demanding and time consuming to crush, thus more expensive to exploit.

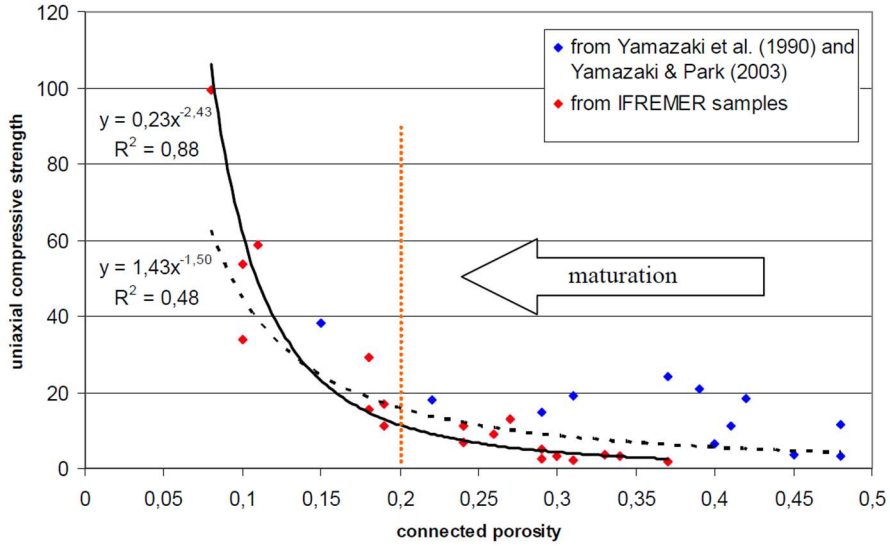

Figure 2-5 – Uniaxial compressive strength versus connected porosity (Waquet & Fouquet, 2010).

High Hydrostatic Pressures

There is little knowledge on the effects of high hydrostatic pressures on mechanical properties of rock; most importantly UCS, Young's modulus, and porosity (Waquet, et al., 2011). The apparent strength of a rock depends on the deformation rate (i.e., drainage effects of pore fluid) and the hydrostatic pressure, as the latter limits the drainage effect (Helmons, et al., 2014). Thus, rock has a ductile behavior under high hyperbaric pressures. For high-pressure cutting, "*[…] crack initiation and crack propagation becomes more difficult, resulting in high cutting forces and high power consumption*", as argued by Alvarez Grima, et al. (2011) and shown in Figure 2-6 (b). In shallow-water, the cutting process is brittle, causing large chips to be formed by tensile cracks. As described by Jackson & Hunter (2007), the major difference between rock cutting subsea and on land, is that *"as a chip of rock is broken out, a cavity is created, and hence a pore suction. This needs to be balanced by water flow either via the crack or through the rock itself. The viscosity of the water reduces the speed at which the chip can leave the host rock matrix compared to the same situation in air"*. Furthermore, the slow release of chips from the rock matrix makes them more likely to be broken multiple times by cutter picks, wasting additional energy (Jackson & Clarke, 2007). Experiments performed by Waquet, et al. (2011), placing a rock sizer in a pressure chamber in up to 200 bar, concluded that pressure conditions have no significant effect on the particle size distributions (i.e., reduction ratio – input versus output size). However, a substantial effect on energy consumption was found, with a required power of up to 3.5 times that of atmospheric conditions.

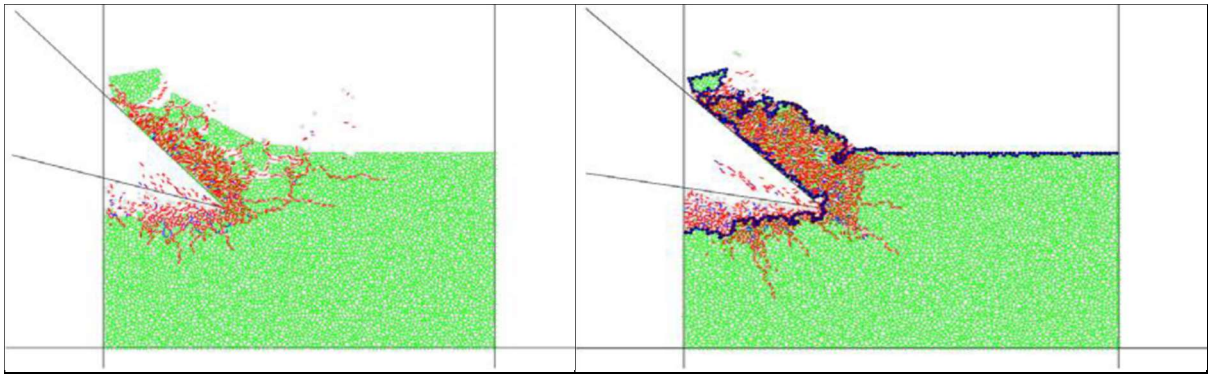

(a) Brittle behavior in shallow water (b) Ductile behavior in deep water

Figure 2-6 – Rock cutting mechanism (Alvarez Grima, et al., 2011).

2.5 Arctic Mid-Ocean Ridge

The parts of the Arctic Mid-Ocean Ridge (AMOR) that lie within the NCS stretches from 71°N to 79°N. The southern part is the 550 km Mohns Ridge, which transitions into the 500 km Knipovich Ridge through an 80° bend at 74°N, see Figure 2-7. See Appendix Q for a more detailed map of the Norwegian continental shelf. Pedersen, et al. (2013) describes the seafloor bathymetry and characteristics for known hydrothermal vents and sulfide deposits, summarized in Table 2-3, and is the basis for this chapter. These vent fields are believed to originate from axial volcanic constructions, rifts within axial volcanic zones, rift valley fault walls and detachment faults, and fracture zones or transverse vault zones

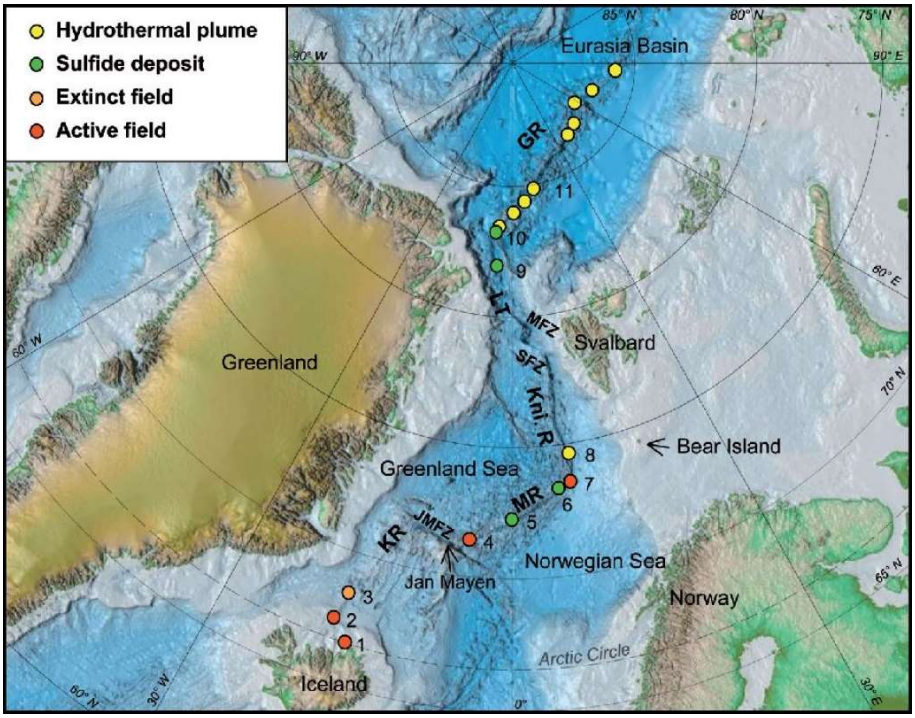

Ridges: MR is Mohns Ridge; and Kni. R is Knipovich Ridge.
Vent fields: (4) Jan Mayen, Soria Moria, and Troll Wall; (5) Copper Hill sulfide mineralized breccia; (6) Mohn's Treasure sulfide deposit; (7) Loki's Castle; and (8) hydrothermal plume.

Figure 2-7 – Active and extinct vent fields along the Arctic Mid-Ocean Ridge (AMOR) (Pedersen, et al., 2013).

Table 2-3 – Known vent fields along the AMOR on the NCS[3]. Based on Pedersen, et al. (2013).

Vent Site	Latitude	Longitude	Location	Depth [m]	Temp. [°C]	Type
Soria Moria	71°15'N	05°48'W	SW MR	700	270	Active white smoker
Troll Wall	71°17'N	05°46'W	SW MR	550	270	Active white smoker
Copper Hill	72°32'N	02°10'E	C MR	900	N/A	Extinct smoker, sulfide deposit
Mohn's Treasure	73°27'N	07°12'E	NE MR	2,600	N/A	Sulfide deposit
Loki's Castle	73°33'N	08°09'E	NE MR	2,400	317	Active black smoker

2.6 Loki's Castle Vent Site

2.6.1 Site Characteristics

The Loki's Castle vent field (73°33′ N, 08°09′ E) is located at the crest of a 30 km long AVR where the AMOR bend at 73°N. The AVR summit is at a water depth of 2,000 m, about 1,300 m above the valley floor, as seen in Figure 2-8 (a). Northeast of the summit area, along a crest of the axial valley ridge (AVR), there is a 12 km long, 200-500 m wide and 100-150 m deep rift, see Figure 2-8 (b). Loki's Castle is located on the northwestern margin of the rift, 4 km from the summit. The vent field consists of five black smokers at 2,400 m depth, which are 11 m tall and emit fluids of 317°C and pH 5.5. They are situated on a hydrothermal mound that is about 20-30 m high and 200 m across. Figure 2-9 gives a detailed view of the bathymetry around the two hydrothermal vents that constitute Loki's Castle, and the assumed extent of the hydrothermal mound is indicated by the stippled line.

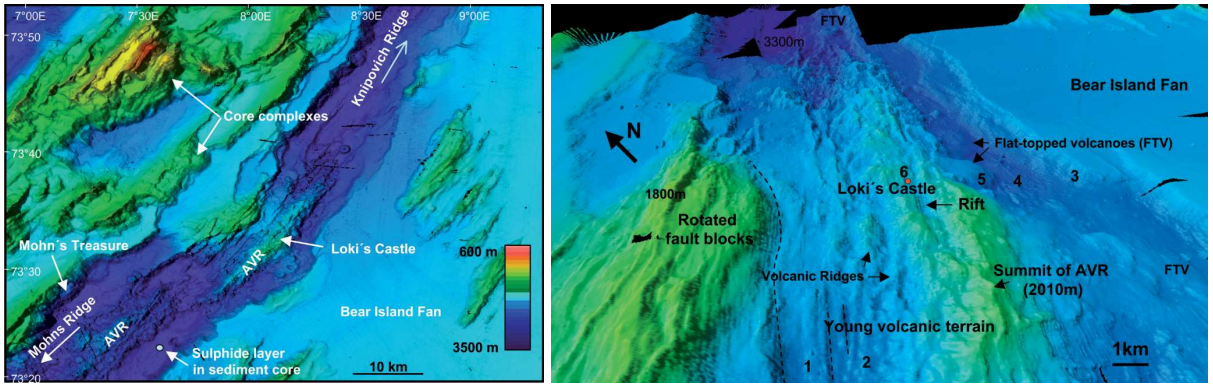

(a) Mohns/Knipovich ridge transition zone (b) Loki's Castle vent field

Figure 2-8 – Location of Loki's Castle (Pedersen, et al., 2013).

[3] SW stands for southwestern, C for central, NE for northeastern, and MR for Mohns Ridge.

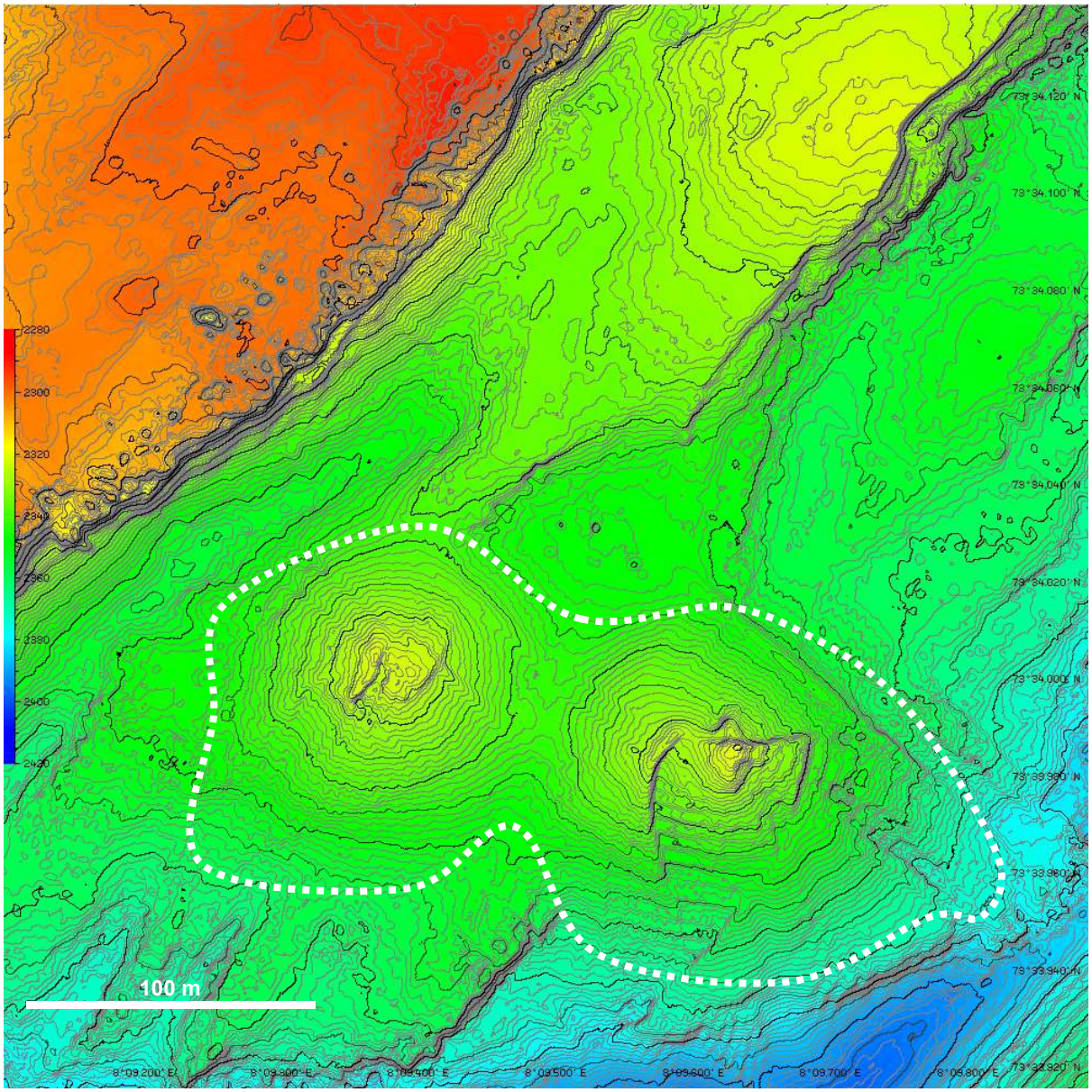

Figure 2-9 – Detailed bathymetry of Loki's Castle (Prof. Rolf B. Pedersen/UiB), (Økland & Pedersen, 2015).

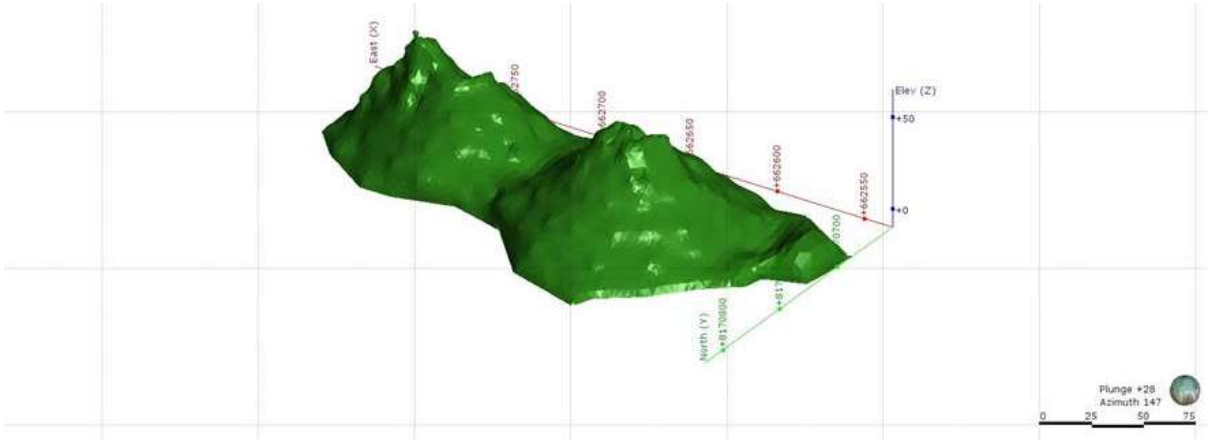

Figure 2-10 – Volumetric model of Loki's Castle, ref. Figure 2-9 (Assoc. Prof. Steinar Ellefmo/NTNU).

2.6.2 Deposit Characteristics

General

As stated by Ellefmo & Frimanslund (2015), the distributions describing the metal grades and the ore tonnage are characterized by their most likely value (mode) and average value (mean), in addition to their standard deviation. The median relates to the P_{50} value. All distributions have a long tail towards the right (i.e., extremes) with a few very high values.

Resource Estimates

The resource estimate below is performed by Associate Professor Steinar Ellefmo at NTNU for the entire AMOR as a whole (i.e., at play level in geological terms). These estimates are based known hydrothermal vent sites or SMS deposits along the ridge, as well as being coupled with statistical data on the likelihood of such sites being present based on other mid-ocean ridges. In Table 2-4, a P75 for copper of 5.04 % corresponds to a 75 % chance of the copper grade being larger than 5.04 %, while a P25 of 6.62 % shows that there is a 25 % chance of a copper grader larger than 6.62 %.

Table 2-4 – Resource estimate for AMOR at play level (Assoc. Prof. Steinar Ellefmo/NTNU).

Metal Grades	Mean	Std. dev.	F100	F75	F50	F25	F0
Cu [%]	5.90	1.35	3.00	5.04	5.78	6.62	10.90
Zn [%]	6.08	1.82	2.66	4.88	5.84	6.94	13.34
Au [ppm]	1.58	1.91	0.07	0.61	1.06	1.82	12.80
Ag [ppm]	90.90	44.10	19.20	62.30	82.90	109.00	284.00

Estimated Ore tonnage

Based on NTNU's low-resolution bathymetric data of the AMOR (which have been gathered earlier), a three-dimensional model of the seafloor existed. By using the bathymetric curves and the coordinates of Loki's Castle in Figure 2-9, a volumetric model of the deposit could then be included in the same three-dimensional seafloor model, as seen in Figure 2-10. The ore tonnage of the modelled deposit is about 500,000 m^3. Earlier performed estimates by Associate Professor Steinar Ellefmo at NTNU assess Loki's Castle to be in the range of $1.5 \cdot 10^6$ t and $1.75 \cdot 10^6$ t depending on whether a specific gravity of 3 or 3.3 is used as the ore density, respectively. These are conservative estimates, assuming no ore "below" the seafloor, and are summarized in Table 2-5. According to Økland & Pedersen (2015), the University in Bergen (UiB) estimates the deposits at Loki's Castle to be 25-35 m tall and cover 60,000 m^2, having a tonnage of $1.2 \cdot 10^6$ t for a 5-m layer and $2.4 \cdot 10^6$ t for a 10-m layer.

Table 2-5 – Estimated ore tonnage at Loki's Castle (Assoc. Prof. Steinar Ellefmo/NTNU).

	Mean	Std. dev.	F100	F75	F50	F25	F0
Ore Tonnage [10^3 t]	854.80	2,985.00	1.61	15.00	72.30	394.00	22,947.00

CHAPTER 3
Literature Review

3.1 Metal Market

3.1.1 Mining Industry

As argued by World Economic Forum (2015, pp. 6-7), mining and metals are essential to the global economy and societal development being at the beginning of most value chains as a supplier of essential materials and products. Thus, they generate trade, employment and economic development on a global scale. Figure 3-1 illustrates the market share (in revenue) of various group of metals within the mining industry, as well as the industries they serve. Properties and general characteristics of the most relevant metals for SMS deposits are listed in Table 3-1.

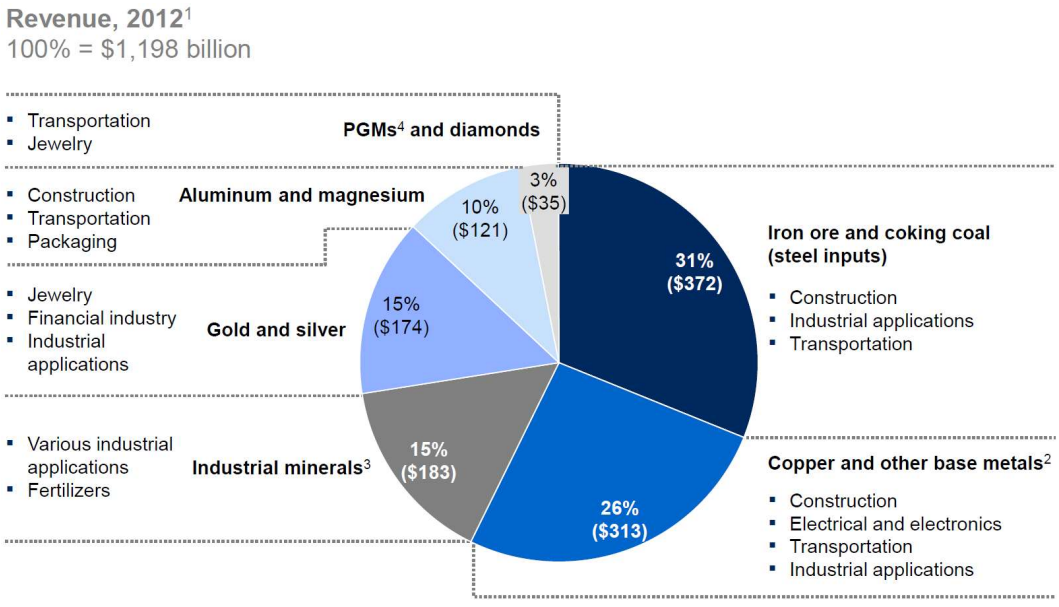

1 Excludes thermal coal and uranium (which are included in the energy commodities).
2 Refers to metals that oxidize or corrode relatively easily, such as copper, lead, tin, and zinc.
3 Industrial minerals, ferroalloys, and others.
4 Precious group metals.

Figure 3-1 – Turnover in the mining industry (McKinsey Global Institute, 2013, p. 18).

Table 3-1 – Metal parameters (Rudenno, 2012, pp. 434-492).

	Copper	Gold	Silver	Zinc
Symbol	Cu	Au	Ag	Zn
SG [-]	8.9	19.3	10.5	7.15
Melting Point [°C]	1,100	1,060	960.5	419
World Production [t]	$16.1 \cdot 10^6$	2,700	21,687	$12.4 \cdot 10^6$
World Reserves [t]	$690 \cdot 10^6$	80,000	481,942	$250 \cdot 10^6$
Consumption	Electrical, automotive, and chemical industries	Jewelry and electronics	Industrial applications (e.g., electronics, photography, batteries, mirrors, and manufacture of coinage, plate and jewelry)	Anti-rust coatings (galvanizing), alloys (e.g., brass), and pigments.
Average Grades	0.25-2 %	0.2-25 ppm	50-160 ppm	5-20 %
Mill Recovery [%]	85-95	60-98	36.7-70.6	69.5-89.1
Payable Metal from Refinery [%]	96.5	99.8-99.95	95-99	85

3.1.2 Historic Prices

Over the 1900s, the annual change in real metal prices was -0.2 % on average (McKinsey Global Institute, 2013, p. 3). The negative development (in real terms) was driven by technology improvements, discovery of low-cost deposits, and shifts in demand. Generally, a country's metal consumption grows together with its per-capita income until a certain threshold, which lies at about 15,000-20,000 USD. The growth coincides with a period of industrialization and building of infrastructure. At higher incomes, the growth becomes services-driven as per-capita income stagnates (McKinsey Global Institute, 2013, p. 19). However, countries have different development paths (e.g., China is more urbanized than India), and the commodity mix demanded by a country changes with its development. For example, an early stage (or low-GDP stage) is characterized by demand for steel-like metals, while a late stage (or high-GDP stage) by demand for platinum-like metals. However, the nominal metal prices have increased by 176 % on average since 2000, which corresponds to an annual increase of 8 %. The largest price increase is seen for gold, and was mainly due to rising production costs, few new discoveries of high-grade deposits, and it being considered by investors as safe during the volatility of the financial crises. Since the millennium, copper has increased by 344 % in nominal terms. Demand and supply are regarded the primary drivers for the later price trends (McKinsey Global Institute, 2013, p. 10). Uneven economic recovery and divergent monetary policies in counties continuously generate volatility and a negative price development on metal prices (PricewaterhouseCoopers, 2015, p. 24). In 2014, prices decreased by 6 % due to additional supply and weaker demand growth, primarily from China. Based on annual commodity price data from the World Bank from 1960 until today, Figure 3-3 shows the fluctuations in metal prices – normalized to their respective real 2010 values. Figure 3-4 and Figure 3-5 illustrate how the prices of copper and zinc, and gold and silver, move together.

McKinsey Global Institute (2013, p. 20) ascribes the rise in overall metal prices to the following factors:

- Demand from emerging markets (e.g., China)
- Changing cost of supply
- Geological issues
- Input cost inflation (especially energy)

Cost of supply is the main differentiator and geology the main driver of metal prices, as seen in Figure 3-2. Considering gold, more than 45 % of cost inflation in the period 2001-2011 was due to geological factors, and additional 30 % from shortages of inputs, including equipment and skilled labor. Strong demand yields higher cost of supply, as producers must develop supplies in regions with a higher cost regime (McKinsey Global Institute, 2013, p. 20). According to McKinsey Global Institute (2013, pp. 21-24), longer-term trends that shape the market are: rising extraction costs with more challenging access to supply; harder to fund new projects as investors focus on strong cash returns and avoid high-risk locations; new, large-scale projects require sufficiently sized mining companies; shortages in skilled labor drives rising labor costs; expected increase in future demand from emerging markets; demand generated by renewable technologies and electric vehicles; introduction of costs on inputs affecting the environment (e.g., carbon and water); and disruptive demand-side technologies (increasing usage efficiency) and increased recycling.

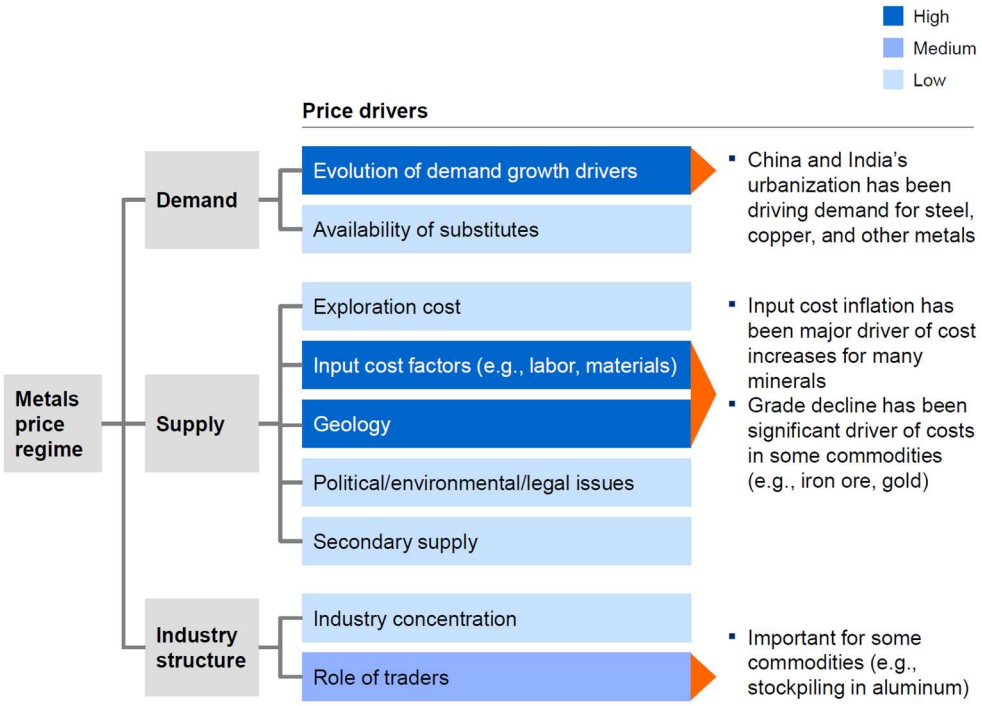

Figure 3-2 – Drivers of metal prices (McKinsey Global Institute, 2013, p. 21).

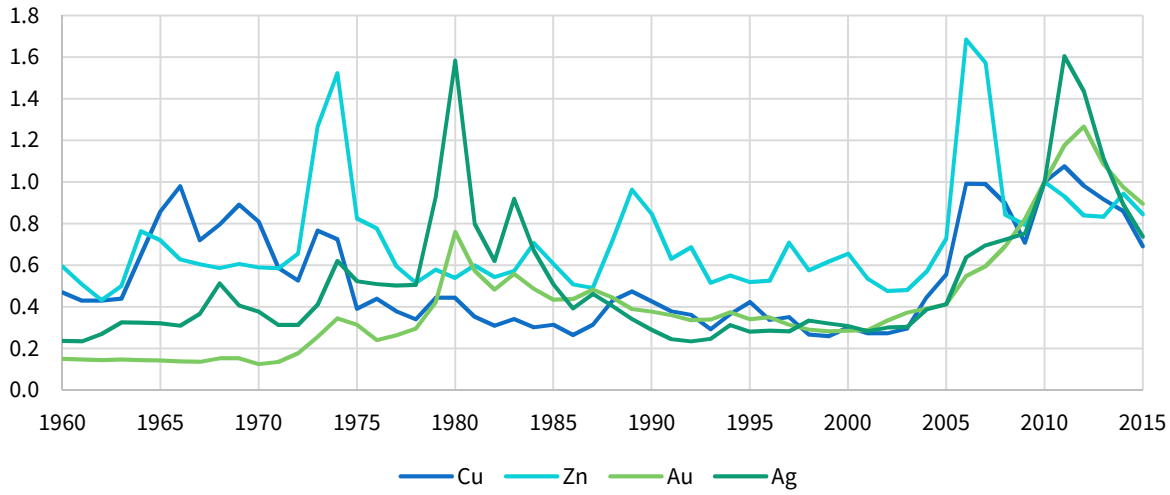

Figure 3-3 – Metal prices, ratio of real 2010 USD (The World Bank Group, 2016).

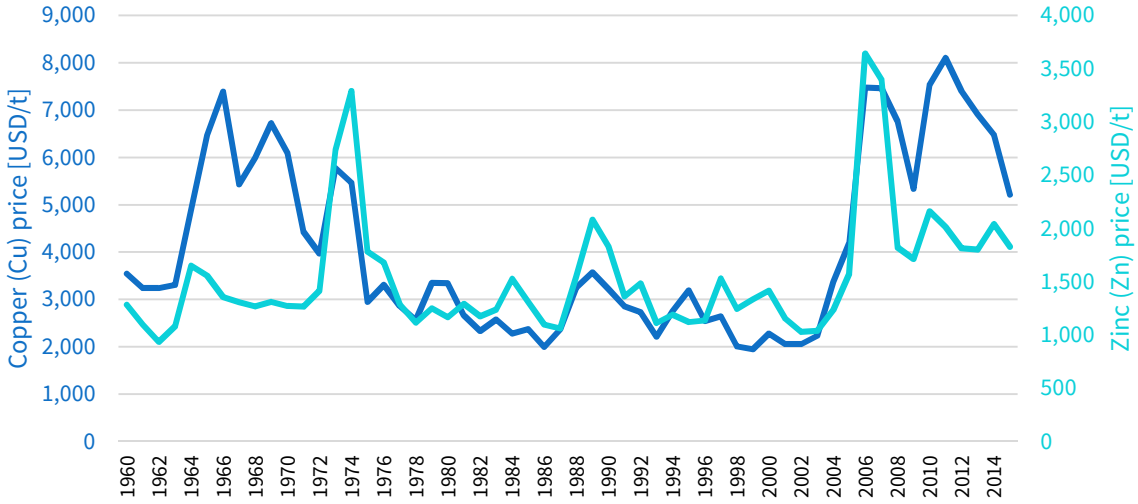

Figure 3-4 – Historic copper and zinc prices, real 2010 USD (The World Bank Group, 2016).

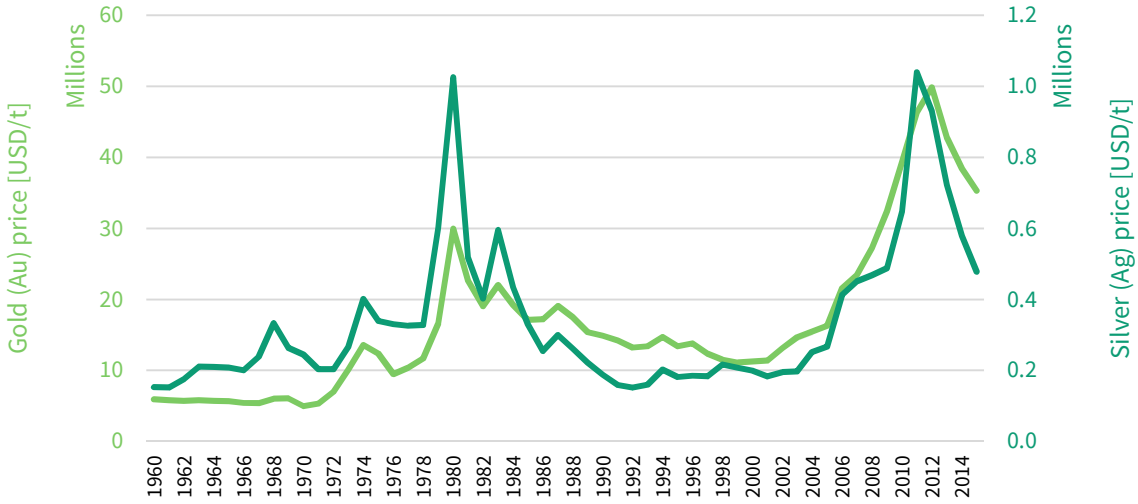

Figure 3-5 – Historic gold and silver prices, real 2010 USD (The World Bank Group, 2016).

3.1.3 Price Correlation and Volatility

Correlation

As stated by McKinsey Global Institute (2013, pp. 7-10), commodity prices have been increasingly closely correlated the last three decades, as seen in Figure 3-4 and Figure 3-5. Based on historic price data, every 10 % increase in energy prices is associated with an increase of 4-5 % in metals and 1 % for raw materials. There are disputes with regards to whether the growing role of financial markets in commodity trading, such as commodity index funds, have caused financial indexes and resource prices to move together, or that the economic cycle has pushed both in the same direction. The following factors are identified by as important drivers of correlation in commodity prices:

- Rapid growth in resource demand from China
- Resource prices as input costs of other resources[4]
- Substitution between resources enabled by technology advances

Volatility

The mining industry is characterized by volatility in metal prices, which is measured by the standard deviation from the mean commodity price (McKinsey Global Institute, 2013, p. 5). A report by EY (2014) identifies metal price and currency volatility as the sixth most important business risk for the mining and metals industry. McKinsey Global Institute (2013) compares historical metal prices to those of other main commodity groups, which all show an increasing degree of volatility, and metal prices have a lower volatility than prices of food, non-food agriculture, and energy. Energy prices have been the most volatile since 2008 (McKinsey Global Institute, 2013, p. 10). Table 3-2 shows historic volatility in metal prices.

Table 3-2 – Metal price volatility (McKinsey Global Institute, 2013, p. 33).

Interval	Cu [%]	Zn [%]	Au [%]	Ag [%]
1980 (Q1) – 1999 (Q4)	25.9	26.2	18.8	59.9
2000 (Q1) – 2013 (Q1)	56.2	49.6	63.8	74.1
2008 (Q1) – 2013 (Q1)	22.3	17.6	26.3	38.3
2012 (Q1) – 2013 (Q1)	1.1	3.1	2.8	4.6

Regarding commodity prices in general, McKinsey Global Institute (2013, pp. 5-6) argues that while short-term volatility is driven by factors such as droughts, floods, labor strikes, and export restrictions. As stated by PricewaterhouseCoopers (2015, p. 10), short-term price volatility requires that miners "*develop more flexible operating strategies, adaptable mine plans including phased expansions and partial curtailments*". Longer-term volatility is driven by structural supply issues, as supply is increasingly inelastic, thus less able to adjust quickly to changes in demand. This is because new reserves are generally more challenging and expensive to access, with new discoveries being flat despite a quadrupling in exploration spending (McKinsey Global Institute, 2013, p. 6). Nearly half of new copper projects are developed in regions with high political risks, which increase the risk of disruptions in supply, as well as increased inelasticity of supply. Hence, small changes in demand may result in significant price changes. Long-run marginal costs are also increasing, supporting that the above volatility trend will continue (McKinsey Global Institute, 2013, p. 6). In line with EY (2014, p. 29), factors contributing to volatility in the medium term are: increased regulations, such as export ban on

[4] Energy accounts for about 25-40 % of the cost of steel, and steel makes up around 30 % of the capital cost of new oil projects (McKinsey Global Institute, 2013, p. 8).

unprocessed ores and export taxes on mineral concentrates in Indonesia; divergent central bank policies; geopolitical risk – mainly relations between Russia and Western countries; provision of credit to traders; and withdrawal of banks from commodity markets.

3.1.4 Copper Production and Grade

Like hydrocarbons, mineral resources are generally non-renewable, as their formation rate is slower than their consumption rate (Fouquet & Lacroix, 2014). In terrestrial copper mines, a steady decrease in grades has been observed the last century globally. Thus, more ore must be mined and processed to obtain the same metal volume, as seen from Figure 3-6 (a). Compared to terrestrial grades, which have average concentrations starting at about 0.7 %, SMS deposits can have ten times as high concentration. Both copper and gold are used in a wide range of industries and products, and the consumption of copper has grown rapidly. The world's copper production has grown rapidly since the mid-1900s, being 8.1 % and 2.6 % in 2013 and 2014, respectively. The total refined copper production in 2013 was $21.2 \cdot 10^6$ t (Batker & Schmidt, 2015). However, the production does not make up the growth in demand following economic growth in emerging economies. For the period 2009-2020, the size of the middle class is projected to increase from 1.8 to 3.2 billion, and further to 4.9 billion by 2030. The majority of the population grown will be seen in Asia (SPC, 2013). Currently, China utilizes about 40 % of the world copper production (Batker & Schmidt, 2015). With the decline in accessible reserves, a peak in copper production is projected around 2040, see Figure 3-6 (b). As Europe is increasingly dependent on metal import, it faces a high risk of shortage (Fouquet & Lacroix, 2014). In 2014, Chile was the world's largest producer at $5.8 \cdot 10^6$ t, or more than 30 % of the global copper production, as seen in Figure 3-7.

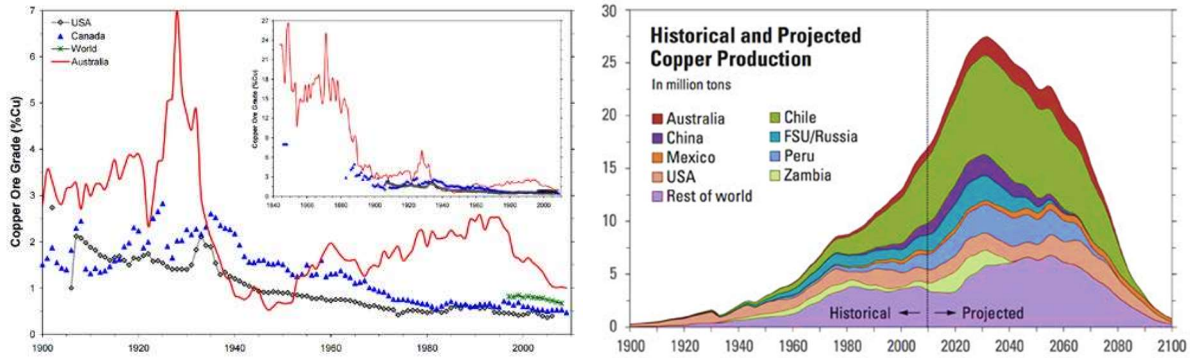

(a) Declining copper grade, 1900 to present (b) Total copper production, 1900 to 2100-forecast

Figure 3-6 – Historical copper data (Batker & Schmidt, 2015, pp. 10-13).

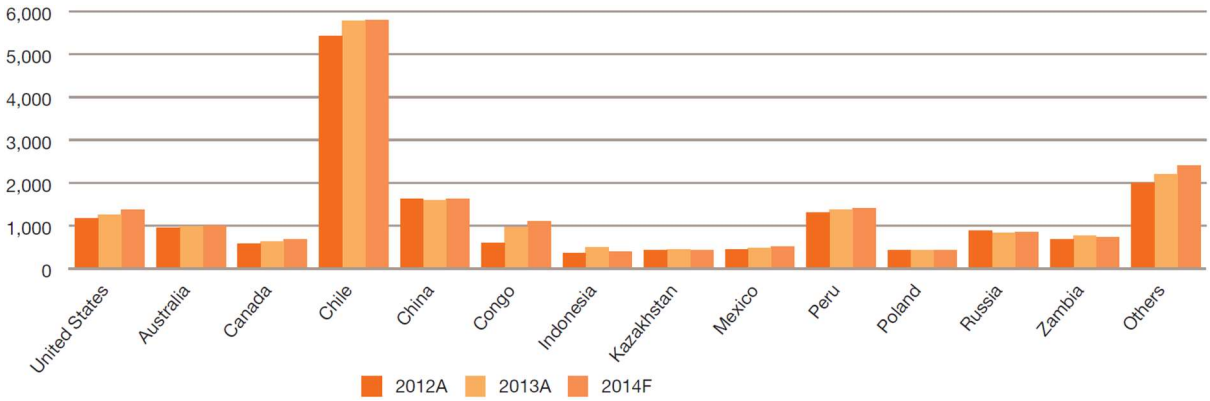

Figure 3-7 – Global copper production, 2012- 2013 and 2014 forecast (PricewaterhouseCoopers, 2015, p. 30).

3.2 Relevant Aspects from Open-Pit Mining

3.2.1 Mining Operations

As both terrestrial mining and most subsea mining concepts have a mining process that is a chain of individual unit operations, each unit relies on the operations of the upstream units (Galar, et al., 2014). Any unnecessary interruptions or bottlenecks will affect the entire chain of operations, and may lead to underutilization of capacity elsewhere. Thus, a key challenge for such an operation is to maximize the production capacity, which according to Lewis & Steinberg (2001) *"[…] is a function of availability, utilization, and performance"*. When considering operational planning and mining site layout, deep-sea mining of SMS deposits is similar to traditional open-pit mining, see Figure 3-8. According to Arteaga, et al. (2014), long-term decisions affecting the exploitation are made through so-called *strategic planning*, and include selection of mining method, processing route, mining sequence, operation size, and cut-off variables. *Tactical planning* is the routine planning activities, which includes operation ramp-up, medium- and short-term production plans, budgets, equipment deployment, and production scheduling on a monthly, weekly, or daily basis. Approach applied at open-pit sites (SRK Consulting, 2010, p. 184):

1. Site establishment
2. Cut
3. Gather and transport
4. Clean-up

Figure 3-8 – Bingham Canyon Mine near Salt Lake City, Utah, USA (Scott T. Smith/CORBIS)[5].

[5] http://www.corbisimages.com/stock-photo/rights-managed/IH200382/kennecott-copper-mine, accessed April 18, 2016.

3.2.2 Site Terminology

As described by Arteaga, et al. (2014), open-pit mining takes place in sequential steps called *pushbacks*. Since the ore is located in the deepest part of a pushback, a majority of the first material excavated in each pushback is waste material. The *stripping ratio* defines the ratio of overburden volume (or waste material) moved per ore tonnage exploited. A stripping ratio of 3:1 means that 3 m^3 of waste material is moved per 1 m^3 ore that is mined. The mining rate is governed by two factors. The first is the *pushback design*, which determines pushback size and shape, as well as characteristics of benches and access routes. It defines the final pit and the extraction sequence. The second is the *load equipment selection*, or the number of shovels or front-end loaders used in the operation, which defines the mill and mine size. The *scheme of exploitation* is the deployment of loading equipment during the depletion of the benches of each pushback, determines the extraction sequence. A pushback is depleted in *benches*, i.e., layers of a particular height and slope angle, as seen in Figure 3-9. The separate layers of benches are distanced by a *berm width* to ensure the stability of the pit wall. Different layers of a pushback are connected by *road ramps*. The overall wall slope angle is determined by the heights and the slope angles of benches, and the width of berms and ramps. A principle ramp provide access to several benches, and auxiliary ramps provide accessibility between benches in operation.

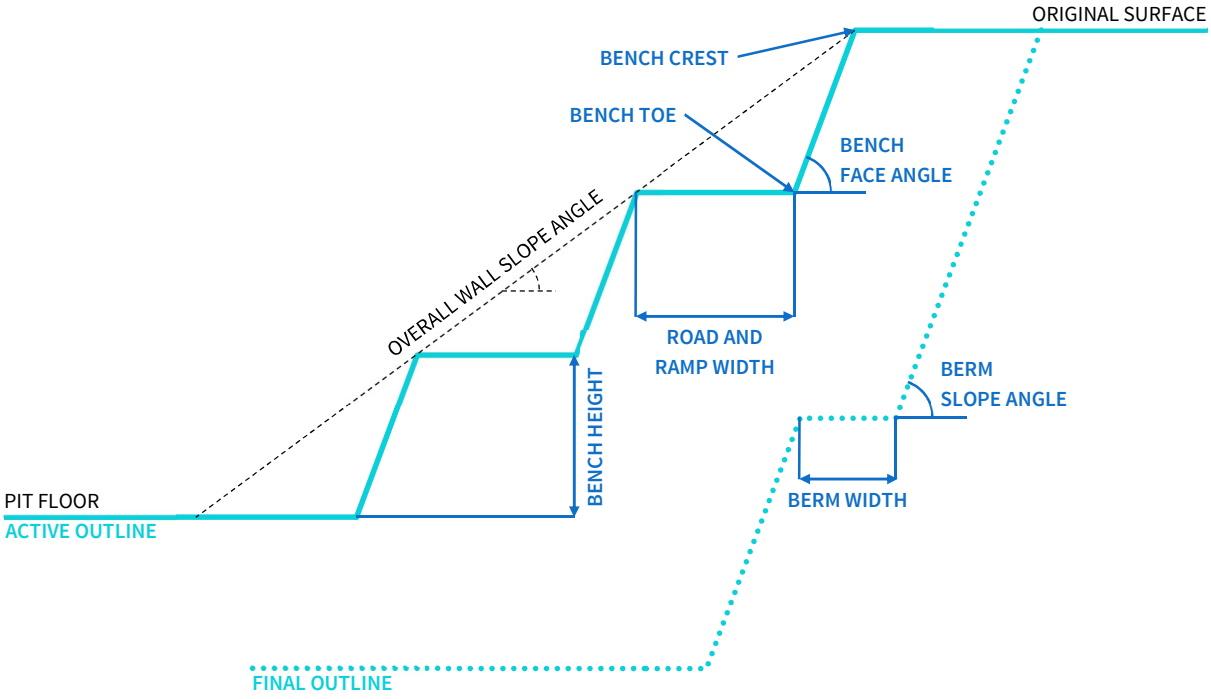

Figure 3-9 – Profile of open-pit mine. Modified from Arteaga, et al. (2014).

3.2.3 Mining Tools Operations

Cutter head forces, torques, and production rates depends on the cutting mode of the seafloor mining tool. Rotating drum cutters can work in the following cutting modes (Jackson & Clarke, 2007), as illustrated in Figure 3-10:

- **Sumping** (or collaring), where the cutter is pushed directly into the rock
- **Trenching**, where cutter extends the trench from the inside in a direction orthogonal to its rotational axis
- **Transverse cutting**, where cutter extends the trench from the inside in a direction parallel to its rotational axis

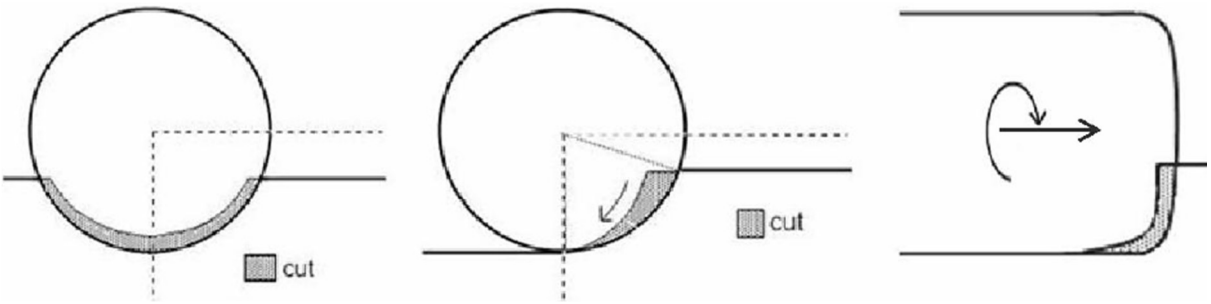

(a) Sumping (b) Trenching (c) Transverse cutting

Figure 3-10 – Cutting modes (Jackson & Clarke, 2007).

An excavator can operate, thus deploy its cutter head, in the following modes (Jackson & Clarke, 2007):

- **Lawn moving** – the cutter head is fixed at one end of the excavator while it moves along the seafloor in trenching mode. Hence, ore is continuously mined as the excavator advances. The simple set-up gives a lighter and smaller machine. The required normal cutting force on the cutter head is provided by its own weight. Despite being the simplest configuration, "lawn moving" requires the excavator to cover a large area and be kept in constant motion. Thus, the wear on the excavator's tracks is larger than for other modes.
- **Open-pit mining** – a boom-mounted cutter head (such as an open-pit mining shovel) in trenching or transverse mode mines a steep face in front of the excavator. Hence, the cutter head is moved in two or more degrees of freedom (DOFs), allowing the excavator to be stationary until having fully excavated the volume within its reach.
- **Scything** is an intermediate mode of the two above, in which the cutter head is moved in one DOF. Horizontal swaths, a back-and-forth motion in trenching or transverse mode, is performed in front of the excavator as it advances. The entire depth of the cutter head is only engaged at the center of the swath motion, while penetration depth is smaller towards each side. "Scything" does not require precise alignment of the excavator, as the cutter head is moved entirely in and out of the rock for each swath, and is oriented at right angles to the excavator's path.

Jackson & Clarke (2007) argue that the "open-pit mining" and "scything" modes require a more complex machine set-up, but have less track maintenance and are capable of handling rugged terrain. Another operational advantage is having the machine stationary in one position for a longer period of time. Excavator designs that require a precise cutter alignment (i.e., repositioning of the excavator or cutter head) after repositioning reduce the operational efficiency. Furthermore, excavation modes that require the cutter head to be moved in and out of the rock are less efficient.

3.3 Production Systems for Deep-Sea Mining

3.3.1 History of Subsea Mining

Deep-sea mining has been a hot topic in academia periodically since the 1970s, as described in Herbich (1978). In the late 1970s and early '80s, enthusiasm for manganese nodules triggered several pilot tests at Clarion-Clipperton Fracture Zone (CCZ) in the Pacific Ocean at depths exceeding 5,000 m (Knodt, et al., 2016). Considering shallow-water deposits, offshore dredging for gold was performed outside Alaska in the late 1980s (Garnett, 1996). In somewhat deeper waters, at 100-150 m depth off the west coast of Namibia and South Africa, diamonds were discovered in the 1960s. Subsidiaries of De Beers have performed large-scale exploration of subsea diamonds since 1991 using a fleet of retrofitted vessels (Richardson, 2007). Despite the relevant operational experience of De Beers, little technology is transferable to operations at greater depths and for other materials than sand. Another example of shallow-water, low-tech operations is offshore mining of tin outside Thailand (Garnett, 1996).

3.3.2 General Features

In general, a subsea mining system is built around the concept of disaggregating the minerals on the seafloor using remotely operated excavators, before vertically transporting an ore-seawater slurry to a surface vessel, which is either dynamically positioned or moored. The slurry is dewatered, a process in which all solid particles are retained, and the mineral-rich ore is stored and subsequently shipped to shore for further processing in an onshore facility. Any excess water is disposed near the seabed to avoid biological and environmental concerns associated with mixing of seawater volumes originating from different depth layer.

Using the analogy of Figoni & Chand (2014), a typical system layout is divided in three main components, as illustrated in Figure 3-11 for a system concept by IHC:

- **Seabed System** (SS) defines various types of remotely operated productions tools performing the mining operation on the seafloor, mainly based on technologies from terrestrial mining.
- **Underwater Transportation System** (UTS) are any equipment connecting the mining operation on the seafloor with the sea surface, thus performing the vertical transporting the ore. Lifting systems from the dredging industry its, as well as riser system designs and lifting technologies from offshore O&G developments, are applied.
- **Topside System** (TS) describes some sort of surface vessels that serves at the base for the operation, which depends on the environmental conditions at the site of operation. Most system architectures have a ship-shaped TS, but semi-submersibles and barges are also proposed. With respect to vessel design and arrangement, there are many similarities with drillships and production vessels, such as Floating Production, Storage and Offloading (FPSO) and Floating, Drilling, Production, Storage and Offloading (FDPSO) vessels. Ore processing solutions onboard the vessel, such as a dewatering system, originate from terrestrial mining, while ore handling technologies are taken from those used in traditional bulk shipping.

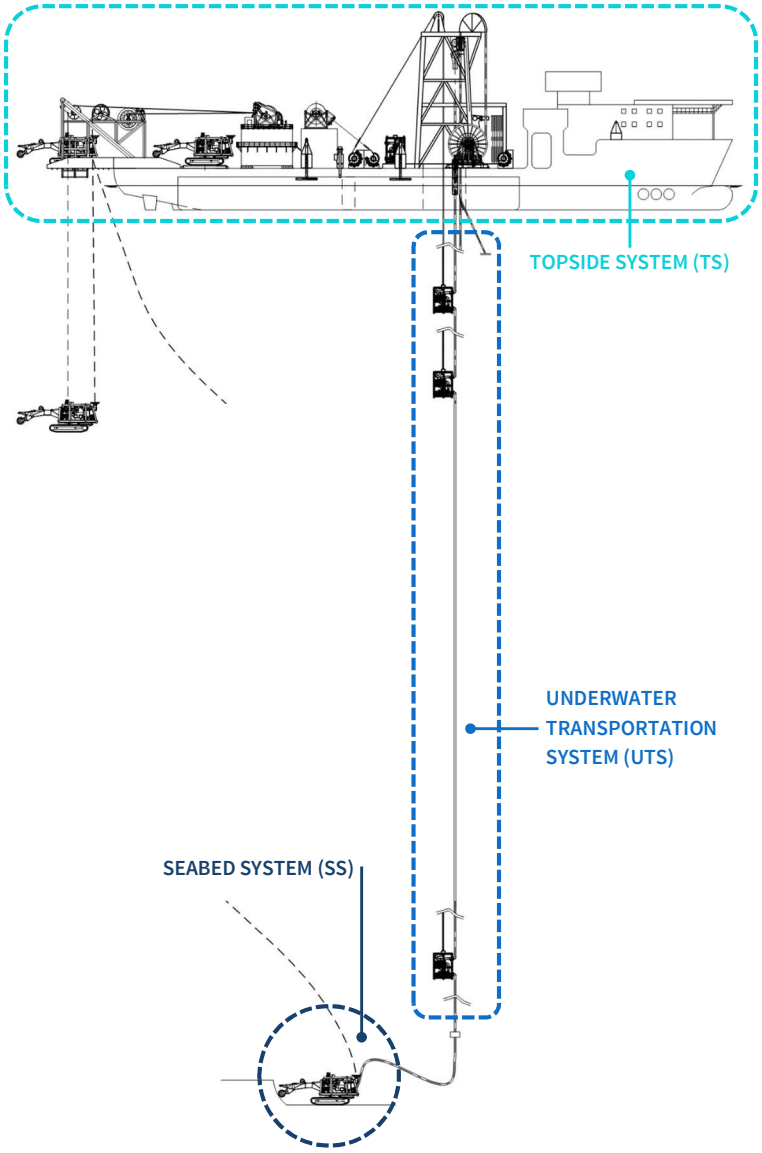

Figure 3-11 – Subsea mining system by IHC. Modified from van Wijk (2016, p. 4).

3.3.3 Vertical Transportation by Hydraulic Lifting

In a UTS based on the concept of hydraulic lifting, in which the ore is transported to surface as a water-ore slurry, the selection of pump system determines the overall layout of the slurry lifting system. In the dredging industry, transporting solid particles as slurry has been used for bulk relocation of smaller particles and lifting of larger particles in shallow water (Leach, et al., 2012). Hydraulic lifting has been used to transport mined products both vertically and horizontally in terrestrial mining, especially within coal mining. Already in the late 1970s, slurry with large coal particles of up to 60 mm was transported from depths of about 1,000 m. Flexible risers can be used in shallower waters than 500 m (Heeren, et al., 2013). The following pump systems enables hydraulic lifting (Figoni & Chand, 2014), see Figure 3-12:

- Positive displacement pumps
- Multi-stage centrifugal pumps
- Air-lift systems

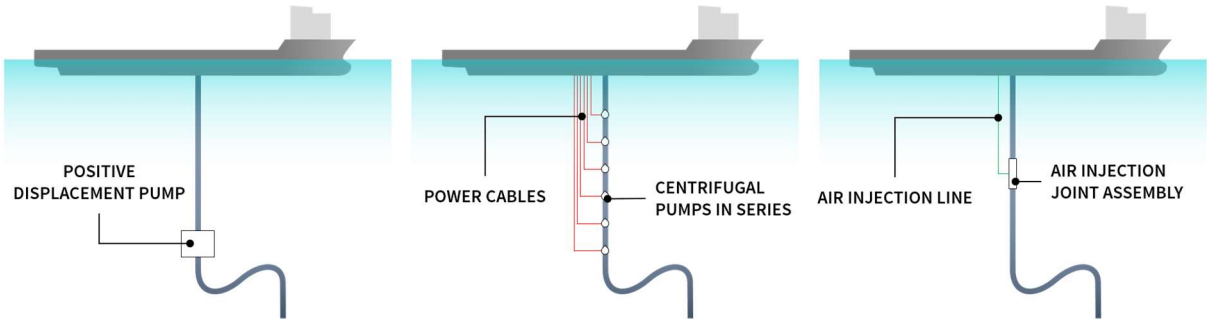

(a) Positive displacement pump (b) Multi-stage centrifugal pump (c) Air lift

Figure 3-12 – Vertical transportation by hydraulic lifting. Modified from Leach, et al. (2012).

Positive Displacement Pumps

The layout of the different systems are described by Leach, et al. (2012). A positive displacement (PD) pump operates in the low flow rate, high pressure regime, thus one pump module is sufficient. Several pump chambers maintain flow control for varying slurry parameters. In such a system, the pump module is mounted on the lower end of the production riser suspended below the surface vessel. The required flow velocity, which is defined as the lowest flow velocity at which the largest particle will not settle out in the flow stream, depends on particle size and density, in addition to the transport fluid velocity (Judge & Yu, 2010). Hence, it is obtained by selecting pump characteristics and riser diameter. For a constant flow rate, the riser diameter decreases, and both the required discharge pressure of the pump and the velocity increase, since the required pressure head depends on the slurry density and frictional losses from the fluid flow. Judge & Yu (2010) state that *"the minimum flow velocity, rate and pressure must be established prior to selecting a slurry pump to transport the slurry to the surface, and the horsepower required to drive the pump must be calculated to size the power generation equipment required on the surface vessel"*. Further, the ideal pump design satisfies the following criteria:

- Maintain a constant flowrate, or adjust its flowrate, for varying fluid density
- Handle varying solid size and concentration
- Provide the required discharge pressure for varying densities or concentrations

Multi-Stage Centrifugal Pumps and Air Lift Systems

In contrast to PD pumps, *centrifugal pumps* operate in the high flow rate, low pressure regime. Hence, multi-staging (i.e., having several pumps in series along the production riser) is required to obtain the required lifting height. Each pump has an individual power supply, making the system more complex and less efficient (Leach, et al., 2012). Generally speaking, centrifugal pumps are extensively used for slurry lifting purposes. The *air lift system* is based on air supplied from compressors onboard the surface vessel. Nitrogen is typically used, being a non-corrosive, non-flammable inert fluid. Air is injected into the flow at a special joint in the production riser through an independent injection hose. As the air rises and expands up the riser string, the fluid is lifted. The air reduces the relative density of the fluid within the riser, creating a differential pressure at the lower end of the riser, which induces a lifting force on the slurry.

Pros and Cons

Based on Leach, et al. (2012), advantages and disadvantages of the different system designs are summarized in Table 3-3. The selection is an optimization of pump efficiency, power consumption, and maintenance requirements. When considering cost and time related to maintenance and repair, the air lift system is advantageous having all pump systems at the topside. Both the air lift system and the displacement pump are sensitive to the slurry properties, such as particle size. Air lift requires large

amounts of energy and is currently not scalable to meet the production rates for projects to be economically feasible. However, a positive displacement is advantageous when it is installed close to the seabed, due to its ability to dispose the tailing from the dewatering process directly to the sea without the need of a return pipe separate from the production riser, as seen in Figure 3-22 (b).

Table 3-3 – Comparison of slurry lifting systems (Leach, et al., 2012).

	Advantages	Disadvantages
Positive Displacement (PD) Pumps	• High pressure output (enabling a single stage pump set) • Mechanically simple with few moving part, hence reduced erosion rates and maintenance requirements • Multiple chambers (enable maintained flow control for varying slurry parameters) • Additional chambers can be added for improved redundancy • Either electric or hydraulic power	• Non-continuous flow (with a single chamber) • Low flow rate (with single chamber compared to centrifugal pumps) • Limited particle size (due to in-line check or actuated valves) • Does not have capacity to provide suction, hence slurry must be pumped into the pump chamber
Multi-Stage Centrifugal Pumps	• No flow path restriction (due to no in-line valves) • Provides suction, hence combines both collecting and lifting (i.e., pumping) functions	• Complexity of multiple pumps with individual power supplies within the riser • By-pass valves in case one pump fails • Production rate reduced by periodically pump maintenance (i.e., replacement of impellors) • Lower efficiency (compared to PD pump) • Delivered volumetric concentration is limited to 8 % (number of pumps vs. required head)
Air Lift Systems	• No submerged mechanical pumping system, hence improved reliability and reduced maintenance • Simple system • Combines both collecting and lifting functions • No flow path restriction (due to no in-line valves)	• Complex three-phase flow • Sensitive to slurry inlet parameters (e.g., particle size, flow rate, and slurry density) • Air/slurry energy (related to particle velocities, and air volume and pressure) • Low efficiency, hence high power consumption • Large dynamic riser joints not developed

3.3.4 Current Status and Technological Challenges

Currently, the exploration technology is well advanced, resulting in an increasing number mineral deposits being discovered in the oceans. However, the production technologies are less developed. Despite decades of efforts in academia, few full-scale systems having been designed and just a handful of pilot tests have been performed. The general lack of operational experience (from other than shallow-water dredging-like subsea mining operations) can be compensated for with parallels to various offshore O&G operations. Furthermore, technical solutions and operational experience from activities in the harsh environment of the North Sea and the ultra-deep waters of the Gulf of Mexico can be utilized in the now field of deep-sea mining. Today's commercial system concepts for deep-sea mining adopt existing technologies from the shipping, offshore oil and gas, traditional land-based mining, and sediment dredging industries – partly because using proven technology for new applications is easier with respect to approval from classification societies (Figoni & Chand, 2014). The general idea of most production system architectures is having remotely operated tools (e.g., crawlers or a grab) crushing and collecting ore on the seafloor. A slurry of ore and seawater is transported through a riser to a surface vessel, where it is dewatered and stored before being shipped to shore.

IHC and Technip are the leading industry players on research and development (R&D) within the field. Shallow-water subsea mining operations have many parallels to dredging, and technologies and solutions for such operations are mainly developed by IHC. Technip has been on the forefront of deep-sea mining development (i.e., deepwater production system for harsh environment operations) utilizing their competence from offshore O&G. While multi-staged centrifugal pumps and air lift systems are proven for shallow waters, only positive displacement (PD) pumps are proven in dual gradient drilling (DGD) operations down to 2,500 m, on which the production system of Nautilus Minerals is based. However, there is no experience with operating such a pump with the high erosion rates seen in SMS mining. The Solwara 1 project of Nautilus Minerals is the first commercial full-scale exploitation of SMS deposits, and is planned to commence in 2018 off the coast of Papua New Guinea in water depths of about 1,600 m. The site and production system are described in detail in Chapter 3.6.

The main technological challenges for mining systems are: Predicting the behavior of large-particle, multi-phase flow in small-diameter rigid and flexible risers; reliability of remotely controlled excavators in design and operation in an environment with violent vibrations, and high wear rate and ambient pressures; hyperbaric crushing of rock is more energy demanding, and current rock crushing models does not apply. As concluded by Alvarez Grima, et al. (2011), *"soil conditions determine the optimal cutting or excavation method. The cutting process determines the input for the vertical hydraulic transport model in terms of particle shape, particle size distribution and production rates. The internal flow, including plug formation and possible riser blockage, represents one of the boundary conditions […]"* for dynamical modeling of the riser system. The sum of the internal and external loads gives the corresponding riser deflections, and the system layout determines the dynamical motion due the loads.

3.4 Relevant Operational Experience

3.4.1 Remotely Operated Subsea Equipment

General Outline

To establish a basis from which to assess the expected efficiency and availability of running remotely operated mining crawlers, various types of subsea equipment have been evaluated. As described by Hallset (2006), intervention, maintenance and repair (IMR) operations related to subsea O&G infrastructure are typically performed by remotely operated vehicles (ROVs) equipped with specialized hydraulic tools. For tools too heavy to be carried by an ROV, a remotely operated tool (ROT) system is used, which is stationary and lowered on a winch either separately or as mounted onto another equipment. The launch and recovery system (RALS) of such systems are essentially the same as those designed for subsea mining crawler (despite the latter being considerably heavier – up to 350 t dry weight). In the following, operational aspects of remotely operated deep-sea mining are comparted to existing experience from subsea trenching and dredging operations, as well as heavy work class ROVs.

Cable Trenching

Nexans delivers a range of cables and cabling solutions both for onshore and offshore applications, and has developed the Capjet system for subsea trenching of cables. The system uses water-jetting for both propulsion and trenching, and is manually operated from a surface vessel using visuals from cameras mounted on the unit itself, and additionally from an ROV flying alongside. A typical trenching job takes a couple of days with continuous operation. When planned maintenance is to be performed, the Capjet unit on the seafloor is retrieved and another unit is deployed. Clauses in Nexans' contracts allow them to accumulate "unused" maintenance hours on the daily operations plan up to a total of 24 h or 48 h. Downtime beyond the scheduled repair hours are registered as breakdown time, and amounts to 5-6 % of the total operational time per annum.

Seafloor Leveling Prior to Pipe Lay

As part of the Ormen Lange subsea field development during the 2004-2005 seasons, Nexans developed two prototype dredging units called Spider, see Figure 3-13 (a). To cope with highly sloping seafloor terrain, the design was inspired by the Menzimuck – a forest logging machine. The Spiders prepared the steep and uneven seabed prior to installation of pipelines and umbilicals for tie-back to shore, being operable in terrain with slopes up to 40° in both axes. In the dredging process, as described by Eklund & Paulsen (2007), *"the soil is cut in pieces by a jetting system and then transported away through a suction pump, everything operated through a 3D model of the seabed bathymetry and the animated movements of the working parts of the Spider"*. The virtual model is continuously updated with changes in the terrain caused by the Spider's progress. The grabber, mounted to a telescopic arm, was primarily used to loosen material, but capable of lifting 2.7 t in case large rocks need to be moved. The job commenced with only one Spider in operation. Experiencing breakdown rates as high as 50 % in the first months of operations, a larger Spider was built and put into operation in the second campaign season to comply with the operational progress required by Hydro. However, the units were connected to the same surface vessel and seldom operated in parallel to maximize the capacity. With both Spiders in operation, the overall steady-state downtime was about 25-30 %. In addition, there was hidden downtime related to repairs and modifications performed when waiting for other operations to complete. Eklund & Paulsen (2007) states that the overall daily processed volume was somewhat lower than anticipated.

Work Class ROV Operations

Remotely operated vehicles (ROVs) in the heavy work class are characterized by having an electro-hydraulic power exceeding 150 hp and a water depth rating of 2,000-5,000 m. Oceaneering holds 36 % (336 of 937) of the worldwide ROV fleet and the majority (57 %, 127 of 222) of the offshore drilling support market (Oceaneering, 2015). Subsea 7 and Fugro are the second and third largest players, respectively. Hence, the downtime of the Oceaneering fleet is representative for heavy work class ROVs in general, as their fleet mainly consists such vehicles. Oceaneering's publicly reported downtime is in the range of 1.6-0.14 % for the period 2005-2013. Oceaneering (2010) defines downtime as *"any time we are called on to make a dive and unable to respond, or become inoperative during a scheduled/requested dive"*. However, failure of the following is not considered as downtime on Oceaneering's behalf (Oceaneering, 2010): (i) components or subassemblies that does not prevent the operation to be completed; (ii) ROV system equipment not belonging to Oceaneering; and (iii) other facility downtime, like vessel systems. Further, for every 24 h of diving Oceaneering gets 2 h of repair and maintenance time (up to 25 h per month) as per contract. Taking the above clauses into consideration, the actual downtime due to random failures on Oceaneering's equipment, when including third-party tools, is likely to be higher than the ones stated publically.

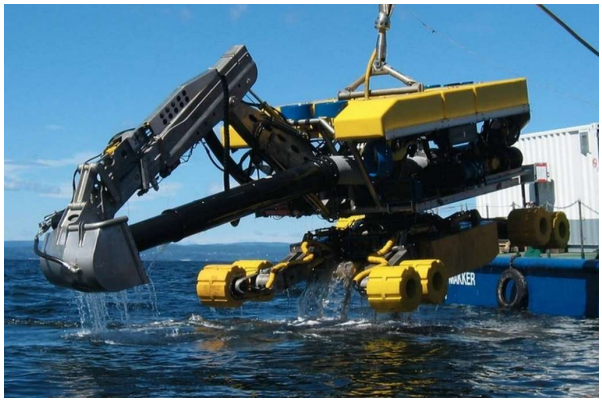

(a) Nexans' Spider unit (Hydro)

(b) Dredging machine (Soil Machine Dynamics)

Figure 3-13 – Examples of remotely operated subsea tools.

Lake and Costal Dredging

Based on various reports on dredging operations in the U.S., like as Honeywell (2009) and Dredging Supply Company (2010), a reasonable sum of planned and unplanned downtime for such operations are in the range of 25-30 % of the total operations time. Although, it is dependent on the cut thickness and dredge template shape. Only a part of the total downtime is related to equipment breakdown and repair. The remaining downtime is due to refueling, environmental conditions, and (de)mobilization. The main components of a dredging system are: dredge; booster pump(s); and other mechanical apparatus, like cables and hoses. Operation recordings suggest that the failure rates are in the range of 3-17 % (Dredging Supply Company, 2010).

3.4.2 Subsea Diamond Mining

As briefly mentioned in Chapter 3.3.1, subsidiaries of DeBeers operate a fleet of five specialized diamond mining vessels along the South African and Namibian coastlines at water depths of 90-140 m, which constitute the only operational experience from commercial subsea mining. The recovery takes place by two methods, as illustrated in Figure 3-14:

- **Crawler (horizontal mining)**, remotely operated from a surface vessel to which it is connected by flexible hoses, is electrically powered and limited to 200 m water depth. Hydraulic systems are used to maneuver the unit and control its boom (Environmental Protection Authority, 2014). Sand and silt are sucked up by vacuum through a nozzle using a centrifugal pump, which is driven by an electric motor. The mining vessel Mafuta has a crawler weighing 286 t and a transport riser pipe with a diameter of 0.7 m. Its capacity is about 1,000 m^2/h (Reuters, 2014).
- **Large Diameter Drill (LDD) (vertical mining)** is used in areas with rocky and uneven seabed. As described by Ship & Offshore (2010), the air lift vertical drilling system is delivered by Aker Wirth, and consists of a 6.8 m diameter rotating drill bit connected to the end of a conventional drill sting. The heave compensating system, from which the 113-t heavy drill equipment (excluding the drill string) is suspended, is limited to heave motions of 6 m and rolls and pitch motions of 10°. After drilling through the diamond-bearing overburden layer down to the bed rock, which takes about five minutes, the drill bit is lifted just clear of the seabed while repositioning the vessel. Station-keeping is done by four anchor lines in conjunction with dynamic positioning (DP). Compressed air (from nine surface compressors) is injected right above the drill bit while drilling, taking a slurry of seawater and loosened material to the surface.

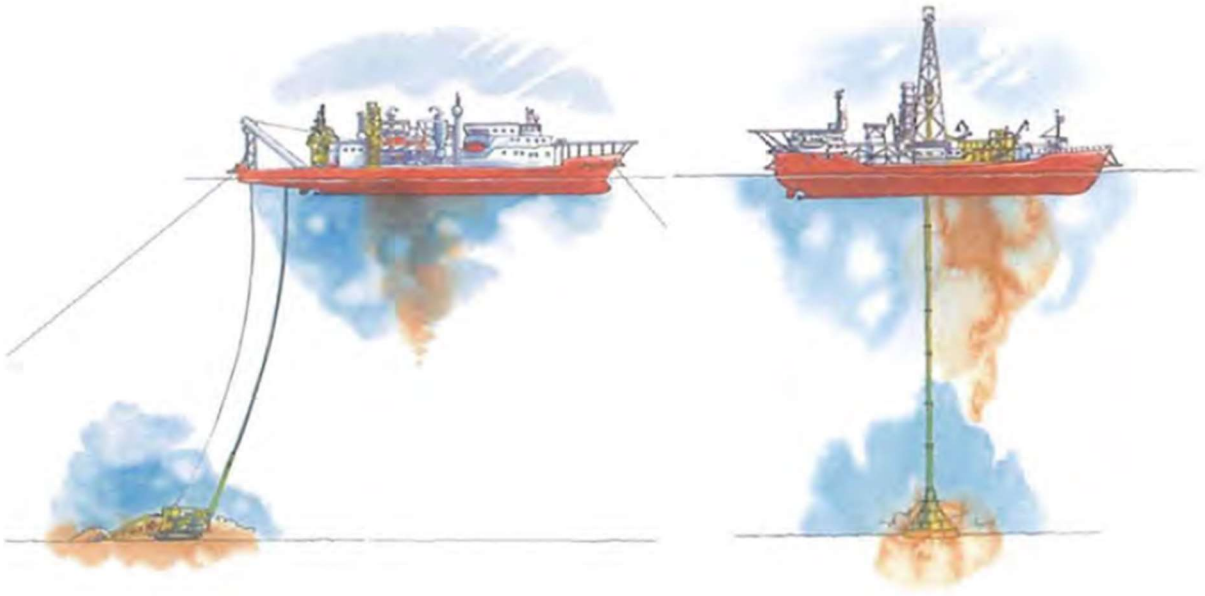

(a) Crawler (b) Large Diameter Drill (LDD)

Figure 3-14 – De Beers' subsea diamond mining systems (Environmental Protection Authority, 2014).

Once the diamond-rich sediments reach the surface vessel, *"the sediment enters an unceasing production line where it is automatically sized and separated, and the diamonds sealed in cans"*, all performed automatically (De Beers Group, 2014). As described by Richardson (2007), the slurry is discharged into a spiral-type partial de-aeration chamber. Subsequently, it is transferred to a processing plant, and is equally split by slitter launders (i.e., sloping chutes) prior to dewatering and sizing. The flows are presented onto two vibrating screens. In addition, the plant comprises of scrubbers, screens, ball mills, density change circuit, driers and x-ray machines. According to De Beers Group (2014), *"once the diamonds are extracted, the sediment is returned to the seabed [...]"*. Once a month, the deposits are airlifted by helicopter for further processing onshore.

Operational experiences and procedures are as follows (Environmental Protection Authority, 2014):

- 400 t of sediment are pumped aboard every hour (De Beers Group, 2014, p. 72).
- The vessels and the LDD system operate offshore for 3 years before being overhauled.
- The LDD system has a capacity of 3,500 m^3/day, and an availability of 98 % (Ship & Offshore, 2010). About 7,400 mining hours per year yield an excavation efficiency of 84 %, as seen in Figure 3-15 for the vessel Grand Banks.
- The operation is exposed to strong southern coastal winds throughout the year, and is unprotected against westerly South Atlantic weather systems during the winter.
- The mining operation follows a grid system, and mining blocks are depleted in a regular pattern.
- The vessels operate continuously throughout the year with crew members working 8-h or 12-h shifts, and rotate 28 days on/off. Crew transfer is done by helicopter.
- Mineral reserves are developed on a rolling basis, with survey and sampling conducted in parallel to mining operations (Richardson, 2007).

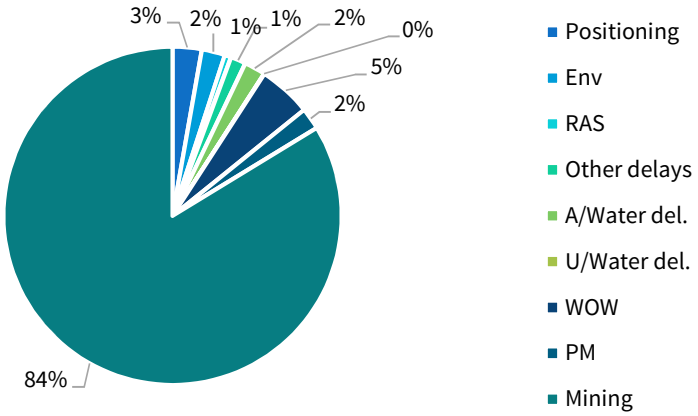

Figure 3-15 - Utilization of DeBeers' vessel Grand Banks in 2005 (De Beers Marine Namibia, 2006).

3.5 System Concepts and Technological Findings by Technip

3.5.1 Background

Since 2008, Technip has had an ongoing R&D campaign on subsea mining with focus on exploitation of SMS deposits in deep waters using hydraulic lifting (Technip, 2008). The company is granted the contract for engineering, procurement, construction and management (EPCM) of all components of the Riser and Lifting System (RALS) for Nautilus Minerals' Solwara 1 project. In the last eight years, Technip has published the below work on system design and various physical aspects:

- **Characterization of seafloor massive sulfides (SMS)**
    - Geotechnical properties, including maturation threshold, in hydrothermal sulfide mounds by Waquet & Fouquet (2010)
- **Flow assurance and operability**
    - Large-scale experiment for flow correlation validation and abrasion testing by Parenteau (2012)
    - Development and large-scale validation of a liquid-solid solver for two-phase transient flow in riser systems by Beauchesne, et al. (2015)
    - Validation of 1-D steady-state flow assurance models for air-lift pumping by Beauchesne, et al. (2015)
- **Mining and rock conditioning**
    - Effects of deep-sea hyperbaric conditions on crushing of SMS deposits by Waquet, et al. (2011)
    - Preliminary design of a trench cutter for mining of SMS deposits at 2,000 m water depth by Spagnoli, et al. (2016)
- **Field architecture** with screening of available deep-sea mining field architecture for both calm and harsh water environments
    - Closed-loop steep wave configuration of flexible pipe using a Subsea Crushing and Feeding Unit (SCFU) by Parenteau, et al. (2013)
    - Nautilus Minerals' system concept, and an open-loop steep wave configuration of flexible pipe (developed for Nepture Minerals for harsh conditions) by Espinasse (2010)

3.5.2 System Design

Design Input

When developing a riser and lifting system for subsea mining purposes, the following factors are considered as required input in a design process:

- Riser design and acceptance criteria
- Riser configuration options
- Vessel properties (e.g., offset, RAOs, and compartment flooding)
- Seabed properties and pipe-soil interaction
- Environmental conditions (i.e., sea states, current, and wave)
- Ancillaries design (e.g., water return lines as part of rigid riser bundle)
- Riser content (e.g., volumetric ratio[6], density of phases)

Riser Design and Acceptance Criteria

As in any project, there will be design criteria from the customer with respect pressure, shape, and length of the riser(s). Flow assurance requirements defines a production operating envelope that establishes requirements on pressure profile, internal diameter (ID) and flow concentration of the production riser. Generally, the internal pressures encountered in deep-sea mining applications are at the lower range of those in offshore O&G.

The so-called "line structure", or the selection of riser design, are one out of the two following:

- **Rigid riser**, which is very similar to a conventional marine drilling riser (see Figure 3-16), consist of tubular midsections with riser connectors in the ends. Drilling riser joints are typically 30 ft (9.14 m) or 50 ft (15.24 m), and the choke and kill lines which are attached to each side of the main bore corresponds to the water return lines seen in subsea mining applications (Bai & Bai, 2012, pp. 829-834).
- **Flexible risers** have been found suitable for production and export risers, as well as flowlines. These multi-layer composite pipes have low relative bending to axial stiffness, which is enabled by layers slipping past each other when loaded. High-stiffness steel armor layers provide strength and low-stiffness polymer sealing layers provide fluid integrity: Several layers of stainless steel (e.g., carcass) wire resist the external pressure; the internal polymer sheath is a barrier ensuring internal fluid containment; the pressure armor in carbon steel resists hoop pressure; the tensile armor in carbon steel resists tensile loading; and the external sheath is an external fluid barrier (Bai & Bai, 2012, pp. 858, 875). The composition of a flexible riser design by Technip is shown in Figure 3-17.

[6] The volumetric ratio is the percentage that solids constitute of the slurry flow as a whole.

Figure 3-16 – Marine drilling riser joint with protection fins and stacking rings (Aker Solutions, 2010).

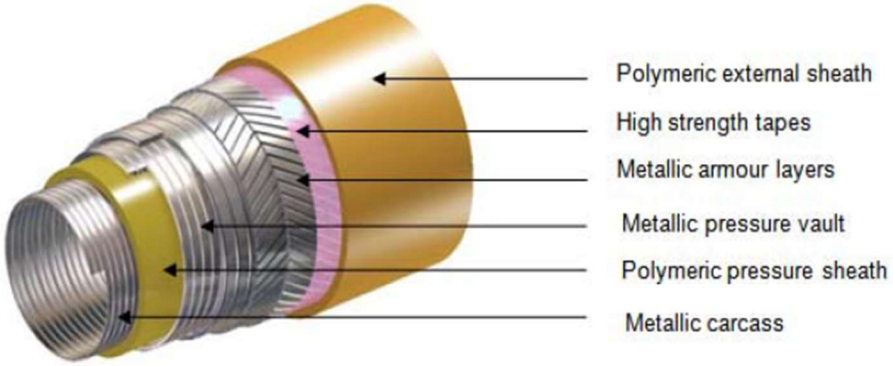

Figure 3-17 – Conventional flexible steel wire armors by Technip (Do & Lambert, 2012).

Since the late 1970s, flexible pipes have been used for offshore oil and gas applications at water depths down to 8,000 ft (2,438 m), pressures up to 10,000 psi (69 MPa), and temperature up to 150 °F (66 °C) (Bai & Bai, 2012, pp. 874-875). Internal flow is not an issue for rigid risers. Vortex-induced vibrations (VIV) is not critical for flexible riser. However, it is a concern for rigid risers. The relative diameters and gaps of the riser bundle (i.e., main bore with choke and kill lines) has an influence on VIV, as evaluated by Vandiver, et al. (2009). With reference to Technip (2011), other advantages of rigid risers are: quick connect-disconnect time; robust fatigue performance; small footprint; low bend radius corresponding to shorter point-to-point length, shorter crossings, and no free spans; robust built-in insulation; corrosion resistance; dynamic stability; limited upheaval buckling; and re-routing (re-use).

Based on a selected "line structure" design that fulfills the requirements to flow assurance, a global analysis of the system is performed in which all external factors are taken into considerations (e.g., wave, current, depth or submerged weight, buoyancy, and seafloor conditions). The density of the riser content is of concern with regards to mechanical analysis. First, an extreme analysis is performed to evaluate the mechanical resistance to extreme loading. It is based on metocean data for the given location of operation, and the criterion is the maximum allowed stress in the riser. Secondly, an interface analysis is performed considering interaction between riser and umbilicals with respect to the position of the surface vessel, with no clashing between adjacent equipment as the criterion. Clashing between risers and umbilicals (e.g., twisting of umbilicals around the riser) is a considerable issue for the concept of Nautilus Minerals. Finally, a fatigue analysis in which VIV and flow-induced vibrations are considered, and the mechanical resistance due to fatigue during the field life is assessed, with a fatigue life greater than service life as the criterion. The analysis results in an adequate configuration for the system. Relevant classification rules for analysis are API RP 2RD, DNV-RP-C205, and DNV-RP-F203.

Riser Configurations

An advantage of flexible risers can that they can be hung off the side of the surface vessel, such as with the riser balcony in Figure 3-18 (b). However, it limits the vessels maneuverability when the flexibles are connected. Other mooring arrangements used for ship-shaped offshore structures include turret mooring and swivel-stack systems, a seen in Figure 3-18 (a), in addition to articulated towers, and soft yoke systems (Paik & Thayamballi, 2007, p. 9), which allow the unit to rotate (weathervane) according to the direction of external forces. Thrusters can provide the system additional restoring force.

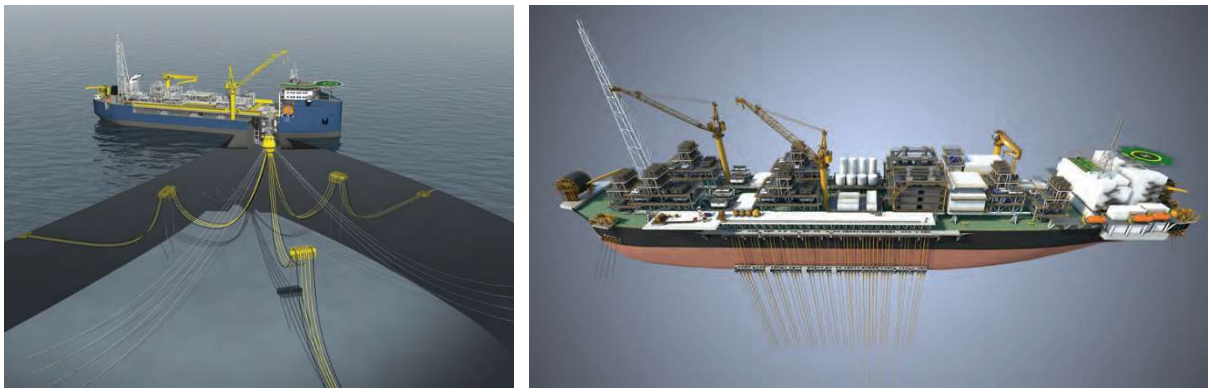

(a) Turret-moored (b) Spread-moored with riser balcony

Figure 3-18 – Mooring arrangements for FPSO vessels (National Oilwell Varco, 2013).

Depending on the environmental conditions at the site of operation, Technip proposes the following riser configurations for subsea mining applications, which is based on their existing product portfolio for O&G concepts:

- **Steep-wave configuration** with a flexible riser allows decoupling of the motions of the surface vessel and the riser anchor. This configuration, as well as others used for oil and gas applications, are shown in Figure 3-19. An ideal flexible riser for deep-sea mining applications will allow operations in H_S of 10-12 m and have a lifetime of two years with respect to erosion rates. Thus, one flexible riser would last throughout the entire mining operation at a typical SMS deposit.
- **Free-Standing Hybrid Riser (FSHR)**, as shown in Figure 3-20 (a), maximizes the vertical component of the riser by combining a rigid riser pipe with a flexible jumper. Experiments shows a significantly lower wear-rate in vertical sections, see "**Error! Reference source not found.**" below. However, the FSHR configuration is more complex and less cost efficient than more traditional free hanging flexible risers and steel catenary risers, and allows disconnection of the risers in case of hurricanes (Remery, et al., 2008). A modified version of the FSHR is the Free Standing Flexible Riser (FSFR), see Figure 3-20 (b), which reduces the requirement for large offshore equipment (high lifting and top tension capabilities) during installation.
- **Rigid riser** is simple and cheap. When applied at locations characterized with harsh environment, the heave compensation of the suspended riser string becomes very expensive – in terms of development costs, as it will require a derrick similar to of a drillship, as well as operating costs due to the large pumping volumes of the heave compensation system.

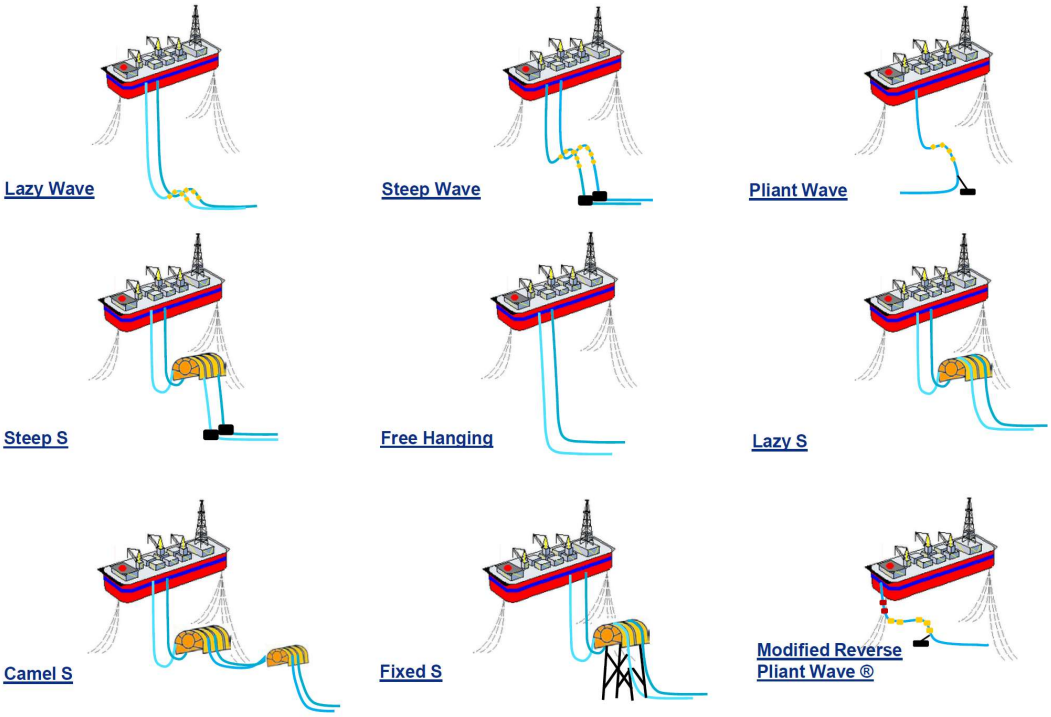

Figure 3-19 – Riser configurations for offshore O&G applications. Modified from Technip (2011).

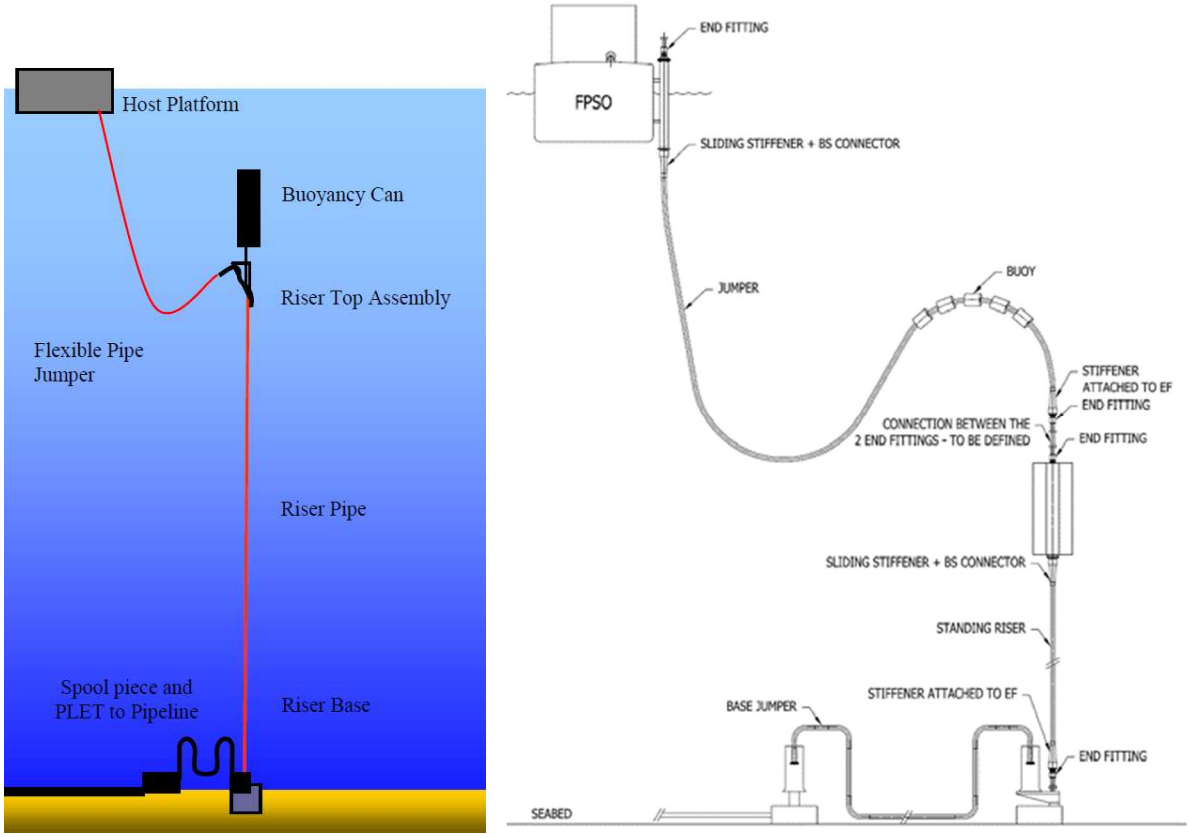

(a) Free-Standing Hybrid Riser (FSHR) (b) Technip's Free Standing Flexible Riser (FSFR)

Figure 3-20 – Free-standing risers (Remery, et al., 2008)

3.5.3 Concepts for System Architecture

Generally, and Technip has incorporated their current product portfolio from offshore O&G. All the process flow systems proposed by Technip are based on the sequence in Figure 3-21. Technip suggests three different lifting solutions for their process flow systems, all based on hydraulic lifting, which are seen in Figure 3-22 (a)-(c) and described by Parenteau, et al. (2013):

- Closed-loop system (using either water or mud as transportation fluid)
- Positive displacement (PD) pump system
- Air-lift system

Figure 3-21 – Process flow system for deep-sea mining by Technip.

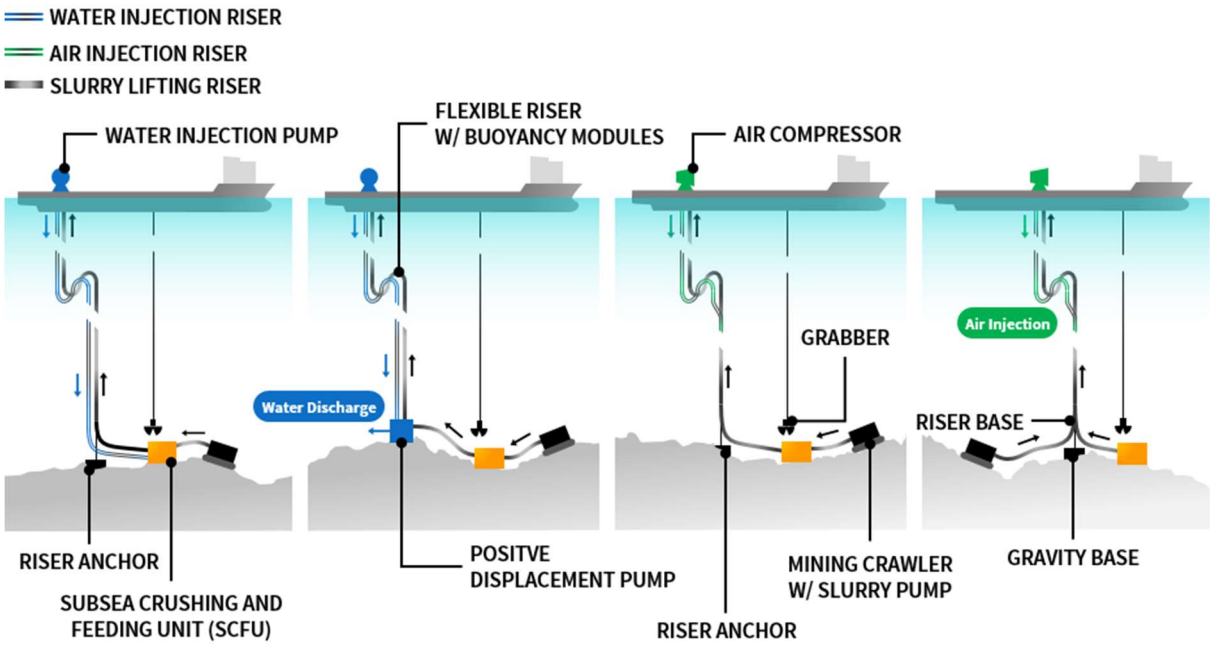

(a) Closed-loop (b) PD pump (c) Air lift (d) Neptune Minerals

Figure 3-22 – Technip's system concepts with flexible flowlines.
Based on Parenteau, et al. (2013) and Yu & Espinasse (2009).

Separate flexible risers are used for slurry and return (lifting medium) flow. The risers are anchored to the seabed in a "steep wave" configuration to decouple the forces and movements of the surface vessel from the seafloor equipment. In addition, it allows relocation of the surface vessel, or disconnection and temporarily abandonment due to extreme weather. Buoyancy modules of syntactic foam mounted to parts of the flexible risers provide the shape configuration (Espinasse, 2010).

The closed-loop and PD pump systems use a topside-mounted water injection pump, while the air lift system has a standard air compressor topside. In the closed-loop configuration, the slurry never passes through the pump, enabling the use a standard pump tolerable to small particle fines (Parenteau, et al., 2013). This high-pressure water flow passes through the Seafloor Crushing and Feeding Unit (SCFU), which is described in detail below. In the two other system configurations, a suction hose takes the

crushed material from the SCFU to the riser base (Espinasse, 2010). The PD pump system is based on the rigid riser system developed for Nautilus Minerals, and the weight of a pump module as an anchor for the flexible risers. Within the pump module, the slurry passes through a series of chambers divided by elastomer membranes that raises the pressure above the hydrostatic head required to reach surface (Leach, et al., 2012). The close-loop and air lift systems are advantageous with respect to maintenance, having the pump located topside.

All three concepts for system architecture proposed in Parenteau, et al. (2013) combine vertical and horizontal exploitation systems. The vertical system consists of a remotely operated grabber capable of collecting both chimneys and surrounding top layers, while the horizontal system comprises a mining crawler. The grabber is proven technology in the field, and current designs are capable of moving 100 m in lateral direction (Espinasse, 2010). The mining crawler has an integrated dredge pump that pumps the cuttings to the riser base. The two systems produce to common unit on the seafloor, the SCFU, which gathers and breaks the rocks down to a certain particle size for easier transportation to surface. The crushing takes place through a three-stage braking process, similar to that of a terrestrial mining sizer, that induces stresses to take advantage of natural weaknesses of the rock. A direct high-torque drive system exposes the rock to tension and shear by driving two rotors with large teeth at low speed in opposite directions (Parenteau, et al., 2013). A rock sizer *"breaks the rock in tension and shear exploiting the weakness of rock material in tension and shear"*, as stated by Waquet, et al. (2011). The center distance of the small-diameter shafts onto which the teeth are mounted determines the maximum size of the processed material, and the length of the inlet affects the volume of material that can be processed in a given time (MDM Group, 2011). The unit temporarily stores the crushed material in storage tanks, thus ensures a continuous feed of slurry into the flexible riser. The injection of solids into the high-pressure water flow in the flexible riser needs to be controlled to avoid clogging and abrasion damage. This is done by a plane with adjustable inclination at which the particles slide down, or by using a slurry gate valve with variable opening. The overall functionality of the SCFU is summarized in Figure 3-23.

Figure 3-23 – Functionalities of Technip's Subsea Crushing and Feeding Unit (SCFU).

An alternate version of the air lift system, described in Espinasse (2010) and seen in Figure 3-22 (d), was developed for Neptune Minerals for a deep-sea mining prospect north of New Zealand. The environmental conditions at the site are similar to the North Sea, with a significant wave height H_s of 8 m for a 10-year return period (Yu & Espinasse, 2009). The sea state for a 100-year return period is characterized by an $H_{s,100}$ of 9.5 m and a peak period $T_{p,100}$ of 12.4 s. Espinasse (2010) states that *"the most frequent environment is a moderate wind sea of short period with an* H_s *of 2 m"* and that *"cumulative sea states of* H_s *larger than 3 m account for an average of 56 days per year"*. The initial concept does not use a grabber. The mining crawler produces directly into the production riser. In case of an unplanned shutdown of the riser system, a dump valve is located at the riser base. An ROV equipped with jet suction and connected to the riser base by a jumper was intended to perform a clean-up run and recover sediments and loose rocks prior to commencing the mining operation.

3.5.4 Wear Rates and Riser Durability

Deep-sea mining of SMS deposits is characterized by transportation of large and dense solid particles in pipes with relatively small diameters (8-10 in). Existing theory from offshore O&G, dredging, hydraulic coal transportation, and oil sand is not directly applicable, as these involve small particles in large-diameter pipes. For SMS mining, 50 % of the particles are assumed to exceed 25 mm, while 25 % exceed 50 mm, and the particle density ranges 2.5-4.0 SG. For flexible risers in a steep-wave configuration, the majority of the pipe segments are vertical. As discussed by Parenteau (2012) and Beauchesne, et al. (2015), large-scale onshore experiments of such flowlines have been performed to study inner pipe wear mechanisms for different system architectures and flow conditions. The aim has been to establish an inner pipe material that provides the highest wear resistance per unit cost, in addition determining the durability of flowlines under near-operational conditions. Parenteau (2012) describes two relevant wear mechanisms, which are illustrated in Figure 3-24:

- **Cutting wear** (or impact erosion) is removal of the inner pipe material due to sharp points on the abrasive particles in the flow. It is the surface roughening seen in straight vertical flow, characterized by a low wear rate.
- **Deformation wear** (or abrasive erosion) results from fatigue of the inner pipe material due to repeated impact of solid particles. It is the gouging wear corresponding to large/intense removal of material at inclined and horizontal segments due to high stress deformation induced by a solid bed at the pipe bottom, and is characterized by a high wear rate.

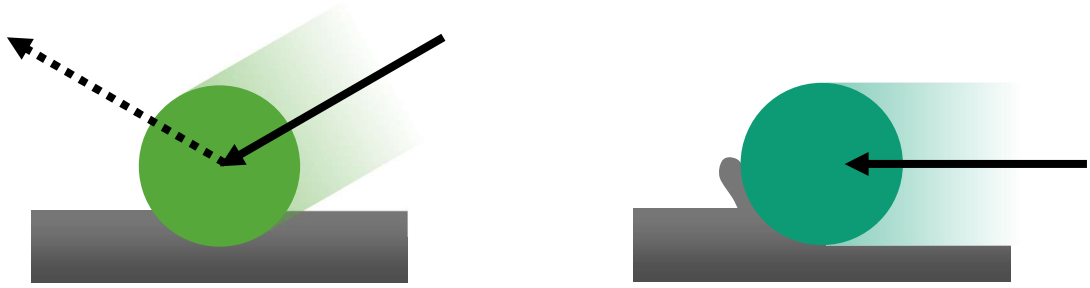

(a) Deformation wear (b) Cutting wear

Figure 3-24 – Wear mechanisms. Modified from Parenteau (2012).

Parenteau (2012) concludes that particle size and concentration increases the wear rate the fastest, while slurry flow velocity has little impact on the wear rate. Straight vertical spools had lower wear than inclined and horizontal spools, and the centrifugal effects in sag bends increase the observed wear rate.

3.6 Nautilus Minerals: First Commercial Subsea Mining Operation

3.6.1 Company Overview

As presented in Nautilus Minerals (2015, pp. 30, 48), the Australia-based Nautilus Minerals is a seafloor resource exploration company listed on the Toronto Stock Exchange (TSX: NUS) and quoted on OTCQX International (OTCQX: NUSMF) and Nasdaq International Designation program. It is the first publicly listed company to commercially explore and develop the ocean floor for SMS deposits and nodule deposits. Their main focus is to demonstrate the seafloor production system and establishing a pipeline of development projects to maximize the value of mineral licenses and exploration applications held in various locations in the Pacific Ocean. The company's proposed core operation is extraction of economically viable discoveries of copper, zinc, gold and silver.

3.6.2 Solwara 1 Project

General

Solwara 1 is the principal project of Nautilus Minerals, planning to commence exploitation of SMS deposits in the first quarter of 2018, as described in Nautilus Minerals (2015, pp. 9, 30, 48), using the production system in Chapter 3.6.3. Solwara 1 is a joint venture comprising Nautilus Minerals (85 %) and the Independent State of Papua New Guinea's nominee, Eda Kopa (Solwara) Limited (15 %). The Solwara 1 field (3.789° S, 152.094° E) is located approximately 50 km north of Rabaul, which lies on the north-east coast of the island of New Britian, as seen in Figure 3-25. The field lies within the territorial waters of Papua New Guinea (PNG) in the Bismarck Sea, and is part of mining lease ML154 granted by the government of PNG in January 2011 (Golder Associates, 2012, p. 2). The deposit occurs on a small ridge on the north-western flank of the North Su volcanic center at water depths ranging 1,500-1,660 m, see Figure 3-26. The flank and crest of the volcanic mound extends 150-200 m above the surrounding seafloor, with relatively steep slopes generally ranging 15-30° (Golder Associates, 2012, p. 2). The total extraction area is small, and covers about 1200 m × 600 m or 0.1 km² (Nautilus Minerals, 2014). The deposit's sulfide-rich chimneys have a height of up to 10-15 m, and occur in discrete fields separated by unconsolidated sediments and local volcanic flows. Locally, there is hydrothermal activity. Figure 3-27 provides a more detailed view of the geology at Solwara 1. Bathymetric maps are found in Appendix A and an early-phase project flow chart is found in Appendix B.

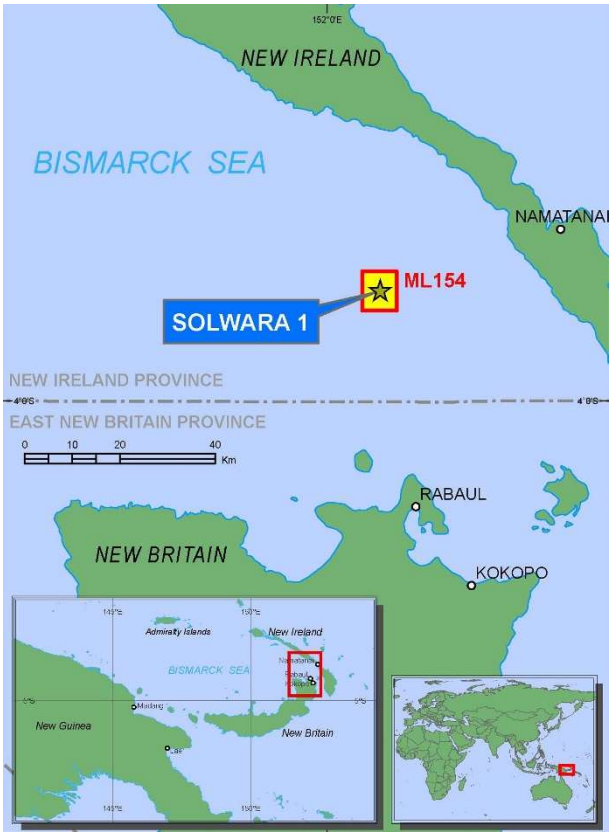

Figure 3-25 – Location of Solwara 1 field in the Bismarck Sea (Nautilus Minerals).

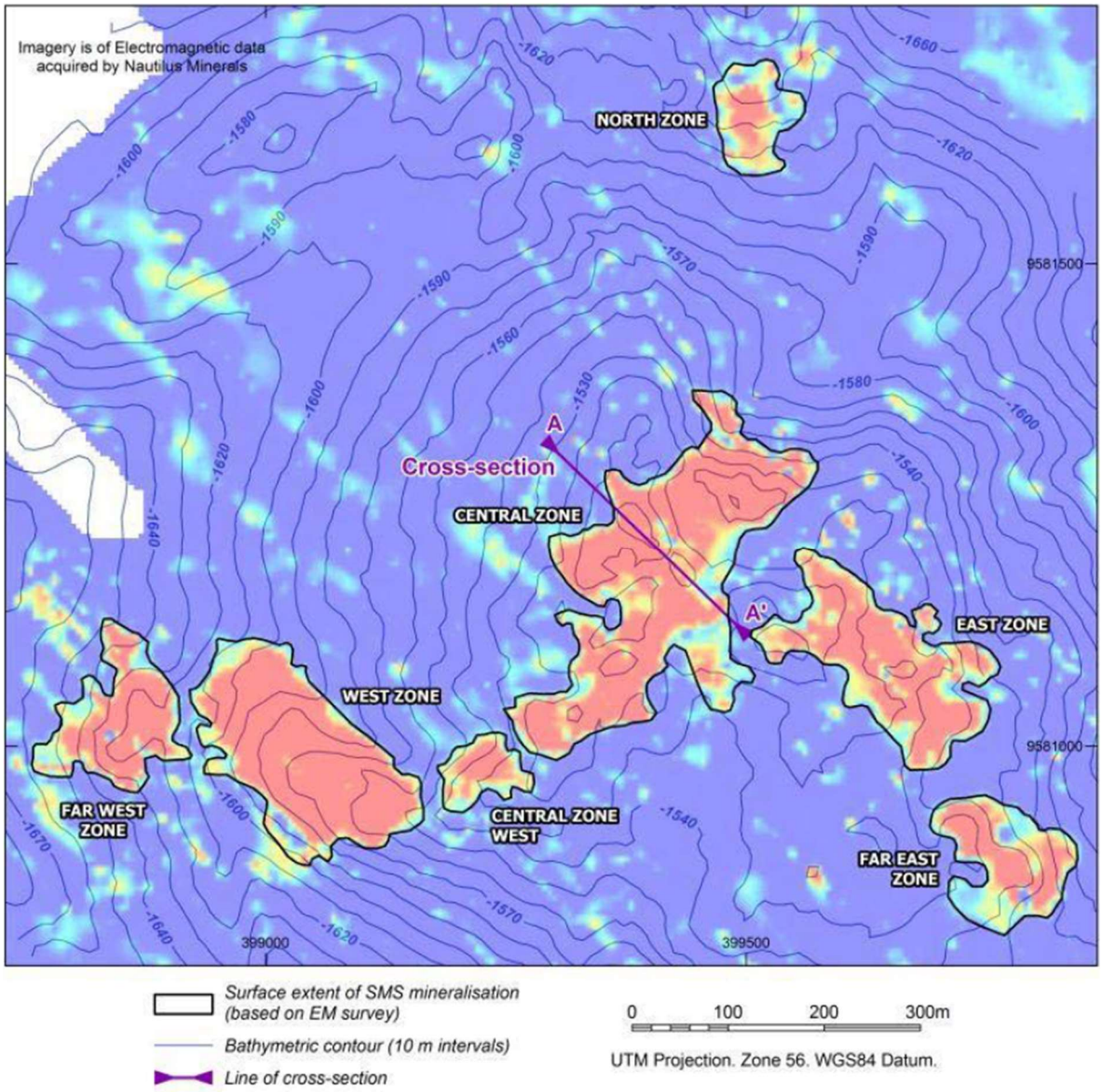

Figure 3-26 – Bathymetric map of Solwara 1 outlining mineralized areas (Golder Associates, 2012, p. 33).

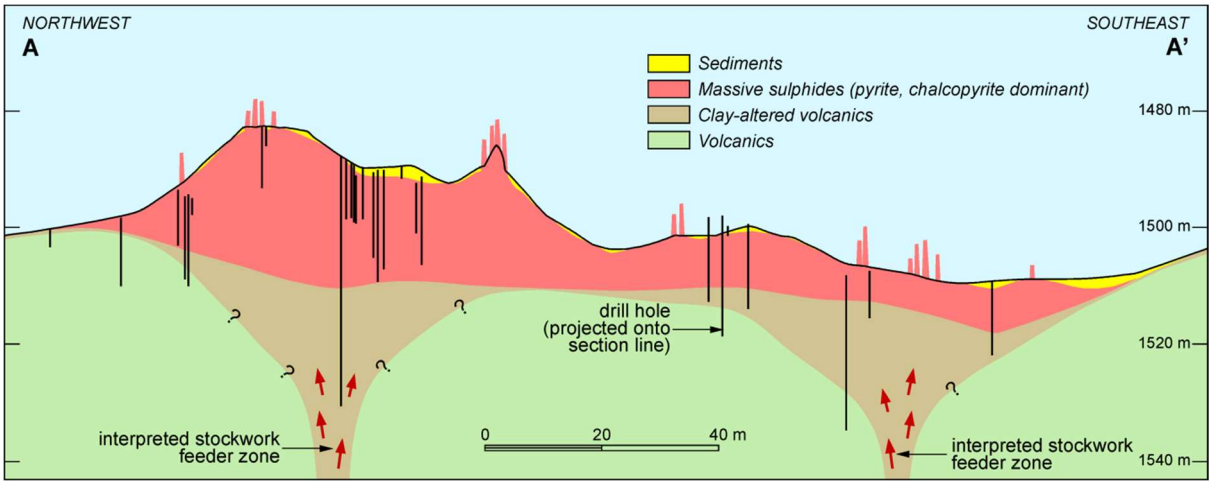

Figure 3-27 – Cross-section A-A' through Central Zone, looking northeast (Golder Associates, 2012, p. 10).

Resource Estimates

Nautilus Minerals has mapped Solwara 1 through four drilling campaigns between 2006 and 2011 (Golder Associates, 2012, p. 3), resulting in the resource estimates presented in Table 3-4 and Table 3-5. The indicated resource estimate corresponds to contained Cu and Au of 74,160 t and 4,695 t, respectively (Nautilus Minerals, 2014, p. 17).

Table 3-4 – Indicated resource estimate for Solwara 1 (Golder Associates, 2012, p. 6).

Domain	Tonnage [10^3 t]	Cu [%]	Au [g/t]	Ag [g/t]	Zn [%]
Sulfide Dominant	1,030	7.2	5.0	23.0	0.4

Table 3-5 – Inferred resource estimate for Solwara 1 (Golder Associates, 2012, p. 6).

Domain	Tonnage [10^3 t]	Cu [%]	Au [g/t]	Ag [g/t]	Zn [%]
Chimney	80	11.0	17.0	170.0	6.0
Consolidated Sediment	27	4.1	4.5	49.0	1.4
Sulfide Dominant	1,330	8.1	5.8	25.0	0.6
Inferred Total	**1,440**	**8.2**	**6.4**	**34.0**	**0.9**

Environmental Conditions

As described by Golder Associates (2012), Solwara 1 is mostly protected against significant sea states from most directions due to its surrounding islands. Thus, the total wave action is caused mostly by locally generated wind waves ($T_p > 7$ [s]) in the same direction as the seasonal monsoons, with minor contributions from swell waves ($7 < T_p \leq 19.5$ [s]) generated in distant regions of the Pacific Ocean. Seasonal monsoons are towards the northwest in summer (February to April), and southeast in winter (June to September). Figure 3-28 shows the annual exceedance probability for significant wave heights, and Table 3-6. the significant wave heights H_s and spectral peak periods T_p for various return periods yielding minimal downtime due to weather.

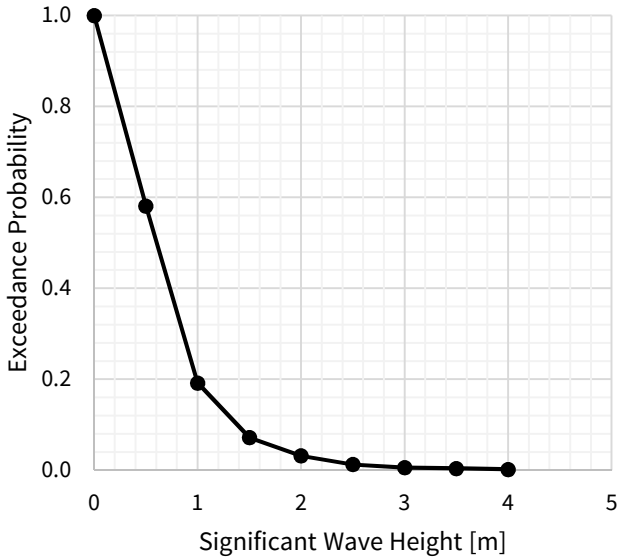

Figure 3-28 – Annual exceedance probability for Solwara 1. Based on data from Golder Associates (2012, p. 22).

Table 3-6 – Extreme design conditions for Solwara 1 (Golder Associates, 2012, p. 24).

Return Period [year]	H_s [m]	T_p [s]
1	3.08	8.90
10	4.40	9.37
100	5.61	10.50

3.6.3 Seafloor Production System

System Outline

As described by Nautilus Minerals (2016, pp. 27-31), Nautilus Mineral's concept for mineral extraction, the so-called Seafloor Production System, comprise the following elements:

- Seafloor Production Tools (SPTs)
- Riser and Lifting System (RALS), including the Subsea Slurry Lift Pump (SSLP)
- Production Support Vessel (PSV) with Dewatering Plant (DWP)
- Load-out and transportation to a third party processing facility for toll treatment or direct sales

SPTs will be used to excavate the SMS material from the seafloor, which will be pumped as slurry to the PSV via the RALS. The pumped slurry will be dewatered at surface and the solid material eventually offloaded into bulk carriers for transportation to a concentrator treatment plant for subsequent processing and/or direct sales. Figure 3-29 illustrates the main components in the system. Annual production target is $1.3 \cdot 10^6$ t. When moving to a new site, installation of the production system is expected to take about three days[7] through several steps.

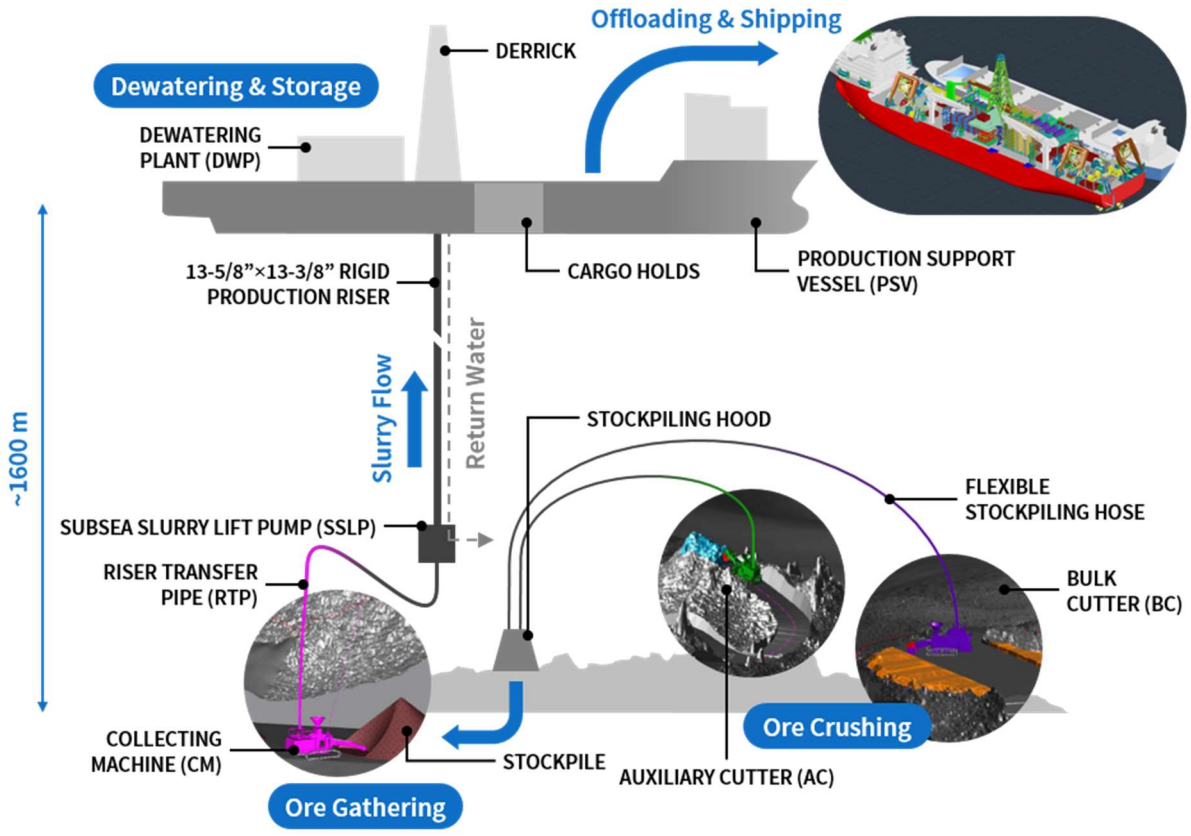

Figure 3-29 – Overview of Nautilus Minerals' seafloor production system.
Modified from Nautilus Minerals (2015).

[7] E-mail from Johann Rongau, Study manager, Technip Innovation and Technology Centre, May 5, 2016.

Seafloor Production Tools

On the seafloor, the excavation of the SMS deposits are performed by Seafloor Production Tools (SPTs), remotely operated robots with track shoes, as described by Nautilus Minerals (2016, pp. 29-30), SRK Consulting (2010, pp. 145-146), Smith (2011) and Ridley, et al. (2011). The vehicles are designed and built by the British company Soil Machine Dynamics (SMD), which is a market leader in offshore and subsea trenching and remotely operated vehicles. The design of the SPTs are based on consolidation of technologies from the offshore O&G, telecommunications, trenching, marine dredging and mining industries. The operational approach for the SPTs is analogous to surface mining systems, where a flexible and mobile machine prepares the site followed by a dedicated bulk production system. The typography (up to 20° slopes) of the Solwara 1 site requires the seafloor operation to be divided in three subsequent tasks, each carried out by a separate vehicle, see Figure 3-30 and Table 3-7:

- **Auxiliary Cutter** (AC) is primarily designed to access and prepare level landing and work areas (benches), being capable of working in rough terrain and equipped with boom-mounted, counter-rotating cutter heads. It is designed to pump overburden away from the mine site and to pump cut materials to a central seabed location as required.
- **Bulk Cutter** (BC) cuts at higher productivities in the prepared areas, to which it is limited, and to pump cut materials to a central seabed location as required. It crushes and sizes the material using a drum cutter with picks.
- **Collection Machine** (CM) gathers the cut material from the seafloor and pump it to the RALS. It sucks the ore-seawater slurry in through a crown cutter using internal dredge pumps.

Figure 3-30 – From left: Collecting machine; bulk cutter; and auxiliary cutter (Nautilus Minerals)[8].

Table 3-7 – Design parameters for seafloor production tools (SPTs) (Nautilus Minerals, 2016, pp. 14-16).

	Length [m]	Width [m]	Height [m]	Weight [t]	Power [MW]
Auxiliary Cutter (AC)	15.8	6.0	7.6	240	2.0
Bulk Cutter (BC)	14.2	4.2	6.8	280	2.5
Collecting Machine (CM)	16.5	6.0	7.6	180	1.8

[8] http://www.rovplanet.com/news/news?id=367, accessed Mars 25, 2016.

According to Ridley, et al. (2011), a high level of wear is expected to the cutting drum pics, crown cutter, and slurry circuits. SMD has applied the rules and regulations of DNV in the design with respect to vibration and fatigue issues, and finite element analyses have been performed to ensure structural integrity and optimize fatigue lifetime. Due to the high-vibration operational conditions of the equipment, larger bearings are used and sensors for vibration monitoring and dual-redundant rotational speeds are mounted the vehicles. Furthermore, the high hydrostatic pressure requires adaptation and altered assembling comparted to terrestrial mining equipment. The material strength of the ore, accounting for hyperbaric effects, are within the strength of materials currently being exploited (Ridley, et al., 2011). The risk of SPTs tipping in highly sloping terrain due to reduced visibility or drift-off is reduced by having reliable control and monitoring systems that make the operator aware of the position and status of the vehicle. The vehicles are controlled from a control room, similar to those used for ROV operations, with 15 monitors per vehicle providing visuals, operational status and logging. In addition, there will be a 3-D sonar system and a real-time virtual seascape (of the seabed and the vehicle's actions) for each vehicle, updated in real time (Ridley, et al., 2011).

Launch and Recovery System

The SPTs are deployed and retrieved from the surface vessel, dynamically positioned above the mining site, by the Launch and Recovery System (LARS). It comprises A-frames, winches, spooling device, active heave compensation device, sheave units, hydraulic power units (HPUs), electric power units, and deck control cabins. The breaking strength of the lifting wires start at above 1,000 t (Chopra, 2016), and the A frame is seen in Figure 3-31 (a). Individual umbilicals run to each SPT, providing power, communication and control. They are reeled onto three separate umbilical winches, see Figure 3-31 (b), which are designed, procured and assembled at SMD (Nautilus Minerals, 2015, p. 9). Norwegian AxTech has delivered the three LARS packages to SMD, which handle loads of 250 t plus wire weight for a maximum operating depth of 2,500 m. Each of the HPUs for operation of the winches and A-frames has a total installed power of approximately 2.2-2.4 MW.

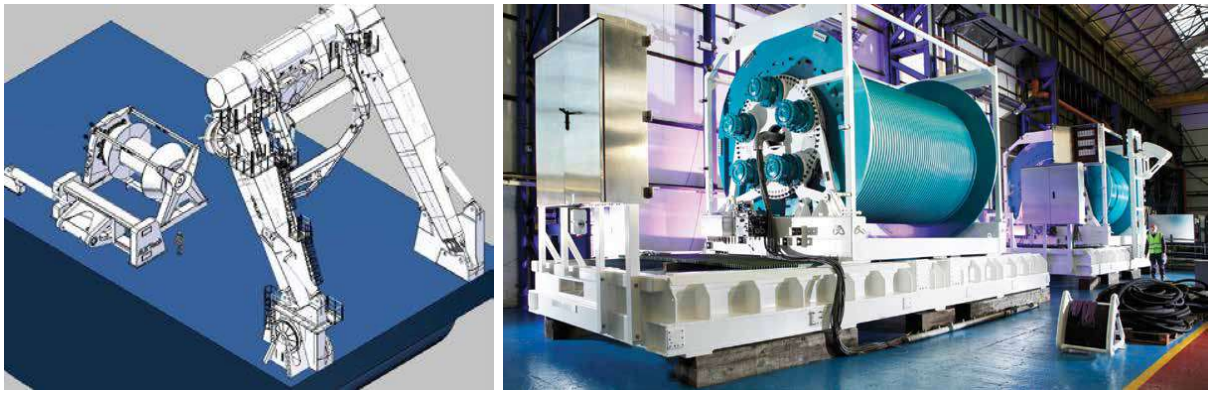

(a) A-frame and lift winch drum (b) Umbilical winch

Figure 3-31 – Launch and Recovery System (LARS) (Nautilus Minerals, 2015).

Stockpiling Hood

To maximize the gathering efficiency of the CM by keeping it stationary, as well as avoiding plume dispersion, the crushed ore is concentrated in stockpiles built up using a moveable stockpiling hood. Jones, et al. (2014) describe the general features of the stockpiling hood, which receives slurry from both the AC and BC through flexible stockpiling hoses, see Figure 3-32. The slurry inlet (i.e., hood roof), hood walls, and seafloor define a cavity where a stockpile can be built up. The frame of the stockpiling hood is covered with a water permeable material, such as a filter fabric or geotextile, making up the walls of the hood, as well as capturing and containing seafloor material present in the slurry, while simultaneously

permitting egress of water from the slurry. The conically shaped stockpiling hood has an open bottom and consists of two modules, as seen in Figure 3-33 (b), which are brought together down on the seafloor. This feature enables separate deployment from the surface vessel without exceeding the weight limits of a surface vessel's cranes.

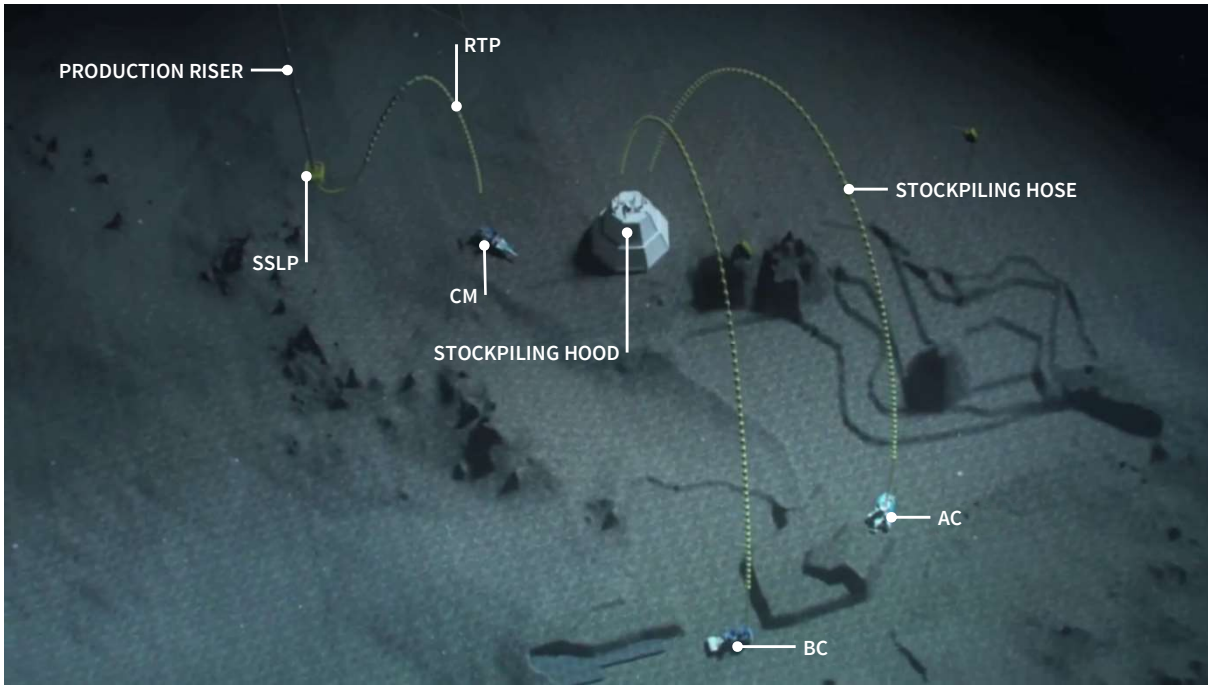

Figure 3-32 - Elements featuring the subsea operation (Nautilus Minerals).

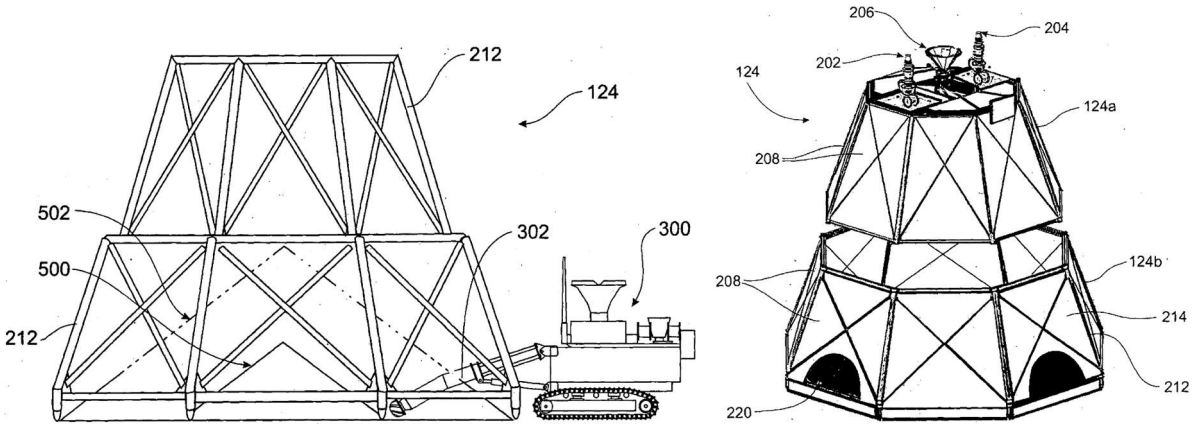

(a) Bare frame in scale with Collecting Machine (CM) (b) Separated frame with geotextile cover

Figure 3-33 – Stockpiling hood (Jones, et al., 2014).

Riser and Lifting System

Components and technology of the Riser and Lifting System (RALS) are adapted from offshore O&G industry. As described by Nautilus Minerals (2016, p. 31), Technip USA was awarded an EPCM contract for the over-all system design, and GE Hydril a supply contract for the design and build of an Subsea Slurry Lift Pump (SSLP). Technip's EPCM contract includes the subsea pump, riser, surface handling system, and ancillary equipment. According to Nautilus Minerals (2015, pp. 9, 30), General Marine Contractors does the fabrication of the riser system, using various other contractors to provide required items of equipment. Sichuan Hong Hua Petroleum manufactures the riser handling equipment, and the seawater pumping systems are delivered by SPX Clyde Union (Nautilus Minerals, 2015, p. 30).

The RALS consists of the following components (SRK Consulting, 2010, pp. 146-147):

- Riser – a rigid riser bundle with a main bore for slurry/production flow and two water injection lines for return water (with connectors, flex joints, and accessories)
- Riser Transfer Pipe (RTP) – a flexible jumper consisting of several hoses bolted together
- Subsea Slurry Lift Pump (SSLP)
- Surface seawater pumps (pressure supply system)
- Pull-in skid
- Derrick
- Riser handling systems

With reference to Figure 3-34, the general outline of the RALS is as follows: The slurry is pumped from the CM via the RTP to the SSLP, which is located at the lower end of the gravity-tensioned, rigid riser, suspended below the PSV. The SSLP overcomes the required pressure heat the to life the slurry to surface. The riser itself is similar to a traditional marine drilling riser, and is run using derrick and draw works systems. The properties of the RALS are found in Table 3-8, and the weights of the combined riser string and SSLP in Table 3-9. A detailed drawing on the RALS is enclosed in Appendix C. The production riser is designed for 2,500 m, and Nautilus Minerals has ordered 1,700 m with an 800 m option (Technip, 2008). Figure 3-35 (a) and (b) show the riser hang-off structure with spider at the top-end termination, as well as the difference between standard and striked joints of riser bundle. The pull-in skid for the SSLP, situated on the port side at the base of the derrick, is shown in Figure 3-36. Figure 3-37 show the riser joints with and without buoyancy modules, as well as GMC's rapid riser connection that can be made without top drive equipment, using a vessel crane and installation tooling (GMC, 2016).

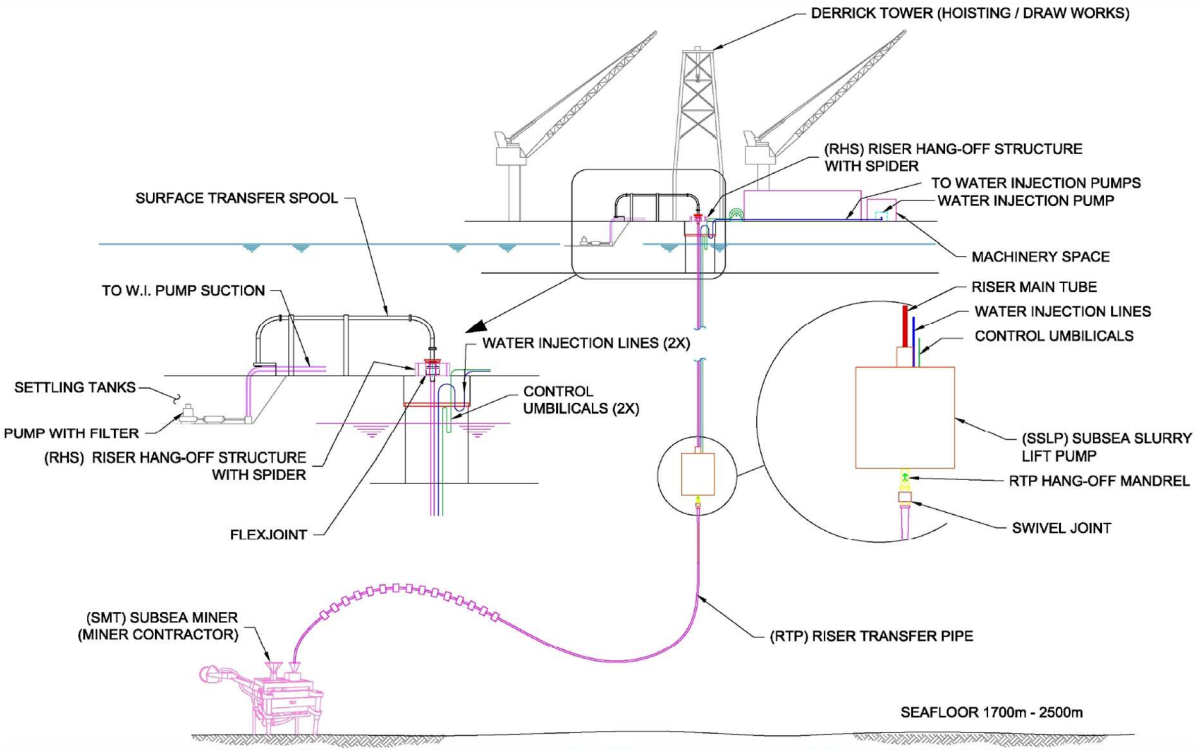

Figure 3-34 – Riser and Lifting System (RALS) for Solwara 1 (Yu & Espinasse, 2009).

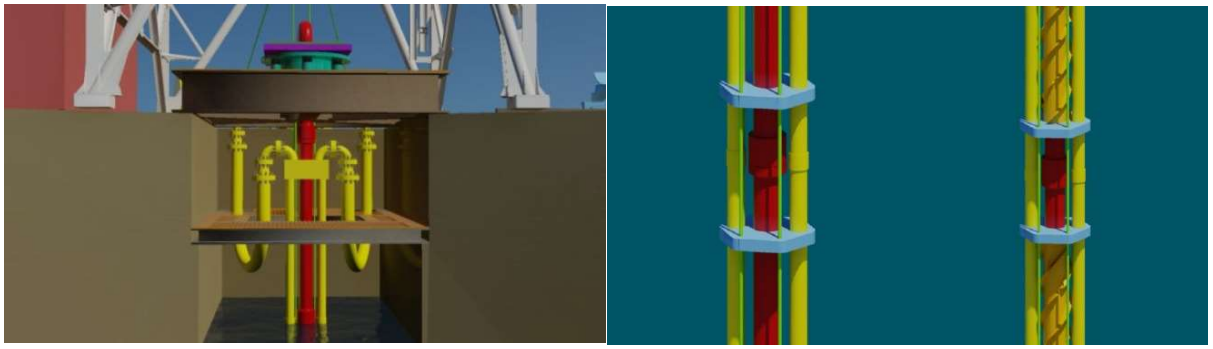

(a) Top-end riser termination (b) Standard (left) and striked (right) riser joint

Figure 3-35 – RALS components (Yu & Espinasse, 2009).

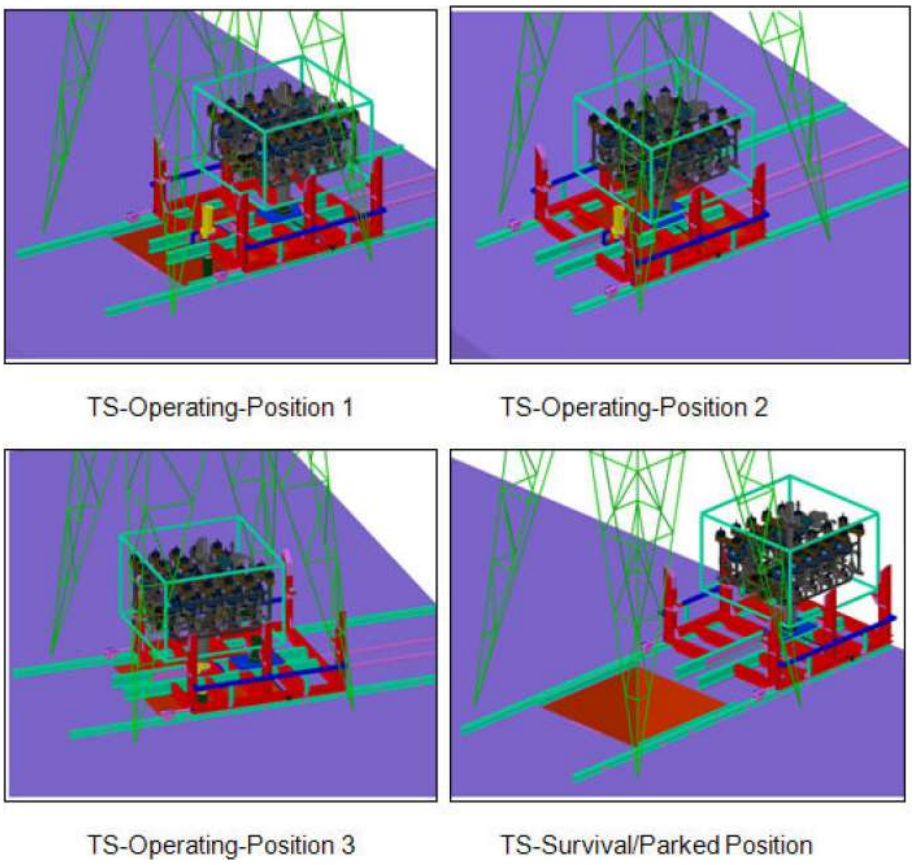

Figure 3-36 – Pull-in skid (Yu & Espinasse, 2009).

Considering internal wear of the various riser system components, the steel production riser is not fitted with internal sleeves, and the jumper is in rubber. To avoid dragging of the flexible RTP along the seafloor, buoyancy modules are mounted from the CM to about ⅔ of length of the RTP, which provide an S-wave configuration. There is a break-away coupling between the SSLP and RTP in case of surface vessel drive-off. The jumper connector part below the pump is not buoyant and will fall, but the rest of the RTP is buoyant. For a re-connect operation, an ROV with proper tooling is used to recover and reconnect the jumper. According to Technip, the heave compensation is rated for a 5 m sea state, and the wave criteria for running/pulling the SSLP through the splash zone is about 1 m (corresponding to a "calm" sea state). The make/break connection time for the riser bundle string is less than 2 min per connection for final make-up (GMC, 2016). the riser's top tension factor $TTF = TT/W_s$ at 1.26 is similar to other top-tensioned risers, and its first natural periods are less than 4 s (Yu & Espinasse, 2009).

Table 3-8 – RALS properties. Based on SRK Consulting (2010, pp. 164-174) and Technip (2008).

	Length [m]	ID [in]	OD [in]	WT [in]	Comment
Main vertical riser, standard	500	12-1/8	13-3/8	5/8	Runs 0-500 m below surface. 62 ft (18.9 m) make-up length.
Main vertical riser, straked	1200	12-1/8	13-5/8	3/4	Runs 500-1700 m below surface. 62 ft make-up length.
Water injection lines	1700	7	8-5/8	4/5	Runs 0-1700 m below surface. 62 ft make-up length.
Riser transfer pipe (RTP)	150-200	10			20 m bolted sections.

Table 3-9 – Weight of riser string and SSLP (SRK Consulting, 2010), (Yu & Espinasse, 2009).

	Condition	Weight [t]
Riser string (excl. SSLP), W_s	Submerged	434
SSLP, W_p	Submerged	112
Riser string (incl. SSLP)	In air	694
Top Tension (Riser string, incl. SSLP), $TT = W_s + W_p$	Submerged, non-operating	546
Top Tension (Riser string, incl. SSLP)	Submerged, operating (12 % slurry)	591

(a) Buoyancy joints (with protectors) (b) Pins of standard joint

Figure 3-37 – Riser joints (GMC, 2016).

Subsea Slurry Lift Pump

The Subsea Slurry Lift Pump (SSLP) is a ten-chamber positive displacement (PD) pump, and was originally developed by GE Hydril to pump drilling fluids and cuttings in dual-gradient drilling (DGD) for water depths up to 2,500 m. In the initial design, electrically driven hydraulic pumps drove the pump chambers. To minimize the pump's complexity and lower the risk associated with high-voltage electrical power, pressurized return water from the DWP on surface provides hydraulic power for the SSLP. In a PD pump, a constant volume is swept with each pump stroke, hence a constant stroking speed gives a constant flowrate. As discharge pressure changes with fluid properties or solids concentrations, the pump's power is adjusted to deliver the required combination of flow and pressure. Hence, it is capable of remaining within its operational window for varying flow conditions. By having power generating pumps and motors on the surface, components are easily accessible and can be replaced or repaired without pulling the riser. In addition, a parallel surface system can be installed for redundancy. The return fluid in drilling has a lower specific gravity (SG) than the slurry for SMS mining. Compared to mining slurry, the highly non-Newtonian drilling fluid has a high viscosity and low mixture flow velocity,

allowing lower fluid velocities without experiencing fallout. However, these characteristics yield a larger pressure head to overcome. The differences in flow parameters for the two applications are seen in Table 3-10. In typical mining conditions, the volumetric concentration of solids is 12 %, and 80 % and 100 % of the passing material is smaller than 25 mm and 50 mm, respectively.

Table 3-10 – DGD pump versus SSLP. Based on Judge & Yu (2010) and Leach, et al. (2012).

Design Parameter	Unit	DGD Pump	SSLP
Cutting material		Clay, rock and gumbo	SMS ore
Cutting material size	[mm]	25-50	D_{80}=25, D_{100}=50
Cutting material density, SG	[-]	< 2.6	2.5-3.8 (3.3 avg.)
Transport fluid viscosity	[Pa · s]	>> $1.78 \cdot 10^{-3}$	< $1.78 \cdot 10^{-3}$
Fluid mixture density, SG	[-] / [ppg]	1.08-1.67 / 9-14	1.08-1.56
Lift pressure	[MPa] / [psi]	45 / 6,600	21 / 3,000
Nominal mixture flow rate	[m^3/h] / [gpm]	275 / 1,200	818-863 / 3,600
Max. particle slip speed, V_s	[m/s]	<< 0.8 (SG = 2.6, D = 50 mm)	0.91 (SG = 3.3, D = 50 mm)
Riser ID	[m] / [in]	0.48 / 18.75	0.308 / 12.125
Nominal mixture velocity, V_m	[m/s]	1.4	3.0
V_m/V_s ratio (for max. particle)	[-]	< 1.75	> 3.2
Particle UCS	[MPa]	Mostly lower than SMS	0-65 (18 avg.)

The SSLP assembly consists of two modules, each containing five PD pumps chambers (Leach, et al., 2012). The chambers are filled with slurry by pressure from the centrifugal pumps of the CM, fed through the RTP. By having multiple pump chambers, a consistent pressure and flow regime is maintained while providing redundancy. The pump module has an in-air weight of about 150 t, and dimensions of 6.5 m × 6.5 m × 6 m, see Figure 3-38. The pump has hydraulically actuated valves with clear flow paths, allowing large solids to pass through (Leach, et al., 2012). The actuated valves, isolating the chambers, are selected to ensure having sufficient force to shear any solids blocking its path and obstructing valve closure (Judge & Yu, 2010). Two small umbilical cables provide electrical power to two hydraulic power units (HPUs) that control the opening and closing of pump valves. Bundled in these cables are fiber optic lines through which operating data is transmitted, such as pressure, temperature, and valve and pump positioning (Yu & Espinasse, 2009). As described by Judge & Yu (2010), each pump chamber houses an elastomeric diaphragm (i.e., membrane) acting as a barrier element between the slurry (process fluid being pumped) and the seawater. The latter is the power fluid generating the diaphragm movement to push the process fluid without being exposed to differential pressure fluid up the return line. Typically, the SSLP is suspended 150 m above the seafloor.

Every 10^6 cycles, corresponding to six months of continuous operations, the SSLP must be pulled to replace the elastomer (Leach, et al., 2012). The most critical components of the SSPL are those exposed to the rocks; the pump chamber diaphragm, pipework and fittings, and slurry valves (Leach, et al., 2012). Test runs of the pump show minimal erosion rates to valves and piping. The power requirement of the pump unit is about 4 MW and 6 MW for an operational depth of 1,700 m and 2,500 m, respectively (Yu & Espinasse, 2009). Estimated power consumption for various operational scenarios for 6,000 t/day continuous operation at 2,500 m depth are listed in Appendix J.

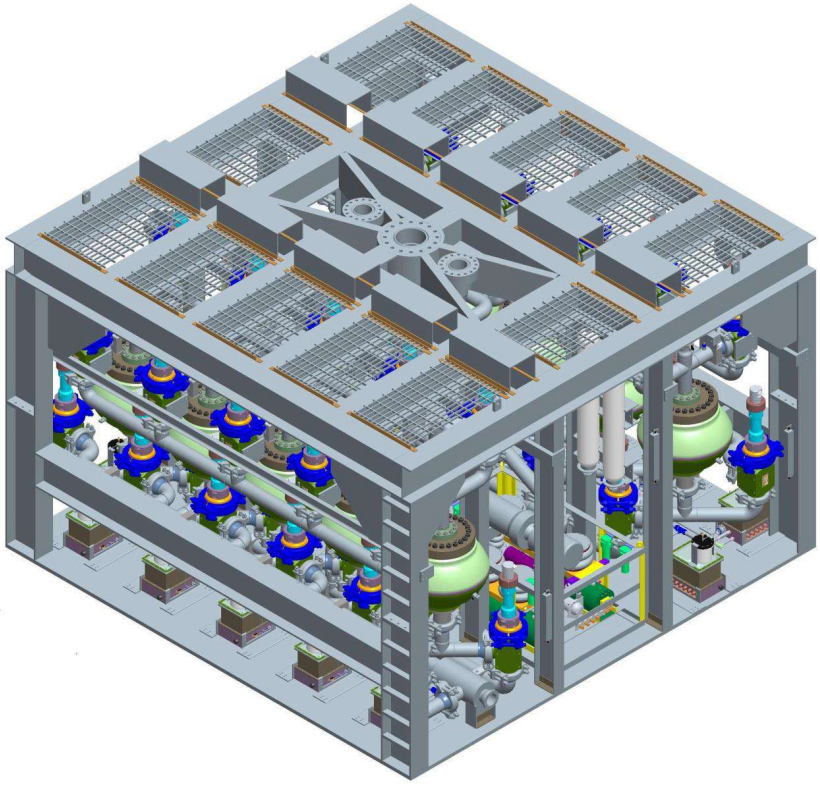

Figure 3-38 – SSLP (Nautilus Minerals, 2016).

(a) Frame

(b) Chamber and valve banks

(c) Umbilical reels

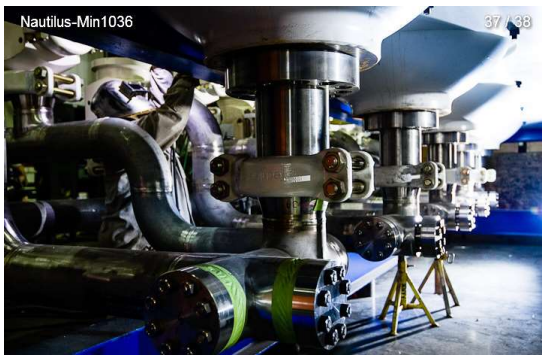

(d) Manifold pipe work

Figure 3-39 – SSLP components (Nautilus Minerals, 2015).

As described by Judge & Yu (2010), additional chambers are added to increase the available flow rate. Each pump chamber is equipped with four actuated valves to control the chamber in- and outflow, and allow the opening and closing of each chamber to precisely overlap to avoid pulsating flow at the inlet and outlet. Smaller (de)compress valves, which are not shown, allow the chamber pressure to be raised to match the discharge pressure (or lowered to match the fill pressure). The total volume of process fluid in all the pump chambers is kept constant. The principle of such a lift pump consists of three cycles, and is shown in Figure 3-40 for a three chamber set-up:

- **Fill cycle** – the left chamber has open process fluid inlet and seawater outlet valves, and closed process outlet and seawater inlet valves. The process fluid is force into the chamber. Meanwhile, the middle chamber is pumping out. Its process fluid outlet and seawater inlet valves are open, and the seawater being pumped into the middle chamber forces the diaphragm downward, expelling the process fluid into the return line. Once the middle chamber's diaphragm reaches the bottom, the process fluid outlet and seawater inlet valves close, trapping the discharge pressure inside the chamber. A decompress valve opens when all the actuated valves on the chamber are closed, lowering the chamber pressure to the inlet pressure.
- **Compression cycle** commences when the left chamber is full, and the process fluid inlet and seawater outlet valves are closed. A compress valve is opened, which allows flow from the seawater supply line coming from the surface vessel (which is maintained at the pump discharge pressure) to compress the chamber up to the discharge pressure. Thus, no sudden pressure drop occurs when the process fluid discharge valve is opened.
- **Flow cycle** enables pulsation-less flow. Before the nearly empty center chamber reaches the end of its stroke, the full and compressed right chamber has its process fluid outlet and seawater inlet valves opened. Hence, flow can be established out of the right chamber prior to closing the center chamber, avoiding a spike in discharge pressure.

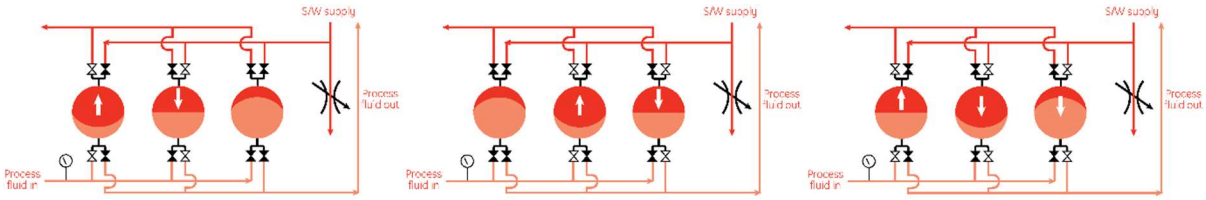

(a) Fill cycle (b) Compression cycle (c) Flow cycle

Figure 3-40 – The working principle of a mud lift pump (GE Oil & Gas, 2011).

Production Support Vessel

The Production Support Vessel (PSV), described by Nautilus Minerals (2016, p. 31) and Chopra (2016), serves as the floating platform for mobilization and remote operation of the SPTs, and will host an on-board refinery and processing unit, in addition to the control center for seabed operation. The design is similar to vessels for subsea construction, drilling and production seen in the offshore O&G industry, and is characterized as a "*combination of a drillship, bulk carrier, tanker, and an offshore construction vessel*" by Chopra (2016). The vessel is currently under construction at the shipyard of Fujian Mawei Shipbuilding in southeastern China, with an expected delivery date in the end of 2017. Nautilus Minerals will charter the PSV from Marine Assets Corporation (MAC) for minimum a five-year period at a daily rate of 199,910 USD, with options to either extend the charter or purchase the vessel (Nautilus Minerals, 2014). MAC, which is based in Dubai, specializes in delivering new-builds for the offshore industry, and provides the marine management of the PSV. Main vessel specifications are listed in Table 3-11. General arrangements are seen in Figure 3-41 and Figure 3-42, as well as in Appendix D.

Table 3-11 – Final vessel specifications (Chopra, 2016).

Length Overall (LOA) [m]	227.0
Width [m]	40.0
Depth [m]	18.2
Draft [m]	13.2
Accommodation [PAX]	199
Power [MW]	31
No. of Diesel Generators	6
Minimum Total Cargo Hold Capacity [t]	45,000
Fresh Water [m^3]	31,500
Fuel Oil [m^3]	10,500
Water Ballast [m^3]	40,000
Propulsion	Diesel-Electric
Classification Society	ABS
Dynamic Positioning Class Notation	DPS-2 EHS-F

As stated by Chopra (2016) and SUT (2015), MacGregor has delivered two knuckle-boom cranes. The main crane is heave compensated, and rated to an operational depth of 2,500 m and a safe working load (SWL) of 200 t. It will provide lifting support to the subsea mining operation. The auxiliary crane is a smaller (SWL of 100 t), supporting aft-deck and ship-to-ship operations. Knuckle-boom cranes are preferred for offshore applications due to compact dimensions and an ability to reduce the effect of ship motions on suspended loads. Deployment and retrieval of SPTs require low freeboard. A freeboard of about 5 m for empty cargo holds is ensured by a 52 ballasting tanks with a total capacity of 40,000 m^3. A total cargo hold capacity of 45,000 t is divided between four cargo measuring 24.8 m × 20.8 m each; two on each side of the 10 m × 10 m moon pool, which is located amidships. The outermost wing tanks are for water ballast, while the inner wing tanks (up to tween deck) are fuel oil tanks. The integrated control systems are delivered by Kongsberg Maritime, comprising dynamic positioning (DP), marine automation, information management, and navigation systems. The vessel is equipped with five azimuth thrusters and two bow thrusters, all of which are listed in Table 3-12 and provided by Rolls-Royce Marine together with the main engines. The design criteria for station-keeping is H_s of 2 m for all directions and a movement radius of approximately 5 m from the RALS. All electrical installations are done by Siemens. Power is supplied by six diesel generators of equal capacity; two in each of the three separate engine rooms that make up watertight compartments, all with separate supporting and auxiliary systems. Thus, each engine room makes up one redundant group. The defined worst-case failure is loss of any two diesel generators within one group, two bow thrusters, or one azimuth thruster.

Table 3-12 – Overview of installed thrusts. Based on Chopra (2016).

Thruster Type	Location	Number	Power [kW]
Azimuth	Aft	3	3,000
Azimuth	Fore	2	3,500
Bow Tunnel	Fore Peak	2	2,000

The diesel-electric vessel is designed according to ABS class notations, including Dynamic Positioning System (DPS) and Enhanced System (EHS) of type DPS-2 EHS-F (Chopra, 2016). The definitions of the various DP notations according to American Bureau of Shipping (ABS) (2013, pp. 2, 8, 42) are as follows:

- **DPS-2** denotes vessels "*[...] fitted with a dynamic positioning system which is capable of automatically maintaining the position and heading of the vessel within a specified operating envelope under specified maximum environmental conditions during and following any single fault, excluding a loss of compartment or compartments*", and requires that "*[...] a loss of position may not occur in the event of a single fault in any active component or system, excluding a loss of compartment or compartments*"
- **EHS-F** is a "*[...] supplement for DPS-2 vessels with fire and flood protection implemented based on the fire risk level*"

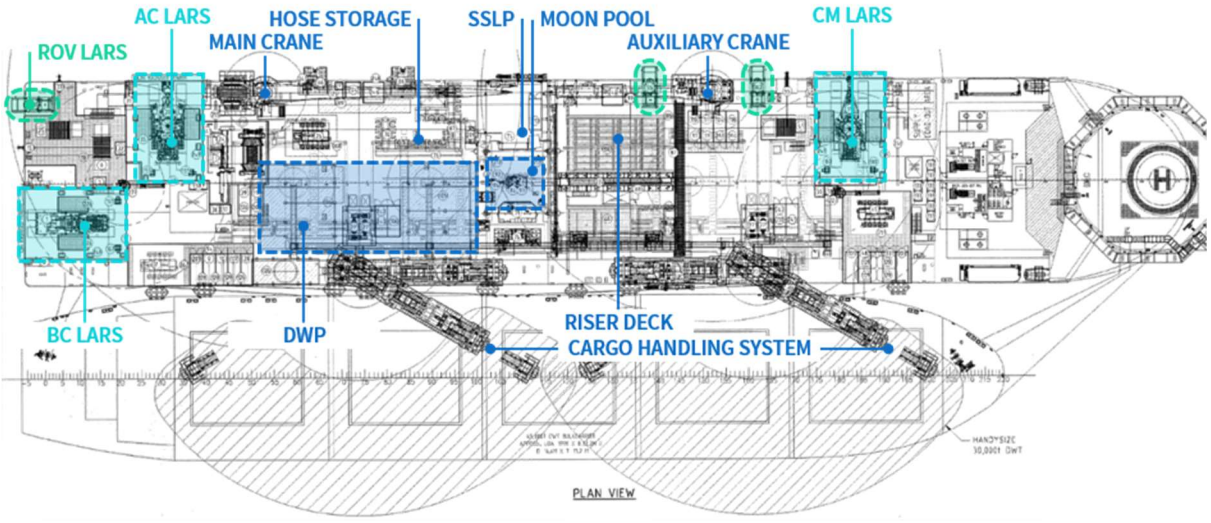

Figure 3-41 – Deck arrangement of PSV. Modified from The Naval Architect (2016).

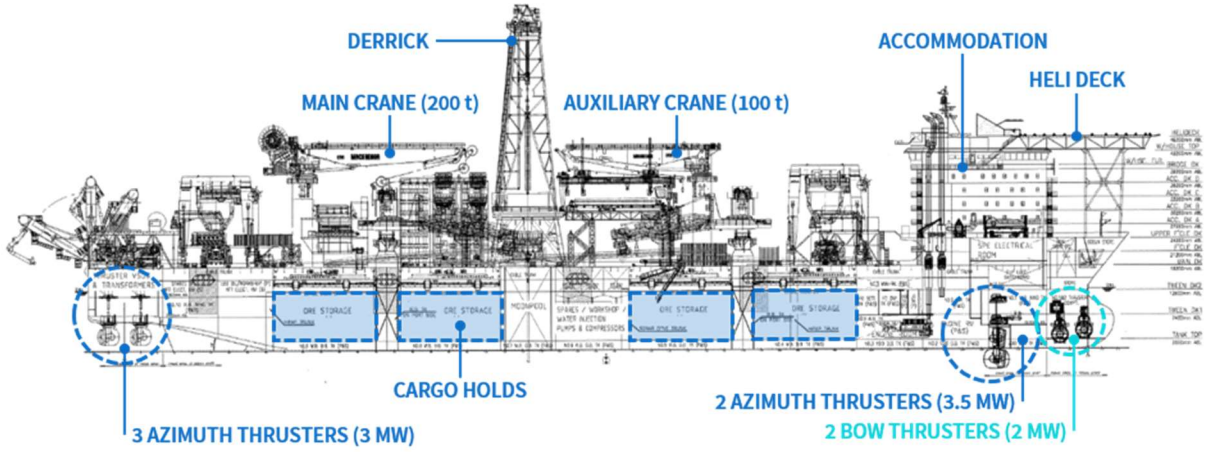

Figure 3-42 – Outboard profile of PSV. Modified from The Naval Architect (2016).

Dewatering Plant

The process design of the Dewatering Plant (DWP) is based on technology from the mineral processing industry (Nautilus Minerals, 2016, p. 31). An initial design study was performed by Parsons Brinkerhoff, and detailed design and construction management are done by DRA Pacific, the Australian subsidiary of a South African materials handling and minerals processing specialist with experience in the offshore diamond mining industry. The Dewatering Plant (DWP) module weighs more than 2,000 t and rises

more than 30 m above deck (Chopra, 2016). The slurry passes through the DWP once it reaches surface, before being loaded and temporarily stored in the cargo holds. The discharged seawater is filtered and pumped back to the seafloor through water return lines in the riser bundle. The process of the DWP consists of the following steps (Smith, 2011):

1. **Screening** by vibrating twin-deck screens
2. **De-sanding** by hydro cyclones and centrifuges
3. **Filtration**, using pressure filters

Cargo Handling System and Side-by-Side Loading Operation

Both the cargo handling system and the loading operation are described by Chopra (2016). The initial vessel design had no internal storage capacity and required at least one barge moored to the PSV at all times. Hence, the production would be shut down in too bad environmental conditions for side-by-side operation. In addition, one side of the vessel would be continuously occupied, limiting possible SPT movements. However, the altered design with internal storage capacity enables continues production. A total of 12 mooring lines, each with a separate winch, will keep the bulk carrier positioned alongside the PSV during the loading operation, see Figure 3-43. The environmental restrictions for the operation is an H_s of 2 m and wind speed of 30 kn. Offloading to the bulk carrier (e.g., handymax, 40,000-50,000 dwt) will be performed once every 8-10 days, and is estimated to take approximately 12 h. The bulk carrier will ship the dewatered ore to an onshore refinery for further processing.

The cargo handling system, which is delivered by Italian Bedeschi SPA, will transport the ore from the cargo holds to the bulk carrier. It is fully enclosed for all-weather operation. The ore density ranges 2.2-3.5 t/m^3. Scrapers and scoopers collect any ore stowed in the holds and feed it into vertical bucket elevators, which transport it to conveyor drop points above deck. The offloading is performed by two conveyor booms, which directly take the ore into the bulk carrier. The booms have sufficient outreach to load all five hulls of the bulk carrier without shifting position laterally, in addition to mechanisms ensuring even distribution. The loading capacity of each boom is 1,600 t/h.

Figure 3-43 – Side-by-side offshore loading of bulk carrier (Nautilus Minerals[9]).

[9] https://vimeo.com/57181759 (screenshots), accessed May 4, 2016.

3.6.4 Mining Operation

Operational Sequence

A proposed mining sequence is shown in Table 3-13, which is optimized by minimizing non-productive time. Nautilus Minerals uses MineSight, a commercial software developed for terrestrial mining, for detailed planning and scheduling of the seafloor mining operation (MineSight, 2014).

Table 3-13 - General mining sequence (SRK Consulting, 2010, pp. 196-197).

Sequence	Task Description	Tool
1	Remove unconsolidated sediment	CM
2	Prepare a level area	AC
3	Gather the ore	CM
4	Fragment the ore to leave a beach of 0.5-1 m height	BC
5	Gather the fragmented ore	CM
6	Repeat steps 4 and 5 until the remnant edges are 4 m high	BC/CM
7	Trim the edges	AC
8	Supplement the mining rate when underutilized	AC
9	Continue the top-down mining sequence to mine subsequent benches according to steps 4-8 to the depth of the commercially viable resource	AC/BC/CM

The AC is the first SPT to be deployed, and will provide access to the mine site (SRK Consulting, 2010). It will clear high points to make landing pads sufficiently large (about 25 m × 35 m) for the BC to commence its work. The AC's boom can swing 11.6 m, and cuts from −1 m to +4 m vertically (Nautilus Minerals, 2014). After clearing the first pad, the AC is lifted (by its main recovery wire) to another high point and repeats its task. Generally, due to the uneven terrain features, the AC will be landed as near to the peaks as possible, and generate an access way by cutting a ramp up to the peak, as seen in Figure 3-44 (a) and (b). It will also even out edges or footwalls that are inaccessible for, or outside the reach of the BC. The BC cuts a 4.2 m wide section, and can operate its drum cutter between −0.5 m to +4 m vertically. It mines parallel strips of ore, as seen in Figure 3-44 (c) and (d), until the site is fully cut to a single pass of cutter depth (0.3-1.0 m). Both the AC and BC are planned to pump ore to a stockpile, which is enclosed by a stockpiling hood, where the CM collects the cuttings, see Figure 3-46. The flowlines connecting the AC and BC with the stockpiling hood (seen in beige) are indicated by the green and purple lines in Figure 3-45, respectively. The figure gives a view of the overall seafloor operation. The CM is also designed to clear material cut by the AC when preparing sites, in addition to unconsolidated sediments. The collecting range of the CM is −2 m and +5 m vertically, and a width of 4 m (Nautilus Minerals, 2014).

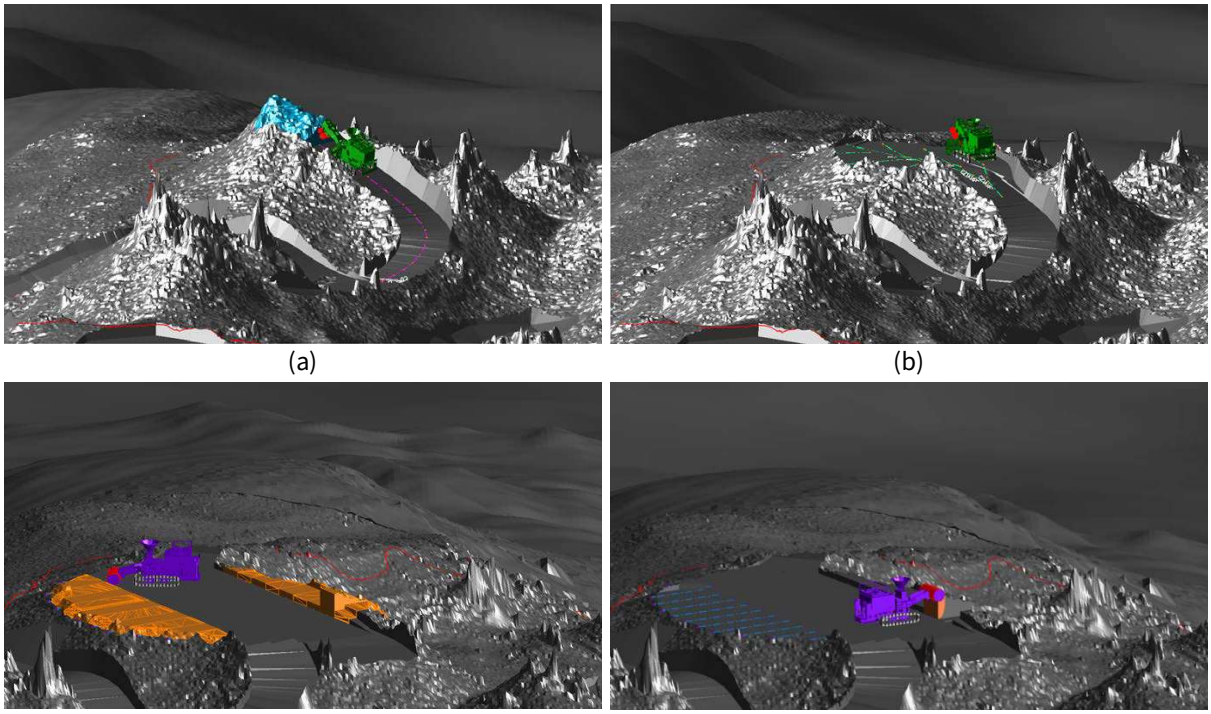

(a) (b)

(c) (d)

Figure 3-44 – Mining sequences: (a)-(b) Auxiliary Cutter; and (c)-(d) Bulk Cutter (Nautilus Minerals, 2015).

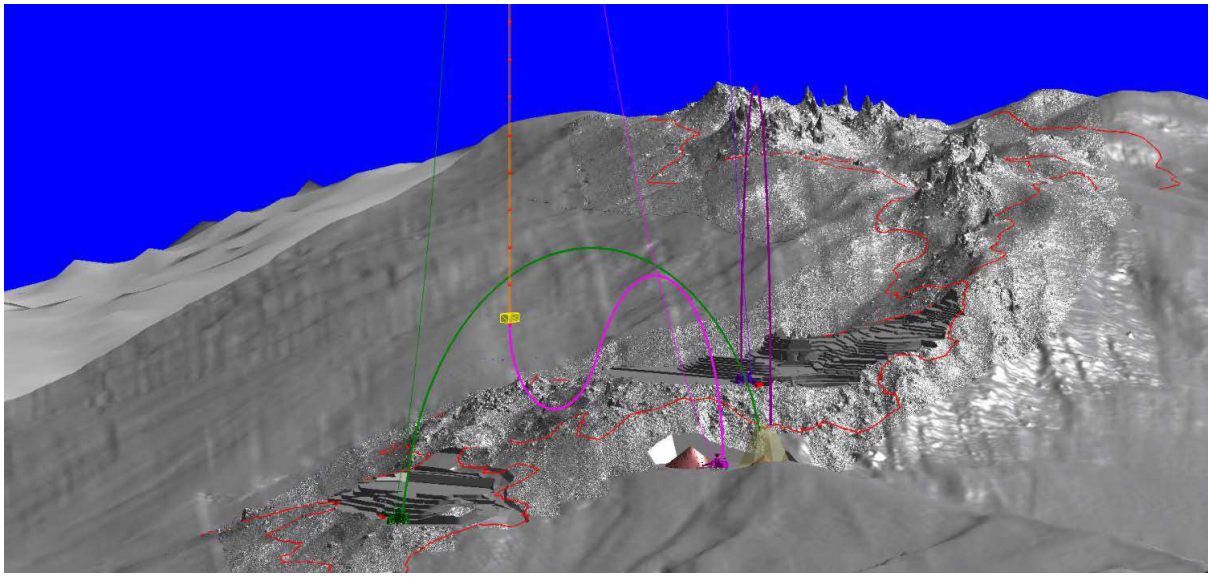

Figure 3-45 – Open mine site (Nautilus Minerals, 2015).

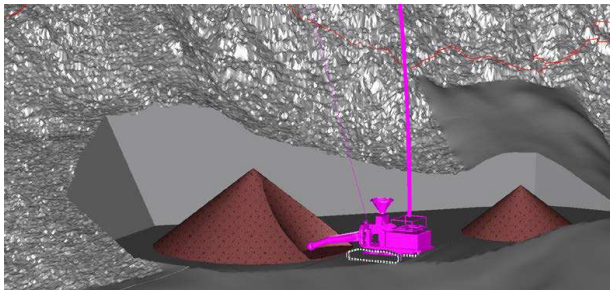

Figure 3-46 – Collecting Machine (CM) collecting a stockpile (Nautilus Minerals, 2015).

Mining Schedule

The mining of the deposit at Solwara 1 is scheduled at 19 months by considering various non-productive time of the SPTs, as presented in SRK Consulting (2010, pp. 196-205). The production schedule in Figure 3-47 represents an average operational year. Continuous operation, equaling 8,760 h per annum, is the available operational time for the overall system, and is called "calendar hours". The "scheduled hours" are the time available for the SPTs to operate, and constitutes 84 % of the year. The resulting "net operating hours" are the actual producing time of the SPTs, and defined as the difference between "calendar hours" and the sum of the downtime classes listed below (highlighted in Figure 3-47). Table 3-14 gives the time classification for the SPTs, and corresponding operational factors are in Table 3-15.

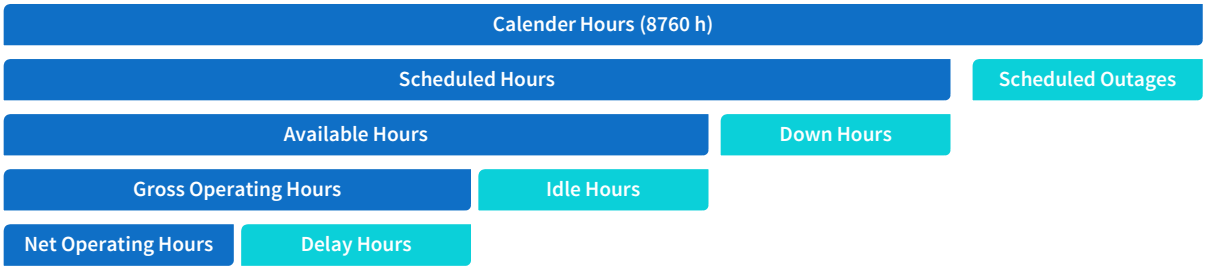

Figure 3-47 – Time classification structure (SRK Consulting, 2010, p. 201).

The different downtime classes are defined as follows (SRK Consulting, 2010, p. 201), see Figure 3-47:

- **Scheduled outages** are any downtime scheduled for the system as whole (i.e., entire mining spread) that affects all sub-operations, such as maintenance of the PSV and RALS, as well as any ramp-up downtime
- **Down hours** are scheduled maintenance with a duration of 24 h every 3.5 days for the AC and BC, and every 6.5 days for the CM
- **Idle hours** are non-productive time while waiting for a previous task to be completed by another piece of the equipment spread
- **Delay hours** are the time required to maneuver on a bench and relocate equipment from the current work place directly to the next work place

Table 3-14 – Time classification for SPTs (SRK Consulting, 2010, p. 202).

	Parameter	AC	BC	CM
a	Calendar Hours	13,608	13,608	13,608
b	Scheduled Outage Hours	2,216	2,216	2,216
c	Scheduled Hours ($a - b$)	11,392	11,392	11,392
d	Downtime Hours	2,073	2,073	1,344
e	Available Hours ($c - d$)	9,318	9,318	10,047
f	Idle Hours	4,963	3,828	3,220
g	Gross Operating Hours ($e - f$)	4,355	5,491	6,826
h	Delay Time Hours	225	1,156	538
i	Net Operating Hours ($g - h$)	4,130	4,335	6,288

Operational factors for the SPTs are defined (SRK Consulting, 2010, p. 201), ref. fractions in Table 3-15:

- **System availability** corresponds to the calendar time that is available for the overall SPTs after considering PSV and RALS maintenance
- **Mining equipment availability** corresponds to the time available for the individual SPTs after accounting for PSV and RALS downtime and SPT maintenance
- **Mining equipment utilization** corresponds to the available time that the SPT is being operated
- **Mining equipment efficiency** corresponds to the operating time that directly translates to cutting or gathering production

Table 3-15 – Operational factors for SPTs, ref. Table 3-14 (SRK Consulting, 2010, p. 202).

Factor	AC	BC	CM
System Availability (c/a)	84 %	84 %	84 %
Mining Equipment Availability (e/a)	68 %	68 %	74 %
Mining Equipment Utilization (g/e)	47 %	59 %	68 %
Mining Equipment Efficiency (i/g)	95 %	79 %	92 %

The RALS maintenance has been assumed to take 7 days each 100 days (SRK Consulting, 2010, p. 193). As the three different mining crawlers follows one another, the second and third vehicle (i.e., BC and CM) depend on the previous vehicle's task to be completed for them to perform their tasks successfully. Thus, the planned maintenance occurs at different times for each SPT to avoid affecting the operation of the two others. The difference between scheduled hours and downtime hours, gives the time the SPTs are available for operation, before unexpected failures or breakdowns occurs. Despite an optimized mining sequence, a significant amount of the available hours is lost as idle hours (i.e., waiting for a previous task to be completed by another tool) and delay hours (i.e., maneuvering on benches and relocating equipment). The net operating hours, which is the actual time the SPTs are exploiting the seafloor deposit, are 36 %, 38 % and 55 % of the scheduled hours (i.e., the total time at disposal for the SPTs) for the AC, BC and CM, respectively. Furthermore, there is a practical limit to the number of vehicles that can be operated at the same time from one surface vessel. Exceeding the limit will result in operational delays and take up deck space that is required for other activities. Launch and recovery of the SPTs will take hours even in the calm waters of the Bismarck Sea. To minimize the time spent on deck for maintenance and repairs, the vehicle designs allow critical and large components to be easily accessed and handled for the service crew, limiting required handling equipment (Ridley, et al., 2011).

Production Profile for Solwara 1

As seen from Figure 3-26, the Solwara 1 site consists of four different zones. Thus, some operational time is used to relocate both the PSV and the SPTs while being in production. It is also reasonable to assume that mining a large continuous zone is more efficient and yields a higher average production rate than mining a smaller, fragmented zone. This is reflected in the production profile and production rate in Figure 3-48 and Table 3-16, where a drop in production is expected when leaving the Central and West zones. A total of $1.9 \cdot 10^6$ t ore is planned to be exploited at Solwara 1 over seven quarters.

Table 3-16 – Production summary for Solwara 1 (SRK Consulting, 2010, p. 203).

		Production Volume [t]							
	Quarter	**Y1, Q1**	**Y1, Q2**	**Y1, Q3**	**Y1, Q4**	**Y2, Q1**	**Y2, Q2**	**Y2, Q3**	
Zone	***Phase***	*Start-Up*	*Prod.*	*Prod.*	*Prod.*	*Prod.*	*Prod.*	*Shutdown*	**Total [t]**
Central and West		202,099	350,660	368,472	397,364	79,434			1,398,029
Fast West						120,707			120,707
East						85,554	235,495		321,049
Far East							56,046	61,209	117,255
Total [t]		**202,099**	**350,660**	**368,472**	**397,364**	**285,695**	**291,541**	**61,209**	**1,957,040**
Days		91	91	92	92	90	91	20	567
Prod. Rate [t/day]		2,221	3,853	4,005	4,319	3,174	3,204	3,060	3,452

Figure 3-48 – Production profile and average production rate for Solwara 1, ref. Table 3-16.

CHAPTER 4
Project Development and Cost Theory

4.1 Project Development in Offshore Oil & Gas

4.1.1 Defining Uncertainties and Risks

Uncertainty and risk are often used interchangeably, but are not the same by definition:

- **Uncertainty** is characterized by something that exist, but cannot be controlled (e.g., exchange rates), and occurs with unknown probability (Gu & Gudmestad, 2012). In a project sense, it refers to "*[...] the range of possible values for project variables*" (Jahn, et al., 2008, p. 365). However, probability distribution for is a way of quantitatively dealing with parameter uncertainty.
- **Risk** is defined as the product of consequence and probability of occurance. Thus, it dependent on one's position – whether or not one are being exposed to uncertainty. Risk occurs with known probability (Gu & Gudmestad, 2012), and project risk is defined by Jahn, et al. (2008, p. 365) as "*[...] the impact of the outcomes on the stakeholders*". Risk can result in of both opportunities (upsides) and threats (downsides), see Figure 4-1.

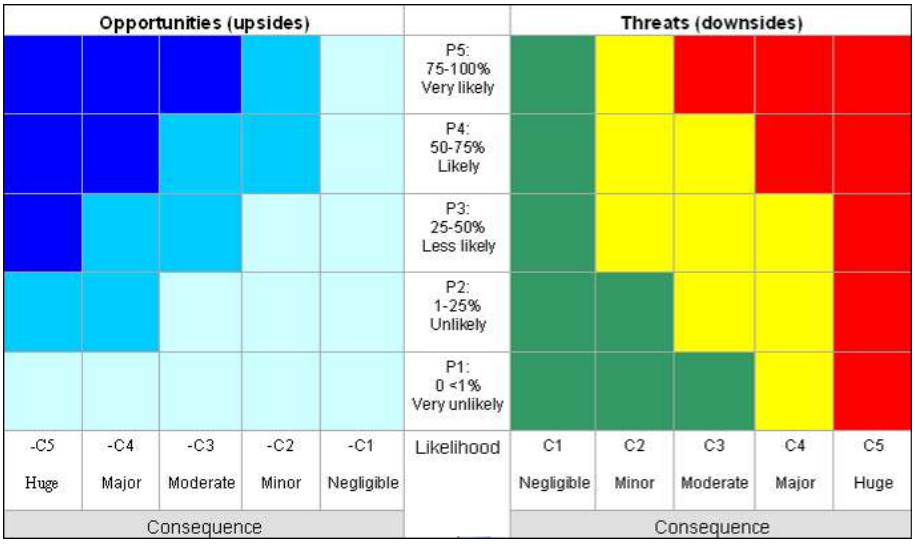

Figure 4-1 – Statoil's risk register matrix (Hembre, 2009).

4.1.2 Scenario Thinking

Pierre Wack at Royal Dutch Shell was one of the first to use scenario planning as part of a process for generating and evaluating strategic options (Wack, 1985). As a consequence, RoyalDutch Shell has been consistently better in their oil forecasts than other major oil companies, and has been the first to see overcapacity in the tanker and petrochemical business, as stated by Schoemaker (1995). Furthermore, Schoemaker (1995) discusses scenario planning as a strategic tool for thinking, and concludes that when contemplating the future, it is particularly useful to consider the following classes of knowledge:

- **Known knowns** are things we know we know
- **Known unknowns** are **t**hings we know we don't know
- **Unknown unknowns** are things we don't know we don't know

4.1.3 Phases of Exploration and Production Projects – Field Life Cycle

Projects for exploitation of petroleum are typically large in terms of complexity, required investments, and overall project cash flow. The phases of an exploration and production (E&P) venture are shown in Figure 4-2, some of which are defined by decisive events, and is similar to that of an offshore mining project. The three main stages are exploration, project development, and operation. The early phases of the project development process are defined as the project planning phases (Gudmestad, et al., 2010, p. 144), as seen in Figure 4-3, consisting of:

- Feasibility study
- Concept study
- Pre-engineering, or front-end engineering and design (FEED)

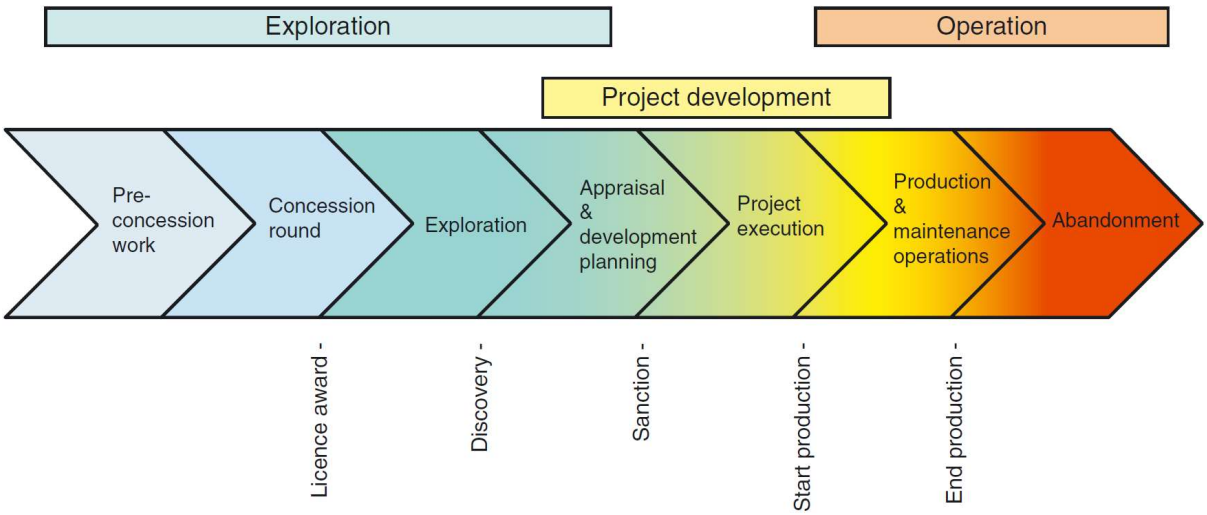

Figure 4-2 – Stages of an E&P venture (Gudmestad, et al., 2010, p. 143).

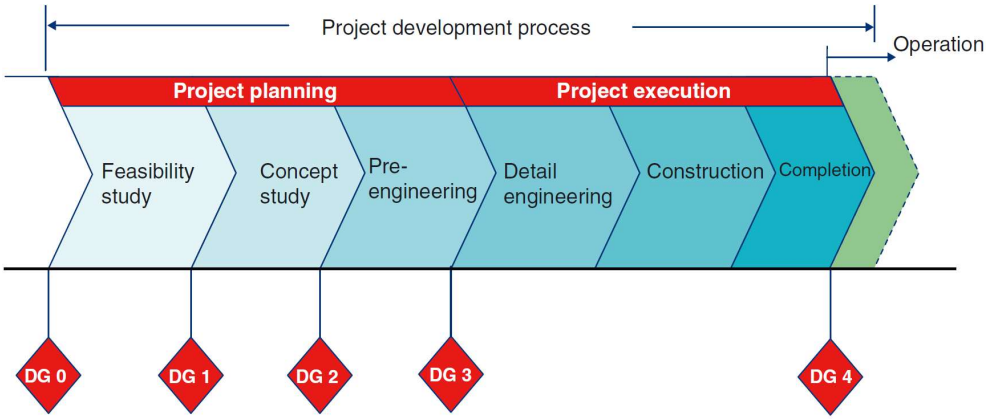

Figure 4-3 – Project development process for investment projects (Gudmestad, et al., 2010, p. 144)

The above phases are followed by the project execution phases. For the scope of this work, only uncertainties and risks related to project development and operation parts of the E&P venture are relevant. Decision gates (DG) are events which mark important decision points, as well as the transition between phases (Gudmestad, et al., 2010, p. 144). In comparison, the development of a subsea mine consists of four discrete phases, as seen in Figure 4-4, in which regulatory issues (e.g., mine licensing) and environmental requirements are managed throughout the process (Searle & Smit, 2011).

Garnett (1996) described such a process as follows:

> *"The multi-phase process leading to successful production starts with sampling, usually by some form of drilling. Estimation of the grade of each sample follows, and its accuracy is affected by the size of the samples, the sample density, and the mathematical procedure used. A cut-off grade is employed to exclude unpayable ground. Mining blocks, each encompassing a minimum number of samples, are selected as part of the total reserve estimation procedure. A proposed mining system may be tested [...] before full-scale production commences."*

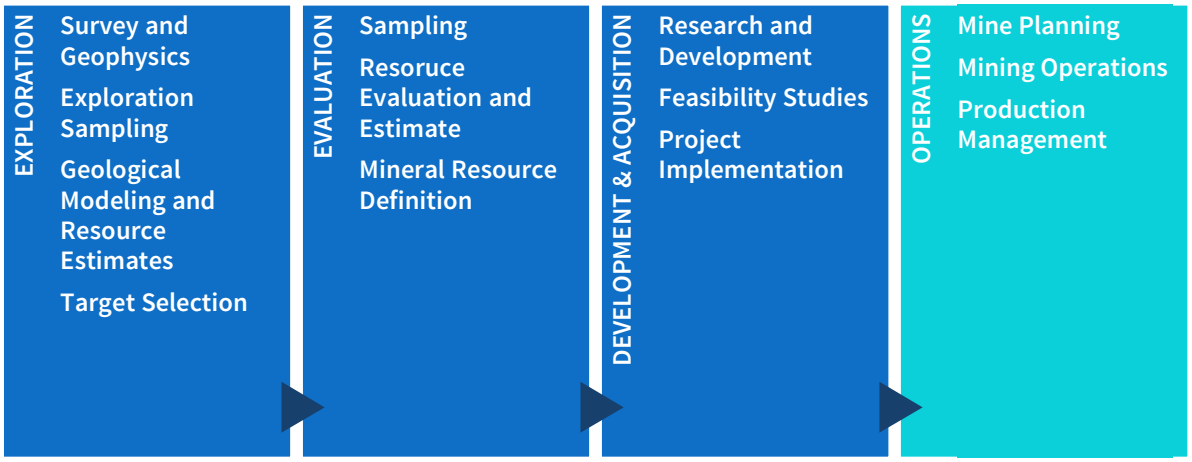

Figure 4-4 – Subsea mining business processes. Modified from Searle & Smit (2011).

Project Development in Statoil

The work of Gudmestad, et al. (2010) is to a large extent based on the methodology applied by Statoil. Statoil deals with uncertainty by applying the cost estimate class system in Table 4-1 for each phase of a project development. As a more detailed look at the process in Figure 4-3, project development in Statoil is divided into four distinct phases, as shown in Figure 4-5, each governed by its own decision gate (Ottervik & Skogdalen, 2013):

- **DG0-DG1 – Business planning** justifies further development of the business case and the establishment of an investment project. Feasibility studies are performed to demonstrate that a concept is technically, commercially and organizationally feasible, and that value chain fit, economic analysis and relevant stakeholder analysis justify further development.
- **DG1-DG2 – Concept planning** identifies alternative concepts, select a viable concept, define and document the selected concept, and develop a design basis for approval. Screening studies identify alternative concepts, and a concept study defines and documents selected concept(s).
- **DG2-DG3 – Business planning** further matures, defines and documents the business case based on the selected concept for project sanction. Any options or technical solutions not selected prior to DG2 shall be decided prior to DG3. A front-end engineering and design (FEED) study matures the business case and prepares execution. If required, any applications to the authorities are issued.
- **DG3-DG4 – Execution** realizes the business case, and includes detail design, procurement, construction (including installation) and completion of the agreed facilities and wells. Furthermore, preparations for start-up, operation and maintenance are done before handover to asset holder and/or operations.

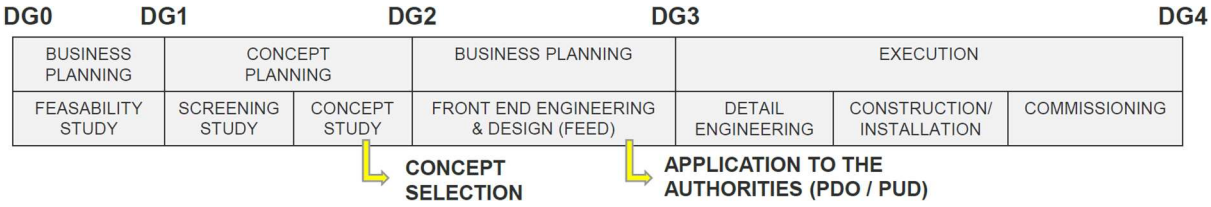

Figure 4-5 – Project development phases in Statoil (Ottervik & Skogdalen, 2013).

Table 4-1 – Statoil's cost estimate classes and characteristics (Gudmestad, et al., 2010, pp. 230-231).

Class	Required At	Description	Cost Estimate Accuracy[10]	Accuracy of Technical Information[10]	Normal Level of Contingency for CAPEX
A	DG0	Prospect Study	N/A	N/A	Not given
B	DG1	Feasibility Study	±40 %	±25 %	25-40 %
C	DG2	Concept Studies	±30 %	±15 %	15-30 %
D	DG3	Pre-Engineering	±20 %	±10 %	10-20 %

[10] 80 % confidence.

4.1.4 Cost and Schedule Estimates in Megaprojects

Uncertainty

Uncertainty rises from a vast range of sources, including social (influenced by political, economic, and social environment), technical (four types: concept, design, technological, and operational), commercial (e.g., demand and supply, cost estimate, production and price, market economy, inflation, interest rate), reservoir or geological, natural environment, management, and health, safety and environment (HSE) (Gu & Gudmestad, 2012). Economical evaluations of oil and gas project are highly affected by uncertainties related to costs, production profile, and product price, which all originate from geological models (Gu & Gudmestad, 2012). As discussed by Gu & Gudmestad (2012), methods for estimation are based on team experience and knowledge, historical data, and subjective evaluation of differences between projects. There are different sources of uncertainty: the subjective nature of the decision-making process; and the probabilistic assessment (i.e., estimate) of a future value. Uncertainty in the estimation model is associated with numerous factors, such as measurement, modelling, methodology, assumptions, and commodity markets.

Deterministic Cost Predictions with Market Adjustment

As an alternative to probabilistic cost analyses, which require market data to be available, deterministic cost estimates can account for future market developments affecting the cost regime by including a market adjustment MA, according to Hall & Delille (2011). MA is found from (1), in which IA are identified quantities and costs, A is allowance, C is contingency, and FI is the forward index at cost mid-point (i.e., the year that most costs are expected to occur); percentage factor based on future market developments The expected cost is the sum of the contributions in Figure 4-6, and the same approach can be applied for both OPEX and CAPEX. A probabilistic cost estimate would include the same factors as listed in Figure 4-6, except for the market adjustment. The 50/50 estimate in Figure 4-7 is as probable to over-run as under-run. Cost overruns are often accompanied by schedule delays, which are defined by Gu & Gudmestad (2012, p. 645) as "*the time overruns either beyond the completion date specified in a contract or the date agreed for a deliverable item*".

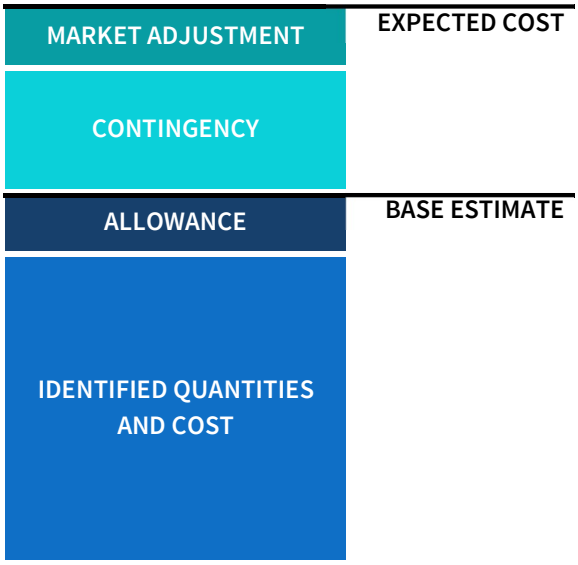

Figure 4-6 – Market adjusted expected cost. Modified from Hall & Delille (2011).

$$MA = (IC + A + C) \cdot FI \tag{1}$$

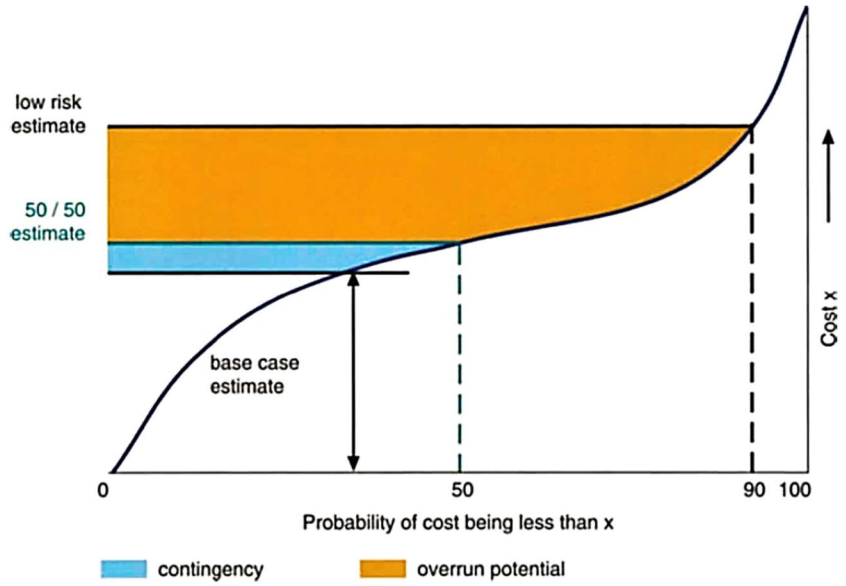

Figure 4-7 – Cost estimates and contingency (Jahn, et al., 2008, p. 334).

Overruns and Schedule Delays

An study of megaprojects[11] in the oil and gas industry by EY (2014, pp. 4-5) states that "*majority of the projects were delayed and/or faced cost overruns when measured against estimates made during the initial stages of the project life cycle*". Considering European projects exclusively, 53 % faces cost overruns and 74 % faces schedule delays. On average the project budgets are overrun by 57 %. Considering contingency allowance (e.g., as a percentage of the project cost), a cost overrun does not necessarily give a budget overrun. Primarily, factors causing cost overruns are material price fluctuations, contractor delay in material and equipment delivery, and inflation, while delays are caused by strikes and border closures, material shortage in market, and delays in material delivery (Gu & Gudmestad, 2012). As stated by Gu & Gudmestad (2012), "*cost overrun causes larger maximum negative cash flow and delayed time to recover the investment and uncertainty in revenue loss. Schedule delay causes delay of construction completion, delayed time to recover the investment and revenue loss.*", see Figure 4-8 and Figure 4-9, respectively.

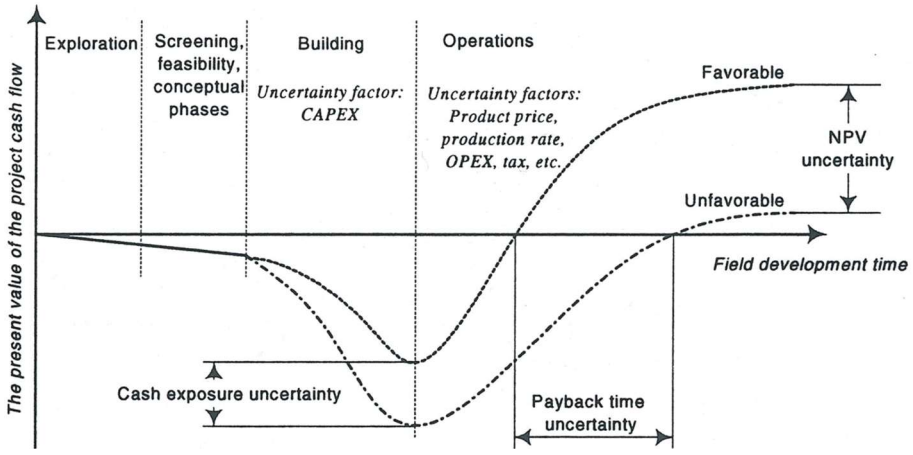

Figure 4-8 – Effect of cost overruns on project NPV (Chamanski, 2002, p. 54).

[11] Based on a review of 365 projects with a proposed investment of above 1 bill. USD in the upstream.

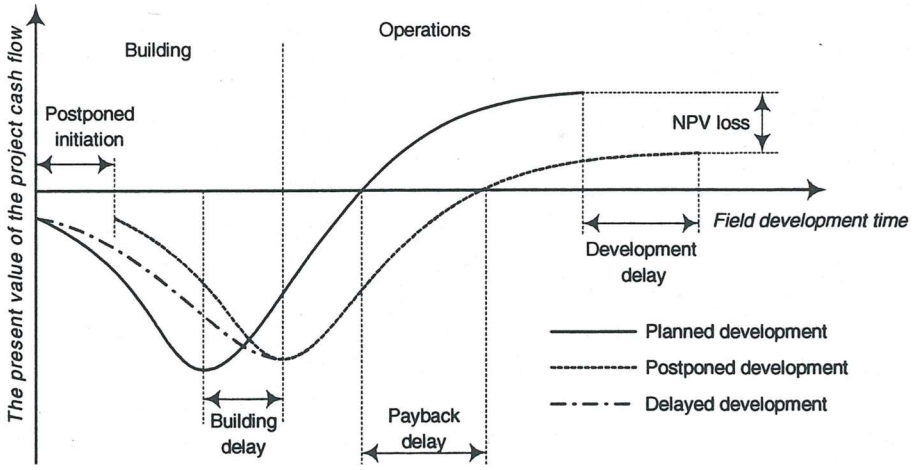

Figure 4-9 – Effect of delays on project NPV (Chamanski, 2002, p. 55).

Project Schedule

A construction schedule of a typical FPSO project (which has many similarities to that of a surface vessel used for subsea mining application when considering new-builds) is broken down into four quartiles, and has a typical duration of about 24 months (Paik & Thayamballi, 2007, p. 39):

1. Engineering and procurement
2. Pre-fabrication and pre-outfitting
3. Vessel erection, outfitting, and process installation
4. Final outfitting, hook-up, commissioning, and completion

The planned schedule of a megaproject is a function of various factors, including the capabilities of the shipyard and its contractors. Paik & Thayamballi (2007, p. 39) list important factors to evaluate when selecting construction facilities for FPSO construction projects:

- Physical facilities, such as steelwork pre-fabrication, and dry-docks
- Management systems, like project management system, quality assurance and quality control procurement, and pre-outfitting experience
- Discipline and trade resources, including engineering manning levels, steelwork and outfitting trade levels, hook-up, and commissioning resources
- Corporate considerations, such as previous offshore sector experience, and fiscal stability

A key challenge in the project process are delays, as briefly discussed by Paik & Thayamballi (2007, p. 39). When a schedule slippage occurs in the first quartiles (i.e., engineering and procurement), recovery is difficult during the second quartiles due to activities (e.g., steelwork pre-fabrication, pre-outfitting, and pipework production) may be significantly affected by the delay.

4.2 Structuring Operational Costs of Vessels and Installations

4.2.1 Life Cycle Cost in Offshore Oil & Gas

The same cost breakdown structure of life cycle cost (LCC) applies for system and subsystems. A general idea is that various mathematical models applicable to subsea oil and gas can be directly transferred to a subsea mining prospect with some adjustments.

Cost Elements

Based on the methodology for subsea systems for oil and gas production Bai & Bai (2012, pp. 183-190), the life cycle costs of a system component can be calculated from (2) when $RISEX$ is excluded. Low pressure in the pumping system combined with a slurry containing only seawater and crushed rock, the environmental risk related to spillage is minimal (at least compared to hydrocarbons). Assuming that mineral oil is used for hydraulic power and control fluid in the SPTs, any component failures and rupturing hoses have a low environmental impact.

$$LCC = CAPEX + OPEX + RAMEX \tag{2}$$

CAPEX are *capital expenditures*, i.e., costs of materials, fabrication and mobilization/installation of the mining system. OPEX, or *operating expenditures*, are costs to perform workovers. Scheduled repairs (i.e., planned maintenance) are included in the OPEX, in addition to fixed and variable costs related to storage of spare modules and spare parts in a warehouse, as well as logistical costs and service contract costs with the supplier of the subsea excavation tools.

RAMEX are *reliability, availability and maintainability costs* associated with component failure. A critical fault will require the operation (i.e., cutting of rock on the seabed) to be shut down, followed by retrieval of the vehicle, diagnostics, and the failed component to be repaired. Unplanned repair costs due to random failures are included in the RAMEX cost. The total RAMEX for each vehicle is the sum of two elements, as in (3), with revenue loss C_p and unscheduled repair cost C_r. The revenue loss C_p is the cost of lost production associated with one or more vehicles being down is. The production income losses are equal to the difference between the net present value (NPV) of the total revenue without and with production deferment. The steps to perform RAMEX cost calculations are illustrated in Figure 4-10.
. C_r is the unscheduled repair cost, i.e., the cost of repairing (or replacing) a failed component. It includes man hours, spare parts, tools and consumables, and consists of two sub-categories:

- **Major faults** require a repair to continue the operation, and is characterized as equipment breakdown.
- **Minor faults** do not affect, or only lower, the production rate. Thus, the repair job is acceptable to be performed as part of the next scheduled repair or maintenance.

$$RAMEX = C_r + C_p \tag{3}$$

In general, the OPEX and RAMEX costs are highly dependent on the rock characteristics, system design, operating procedures, and operational schedule, as this affects the progress in operations, hence the production rate of ore. Lewis & Steinberg (2001) state that *"the optimization of availability and utilization are the primary responsibility of the maintenance and operation groups, respectively, while the optimization of equipment performance"* is a joint responsibility. Hence, good cooperation between the different parts of the organization is paramount in reaching the most optimal operations scheme.

Figure 4-10 – Calculation steps for RAMEX costs. Modified from Bai & Bai (2012, p. 186).

Operational Costs

Using the same methodology and structure as van der Vet, et al. (2015), the total OPEX can be broken down to the following items, as illustrated in Figure 4-11:

1. **Initial costs** occur once and are made in the beginning of the operational life cycle.
    a. **Investment costs**: Procurement of new equipment, such as spare modules and condition monitoring equipment.
    b. **Contract joining fees**: Costs when entering a contract, like the service contract with the vendor (e.g., SMD) of the subsea mining equipment. As the vessel will be in operation for several years once it commences operation along the AMOR, and because of the large consequences unavailability of the SPTs will have on the project cash flow, a long-term contract will be preferred. This will also provide predictability for the operation.
2. **Yearly costs** are Pre-determined or expected (due to a constant failure rate) costs that are repaid on a yearly basis.
    a. **Scheduled repair costs**: The cost of performing maintenance on the equipment, and includes man hours, spare parts, tools, and consumables. Larger repairs or modification when the equipment is brought onshore to a workshop may also be included here.
    b. **Storage costs**: Both fixed and variable costs related to storage of spare modules or spare parts in an onshore facility.
    c. **Logistical costs**: Logistics, such as transportation costs when using carrier companies onshore or helicopter transport for critical parts or crew for the seafloor mining equipment.
    d. **Contract costs**: Yearly costs related to a contract, such as a service contract.
    e. **Others**: Other expenditures related to running the mining equipment on the seabed.

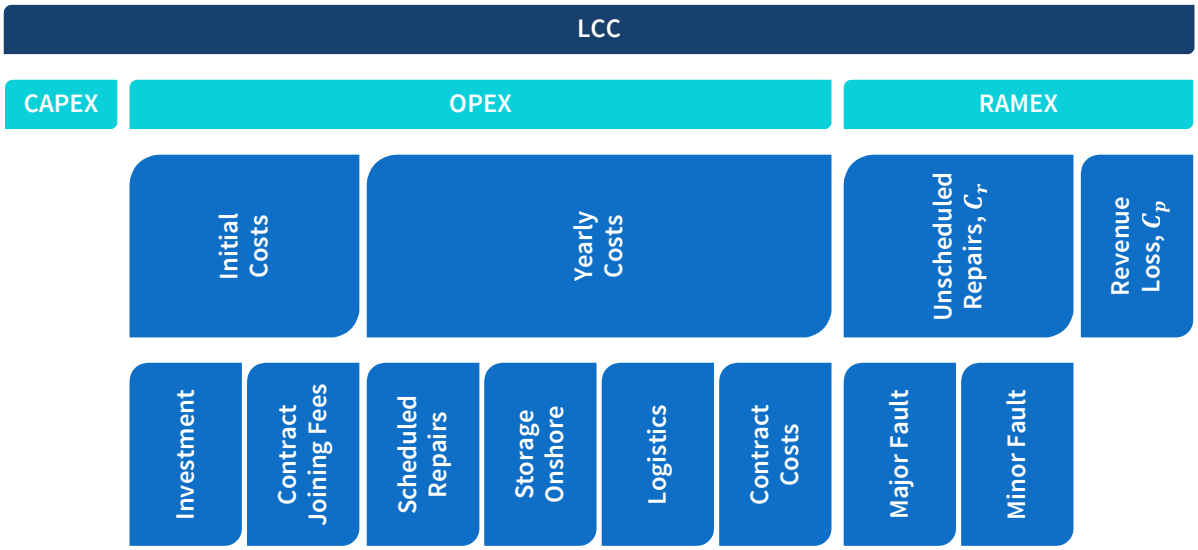

Figure 4-11 – Breakdown of operational costs in offshore oil & gas.

4.2.2 Operational Costs in Terrestrial Mining

Surface or open-pit mining is a capital intensive mining method, with higher productivity and lower costs than underground mining (Arteaga, et al., 2014). CAPEX are mostly related to equipment acquisition for the various unit operations, such as shovels or front-end loaders. Terrestrial mining differs from most other industries in that its main asset is finite and non-renewable, as well as uncertainty related to the ore characteristics and economic drivers of the project (like price and cost). Parallels can be drawn to the oil and gas industry. Today's terrestrial mining operations are highly mechanized and equipment dependent. According to Lewis & Steinberg (2001), costs related to maintenance account for about one third of the total extraction costs in open pit mines in North America. Maintenance constitutes 30-50 % of the direct mining costs, where general and labor costs make up 30 % and 11 %, respectively. Included in these costs are parts, labor, supplies and contractual services, as seen in Table 4-2. In addition, there are numerous hidden maintenance costs, such as production losses, cost of make-up equipment, loss of available capital, excess spares inventory, and increased crew size.

Table 4-2 – U.S. open-pit mining costs (Lewis & Steinberg, 2001).

Item	Fraction
Maintenance General	30 %
Maintenance Labor	11 %
Operations Labor	29 %
Diesel	15 %
Tires	9 %
Other	6 %
Total	**100 %**

4.2.3 Operational Costs in Shipping

Ship Design Criteria

When evaluating the cash flow of a project and selecting the most profitable system designs, "*the minimum cost over the life of the vessel rather than the minimum initial cost*" is sought after, as emphasized by Branch (1998, p. 44).

Key cost drives are listed below (Branch, 1998, p. 49):

- **Initial cost** based on invest budget and required return on capital;
- **Financial conditions** including general funding arrangement, potential operational subsidies, short- and long-term tax allowances, depreciation allowances, provision for inflation and prospective revenues, freight rebates, and commission payments;
- **Direct operating cost** such as crew wages, fuel, stores, maintenance, and port dues;
- **Fixed overheads** such as depreciation, interest on loans, and survey costs.

Ship investments involves the following four main factors (Branch, 1998, p. 44):

1. Shipbuilding cost
2. Operating expenses in trade
3. Cargo and passenger volume
4. Level of tariffs applicable to the traffic forecasts

Breaking Down and Estimating Operational Costs of Ships

Three variable cash flow items affect the financial performance of the ship owner, hence can be altered to manipulate the performance, as illustrated in Figure 4-12 and Figure 4-13:

- **Revenues** received from chartering/operating the vessel
- **Running costs** comprises all costs associated with running the vessel
- **Capital costs** are determined by the method of financing

Stopford (1997, pp. 153-155) discusses factors constraining these variables. The vessel design greatly influences the running costs (e.g., a modern vessel yields higher efficiency and lower costs). Moreover, maximizing the revenue is not only a matter of cutting operational costs and minimizing unit costs on a continuous basis, but also to keep the utilization of the vessel at maximum. The capital costs are mostly fixed after a fleet is purchased and financed, thus do not vary with market conditions. The residual in the cash flow model, highlighted in Figure 4-12, is paid out as dividends or retained within the company. It results after deducting running costs and taxes from the revenue earned from trading the ship. All the cost items in Figure 4-12 and Figure 4-13 are per annum.

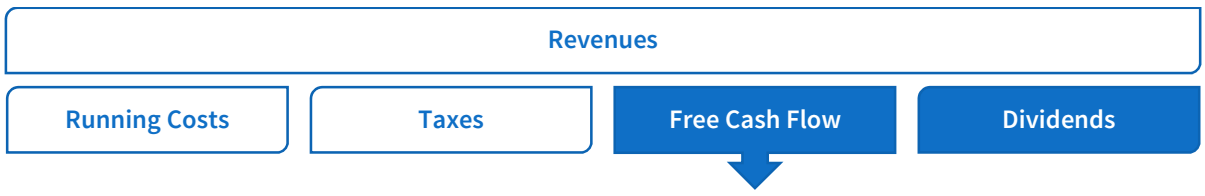

Figure 4-12 – Cash flow model. Residuals are highlighted (Stopford, 1997, p. 154).

According to Branch (1998, p. 68) and Stopford (1997, pp. 153-156), the general cost structure applied in shipping divided the running costs of a vessel into four main elements:

- **Operating costs** constitute all expenses in the day-to-day operation
- **Voyage costs** are costs associated with a specific voyage
- **Cargo handling costs**, representing the expense of loading, stowing and discharging cargo, and only applies to bulk carriers
- **Capital costs**, which also includes dividends (listed separately in Figure 4-12)

Figure 4-13 summarizes all the cost items that go into each of the elements/classes. The capital costs consist of interest charges and principal repayments, which are fixed (regardless of market conditions and the status of the vessel), except for the costs of periodic maintenance. The periodic maintenance costs incur when the ship is dry-docked for major repairs, which is normally done together with special periodic surveys. The operating costs and voyage costs are variable. The percentage that capital cost constitutes of the total annual cost varies between vessel types.

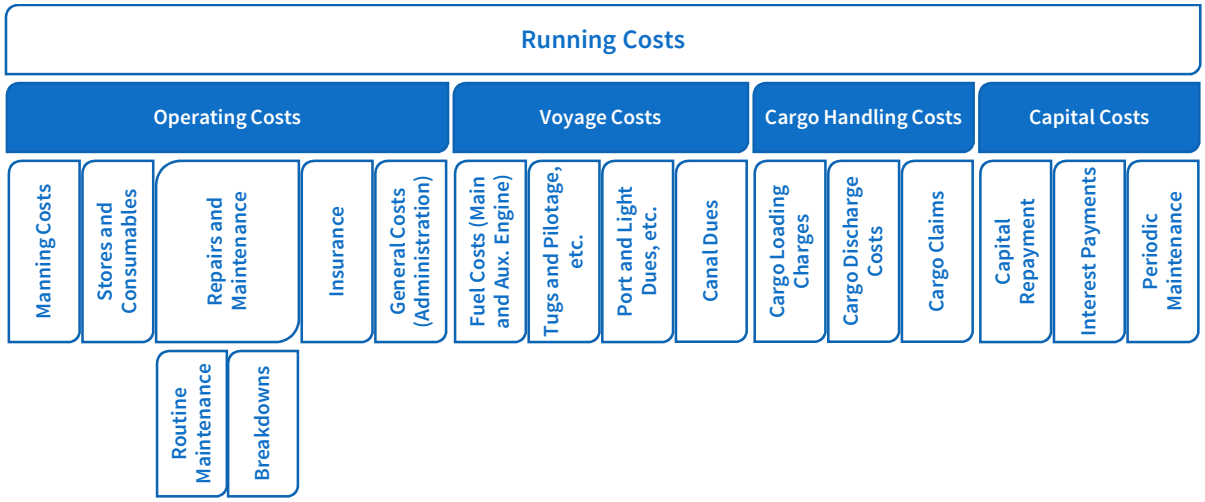

Figure 4-13 – Cost items included in running costs (Stopford, 1997, p. 160).

Factors Affecting Costs

Generally, operational expenditures are influenced by the following three external (market driven) factors (Drewry Maritime Research, 2015, pp. 47, 50):

- **Labor costs**, with labor being directly employed or by subcontractors or specialists;
- **Raw material costs**, with emphasis on oil and energy prices and key metal prices;
- **Exchange rates**, as contracts and purchases are set in different currencies, in this case mainly between USD and NOK.

Generally, the cost of running a vessel depends on three main internal factors:

1. The selected vessel design and main parameters, in addition to the condition of the vessel, make up fundamental cost constraints (e.g., fuel consumption, and number of crew)
2. Bought-in items (e.g., bunkers, consumables, and interest rates) and subject to inflation, and are generally market driven
3. Managing administrative overheads and maximizing operational efficiency

As stated by Branch (1998, p. 73), "*the annual revenue less operating costs must provide an operating surplus to cover the capital repayment schedule over the life of the loan*". Operating expenses rise with inflation and vessel age, among other factors. A detailed overview of factors influencing the running costs of a vessel are listed in Table 4-3, and Branch (1998, p. 125) lists factors affecting the ship operation and the ship cost as follows:

- Age and registration flag of vessel
- Crew nationality and manning scales
- Type of vessel
- Method of investment funding
- Ship management
- Ship operation (e.g., hub and spoke operation)

Table 4-3 – Factors influencing running costs (Stopford, 1997, p. 154).

Cost Item	Factors of Dependency
Revenues	*Cargo capacity*: Ship size; bunkers and store. *Ship productivity*: Operational planning; backhauls; operating speed; off-hire time; dwt utilization; port time. *Freight rates*: Market balance; quality of service; competition.
Operating Costs	Crew numbers; crew wages; stores; lubricants; repairs; maintenance; insurance; administration.
Voyage Costs	Fuel consumption of both main and auxiliary engines; fuel price; speed; port charges; canal dues; tugs.
Cargo Handling Costs	Cargo type; ship design; cargo handling gear; unitization; organization skill.
Capital Repayment	Loan size; loan length; moratorium; currency.
Interest Payments	Loan source; loan size; market interest rate; terms of loan.
Periodic Maintenance	Vessel age; maintenance policy; special survey cycle; regulations.

4.2.4 Introducing Cost Constraints

Crew Selection and Cost

Crew cost is a significant cost item, being the single largest variable cost of operating a ship, and can comprise over half a vessel's total annual operating costs (Branch, 1998, p. 133). Typically, crewing is influenced by the following factors:

- Availability of personnel (e.g., continuity, loyalty, and language of communication)
- Flag registry (i.e., national flag, second register, or flag of convenience) affects requirements regarding bookkeeping, wage levels, employment packages, and vessel inspections
- Experience, skill, certification and training, as shipboard technology is increasingly more demanding
- Travel costs related to trading pattern
- Familiarity with equipment and way of operation
- Maintenance and repair costs are higher with cheaper crews

Port Selection

(Branch, 1998, p. 186) defines logistics as "*the time-related positioning of resources, ensuring that materials, people, operational capacity and information are in the right place at the right time in the right quantity and quality and at the right cost*".

The following criteria for selecting a port are taken from (Branch, 1998, p. 182):

- Amount and type of profitable cargo
- Ship flexibility in design with respect to turnaround time
- Berth layout and backup facilities (such as container stacking area, handling equipment, distribution network, and customs clearance)
- 24/7 operational port with continuous access regardless of weather
- Road, rail and canal (inland waterway transport) communications available
- Strategically situated port; located on or near a shipping lane, remotely located area away from residential areas, and available for expansion
- Political stability and outlook of economic growth of port
- Brand image of port
- Bunker and ship repair facilities availability and charges

CHAPTER 5
Operational Scenario & Assumptions

5.1 Site

Being the most promising hydrothermal vent side with respect to associated SMS deposits that is known along the AMOR, the Loki's Castle vent field (73°33′ N, 08°09′ E) is selected for the operational scenario. The vent site is located at a water depth of 2,400 m, and is further described in Chapter 2.6. The remoteness of the ridge challenges the operation both with respect to safety and supply, with its large distances to mainland Norway and the established heliports and logistics hubs of Hammerfest for offshore O&G operations in the Barents Sea.

5.2 Production System Concept

The production system is based entirely on that of Nautilus Minerals for the Solwara 1 project, which is presented in detail in Chapter 3.6.3. With respect to the seafloor operation, the same mining procedure as described in Chapter 3.6.4 is used at Loki's Castle. The system selection based on these arguments:

- It is the first full-scale, commercial deep-sea mining production system that is detail designed (and under construction). Furthermore, there is a considerable amount of publically available information (including specifications and drawings) on the system compared to other published conceptual system designs.
- The system is designed for operations down to 2,500 m – however for significantly milder environmental conditions than those faced at the AMOR.

Key assumptions regarding the system are as follows:

- The production system (with its rigid production riser) is assumed to be capable of withstanding the environmental loads present at the AMOR without any modifications. However, a realistic concept would use flexible risers, similar to the concepts in Chapter 3.5.3.
- The SSLP is assumed to be shut down at an H_s of 5 m, governed by the heave compensation in the derrick. Emergency disconnect, where the RTP is ditched at disconnection and later recovered by an ROV, is performed at a higher H_s. Reconnection is assumed to be performed ones the sea state returns below the 5-m limit, and reconnection time is assumed short enough to affect the production rate and profile (when back and running on system uptime).

- Station-keeping of the PSV is performed by dynamic positioning (DP) only, and a yearly average thruster load is taken at 50 % of installed thruster effect. Thus, no mooring is used and no anchor handling (i.e., laying of anchor spread) is performed. Anchor lines would be an issue with respect to clashing with the production riser, SPT lifting wires (with clamped umbilicals), and the tether management systems (TMS) of the three ROVs. Furthermore, anchor handling would introduce a high cost which cannot be justified for the relatively short time frame of operation at each vent site.
- To compensate for additional depth (2,400 m at Loki's Castle versus 1,700 m at Solwara 1), both weight and cost of the rigid production riser are scaled based on the numbers of SRK Consulting (2010). Except for this, all system components are unchanged.
- The maximum production rates of the AC and BC are highly fluctuating and essentially lower than those of the CM and SSLP. At all times, at least one of the AC and BC are assumed to deliver a continuous production flow into the stockpiling hood, as their planned maintenance intervals do not overlap. Thus, the average production capacity of the AC and BC is assumed to be equal to the average net productive time of the SSLP and CM, which is the limiting production capacity of the overall system.

5.3 Environmental Criteria for Operations

5.3.1 General Concept

As the operation is based on a specific system concept, the explicit operational criteria for the various system components, and the operations linked to them, are part of the detailed engineering, and neither Nautilus Minerals or Technip have been willing to disclose any restrictions upon request. However, operations with many similarities are performed in offshore drilling, and may serve as a good comparison with respect to environmental criteria/limitations to perform a certain operation.

5.3.2 Taking SSLP Through Splash Zone

Regarding running of the SSLP through splash-zone, two similar types operations are performed from mobile offshore drilling units (MODUs), such as semi-submersible drilling rigs or drillships:

- Running 21-in marine drilling riser with blowout preventer (BOP) and lower marine riser package (LMRP)
- Running of x-mas tree (XMT) on drill pipe

Considering the first case, the weight of a BOP stack (i.e., BOP with LMRP on top) varies greatly with water depth of the wellhead and reservoir characteristics, thus the required pressure rating of the BOP. Those used at Norwegian offshore fields are typically in the weight range 150-300 t. Running of a BOP stack through the splash zone is limited to an H_s of about 2-3 m.

For the second case, to be able to run an XMT on drill pipe additional equipment is needed (e.g., to enable communication with the values in the tree). In the case of a horizontal XMT (HXT), a tree running tool (TRT) is used, and for a vertical XMT (VXT) both a lower riser package (LRP) and emergency disconnect package (EDP) is latched onto the tree. The weight of such a stack, which includes the XMT weight, is up

to approximately 65 t for smaller trees, and closer to 100 t for larger, more complex tree designs. Specific requirements for running these stacks through the splash zone are set by the respective supplier. For a 65 t stack on drill pipe, the limit with respect to H_s ranges 3-3.5 m, and for heave η_3 around 2 m. Typically, maximum allowed pitch η_5 and roll η_4 motions are about 3° double amplitude.

Nielsen (2007, pp. 28-30) lists approximate operational limits for some marine operations. For a drillship in head seas, limits on significant wave height H_s for performing drilling, running casing, and doing BOP and riser handling are 5 m, 4 m, and 3.5 m, respectively.

5.3.3 Stopping SSLP and Emergency Disconnect of RTP

The purpose of the heave compensation system is to hold the riser in constant tension to avoid it collapsing due to excessive stresses from its own weight and environmental forces acting on it. Most MODUs have a heave compensator built into the crown block, a so-called crown-mounted compensator (CMC), at the top of the derrick. A CMC has a typical stroke of 8 m and weight capacity of 450 t (Sangesland, 2008, pp. 24-25).

Applying an H_s limitation of 5 m for the heave compensation system, and assuming that the SSLP would only be operated when the production riser is compensated, the SSLP (hence the production) will be shut down at a significant wave height exceeding 5 m. At a higher H_s, an emergency disconnect of the flexible riser (i.e., jumper running from the CM to the SSLP) would be performed to protect both the jumper and the connected mining tool. At an even higher H_s, large inertia forces acting on the entire riser string due to large motions of the surface vessel, as well as it not being able to keep its position, would require the rigid production riser and SSLP to be pulled. Typically running/pulling speed in offshore drilling are as follows: Drill pipe with workover stack is runs at about 400-500 m/h, and is somewhat limited by the umbilical running simultaneously (which has to be clamped onto the drill pipe at certain intervals); and BOP runs slower, since each riser connection must be bolted together, at an approximate effective speed of 60-70 m/h. Assuming a running/pulling speed of 3.5 joint/h for the 62 ft (18.9 m) joint length (66.15 m/h), this operation would take 34 h (about 1.4 days) for a total riser length of 2,250 m. The water depth at Loki's Castle is 2,400 m, and the SSLP is 150 m above the seafloor.

5.3.4 Offshore Loading Operations

Loading operations between vessels are standard procedure in offshore oil and gas operations. However, such operations are highly governed by restrictions with respect to environmental conditions. From an FPSO, oil, liquefied natural gas (LNG), or liquefied is exported to an export tanker using various layout arrangements depending on the offloading system design. Typical arrangements are tandem offloading, side-by-side offloading, and a catenary anchor leg mooring (CALM) buoy located at a distance from the FPSO. Operational limits for typical offloading systems are given in Table 5-1.

Another standard offshore loading operation are between MODUs and platform supply vessels (PSVs) on daily basis. According to Aas, et al. (2009), offshore (un)loading operations carried out on the windward side must be aborted if H_s excessed 4 m. If there are cranes on different sides of the vessel increase the operability somewhat, as leeward-side operations are limited to an H_s of 4.5 m. Bulk operations (e.g., fuel or brine loading through floating hoses) is more weather sensitive than deck operations. In addition, to ensure that the PSV has excess power to handle unforeseen problems, it cannot utilize more than 50 % of its machinery power to maintain its position alongside the installation

(or MODU). Aas, et al. (2009) also mentions co-called "cherry-picking" (i.e., use a crane to pick a load carrier that is surrounded by other load carrier – containers or baskets – on all sides) not being allowed as a factor that further complicates offshore loading (and giving reduced flexibility with respect to logistics) by making re-routing difficult as most PSV are not equipped with deck cranes.

Table 5-1 – Maximum operating sea state for FPSO transfer systems (FMC Technologies, 2010).

Arrangement	Shuttle Tanker Loading Method	Shuttle Tanker Capabilities	H_s Criteria, Approach and Mooring [m]	H_s Criteria, Offloading and Disconnect [m]	Limiting or Governing Factors
Side-by-Side	Mid-ship manifold	Any tanker	1.5-2.0	2.5-3.0	Shuttle tanker maneuvering and tug support capabilities Relative motions and mooring line loads
Tandem	Mid-ship manifold	Any tanker	2.5-3.0	3.5-4.0	Tug support capabilities for handling of hose Manifold load capability
	Bow	Non-DP shuttle tanker	3.5-4.5	4.5-5.0	Maneuvering capability (approach and mooring) Hawser loads (offloading)
	Bow	Non-DP shuttle tanker	4.5-5.5	5.5-6.0	Shuttle tanker DP capability

5.4 Logistics

For an operation along the AMOR, Large distances from nearest offshore heliport and logistics hubs are challenging with respect to operations and supply. Using a supply base on the mainland seems advantageous when considering accessibility and existing infrastructure. As Hammerfest has a developed harbor, and is already a logistics hub for current O&G activities (e.g., Snøhvit and Goliat). Tromsø is another option, with a harbor and supply base for offshore activities under development at Grøtsund (located north of the city). As seen from the distances in Table 5-2, Loki's Castle is a sailing distance of 30 h away from Hammerfest and Tromsø. Another interesting hub of the seven existing supply bases used by Statoil, see Figure 5-1, is the one at Sandnessjøen.

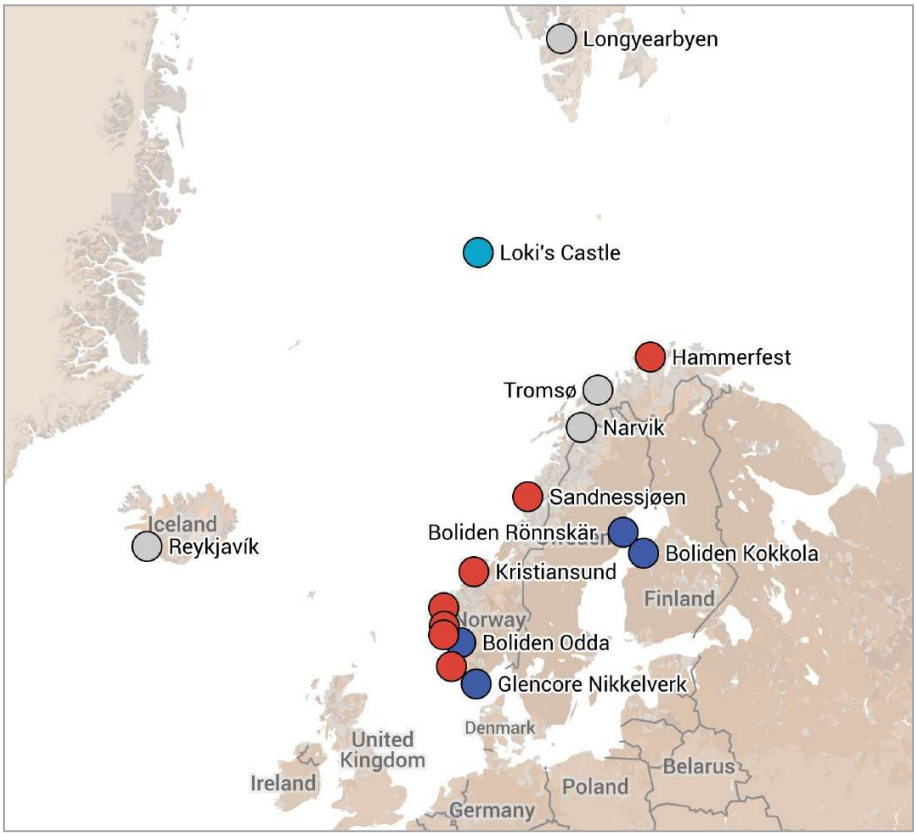

Figure 5-1 – Map of O&G logistics hubs (red), refining plants (blue) and ports (grey) (Google/INEGI, 2016).

Table 5-2 – Sailing time to Loki's Castle [h / days][12].

Port	Distance [nm]	10 kn	11 kn	12 kn
Longyearbyen	313	31.3 (1.3)	28.5 (1.2)	26.1 (1.1)
Hammerfest	337	33.7 (1.4)	30.6 (1.3)	28.1 (1.2)
Tromsø	314	31.4 (1.3)	28.5 (1.2)	26.2 (1.1)
Narvik	377	37.7 (1.6)	34.3 (1.4)	31.4 (1.3)
Odda	906	90.6 (3.8)	82.4 (3.4)	75.5 (3.1)
Kristiansand	1,011	101.1 (4.2)	91.9 (3.8)	84.3 (3.5)
Reykjavik	944	94.4 (3.9)	85.8 (3.6)	78.7 (3.3)

As a baseline for evaluating the technical concept, different operational scenarios are defined, as seen from Table 5-3. Their fundamental difference is whether such an operation will run as a traditional offshore O&G operation with respect to logistics, yielding a high-cost scenario, or as a more simplified, low-cost operation. There are three main logistical aspects/issues associated with an AMOR operation:

- Sufficient frequency for providing supplies, stores and fuel to the PSV and the various equipment of the production system
- Personnel rotation
- Destination for shipping of dewatered ore

[12] Distances are taken from Veson Nautical's distance tables (www.veslink.com/distances).

Table 5-3 – Operational scenarios.

	Scenario A	Scenario B
Type	Low-cost scenario	High-cost scenario
Description	Operational scenario as a cross-over between that seen in offshore drilling and traditional shipping, as well as walk-to-work solutions applied in offshore wind.	Based on a traditional offshore O&G operation of a MODU. A typical logistics chain is seen in **Error! Reference source not found.**.
Shift Rotation	Ideally: 2-4 months on/off Realistically: 3 weeks on/off	2 weeks on / 4 weeks off.
Logistics Outline	Combined vessel acting as supply vessel at approach and as bulk carrier at return. Logistics hub preferably at same location as the refining plant that receiving the ore – alternatively on the sailing route. Personnel is sailed out and a heave compensated gangway is used as a temporary bridge between the vessels – a so-called walk-to-work solution, which is used at offshore wind farms.	Personnel are airlifted by helicopter from mainland (e.g., Hammerfest). Supplies are carried by a supply vessel similar to a platform supply vessel (PSV), while the dewatered ore is picked up by a bulk carrier.

The walk-to-work concept is popular for offshore wind farms using active heave-compensated gangways to mobilize personnel for inspection and maintenance work. ESVAGT's service operation vessels (SOV) for offshore wind farms has such a solution installed, similar to the one seen in Figure 5-2 (a). Walk-to-work solutions are proven in real operations, and are developed by companies like Dutch Ampelmann and Norwegian Uptime.

At full production rate (8,202 t/day for 12 % and 3.3 SG), the cargo hold capacity of the PSV (67,500 t for 3.3 SG) reaches capacity in 8.2 days for the average volumetric percentage of 12 % (i.e., the capacity is independent of SG and varies with volumetric ratio). At 50 % thrust utilization, the average fuel consumption is 103.6 m^3/day, corresponding to 852 m^3 of 8.2 days of operation.

Based on the discussion above, the following requirements are found for the design of a combined supply vessel and bulk carrier:

- A round-trip including offloading time and contingency of maximum 8.2 days
- Active heave-compensated gangway
- A minimum passenger capacity of 52 PAX, which corresponds to one-third of the daily personnel on the PSV or a three-week on/off crew rotation
- Sufficient deck area for supplies, including large and heavy spare part modules for the SPTs
- A minimum fuel capacity of about 1,000 m^3
- Bulk carrying capacity of 20,500 m^3 of ore

(a) Walk-to-work gangway (Uptime)[13]

(b) Supplies to drillship (Rowan Companies)

Figure 5-2 – Combined bulk and supply vessel.

Suggested refineries and ways of transporting the dewatered ore are as follows (Boliden Group, 2016), some of which are marked in the map in Figure 5-1:

- Boliden Odda in Odda, Norway produces pure zinc, zinc alloys, sulfuric acid, and aluminum fluoride.
- Glencore Nikkelverk in Kristiansand, Norway
- Shipping to Narvik and further transportation to the Baltic Sea by train
    - Boliden Rönnskär in Skelleftehamn, Sweden is a copper smelters and recycles copper and precious metals from electronic scrap. The main products are copper, lead, zinc clinker, gold and silver.
    - Boliden Kokkola in Kokkola, Finland is a zinc plant producing pure zinc and zinc alloys, as well as sulphuric acid.
- Kirkenes in Finmark country, Norway has an already existing infrastructure from an abandoned copper mine.
- Svalbard, with its history as a mining community, is a potential site for establishing a processing plant.
- Nussir in Kvalsund municipal, Finnmark county, Norway has a copper plant associated with an upcoming copper mine being established.
- Island – establishing a copper smelting plant utilizing the cheap geothermal energy of the landmass with parallels to aluminum production plants already present.

[13] http://www.uptime.no/wp-content/uploads/FF65925.jpg, accessed May 22, 2016.

5.5 Emergency Preparedness and SAR Helicopter Reach

5.5.1 Risk-Based Emergency Response Times and Capacity

A permanent, remotely located operation, such as the one intended at Loki's Castle, requires emergency preparedness in case of life threatening injuries or health conditions of any of the personnel onboard, as well as man-over-board (MOB) situations, that require immediate evacuation to land. The Norwegian petroleum industry has established four areas of cooperation between operators with respect to external marine and airborne resources, known as the "area-based emergency response", as described by Vinnem (2014, p. 746). The following scenarios form the basis of the emergency response planning:

DFU1: Man over board in connection with work over sea

DFU2: Personnel in sea needing rescue after helicopter ditching

DFU3: Personnel in sea needing rescue after emergency evacuation

DFU4: Collision hazard (from passing and drifting vessels)

DFU5: Acute oil spill

DFU6: Installation fire with external firefighting assistance required

DFU7: Acute injury or illness with external medical assistance required

DFU8: Helicopter crash on installation with severely injured personnel

According to the guidelines of the Norwegian Oil and Gas Association (Norsk olje og gass, 2015), in which the above scenarios are defined, the required capacity and effectiveness of each DFU. Requirements for DFU7: acute medical response time is 1 person and 1 h; and transport to hospital is 2 people in 2 h. For DFU3, a fully loaded helicopter of 21 people should be rescued within 2 h. Following the Petroleum Act, operators are only responsible for picking up of people from the sea within the safety zone, i.e., a radius of 500 m around the installation, as it is assumed that the national emergency services is effective outside the safety zone. Statoil uses six heliports for their offshore operations in Norway: Sola, Stavanger; Flesland, Bergen; Florø, Kvernberget, Kristiansund; Brønnøy, Brønnøysund; and Hammerfest. Statoil has all-weather search-and-rescue (AWSAR) helicopters stationed at Sola and Hammerfest, as well as at the platforms of Oseberg, Statfjord B, and Heidrun. The distance from Flesland to Statfjord B is 114 nm, and from Sola to Oseberg is 126 nm.

5.5.2 Helicopter Types

Loki's Castle is at the absolute maximum range of commercially available helicopters – and that is when considering the run-empty flight range, which is not a realistic operational scenario. There are not any permanent operations, installations or facilities that enable touch-and-go for refueling on the flight path between the site and its nearest airports. Among the current long-range helicopters used in (and configured for) the offshore industry, Airbus Helicopter's Super Puma H225 has the longest range. Additional fuel tanks can be fitted to extend the range. Typically, a SAR configuration of the H225 has capacity of six seats (two pilots and four additional crew) and up to 3 stretchers (Airbus Helicopters, 2016, pp. 6-8, 23), as seen in Figure 5-3 (a). For passenger transport, the capacity is two pilots and 19 passengers. With respect to performance, the H225 has a maximum speed and fast cruise speed of 175 kn and 142 kn, respectively. Its maximum range with all optional central and pod tanks, in addition to the standard fuel tanks, is 613 nm (giving an endurance of 5 h 38 min).

A helicopter currently under development, the AgustaWestland AW609 TiltRotor, enables such remote operations, and is seen in Figure 5-3 (b). Its technical details are described in AgustaWestland (2014), Leonardo-Finmeccanica (2015), and Bristow Group (2015). Bristow Group, a major helicopter service provider to the offshore O&G industry globally, is a collaborative partner in the development of the AW609, with customer delivery beginning in 2018 after an expected receipt of FAA certification in late 2017. The design combines the speed, range and high-altitude, above-the-weather capability (25,000 ft) of fixed-wing aircrafts with the vertical takeoff-and-landing capability and flexibility of rotary-wing aircrafts (helicopters). The maximum range without reserves for a standard fuel tank configuration is 700-750 nm, and is extended to 1,100 nm with additional fuel tanks, allowing transportation of six passengers over a range of 800 nm in about 3 h. Maximum cruise speed is 275 kn. The maximum takeoff weight is 18,000 lb (8,165 kg) for short takeoff and landing (STOL) and 16,800 lb (7,620 kg) for vertical takeoff and landing (VTOL). In offshore configuration with standard fuel tanks, the AW609 can carry up to nine passengers and two crew members, and two engines ensure safe operations even with a single-engine failure. The AW609 is capable of flying in full-icing conditions. An emergency medical services (EMS) configuration allows up to four medics and two stretcher patients. Additionally, a SAR configuration will be available.

(a) SAR configured H225 (Airbus Helicopters)[14]

(b) AW609 TiltRotor (Leonardo-Finmeccanica)[15]

Figure 5-3 – Offshore helicopters from Bristow.

[14] https://www.airbushelicopters.com/website/en/ref/EMS_56.html, accessed June 4, 2016.
[15] http://www.leonardocompany.com/-/aw1238, accessed June 4, 2016.

CHAPTER 6
Methodology

6.1 Probabilistic Cost Estimates

6.1.1 Deterministic versus Probabilistic Modelling

Different ways of estimating the cash flow of future projects are described by Albright & Winston (2015, pp. 812-846), which this and the following sub-chapters are based upon. A *deterministic model* is most often used, in which input variables are taken as averages or "best guesses" based on the information available. As there are often uncertainties associated with one or more of the input variables, this rarely give outputs that are representative of the real case.

To deal quantitatively with the significant uncertainty that is present at an early phase of an engineering project, probability and probability distributions are often introduced. Each random variable, which associates a numerical value with each possible random outcome (Albright & Winston, 2015, p. 140), is linked with a probability distribution, defining possible values for the random variable and the corresponding probability of occurrence. In such a *probabilistic (or simulation) model* is an approximation, and the input variables are entered as probability distributions, which incorporate the associated uncertainty. Numerous simulations are run with different sets of random input values (drawn from each input probability distribution using a randomly generated probability). Each set of drawn input variables represent a scenario and gives particular output(s). Hence, the approach results in probability distributions for the result variables (e.g., project NPV), and is outlined in Figure 6-1. Simulation models are also useful in sensitivity analyses when evaluating the effect of changes in operating conditions. An exact probability model, incorporating the rules of probability, may be very difficult (if not mathematically impossible) to establish. The resulting output from a deterministic model can be considerably different, either lower or higher, than the mean of a similar probabilistic model, which is referred to as the "flaw of averages".

Figure 6-1 – Probabilistic model. Modified from Albright & Winston (2015, p. 814).

6.1.2 Modelling Uncertainty by Monte Carlo Simulations

Probability Distributions and Random Variables

As defined by Walpole, et al. (2012, pp. 81-91), a random variable X is "*a function that associates a real number with each element in the sample space*". The values of the random variable are denoted x. For a continuous random variable X (see Appendix F for definition), the probability of an observed value of X being less than or equal to a real number x is found from the cumulative distribution function (CDF) $F(x)$ as in (4), where $f(x)$ is the probability density function (PDF). Hence, the CDF is a non-decreasing function with values ranging from 0 to 1.

$$F(x) = P(X \leq x) = \int_{-\infty}^{x} f(t)\, dt\,, \quad -\infty < x < \infty \tag{4}$$

The area under the PDF curve bounded by the x axis is equal to 1 when computed over the range of X for which $f(x)$ is defined as in (5). The probability of X taking on a value between the x-values a and b is given by (6). As the potential upside of an uncertain variable is of interest when evaluating projects, the probability of exceedance of $x_{\max}$ is used, found from (7).

$$\int_{-\infty}^{\infty} f(x)\, dx = 1 \tag{5}$$

$$P(a < X < b) = \int_{a}^{b} f(x)\, dx \tag{6}$$

$$P(X > x_{\max}) = 1 - F(x_{\max}) \tag{7}$$

Monte Carlo Simulations

Gu & Gudmestad (2012) describe the Monte Carlo simulation as "*a method for iterative simulation for modelling significant uncertainties in inputs, then the probability distributions of outputs show which value is most likely*". As stated by Haver (2011, pp. 100-102), a Monte Carlo simulation is useful when it is difficult, not possible, or too expensive to make real observation of the random variable(s). To generate the value numerically, a random number between 0 and 1 is generated for the variable y_j (from a random number generator using a uniform distribution; a feature which is supported by most calculators and computer calculation tools, such as MATLAB and Excel). By using the inverted cumulative distribution function F_X^{-1} (e.g., the probability distribution for a cost parameter), a corresponding value for the random variable X is found, as in (8).

$$x_j = F_X^{-1}(y_j), \quad j = 1,2, \dots, n \tag{8}$$

This is repeated for all values of j (representing the number of simulation iterations), giving a sample size n for the random variable X. The solution of a Monte Carlo simulation will always converge to the correct answer if n becomes sufficiently large, assuming that F_X is the true distribution for X (Haver, 2011, p. 102). As emphasized by Kitchel, et al. (1997), a large number of iterations are required to sample each distribution thoroughly and avoid clustering. The latter is an issue for distributions with

low-probability outcomes. Typically, a simulation runs 1,000-10,000 trials (Gu & Gudmestad, 2012). Figure 6-2 shows the general steps of a Monte Carlo simulation.

Figure 6-2 – Steps of Monte Carlo forecasting. Modified from Williamson, et al. (2006, p. 218).

6.2 Spradsheet Modelling of Costs

6.2.1 Background from the Offshore O&G Industry

As defined by Odland (1999, p. 2), "*a cost estimate is defined as the expected final cost of a development*". Probabilistic estimates of drilling costs have been widely performed in the oil and gas industry since the late 1990s, using spreadsheet models to evaluate prospects or to analyze problems that involve uncertainty, like in Conoco described by Murtha & Janusz (1995) and Kitchel, et al. (1997). Earlier these cost estimates were done using deterministic approach, and uncertainty was incorporated using percentage additions and subtractions. Triangular, normal, lognormal, and uniform distribution profiles were selected based on assumed best, worst, and most-likely cases and their likelihood of occurrence. Generally, drilling costs depend on time and depth, in addition to fixed-cost components.

6.2.2 Defining Probability Distributions of Input Variables

According to Williamson, et al. (2006), the choice of distribution in a Monte Carlo analysis is critical when the relative frequency of extreme values is important. The *central limit theorem* applies to most well simulations, as a large collection of different probability distributions are sampled once and summed per iteration of a process repeated a large number of times before the distributions of the sums are examined. The resulting distribution of such an operation has a mean and variance close to the sum of the mean and variance of the individual distributions, in addition to a shape approximating the normal distribution. It follows by the central limit theorem that "*[…] the distribution of the sum of a large number of random variables depends only on the mean and standard deviation of those variables […]*" (Williamson, et al., 2006). This tendency increases with the number of individual distributions. Hence, the selection of distribution type is of less importance, and attention should be given on assigning the correct mean and standard deviation to the input distributions. The potential effect of the central limit theorem is an unrealistically narrow output distribution. The issue is discussed by Akins, et al. (2005), which proposes the some reducing measures listed below:

- Restrict the number of input variables
- Consider uncertainty and avoid using too narrow input ranges (i.e., realistic minimum and maximum values for input distributions)
- Use correlation to introduce dependencies between input variables

Triangular and uniform distributions are widely accepted standards in well and time cost modelling (Akins, et al., 2005). A main assumption is that the actual cost of each input is within an interval bounded

by a minimum and a maximum value (Gu & Gudmestad, 2012). Williamson, et al. (2006) list common pitfalls when choosing distribution parameters:

- Defining the minimum and maximum values from the minimum and maximum of the data values, as it is unlikely that the historical data contains that more extreme values possible.
- Defining the most-likely value as the mean or median of the data set, as give an overestimated or underestimated forecast result for left- and right-skewed forecast input, respectively.
- Relying exclusively on calculated distribution parameters without necessarily understanding the data, or doing proper quality assurance of it.

Murtha & Janusz (1995) and Murtha (1997) states that a particular distribution is indicated by a P_{10} and a P_{90} value (or alternatively using P_5 and P_{95}), along with a measure of central tendency, such as median (P_{50}) or mode. Distributions of time and cost parameters are generally skewed right, giving a tail of large values with a low probability of occurrence The triangular distribution is specified by its minimum (P_0), mode, and maximum (P_{100}). For the normal or lognormal distributions, the corresponding mean and standard deviation can be solved for using a set of basic equations. Using (9), observations of any normal random variable X can be transformed into a new set of observations of a normal random variable Z with mean 0 and variance 1, known as the *standard normal distribution* (Walpole, et al., 2012, pp. 176-177). For the normal distribution, the unknown mean m and standard deviation s are found by rearranging (10) and solving (11). -1.28 and 1.28 are the areas under the standard normal curve corresponding to $P(Z < z)$ for P_{10} and P_{90}, respectively.

$$Z = \frac{X - \mu}{\sigma} \tag{9}$$

$$-1.28 = \frac{P_{10} - m}{s}, \quad 1.28 = \frac{P_{90} - m}{s} \tag{10}$$

$$m = \frac{P_{10} + P_{90}}{2} \tag{11}$$

For the lognormal distribution, X is a lognormal variable with mean m' and standard deviation s', and $\ln(X)$ is normally distributed with parameters m and s. These values are related to the minimum and maximum estimates, P_{10} and P_{90}, by (12)-(14).

$$m' = e^{m+\frac{s^2}{2}} \tag{12}$$

$$s' = m'\sqrt{e^{s^2} - 1} \tag{13}$$

$$-1.28 = \frac{\ln(P_{10}) - m}{s}, \quad 1.28 = \frac{\ln(P_{90}) - m}{s} \tag{14}$$

Conoco refined the true limits to the range for a variable (i.e., class boundaries) by using worst- and best-case assumption, and evaluating the probability and the direction(s) for these boundaries to change in the future (Kitchel, et al., 1997). Industry practice for choosing input distributions for various cost items and required time (or number of days) for an activity are typically modelled by either normal, lognormal, and triangular distributions (Kitchel, et al., 1997). Rig costs are modelled by a uniform distribution in local markets (where there are small variations in day rates), while triangular, normal, or lognormal distributions are used for global operations based on rig specifications, market conditions,

and timing. Costs associated with (de)mobilizing a drilling unit are influenced by location remoteness, rig-standby rates, fuel consumption, and possible upgrades. Uncertainty in cost of time-related services (e.g., boats, aircraft, base/warehouse, mud logging, measurement while drilling (MWD), and rental tools) is related to drilling time spent, hence the respective contractor rates are applied directly (Kitchel, et al., 1997).

6.2.3 Development Costs

General Approach

Considering the CAPEX of the project and each of its sub-systems, the lower estimate, the method described in Chapter 6.2.2 is applied. The P_{10} value is taken as the costs found in SRK Consulting (2010, pp. 210-217) before contingency is added, which is found in Appendix M. The upper value P_{90} is found by taking the P_{10}value, adding 17.5 % contingency (SRK Consulting, 2010, p. 214), and multiplying by 1.57. The latter corresponds to the average cost overrun of 57 % in European oil and gas megaprojects (EY, 2014, pp. 4-5). According to EY (2014, pp. 4-5) based on cost data for 205 out of 365 evaluated European megaprojects, 53 % have cost overruns.

RALS

The estimated CAPEX of the RALS for Solwara 1 is done for an ordered riser length of 1,700 m. However, Nautilus Minerals has an option for additional 800 m giving a total riser length of 2,500 m (Technip, 2008), which also is the maximum design depth for the RALS and SSLP. For an operation at the AMOR, a riser length of 2,500 m would enable operation along the entire ridge, including the 2,300 m water depth at Loki's Castle. Thus, the part of the RALS' CAPEX that is made up by the production riser is scaled by a length factor of $2{,}500/1{,}700 \approx 1.47$.

DWP

The DWP is the sub-system with the most detailed CAPEX estimate with respect to listed cost items. An uncertainty of $\pm$30-40 % is suggested (SRK Consulting, 2010, p. 216), and an additional allowance of 10 % is added to the estimate. Thus, an uncertainty of $\pm$40 % is taken around the

6.2.4 Operational Costs

Breakdown Structure

The OPEX structure of the overall production system is shown in Figure 6-3. Combining the cost structure in shipping with that of offshore O&G, both elaborated on in Chapter 1177510768.172, the cost breakdown in Figure 6-4 is applied in the estimates for the OPEX of the PSV. The highlighted (light blue) costs are daily running costs.

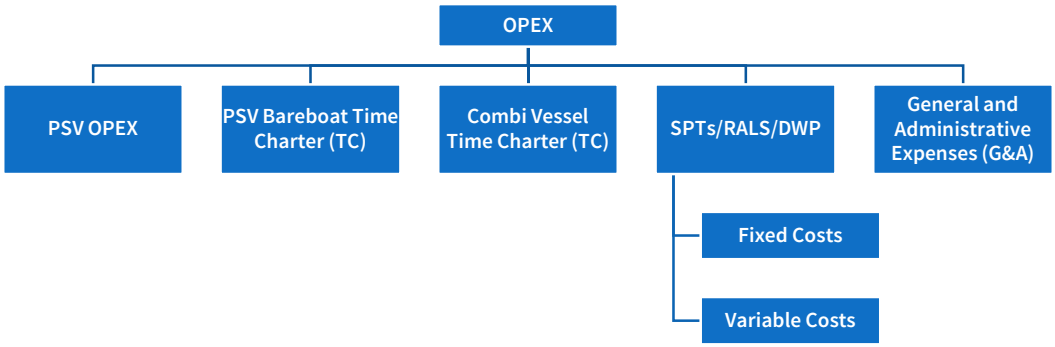

Figure 6-3 – OPEX structure for seafloor production system.

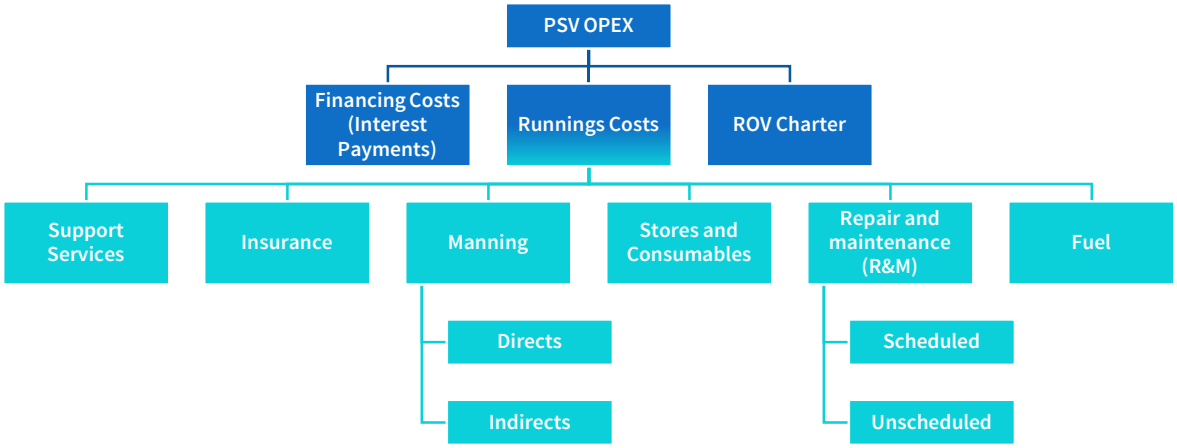

Figure 6-4 – OPEX structure for PSV.

Assumed Input Parameters

The following assumptions are made with respect to fixed OPEX for the overall seafloor production system:

- **Time charter (TC) rates** for the PSV and the combined bulk and supply vessel are based on the collected data and discussion in Appendix H. Ship leasing may occur in the form of a bareboat charter (i.e., chartering a vessel with no crew or provisions included), and is categorized as a financial or operational lease based on whether a non-cancellation clause features in the contract, see Appendix E. Assumed vessel TC rates are found in Table 7-3.
- **General & Administrative Expenses (G&A)** are taken to be constant at $1.5 \cdot 10^6$ USD/year (corresponding to 4,110 USD/day), which is based on a break-even analysis for a semi-submersible by Odfjell Invest (2006, pp. 7-8).
- **SPTs and RALS**
    - **Fixed OPEX** is assumed to constitute two vendor representatives (i.e., two for each of the two systems) at all times. The cost is taken as the average of supervisor and pilot/technicians from Oceaneering (2010). Both the rates and the crew overview are found in Appendix I.
    - **Variable OPEX** is taken as the per-tonnage amount [USD/t] as stated by (SRK Consulting (2010), also seen in Appendix L, and is assumed to cover maintenance and repair of the various production system. Thus, such costs do not accumulative when the production is on halt.

Table 6-1 – Assumed vessel rate distributions, ref. Appendix H.

Vessel Rates	P10 [USD/day]	P10 [M USD/year]	P90 [USD/day]	P90 [M USD/year]
Production Support Vessel (PSV)	199,910	72.967	400,000	146.000
Combined Bulk and Supply Vessel	15,000	5.475	40,000	14.600

6.3 Spreadsheet Models of System Flow Rate and Production Profile

6.3.1 Distribution of Significant Wave Height

The significant wave height H_s is defined as the "*mean of the one-third highest waves*" (Myrhaug & Lian, 2014, p. 14), and its estimator is denoted H_{m0} if it is calculated from a wave spectrum. A given sea state is characterized by significant wave height H_s and spectral peak period T_p. Using the MATLAB code in Appendix O, a joint frequency table (i.e., scatter diagram) of H_{m0} and T_p is established for each month based on the hindcast data. The upper bounds of the T_p classes range from 1-22 s (with a class width of 1 s), and the upper bounds of the H_{m0} classes range from 0.5-18.5 m, using a class width of 0.5 m. The estimate of the cumulative distribution function $F_{H_{m0}}(h)$ (i.e., cumulative probability) of each H_{m0} class is calculated from (15),

$$\hat{F}_{H_{m0}}(H_{m0}) = \frac{n_{H_{m0}}}{n+1} \tag{15}$$

where n is the total number of observations, and $n_{H_{m0}}$ is the number of observations less or equal to H_{m0}. After establishing the scatter diagrams (and corresponding cumulative probabilities), the mean value $\overline{H}$ and standard deviation σ_H can be found for each month. For the 90th percentile P_{90}, there is a 10 % change that the corresponding H_s value will be exceeded that month. In long-term modelling of sea states for unrestricted operations, the maximum allowable significant wave height H_s is found from the annual exceedance probability q, or considered conditionally with respect to the season or month for which operation is planned (Haver, 2014). The probability of exceedance $P(h_m)$ is calculated in Excel after export by using (16).

$$P(H > h_m) = P(h_m) = 1 - F_H(h_m) \tag{16}$$

6.3.2 Environmental Criteria for Operations

Based on the discussion in Chapter 5.3, as well as conversations with industry professionals, the environmental criteria for various operations are listed in Table 6-2.

Table 6-2 – Assumed operational criteria.

Operation	H_s Criterion [m]
SPTs through splash-zone	5.0
SSLP through splash-zone	3.0
Heave compensation of RALS	5.0

6.4 Implementation in GeoX

6.4.1 Overview

As described by GeoKnowledge (2003), GeoX is a software package for exploration prospect risk, resource and value (RRV) assessment of plays and prospects. It is widely used in the industry by more than 100 O&G companies worldwide (Schlumberger, 2012), including Statoil, which uses it for exploration drilling only. GeoX was developed by the Norwegian company GeoKnowledge that was acquired by Schlumberger in 2012. As illustrated in Figure 6-5, the software consists of various modules. Resource and geotechnical risk assessment are performed in "gProspectR" and "gPlayR". By establishing a prospect valuation model in "gFullCycle", a complete analysis of prospect and field economics can be performed, such as for the subsea production system in the case of this thesis. The latter takes costs, tax regime, and commodity prices as inputs, and outputs are discussion trees and project evaluation parameters, such as NPV, IRR and EMV. The economic calculations can be run as either a deterministic or Monte Carlo simulation. Thus, to summarize:

- **"Segment Analysis"** – geological modelling of the recoverable resource(s)
- **"Full Cycle Analysis"** – economical production system (and segment) evaluation by modelling of production profile/rates and costs

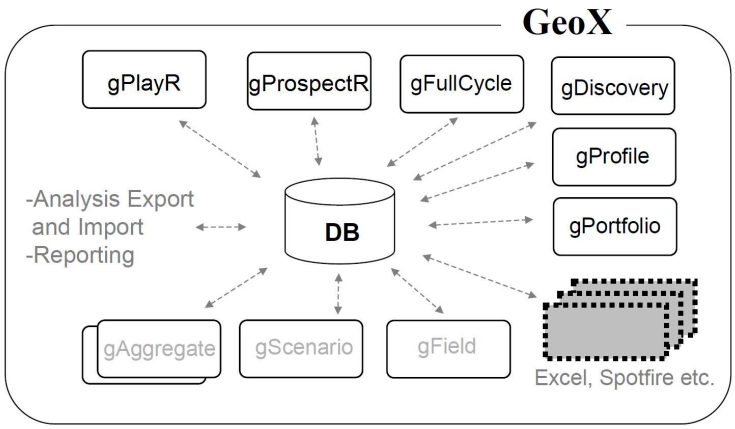

Figure 6-5 – GeoX overview. Modified from GeoKnowledge (2003).

6.4.2 Analysis Build-Up

Figure 6-6 shows the relevant components that go into the "Segment Analysis" in GeoX, which results in a "Resource Diagram" that serves as the basis for the project revenue in the "Full Cycle Analysis".

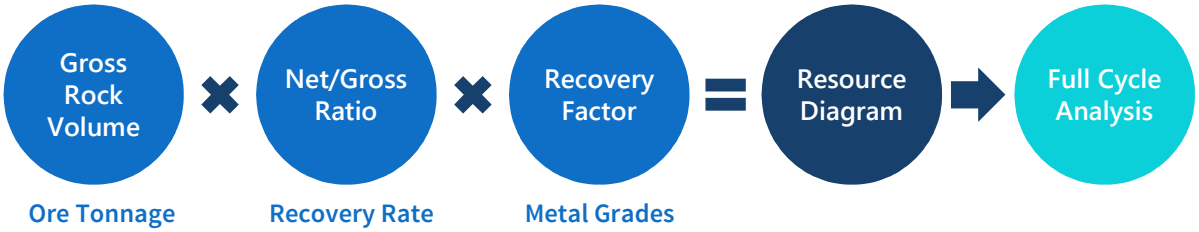

Figure 6-6 – "Segment Analysis" components and export to "Full Cycle Analysis" in GeoX, with corresponding mining terms below.

6.4.3 General Modelling

Terminology
All parameters and units in GeoX are related to O&G terminology. Thus, corresponding parameters when modelling a mining project are applied, as listed in Table 6-3.

Table 6-3 – Converting GeoX parameters from oil and gas to mining terminology.

Original Terms in GeoX	Terms Applied in Analyses
Oil	Copper (Cu)
Non-Associated Gas	Zinc (Zn)
Condensate	Silver (Ag)
Associated Gas	Gold (Au)
Gross Rock Volume	Ore Tonnage
Net/Gross Ratio	Recovery Rate
Recovery Factor	Metal Grades

Case Definitions
Having an as-simple-as-possible baseline simulation is useful as a starting point, as both the number of input parameters and the uncertainty in modelling are reduced to a minimum. The easiest and simplest way to model a deposit in GeoX is by doing a pure "Oil Case" simulation. Thus, oil is the only hydrocarbon (HC) phase that is present and marketable.

Thus, two different approaches are used for the modelling the metal grade of the deposit in GeoX, which is determined when the "Segment Analysis" is defined/constructed:

- **Case I** – The combined grade of the metals is modelled as copper equivalent grade in a "Oil Case" simulation, in which only the oil phase is present.
- **Case II** – The grade of each metal is modelled with individual distributions in a "Multiple Phase" simulation, in which all four hydrocarbon phases are present.

6.5 "Segment Analysis" in GeoX

6.5.1 Ore Tonnage (Gross Rock Volume)

In GeoX, the reservoir volume can be modelled directly as a "Gross Rock Volume". Thus, the ore tonnage is modelled using this parameter. The tonnage distribution (or volume distribution in the case of an petroleum reservoir) should resemble the observed deposits at the hydrothermal vent site, as presented in Chapter 2.6.2. However, when setting the bounds for the distribution, it is assumed that the deposit continuous below the seafloor and downwards into the feeder systems in a cone shape; rather similar to what is seen in Figure 2-2 and Figure 3-27. Hence, the increased distribution parameters in Table 6-4 are applied for the ore tonnage (when compared to the initial estimates in Table 2-5), and corresponds to the lognormal distribution seen in Figure 6-7.

Table 6-4 – Lognormal distribution parameters for ore tonnage [1E6 t]

F99.5	1.0
F0.5	5.0
Mode	2.0

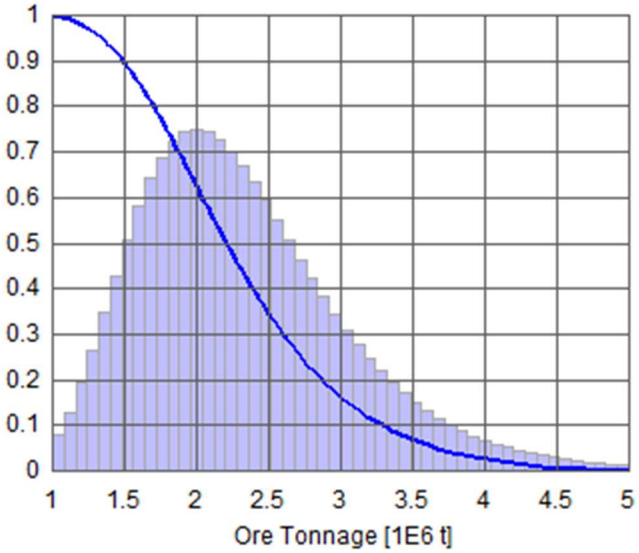

Figure 6-7 – Ore tonnage.

6.5.2 Recovery Rate (Net/Gross Ratio)

Recovery-Over-Estimated Factor in Mining

An important performance factor in mining operations, in addition to production and profit, is the recovery-over-estimated factor R/E, which is defined as the recovered mineral output or grade (i.e., the actual production results) divided by the corresponding expected value (Garnett, 1996). The R/E factor provides a long-term measurement of performance (on a monthly, quarterly, or plan basis), and has the following four components, as argued by Garnett (1996), all of which ideally approaches 1.0:

- **Estimation factor** indicates errors involved in determining the grade and sediment thickness at individual sample sites, and shows typically the greatest deviation from 1.
- **Selection factor** expresses the ability of the mining unit selectively to extract individual blocks at the expected average grade with minimum dilution and losses of ore.
- **Excavation factor** is the amount of total volume of sediments in the mining included within the mining plan that is excavated.
- **Treatment factor** reflects the recovery plant equipment, the conditions under which it is operated, the physical features of the minerals and host sediments, and the throughput rate (of the production system. It approximates the metallurgical recovery of the plant and measures the extraction of potentially recoverable mineral content, not the total.

As further described by Garnett (1996), the *estimation factor* depends on the characteristics of the marine sediments and the contained minerals, the sampling method, the sample size, and the means of sample collection and treatment. The *selection factor* is inversely proportional to the sample spacing, which is dependent on the grade variability, the magnitude of the cut-off grade relative to the average grade, and the desired mining selectivity. Aspects that affects the *excavation factor* include irregularity in bedrock profile, penetration of excavating tool, and short-cut operating procedures.

Recovery Rate

The volume descriptive parameter "Net/Gross Ratio" is defined in GeoX as the "*the proportion of the reservoir thickness made up of sand*", and is used to model the recovery rate accounting for two factors:

- Fraction of the ore volume that is gathered by the SPTs
- Fraction of metal contained within the dewatered ore that is extractable by the refinery plant during the onshore processing

The assumed mining efficiency of the SPTs is the product of fractions taken from SRK Consulting (2010, p. 193), and defines the gathered cut per net ore tonnage. The subsea mining efficiency accounts for ore lost from fines within mining plume and from bench edges settling outside accessible mining zone. It is multiplied with an assumed onshore processing recovery rate that ranges 0.8-1. The resulting recovery rate is assumed normally distributed between the minimum and maximum values in Table 6-5.

Table 6-5 – Recovery rate distributions.

Parameter	Min.	Max.
Design Cut / Net Ore Tonnage	1.00	1.00
Mined Cut / Design Cut Ratio	0.85	0.95
Gathered Cut / Mined Cut Ratio	0.85	0.95
Subsea Mining Efficiency	0.72	0.90
Onshore Processing Recovery	0.80	1.00
Resulting Recovery Rate	**0.58**	**0.90**

6.5.3 Metal Grades (Recovery Rate)

Case I – Copper Equivalent

The general idea of copper equivalent Cu_{eq} is to convert the grades all the individual metals present in a deposit into a corresponding copper grade, and summing them by applying a weight factor consisting of the respective metal grade, price ratio (with respect to copper price), and ore texture factor. Historical values for metal prices, such as those seen in Chapter 3.1.2, are used to establish distributions for the price ratios. Depending on the ore texture (i.e., each metal not being uniformly distributed throughout the volume), the recovery rate of the four metals will be different. This is accounted for by using the typical mill recovery rates that are listed in Table 6-6. Alternatively, a uniform distribution between 0.6 and 0.9 could be applied for the ore texture to indicate the large degree of uncertainty. The copper equivalent $Cu_{eq,j}$ for each iteration j in the Monte Carlo simulation is found from (17),

$$Cu_{eq,j} = \sum_{i=1}^{4} \text{Metal Grade}_i \cdot \text{Price Ratio}_i \cdot \text{Ore Texture}_i \tag{17}$$

and is the sum of the contributions from each of the four metals i, which the product of the probabilistic metal grade, price ratio, and ore texture values for the respective metals. From the approach described above , the copper equivalent is calculate as shown in Appendix N with the MATLAB script in Appendix P. The combined metal grade is modelled using the input parameter "Recovery Rate" for the "Pure Oil" simulation. Figure 6-8 shows the resulting grade distribution, and its parameters as listed in Table 6-7.

Table 6-6 – Mill recoveries (Rudenno, 2012, pp. 434-492).

	Cu	Au	Ag	Zn
Lower	0.850	0.850	0.367	0.695
Upper	0.950	0.980	0.706	0.891

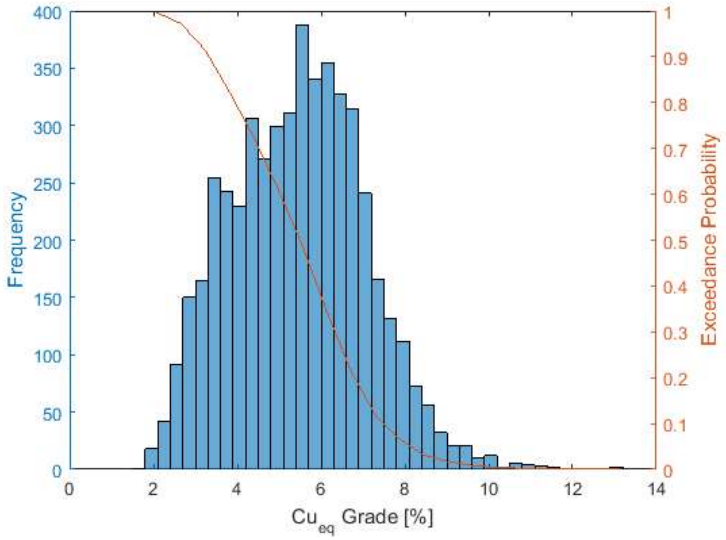

Figure 6-8 – Simulated distribution of copper equivalent grade.

Table 6-7 – Distribution parameters, ref. Figure 6-8.

Parameter	Cu_{eq} Grade [-]
Mean	0.05459
Median, P_{50}	0.05494
Std. dev.	0.01608
$P_{99.5}$	0.02118
P_{90}	0.03327
P_{10}	0.07500
$P_{0.5}$	0.10068

Case II – Individual Metal Grade Distributions

The metal grades are modelled separately using the "Recovery Factor" input parameter for each of the hydrocarbon phases, applying the distributions presented in Chapter 2.6.2.

6.5.4 Risk Factors: Play versus Local Segment Considerations

The Concept of Play-Based Exploration

The concept of play-based exploration (PBE) is based on various levels of geological details, as seen in Figure 6-9 (a), which correspond to the exploration pyramid in Figure 6-9 (b). The level of detail (and the associated cost of acquiring knowledge) increases as one gets closer to the top. The consists of the building blocks seen in which constitutes the following levels (Royal Dutch Shell, 2013, p. 7). Based on definitions of Royal Dutch Shell (2013, pp. 7-8) and Sinding-Larsen (2015, pp. 8-9), the following terms elaborates on the concept of play-based exploration (in ascending level of detail):

- **Basin** is a natural petroleum system that links an active (or once active) source rock to geologic elements and processes that are essential for a hydrocarbon accumulation to exist. Establishing a basin entails verifying essential elements of the petroleum system from which the potential for generating and trapping hydrocarbons are determined, among other features.
- **Play** defines a group of hydrocarbon fields and prospects within a basin, having a chance for charge, reservoir, and trap, and belonging to a geologically related stratigraphic unit. An understanding of the petroleum system in the basin leads to the identification, mapping and quantification of plays, and eventually to identification of "sweet spots".
- **Play segment** is a locally-defined subdivision of a geologic play (or part-play) that is accessible and chosen to be accessed. Segments may have different risks, contract, reservoir parameters, or economic values.
- **Prospect** expresses a potential trap and a group of segments that may be developed as a single economic project. A successful prospect turns into an O&G field when drilled. Many prospects can exist in one play, and one prospect may span multiple plays. Most play execution activity is concerned with defining prospects; seismic evaluation and other maturation activities, and eventually drilling of selected prospects from a portfolio. A geological model is built, before volumetrics, technical risk and confidence are assessed for a range of both models and prospects. Fields and prospects that share common geological controls have the same probability of trapped hydrocarbon being both present and capable of being produced from the formation somewhere in the play segment (Royal Dutch Shell, 2013, p. 26).

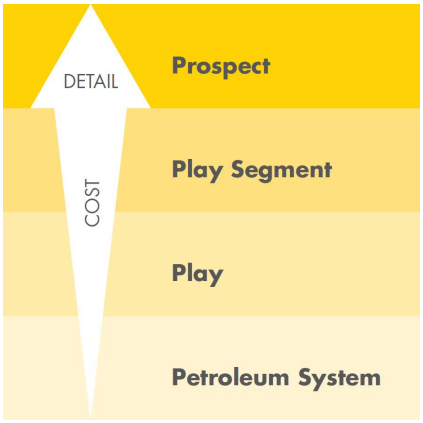

(a) Geological levels of detail

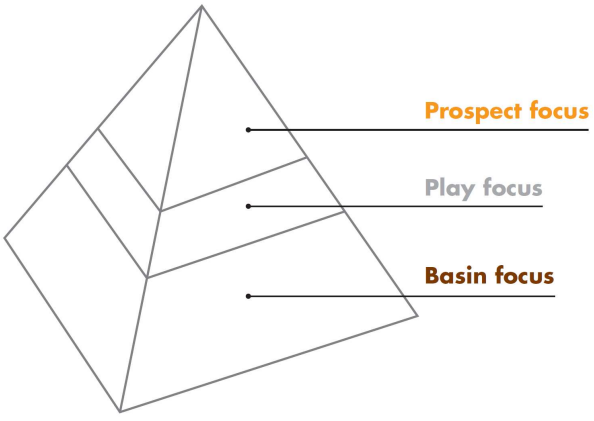

(b) Exploration pyramid

Figure 6-9 – Play-based exploration (Royal Dutch Shell, 2013, pp. 4, 8).

Risk Factors

As described above, the geological features are modelled at different levels; segment level and play level. The resource estimate applied in this thesis is for the AMOR as a whole; at play level. To account for the uncertainty related to whether or not the resource estimate describes the deposit at Loki's Castle, which is defined at segment level, the risk factor for source and migration is set to 0.45. This means that not all hydrothermal vents are expected to be productive (or can accumulate metals). The probabilities for play and segment used in the GeoX simulation are listed in Table 6-8, and are input parameters under "Risk" and "Initial Risk Assessment" in the "Segment Analysis". The marginal play probability and the conditional segment probability are the product of the two columns, respectively. The above gives a dry hole risk for Loki's Castle as a segment is 0.55 (i.e., a probability of 0.45 that the resource estimate is present at the site). Thus, the risked resource curve is 0.45 times the initial curve, as seen in Figure 7-10.

Table 6-8 – Play and segment probabilities.

Risk factor	P(play)	P(segment | play)
Trap and Seal	1.00	1.00
Reservoir Presence	1.00	1.00
Reservoir Quality	1.00	1.00
Source and Migration	1.00	0.45

6.6 "Full Cycle Analysis" in GeoX

6.6.1 General

Notation

Due to issues with modelling gas wells (at such low production rates as note that all the "Full Cycle" analyses are performed for the

Input Parameters

Table 6-9 lists the input parameters that are set as constant for the analyses. Due high degree of financial risk involved with deep-sea mining project, a quite high discount rate would be applied. However, for this analysis uncertainties are captured by the probabilistic approach that is applied, and does not need to be compensated for in the same manner by a high discount rate. Note that Markussen (2000) refers to an unpublished report on calculations performed by Bechtel Corporation for a pilot concept for nodule mining (with 30 % equity and 70 % debt), which have a return of investment (ROI) and a return on equity (ROE) of 21 % and 29 %, respectively.

Table 6-9 – Fixed input parameters for all "Full Cycle" analyses.

Parameter	Value
Project Start Date	January 1, 2016
Net Present Value (NPV) Date	January 1, 2016
Discount Rate	10 %

6.6.2 Production System Modelling

Production System Implementation and Activity Scheduling

The overall production system is modelled by defining two types of "Activities" that are linked to one another, as seen from the arrow in Figure 6-10:

- **"Development" activity** includes modelling the duration of the development phase of the project and associated CAPEX distribution. Furthermore, is allows modelling of individual parts of the production system is split into the "Development Components" below, see Figure 6-11:
  - Seafloor Production Tools (SPTs)
  - Riser and Lifting System (RALS)
  - Dewatering Plant (DWP)
  - Logistics (i.e., combined bulk and supply vessel)
  - General (covers any other parameters for the system)
- **"Field-Based Production" activity** models the production phase, in which parameters for one or multiple wells can be entered.

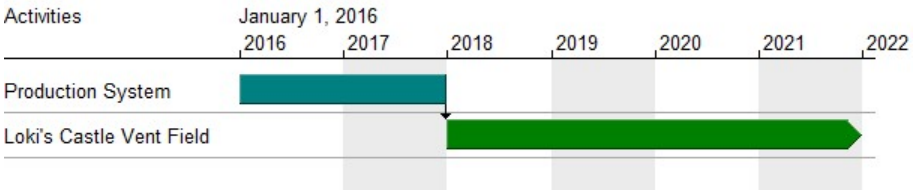

Figure 6-10 – Gantt diagram of activities.

Figure 6-11 – Production system split into "Development Components" under "Development" activity.

Production Capacities

The system's annual average production rate of 3,591 t/day, as found in Chapter 7.1.3, is lower than any of the design capacities of the individual system components. Thus, it is the limiting factor with respect to the production rate. As seen from Figure 6-12, this is modelled as a "Peak Well Rate" under the "Field-Based Production" activity. However, as the daily production "seen by" GeoX is pure metal tonnage only, the average production rate is multiplied with the mean copper equivalent grade (from Chapter 6.5.3), which gives an effective production capacity limitation of 196 t/day in pure metal tonnage. The capacities of the "Development Components" are excluded, as these are not governing the production rate of the system (as follows from the above discussion).

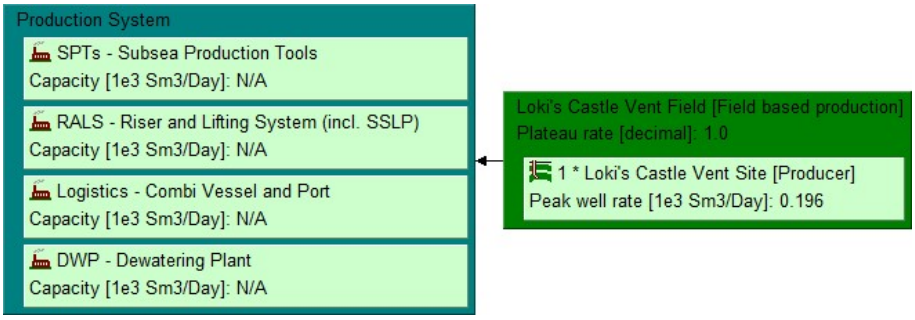

Figure 6-12 – Facilities and producers.

Production Profile and Decline Rate

As a "Field-Based Production" model is selected for Loki's Castle, hence explicit well inputs are not required (e.g., well spacing, and well flow rates). The developer of GeoX, GeoKnowledge, illustrates who to model a sample prospect in Surovtsev, et al. (2012, p. 4). In the "field-based" model, the field output or production volume is determined by three general assumptions, for which following typical values of oil and gas prospects are listed:

- **Peak production as percentage of reserves** is taken as 10 % for a reserve-coverage (RP) ratio of 10 years, which is considered the optimum depletion rate. A wide range of 8-12 % is modelled.
- **Fraction HC remaining at the end of plateau** can be in the range of 40-60 %.
- **Effective decline rate and type** of 10-15 % per annum for an exponential decline model is usual industry practice, as illustrated in Figure 6-13.

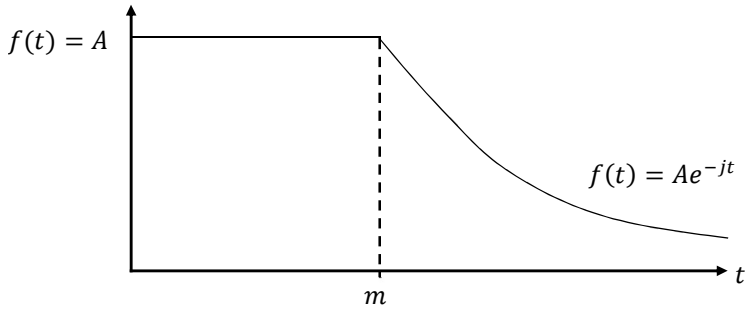

Figure 6-13 – Exponential decline in production volume for an oil well.

The production profile for a mining site has a very steep decline; at least for such a condensed site with respect to ground area as Loki's Castle. In the GeoX analysis, the production profile is manipulated by using the parameters in Table 6-10. Moreover, a "Logarithmic WOR" decline model is applied, in which WOR abbreviates water-oil ratio, with the following factors: WOR of 0.001 at both end of production (EOP); fraction remaining at EOP equal to 0; and fraction remaining hydrocarbon (HC) at start of water production is 0.99. However, which one of these two sets of production profile parameters that govern the resulting production profile is somewhat unclear.

Table 6-10 – Parameters for production profile.

Parameter	GeoX Location	Value
Fraction HC Produced Yearly at Plateau	"Field-Based Production" – "General"	1.0
Fraction Remaining HC at EOP	"Field-Based Production" – "General"	0.01
Well Plateau Factor	"Field-Based Production" – "Well Types" – "Parameters"	0.999

Development and Operational Costs

In GeoX, costs associated with the production system (and the operation as a whole) are introduce in the "Full Cycle Analysis" as described below (with reference to Figure 6-14):

- Costs for the production system in general (modelled under "General") and each of the main sub-systems (modelled as "Development Components") are modelled under one "Development" activity. For each of the "Development Components", fixed development costs (CAPEX), fixed operating costs (F-OPEX), and variable operating costs (V-OPEX) are modelled.
- The long-term charter rate of the PSV is modelled in the "Rig" tab under the "Field-Based Production" activity

For all cost items, a lognormal distribution of type "Ln3HLMn" is applied by giving three input parameters: low estimate F_{90} (equivalent to the 10th-percentile P_{10}, which is exceeded in 90 % of the cases); mean; and high estimate F_{10} (equivalent to the 90th-percentile P_{90}, which is exceeded by only 10 %). Percentiles for the development costs and mean values of the operating costs, which serves as the input parameters for the GeoX analysis, are shown in Chapter 0.

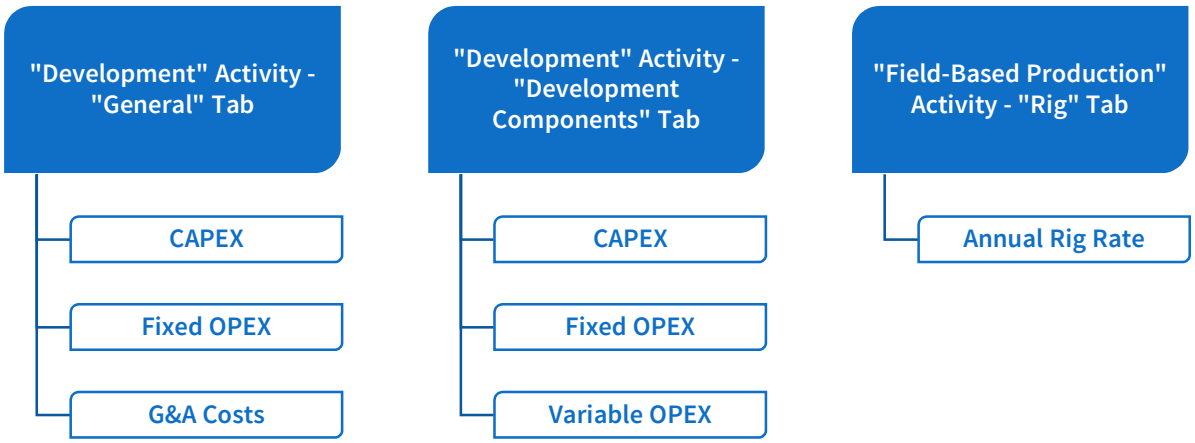

Figure 6-14 – Cost modelling in GeoX.

6.7 Economical Scenarios

The forecasts on commodity prices by The World Bank (2016), as part of the Comodity Markets Outlook for April 2016, are the basis for an estimate for metal prices over the production period (i.e., the timespan over which the project is evaluated). A low, mean and high price is found for each metal, which together constitute the individual values for each economic scenario, as listed in Table 6-11. The data set by The World Bank (2016) has forecasted prices until 2025 in nominal values, and the relative value to their 2013 value is illustrated in Figure 6-15, showing differences in the suggested development path

of the individual prices. When calculating the bounds and mean, the forecasts were rounded (i.e., rounding was applied for the mean/average values, and flooring and ceiling for the low and high values, respectively): copper and zinc prices to nearest 10^3; gold to nearest 10^5; and silver to nearest 10^4. The inflation rate and the growth rate in commodity prices are both set to 0 % in GeoX.

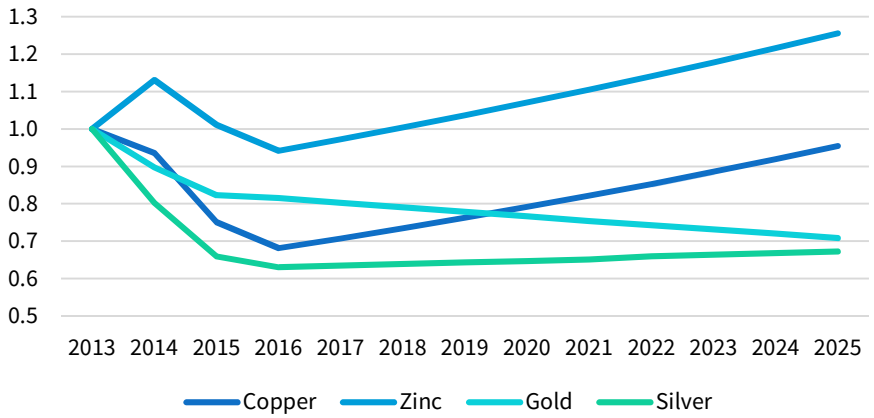

Figure 6-15 – Price development forecast; nominal values per 2013-values (The World Bank, 2016).

Table 6-11 – Metal prices [USD/t] for the economic scenarios.

Metal	Low	Mean	High
Copper	5,000	6,100	7,300
Zinc	1,800	2,100	2,400
Gold	32,200,000	36,000,000	45,400,000
Silver	480,000	530,000	770,000

6.8 Norwegian Fiscal Regimes

The tax regime can be modelled under "Fiscal Regime" in GeoX as part of a "Full Cycle Analysis". However, in this case, the cash flow overview is exported to Excel and taxation is calculated afterwards.

6.8.1 Corporate Tax

For 2016, the Norwegian corporate tax rate is fixed at 25 % (Ministry of Finance, 2016), and losses (i.e., accumulated deficits) may be carried forward indefinitely.

6.8.2 Petroleum Taxation

Regime Overview

KPMG International (2015) elaborates on the change in tax regime for fiscal year 2016:

> *"E&P companies with activities on the NCS and involved in pipeline transportation of petroleum are taxed according to special rules that include a special petroleum tax rate of 51% in addition to the general corporate tax rate of 27%. The budget 2016 proposes to reduce the corporate income tax rate to 25% (down 2%) with a corresponding increase of the "special" petroleum tax rate to 53%. Hence, the marginal tax rate of 78% would continue to apply for 'E&P companies'. […] There are no suggestions in the 2016 budget to amend the 'uplift rules' for capitalized development costs, which today is at 22% (5.5% per year over four years). Hence, the net value of the uplift is slightly increased for E&P companies with activities on the NCS. On the contrary, the tax value of deductions for interest and finance cost under the general corporate tax rate is slightly reduced for most companies."*

Based on Ministry of Finance (2016), as well as various guides by Jansen & Bjerke (2012), Samuelsen (2011), Deloitte Advokatfirma (2014) and EY (2015), the Norwegian petroleum taxation regime is summarized in the following points:

- **General features** are as below:
  - Taxation of upstream actives on the NCS is regulated by rules stated in the Petroleum Tax Act (PTA). If no rules in the PTA are applicable, the rules in the General Tax Act (GTA) applies.
  - The regime consists of direct (i.e., marginal tax) and indirect taxation (e.g., CO_2 and NO_x tax, and VAT).
  - Supplies to be used in upstream activities on the NCS are zero rated with respect to VAT.
  - Taxable income is gross income (i.e., revenue from production on the NCS as well as substitutes for such revenues, but not financial income) minus deductions. Financial income is taxable according to the GTA only.
  - The marginal tax rate is 78 %, consisting of a 25 % ordinary corporate income tax and an additional 53 % resource rent tax. These taxes are calculated independently, as described under "Calculating Taxes".
  - There is no ring fencing system between different licenses or field on the NCS.
  - 50 % of a company's onshore losses may be offset against income from offshore activities that are subject to an ordinary tax rate of 27 %.
  - Losses may be carried forward indefinitely. Tax value (78 %) of unused losses when finally ceasing exploration or production activities on the NCS are refundable by the Norwegian state.
- **Capital allowances** or depreciations are granted when calculating the basis for both the ordinary petroleum tax and the special tax.
  - **Depreciation** – For taxable income subject to a marginal tax rate of 78 %, investments made in offshore production facilities and pipelines used in extraction activities, and installations which are part of such production facilities and pipelines, are depreciated

on six-year, straight line basis (at a rate of 16.66 % per year) from the date that the CAPEX incurred.

- **Uplift** is an additional depreciation only for special tax. This accelerated capital allowance is granted on CAPEX at a total rate of 22 % (i.e., 5.5 % per year over four years) for the 53 % special tax rate.
- If production from a field is abandoned, any undepreciated capital costs subject to straight line depreciation, including uplift not utilized, may be deducted in the last year of production.

- Other investments and assets located onshore (e.g., buildings and office equipment) used in the business of extraction are depreciated on a declining balance method at rates of 0-30 % per year from when the assets are utilized, see Chapter 6.8.3. However, depreciation on such assets are deductible in the offshore regime at the 78 % tax rate.

Calculating Taxes

As described by Jansen & Bjerke (2012, p. 10), the taxation scheme outlined above, under "Regime Overview", is calculated in the following manner:

	Operating income
−	Operating costs
−	Depreciations (6-year, straight line at 16.67 %)
−	Expenses related to exploration, research and development (R&D), plug and abandonment (P&A), and decommissioning
−	Environmental taxes
−	Allocated financial costs
=	General income tax base (at 25 %)
−	Uplift (at 5.5 % per year for 4 years)
=	Special tax base (at 53 %)

6.8.3 Depreciation

KPMG International (2014, p. 3) states that all assets acquired by a business are depreciable if they are either listed in Table 6-12 (with its corresponding depreciation rate) or are documented as having lost value over time. Note that for "Class D" an additional initial depreciation applies, giving a depreciation rate for the first year of 30 %. According to Nautilus Minerals (2015, p. 50), depreciation of the seafloor production system for the Solwara 1 project (and other assets of the company) is calculated over the estimated useful life of the assets on a straight-line basis based on .

Table 6-12 – Rates for different depreciation groups.

Group	Assets	Depreciation Rates [%]
A	Office machines, etc.	30
B	Acquired (purchased) goodwill	20
C	Trucks, buses, etc.	20
D	Cars, tractors, machines, tools, instruments, inventory, etc.	20
E	Ships, vessels, rigs, etc.	14
F	Planes, helicopters	12
G	Electrical plant	5
H	Buildings and plants, hotels, restaurants, etc.	4
I	Business building	2
J	Permanent technical installations in buildings	10

Table 6-13 – Estimated useful life (Nautilus Minerals, 2015, p. 50).

Asset	Life [years]
Leasehold Improvements	3
Plant and Equipment	3-15
Office Equipment	1-20
Motor Vehicles	6-8

6.8.4 Asset Valuation

The resale value is calculated as the 2-year value in Table 6-14, while the annual deprecation is the one used for the ordinary corporate tax regime.

Table 6-14 – Asset valuation.

Class	CAPEX [M USD]	Rate, 1st yr	Value after 1 yr	Rate, 2nd yr	Value after 2 yrs	Exp. Lifetime	Annual Depr.
SPTs	117.541	30%	82.28	20%	65.82	10	11.75
RALS	151.035	30%	105.72	20%	84.58	5	30.21
DWP	28.309	14%	24.35	14%	20.94	15	1.89
General - Integration and Testing	83.439	14%	71.76	14%	61.71	15	5.56
Total	**380.323**				**233.05**		**49.41**

CHAPTER 7
Results

7.1 Estimated Production Rate and Profile

7.1.1 Environmental Conditions

As parts of the seafloor production system have operational limits with respect to environmental conditions, the environmental data for the operational site must be evaluated. Statoil has provided hindcast data for a location (73°61′ N, 08°15′ E) close to Loki's Castle (73°33′ N, 08°09′ E) from the Norwegian hindcast weather database NORA10[16]. The mean value $\overline{H}$ and standard deviation σ_H for each month are listed together with corresponding cumulative probabilities in Table 7-1 and plotted in Figure 7-1.

Table 7-1 – Corresponding H_s for monthly cumulative probabilities, ref. Figure 7-1.

Distr. Parameters	Jan	Feb	Mar	Apr	May	Jun	Jul	Aug	Sep	Oct	Nov	Dec
Mean	3.6	3.5	3.2	2.5	2.0	1.7	1.6	1.7	2.3	2.8	3.1	3.5
Std. dev.	1.6	1.6	1.4	1.2	1.0	0.7	0.6	0.7	1.0	1.3	1.4	1.5
P10	1.6	1.5	1.4	1.0	0.7	0.7	0.6	0.7	1.0	1.2	1.4	1.5
P50	3.0	2.9	2.7	2.0	1.5	1.3	1.2	1.3	1.8	2.3	2.6	2.9
P90	5.4	5.5	4.9	3.9	3.0	2.4	2.1	2.4	3.4	4.3	4.8	5.4

[16] Norwegian Reanalysis 10 km (NORA10) gives wind and waves every 3 h for the entire Norwegian continental shelf and covers the period from September 1, 1957 until today.

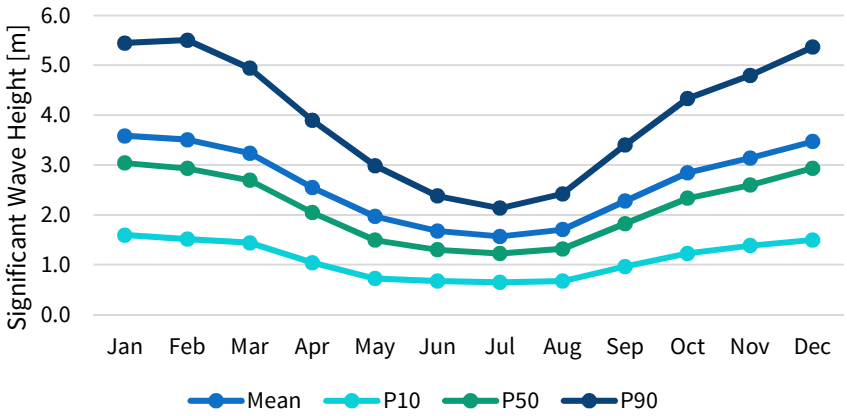

Figure 7-1 – Monthly cumulative probability $P(H_s)$ for H_s.

The probability of exceedance $P(h_m)$ is plotted for February (harshest winter month) and July (mildest summer month) in Figure 7-2. There are some inconsistencies in the function values for the lowest H_s values (due to a too large class width regarding the large number of observations in the lowest range). However, this is not of concern, as the operational limits for H_s being evaluated are in the range 2-5 m. Table 7-2 shows the monthly exceedance probability for some specific H_s values.

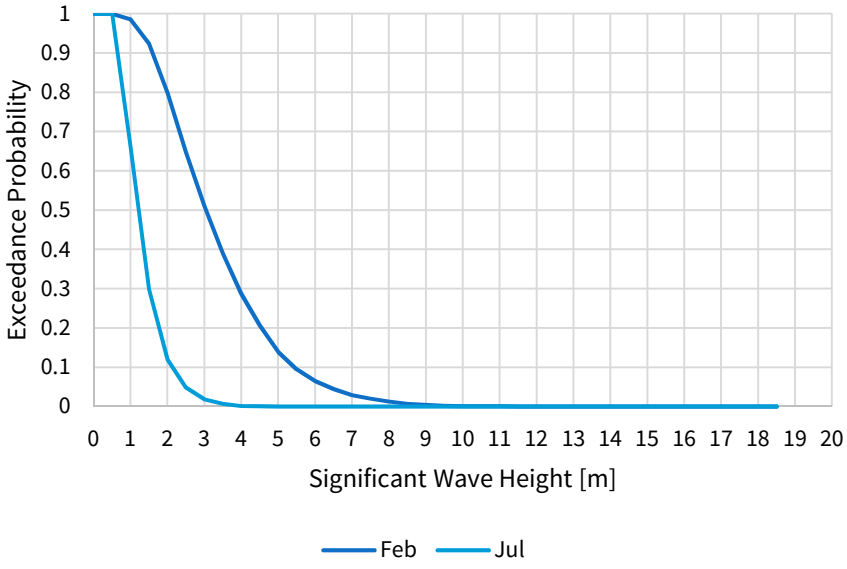

Figure 7-2 – Probability of exceedance for worst and best month (February and July).

Table 7-2 – Probability of exceedance of H_s for each month.

H_s	Jan	Feb	Mar	Apr	May	Jun	Jul	Aug	Sep	Oct	Nov	Dec
2.0	0.798	0.768	0.734	0.515	0.299	0.172	0.119	0.182	0.418	0.619	0.707	0.769
3.0	0.510	0.482	0.412	0.235	0.098	0.032	0.019	0.037	0.151	0.299	0.384	0.482
4.0	0.288	0.269	0.206	0.087	0.026	0.004	0.002	0.007	0.052	0.132	0.189	0.267
5.0	0.139	0.140	0.095	0.030	0.008	0.000	0.000	0.002	0.015	0.050	0.082	0.134

7.1.2 Flow Restrictions and System Capacity

The assumptions made in Chapter 5.2 with respect to limiting factors on the production rate govern the following calculations. The flow restrictions on each sub-system govern the capacity of the production system. According to SRK Consulting (2010, p. 193), the design basis for the CM is a slurry flow rate 1,000 m^3/h, which gives the mean solids flow rates when multiplied with the solids-slurry ratios. Thus, a slurry density of 12 % gives a solids flow rate through the CM of 120 m^3/h. The density of the SMS ore is considered to be constant with respect to water depth. However, the required pumping power increases with depth as the slurry column to be lifted is heavier. The resulting capacities of the CM are calculated for a ore density range of 2.5-3.8 SG given by Leach, et al. (2012), and are shown in Table 7-3.

Table 7-3 – Capacity of Collecting Machine (CM) for various solid-slurry ratios.

Capacity [t/day]	Ore Density, SG	10 %	12 %	14 %
Lower	2.5	6,000	7,200	8,400
Mean	3.3	7,920	9,504	11,088
Upper	3.8	9,120	10,944	12,768

The slurry lift rate of the SSLP is 863 m^3/h, which corresponds to a solids flow rate that ranges 103.56-120.82 m^3/h (for 10-14 %). Technip (2008) states that the design capacity of the RALS is 6,000 t/day, which corresponds well with the calculated lowest capacities in Table 7-4.

Table 7-4 – Capacity of Subsea Slurry Lift Pump (SSLP) for various solid-slurry ratios.

Capacity [t/day]	Ore Density, SG	10 %	12 %	14 %
Lower	2.5	5,178	6,214	7,249
Mean	3.3	6,835	8,202	9,569
Upper	3.8	7,871	9,445	11,019

The DWP also has a design basis at 1,000 m^3/h (SRK Consulting, 2010, p. 176), which gives the same capacity as for the CM. As seen from the calculated value above, the limiting sub-system with respect to flow rate is the SSLP.

7.1.3 Production Profile

System Operability

Availability is defined as the "*probability that a system or component is performing its required function at a given point in time or over a stated period of time when operated and maintained in a prescribed manner*" (Utne & Rasmussen, 2013, p. 8.1), and mathematically as in (18).

$$\text{Availability} = \frac{\text{Uptime}}{\text{Uptime} + \text{Downtime}} \tag{18}$$

In SRK Consulting (2010, p. 202), the system outage (as defined in Chapter 3.6.4) is stated to be 16.3 % of a normalized year – 2,216 h out of 13,808 h for the Solwara 1 schedule. This includes RALS maintenance, which involves retrieving the SSLP (by pulling the entire production riser string) to the

surface vessel. Maintenance is assumed to take 7 days each 100 days (SRK Consulting, 2010, p. 193). Considering that the design lifetime of the elastomeric diaphragm in the pump chambers is stated to be about 6 months of continuous operation (Leach, et al., 2012), it is assumed that the SSLP is overhauled two times per year. Further, assuming that each overhaul will take 7 days at Solwara 1, the duration of each overhaul will be 7.76 days at Loki's Castle when considering the difference in water depth, thus difference in pulling/running time of production riser with SSLP. Both running speed and pulling speed is assumed to be 66.15 m/h (3.5 joint/h).

Table 7-5 – Maintenance cycles for each sub-system.

Component	AC	BC	CM	RALS
Time Between Overhaul (TBO) [days]	3.5	3.5	6.5	174.7
Overhaul Duration [days]	1.0	1.0	1.0	7.8
Effective Maintenance Cycle Duration [days]	4.5	4.5	7.5	182.5
Annual Number of Maintenance Cycles	81.1	81.1	48.7	2.0

The ideal timing for SSLP maintenance is found as the maximum value in Table 7-6, which is the sum of wait-on-weather (WOW) time due to sea states exceeding the criterion of 5 m H_s for combinations of two months half-a-year apart. Thus, SSLP maintenance is chosen to be performed in January and July.

Table 7-6 – Combined WOW of RALS for pair of months half-a-year apart [days].

Jan & Jul	Feb & Aug	Mar & Sep	Apr & Oct	May & Nov	Jun & Dec
4.323	3.973	3.401	2.467	2.724	4.161

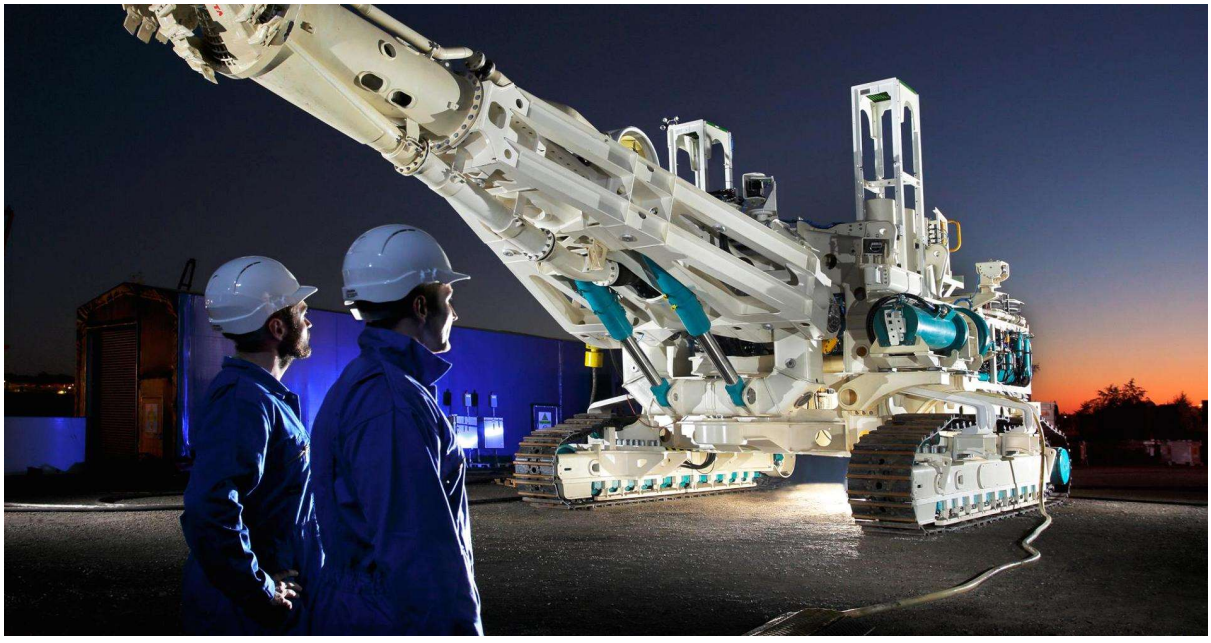

Figure 7-3 – Auxiliary Cutter (AC).

The net operating times in Table 7-8 are found by multiplying the available time (in line *e* and *k*) with the fractions in Table 7-7. The net operating time (in percent of total calendar year) is seen in Table 7-9.

Table 7-7 – Net operating time per available time.

Systems	Net Ops./Avail.
AC and BC	44.3 %
CM and RALS	62.6 %

Table 7-8 – Estimated production schedule for Loki's Castle vent field.

	Parameter [days]	Jan	Feb	Mar	Apr	May	Jun	Jul	Aug	Sep	Oct	Nov	Dec
a	Days per month	31.0	28.0	31.0	30.0	31.0	30.0	31.0	31.0	30.0	31.0	30.0	31.0
b	Vessel outage	3.7	3.4	3.7	3.6	3.7	3.6	3.7	3.7	3.6	3.7	3.6	3.7
c	Scheduled time, AC and BC	27.3	24.6	27.3	26.4	27.3	26.4	27.3	27.3	26.4	27.3	26.4	27.3
d	Maintenance, AC and BC	6.0	5.0	6.0	5.0	6.0	5.0	6.0	6.0	5.0	6.0	5.0	6.0
e	Available time, AC and BC	21.3	19.6	21.3	21.4	21.3	21.4	21.3	21.3	21.4	21.3	21.4	21.3
f	Maintenance, RALS	7.8	0.0	0.0	0.0	0.0	0.0	7.8	0.0	0.0	0.0	0.0	0.0
g	WOW, RALS	2.7	3.4	2.6	0.8	0.2	0.0	0.0	0.1	0.4	1.4	2.2	3.7
h	Total downtime, RALS	10.5	3.4	2.6	0.8	0.2	0.0	7.8	0.1	0.4	1.4	2.2	3.7
i	Scheduled time, CM	16.8	21.2	24.7	25.6	27.0	26.4	19.5	27.2	26.0	25.9	24.2	23.6
j	Maintenance, CM	2.0	2.0	3.0	3.0	3.0	3.0	2.0	3.0	3.0	3.0	3.0	3.0
k	Available time, CM	14.8	19.2	21.7	22.6	24.0	23.4	17.5	24.2	23.0	22.9	21.2	20.6
	Net operating time, CM	**9.3**	**12.0**	**13.6**	**14.1**	**15.0**	**14.6**	**11.0**	**15.2**	**14.4**	**14.3**	**13.3**	**12.9**

Table 7-9 - Net operating time as percent of total calendar year.

System	Jan	Feb	Mar	Apr	May	Jun	Jul	Aug	Sep	Oct	Nov	Dec
AC and BC	30	31	30	32	30	32	30	30	32	30	32	30
CM	30	43	44	47	49	49	35	49	48	46	44	42

Production Rate

As concluded in Chapter 7.1.2, the SSLP is the limiting system component with respect to production rate. When calculating the production volume (see Table 7-10) and the average production rate (see Table 7-11) for each month, a solids flow rate of 8,202 t/day is used, which corresponds to the mean values of both ore density and solids-slurry ratio (i.e., 3.3 SG and 12 %, respectively). The average production rate is found by dividing the monthly production volumes on the total number of days each month, and the annual average production rate of 3,591 t/day is the average of these. The sum of the monthly production volumes gives an annual production volume of 1,309,917 t which corresponds well with Technip annual production target for the Solwara 1 system at $1.3 \cdot 10^6$ t per annum.

Table 7-10 – Monthly production volume (3.3 SG, 12 %).

Jan	Feb	Mar	Apr	May	Jun	Jul	Aug	Sep	Oct	Nov	Dec
75,956	98,504	111,341	116,013	123,430	120,081	89,913	124,350	117,998	117,541	108,966	105,823

Table 7-11 – Average production rate for each month in t/day (3.3 SG, 12 %).

Jan	Feb	Mar	Apr	May	Jun	Jul	Aug	Sep	Oct	Nov	Dec
2,450	3,518	3,592	3,867	3,982	4,003	2,900	4,011	3,933	3,792	3,632	3,414

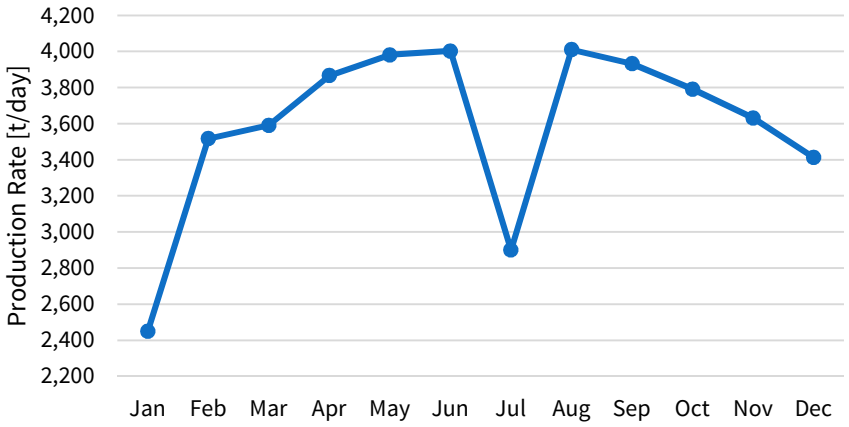

Figure 7-4 – Average production rate for Loki's Castle vent field (3.3 SG, 12 %).

7.2 Estimating Costs

7.2.1 Development Costs

Estimates

For the estimates on development costs, the approach described in Chapter 6.2.3 is used – based on the method of Chapter 6.2.2. The resulting parameters for the lognormal cost distribution is found in Table 2-1. A detailed overview of the CAPEX estimate is found in Appendix M. Looking at the proportion each sub-system makes up of the total development cost, it is seen that the SPTs and the RALS are 26 % and 31 %, respectively. Further, project services and owner's cost are in turn 10 % and 2 %.

Table 7-12 – CAPEX estimates for seafloor production system.

Cost Items [M USD]	P10	P90	Mean	Std. Dev.
SPTs	84.100	155.143	117.541	28.522
RALS	108.065	199.352	151.035	36.650
Logistics	0.000	0.000	0.000	0.000
DWP	15.820	43.374	28.309	11.600
General	105.800	195.175	147.869	35.882
Total			**444.754**	**112.654**

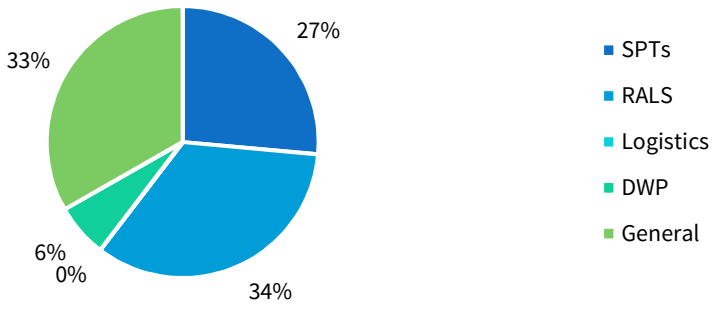

Figure 7-5 – Mean distribution of CAPEX.

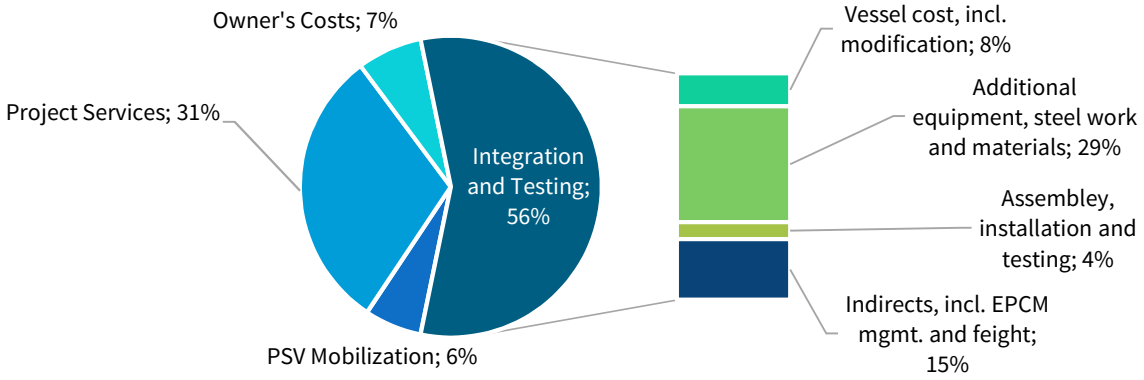

Figure 7-6 – Distribution of General CAPEX.

7.2.2 Operating Costs

Table 7-13 and Figure 7-7 show the overall OPEX for the subsea production system based on the approach described in Chapter 6.2.4. The background for the cost items constituting the PSV OPEX is found in Appendix J. General and Administrative (G&A) expenses are listed separately under "General OPEX", ref. OPEX breakdown structure in Chapter 6.2.4.

Table 7-13 – Overview of OPEX; mean values; variables for mean prod. rate.

Class	Daily Cost [USD/day]	Annual Cost [M USD/year]
General and Administrative Expenses (G&A)	4,110	1.500
PSV OPEX	254,070	92.736
PSV Bareboat Time Charter (TC)	293,351	107.073
Combi Vessel Time Charter (TC)	26,360	9.622
SPTs – Fixed	5,741	2.095
SPTs – Variable @ 3,591 t/day	23,621	8.622
RALS – Fixed	5,741	2.095
RALS – Variable @ 3,591 t/day	23,621	8.622
DWP – Variable @ 3,591 t/day	6,435	2.349
Total	**643,049**	**234.713**

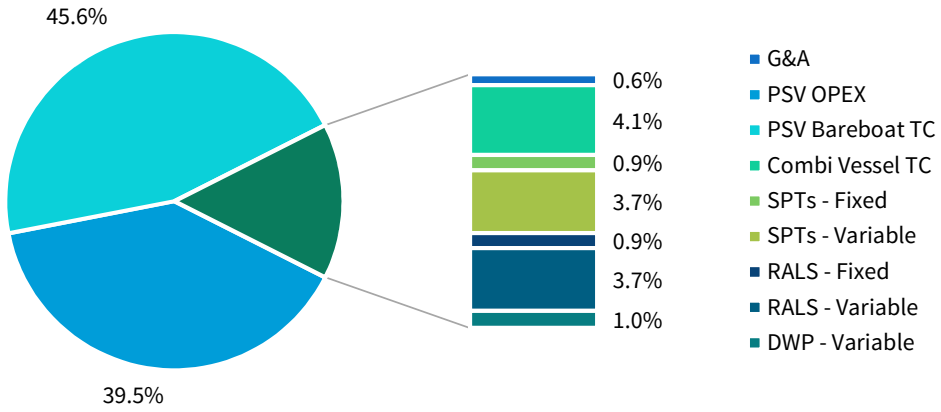

Figure 7-7 – Distribution of OPEX, ref. Table 7-13.

Table 7-14 – PSV OPEX; mean values.

Category	Cost Class	Daily Cost [USD/day]	Annual Cost [M USD/year]	Comments
Financing Costs	Financing Costs – Interest Expenses	11,095	4.050	
ROV Charter	ROV Charter	52,860	19.294	Three heavy work class ROVs, one supervisor, and four crew members per ROV. Oceaneering (2010).
Running Costs	Support Services	15,235	5.561	SRK Consulting (2010)
Running Costs	Insurance	9,374	3.422	75 % of Rowan's Norwegian North Sea cost level, see Appendix J
Running Costs	Manning – Directs	26,575	9.700	Mean of marine crew and drilling crew; in-between risk level
Running Costs	Manning – Indirects	4,054	1.480	Incl. training, catering, and crew transportation. 60 % of "Directs".
Running Costs	Stores and Consumables	28,175	10.284	Value from SRK Consulting (2010) scaled with updated crew number
Running Costs	Fuel	51,790	18.904	See Appendix J
Running Costs	Repair and maintenance (R&M) – Scheduled	49,919	18.220	Average of Rowan's North Sea cost level, see Appendix J.
Running Costs	Repair and maintenance (R&M) – Unscheduled	4,992	1.822	10 % of "Scheduled"
PSV OPEX		**254,070**	**92.736**	

Figure 7-8 – Transocean's drillship Discoverer Americas (Paul Joynson-Hicks/AP/Statoil ASA).

7.3 “Segment Analysis” – Resource Diagram

7.3.1 Case I – Copper Equivalent Grade

The resulting distributions for “Case I” are listed in Table 7-15. Detailed as shown in Appendix R. The “in-place” resource is a way of mapping a certain amount of the deposit’s tonnage to a specific metal. The “recoverable” tonnage is the amount of pure copper equivalent within the deposit, and corresponds to the resource diagram in Figure 7-9 (and the risked diagram in Figure 7-10). Associated uncertainties with the recoverable resources are seen from the tornado diagram in Figure 7-11.

Table 7-15 – Recoverable resources; copper equivalent, ref. Appendix R.

Resource Type [1E6]	Mode	Mean	Std. dev.	F90	F50	F10
Total Recoverable Resources, Cu_{eq}	0.0745	0.0959	0.0405	0.0516	0.0889	0.1500

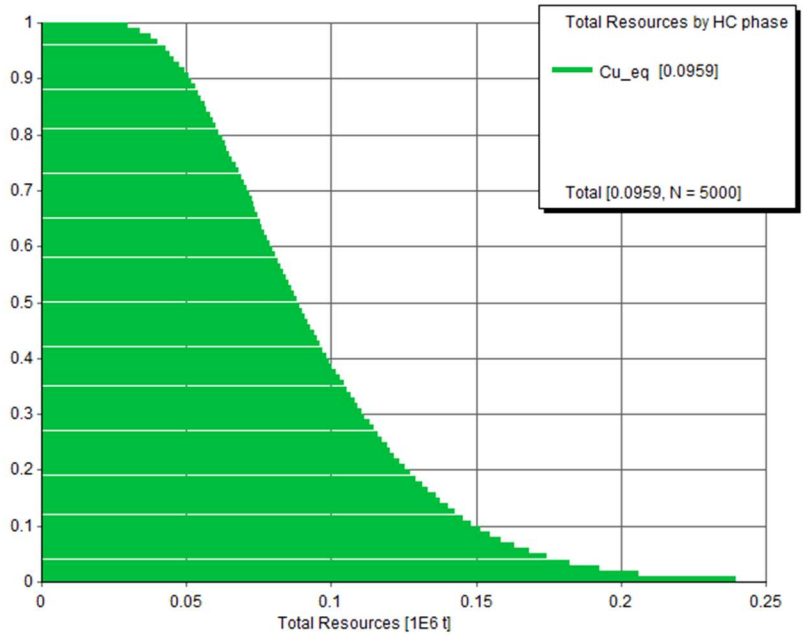

Figure 7-9 – Diagram of total recoverable resources for Case I.

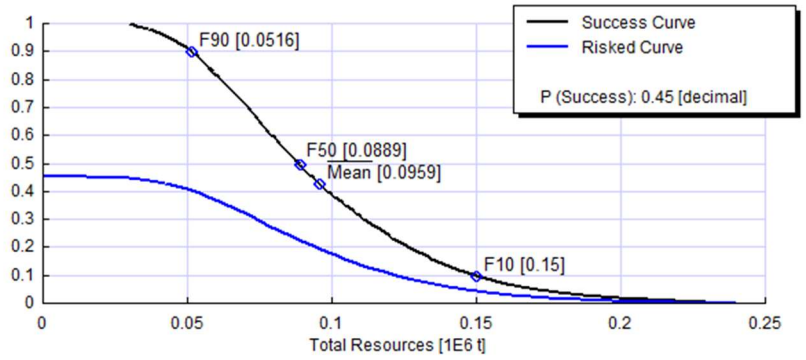

Figure 7-10 – Success diagram of total recoverable resources for Case I.

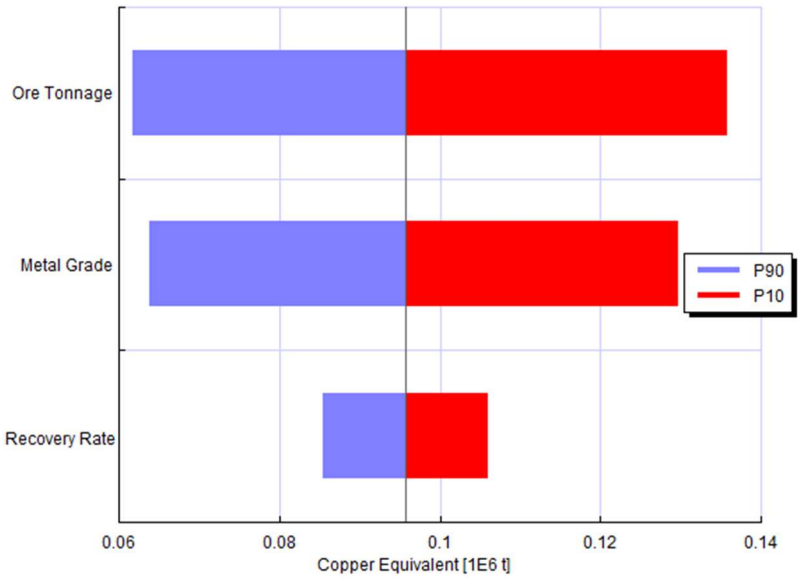

Figure 7-11 – Tornado diagram for copper equivalent.

7.3.2 Case II – Individual Metal Grade Distributions

For Case II, the "recoverable" tonnage of each metal is seen in Table 7-16 with the corresponding resources diagrams in Figure 7-12 and Figure 7-13. Figure 7-14 shows the effect of each metal grade distribution on the overall recoverable tonnage.

Table 7-16 – Recoverable resources for Case II, ref. Appendix R.

Resource Type	Mode	Mean	Std. dev.	F90	F50	F10
Cu [1E6 t]	0.0392	0.0511	0.0207	0.0287	0.0474	0.0786
Au [1E9 t]	4.96E-07	1.72E-06	1.77E-06	3.31E-07	1.17E-06	3.74E-06
Zn [1E9 t]	0.0382	0.0556	0.0249	0.0288	0.0508	0.0896
Ag [1E6 t]	4.86E-05	0.000086	5.04E-05	3.48E-05	7.49E-05	0.00015
Total Recoverable Resources [1E6 t]	**0.0848**	**0.107**	**0.0434**	**0.0599**	**0.0986**	**0.164**

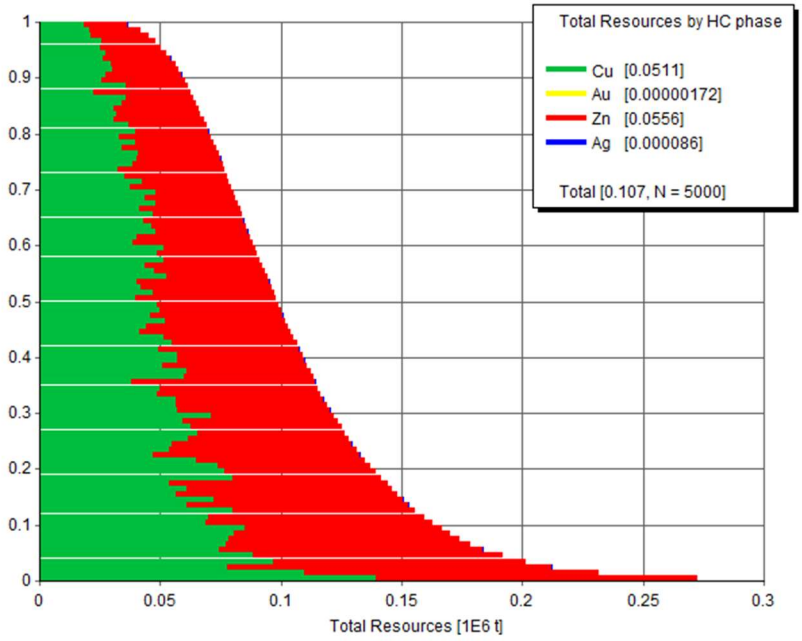

Figure 7-12 – Diagram of total recoverable resources for Case II.

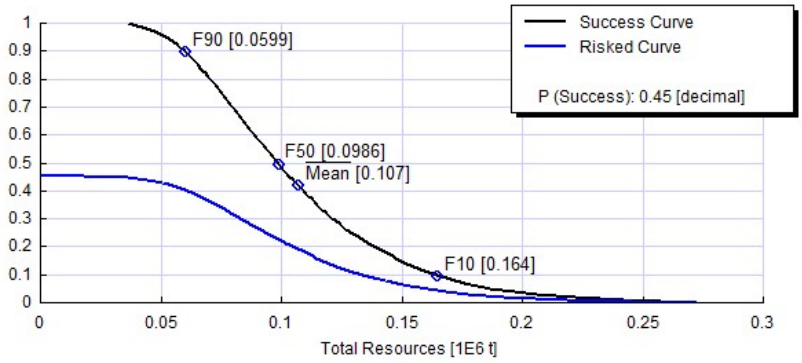

Figure 7-13 – Success diagram of total recoverable resources for Case II.

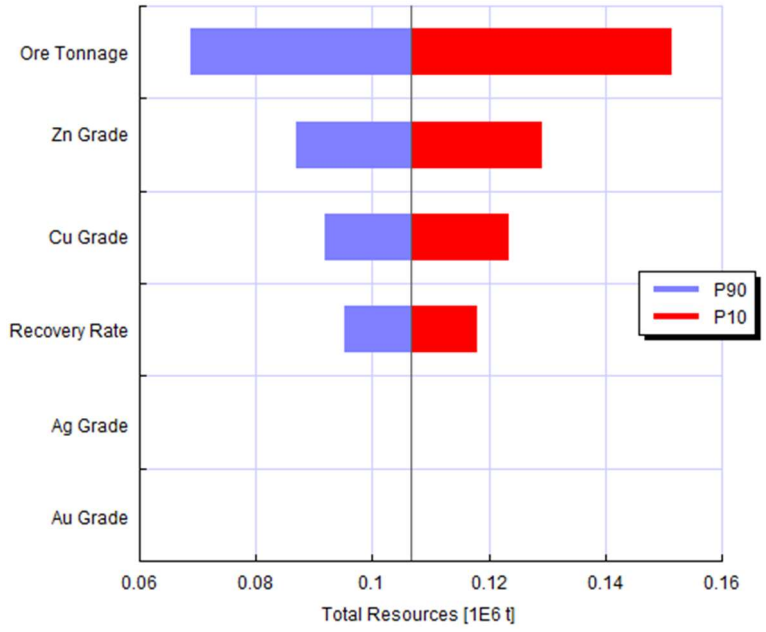

Figure 7-14 – Tornado diagram of total recoverable resources for Case II.

7.4 "Full Cycle Analysis" – Production Profile and Cash Flow

7.4.1 Production Rate and Volumes

As briefly discussed in Chapter 6.6, only the copper equivalent case (Case I) is modelled in the "Full Cycle Analysis" due to issues arising when modelling gas wells and small production rates. Figure 7-15 shows the mean production profile for copper equivalent. However, the values are average daily production rates based on the annual production volumes. The box plots in Figure 7-16, in which an "×" marks a mean value, show the distribution in production rate for each year. The corresponding average daily and annual production tonnage is listed in Table 7-17 and Table 7-18.

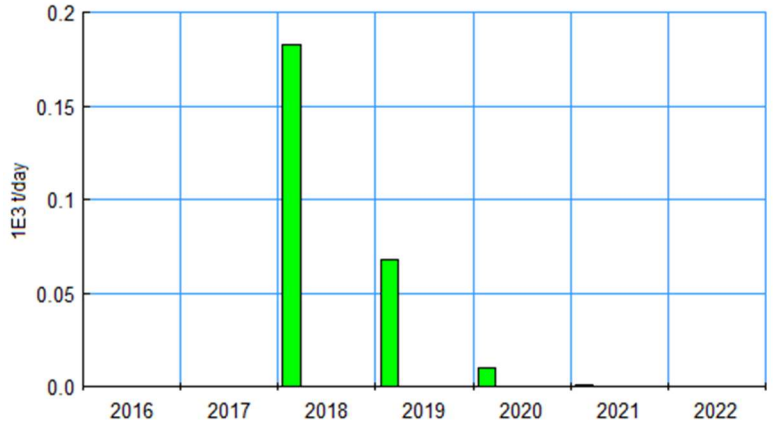

Figure 7-15 – Production profile (in average daily production rate); copper equivalent.

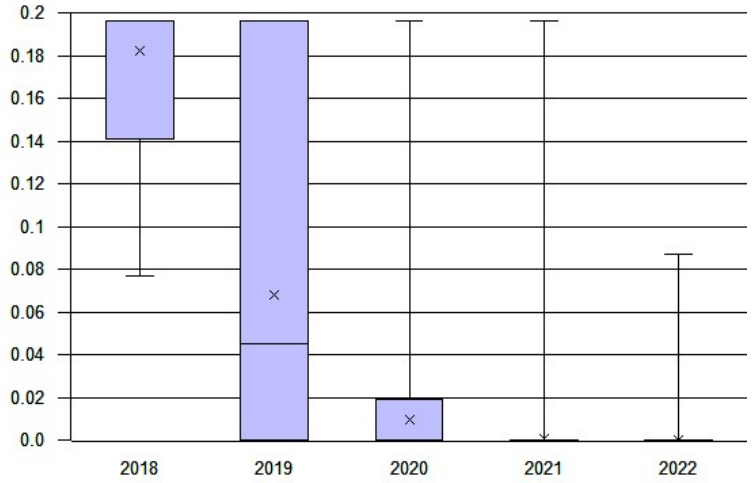

Figure 7-16 – Distribution of average daily production rate [1E3 t/day]; copper equivalent.

Table 7-17 – Daily production profile; copper equivalent.

Daily Production Profile	2018	2019	2020	2021
Total Resources [1E3 t/day]	0.18	0.07	0.01	0.00

Table 7-18 – Annual production profile; copper equivalent.

Annual Production Profile	Total	2018	2019	2020	2021	2022
Total Resources [1E6 t]	0.10	0.07	0.02	0.00	0.00	0.00

7.4.2 Distributions of Cash Items

Revenue

The revenue from the cash flow overview is directly linked to the production rate (in Chapter 7.4.1), as it is only multiplied with the respective economic scenario (i.e., metal price) to generate the revenue. The distributions of revenues are shown in Figure 7-17 (a)-(c).

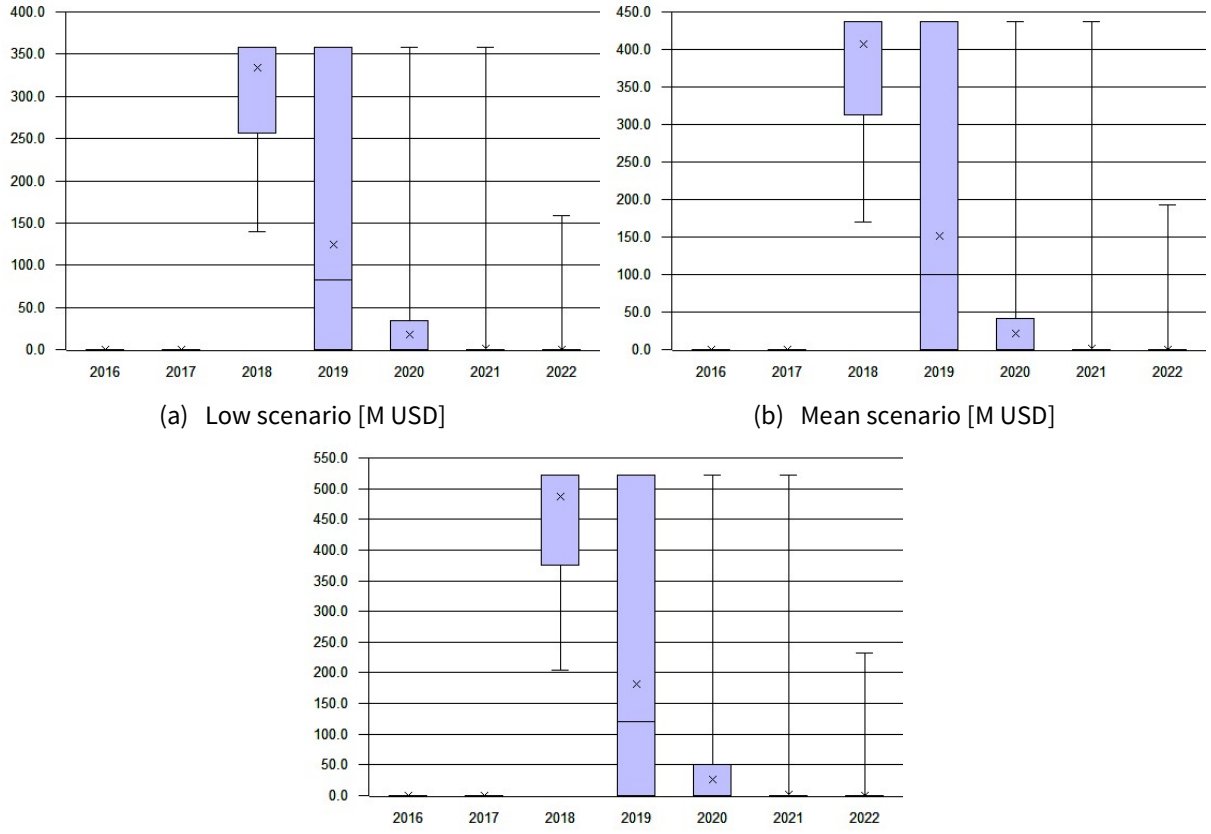

(a) Low scenario [M USD]

(b) Mean scenario [M USD]

(c) High scenario [M USD]

Figure 7-17 – Distributions of revenue.

CAPEX and OPEX

Furthermore, the distributions of project CAPEX and OPEX are found in Figure 7-18.

(a) CAPEX [M USD] (b) OPEX [M USD]

Figure 7-18 – Box plot of cost uncertainty.

7.4.3 Cash Flow for Corporate Tax Regime

Low Price Scenario

Table 7-19 shows the expected free cash flow (FCF) for the low economic scenario at 5,000 USD/t.

Table 7-19 – Expected FCF; corporate tax regime; low scenario (5,000 USD/t).

Year	**2016**	**2017**	**2018**	**2019**	**2020**	**2021**	**2022**	**2023**
Financial Year	0	1	2	3	4	5	6	7
Production Year			1	2	3	4	5	6
Adjusted Revenue			333.34	143.57				
Adjusted OPEX	(1.50)	(1.50)	(227.01)	(97.77)				
Selling of Prod. System				233.05				
EBITDA	(1.50)	(1.50)	106.33	278.85	0.00	0.00	0.00	0.00
Depreciation			(49.41)	(49.41)	(49.41)	(49.41)	(49.41)	(49.41)
EBIT	(1.50)	(1.50)	56.92	229.44	(49.41)	(49.41)	(49.41)	(49.41)
Income Tax at 27%	0.38	0.38	(14.23)	(57.36)	12.35	12.35	12.35	12.35
Net Income	(1.13)	(1.13)	42.69	172.08	(37.06)	(37.06)	(37.06)	(37.06)
Plus: Depreciation	0.00	0.00	49.41	49.41	49.41	49.41	49.41	49.41
Less: CAPEX	(221.29)	(221.29)	0.00	0.00	0.00	0.00		
Free Cash Flow (FCF)	(222.42)	(222.42)	92.10	221.49	12.35	12.35	12.35	12.35
Disc. Factor at 10%	*1.000*	*0.909*	*0.826*	*0.751*	*0.683*	*0.621*	*0.564*	*0.513*
Disc. FCF	**(222.42)**	**(202.20)**	**76.12**	**166.41**	**8.44**	**7.67**	**6.97**	**6.34**
NPV	**(182.09)**							

Mean Price Scenario

Table 7-20 shows the expected FCF for the mean metal price scenario.

Table 7-20 – Expected FCF; corporate tax regime; mean scenario (6,100 USD/t).

Year	2016	2017	2018	2019	2020	2021	2022	2023
Adjusted Revenue			406.67	175.17				
Adjusted OPEX	(1.50)	(1.50)	(227.01)	(97.78)				
Selling of Prod. System				233.05				
EBITDA	(1.50)	(1.50)	179.66	310.44	0.00	0.00	0.00	0.00
Depreciation			(49.41)	(49.41)	(49.41)	(49.41)	(49.41)	(49.41)
EBIT	(1.50)	(1.50)	130.25	261.03	(49.41)	(49.41)	(49.41)	(49.41)
Income Tax at 27%	0.38	0.38	(32.56)	(65.26)	12.35	12.35	12.35	12.35
Net Income	(1.13)	(1.13)	97.69	195.77	(37.06)	(37.06)	(37.06)	(37.06)
Plus: Depreciation	0.00	0.00	49.41	49.41	49.41	49.41	49.41	49.41
Less: CAPEX	(221.29)	(221.29)	0.00	0.00	0.00	0.00		
Free Cash Flow (FCF)	(222.42)	(222.42)	147.10	245.18	12.35	12.35	12.35	12.35
Disc. FCF	**(222.42)**	**(202.20)**	**121.57**	**184.21**	**8.44**	**7.67**	**6.97**	**6.34**
NPV	**(118.83)**							

High Price Scenario

The expected FCF for the corporate tax, high scenario is listed in Table 7-21.

Table 7-21 – Expected FCF; corporate tax regime; high scenario (7,300 USD/t).

Year	2016	2017	2018	2019	2020	2021	2022	2023
Adjusted Revenue			486.70	209.63				
Adjusted OPEX	(1.50)	(1.50)	(227.01)	(97.78)				
Selling of Prod. System				233.05				
EBITDA	(1.50)	(1.50)	259.69	344.90	0.00	0.00	0.00	0.00
Depreciation			(49.41)	(49.41)	(49.41)	(49.41)	(49.41)	(49.41)
EBIT	(1.50)	(1.50)	210.28	295.49	(49.41)	(49.41)	(49.41)	(49.41)
Income Tax at 27%	0.38	0.38	(52.57)	(73.87)	12.35	12.35	12.35	12.35
Net Income	(1.13)	(1.13)	157.71	221.62	(37.06)	(37.06)	(37.06)	(37.06)
Plus: Depreciation	0.00	0.00	49.41	49.41	49.41	49.41	49.41	49.41
Less: CAPEX	(221.29)	(221.29)	0.00	0.00	0.00	0.00		
Free Cash Flow (FCF)	(222.42)	(222.42)	207.12	271.03	12.35	12.35	12.35	12.35
Disc. FCF	**(222.42)**	**(202.20)**	**171.17**	**203.63**	**8.44**	**7.67**	**6.97**	**6.34**
NPV	**(49.81)**							

7.4.4 Cash Flow for Petroleum Tax Regime

Low Price Scenario

Table 7-22 shows the expected FCF for the low scenario with petroleum tax regime.

Table 7-22 – Expected FCF; petroleum tax regime; low scenario (5,000 USD/t).

Year	**2016**	**2017**	**2018**	**2019**	**2020**	**2021**	**2022**
Financial Year	0	1	2	3	4	5	6
Production Year			1	2	3	4	5
Adjusted Revenue			333.34	143.57			
Adjusted OPEX	(1.50)	(1.50)	(227.01)	(97.77)			
Selling of Prod. System				233.05			
EBITDA	(1.50)	(1.50)	106.33	278.85	0.00	0.00	0.00
Depreciation	(36.88)	(73.76)	(73.76)	(73.76)	(73.76)	(73.76)	(36.88)
General Income Tax Basis (EBIT)	(38.38)	(75.26)	32.57	205.08	(73.76)	(73.76)	(36.88)
Income Tax at 27%	9.60	18.82	(8.14)	(51.27)	18.44	18.44	9.22
Uplift	(24.34)	(24.34)	(24.34)	(24.34)			
Special Tax Basis	(14.04)	(50.92)	56.91	229.43	(73.76)	(73.76)	(36.88)
Resource Rent Tax at 51%	7.44	26.99	(30.16)	(121.60)	39.09	39.09	19.55
Net Income	(28.79)	(56.45)	24.43	153.81	(55.32)	(55.32)	(27.66)
Plus: Depreciation and Uplift	61.22	98.11	98.11	98.11	73.76	73.76	36.88
Less: CAPEX	(221.29)	(221.29)	0.00	0.00	0.00	0.00	
Free Cash Flow (FCF)	(188.85)	(179.63)	122.53	251.92	18.44	18.44	9.22
Disc. Factor at 10%	*1.000*	*0.909*	*0.826*	*0.751*	*0.683*	*0.621*	*0.564*
Disc. FCF	**(188.85)**	**(163.30)**	**101.26**	**189.27**	**12.60**	**11.45**	**5.20**
NPV	**(61.62)**						

Mean Price Scenario

Table 7-23 shows the expected FCF for the mean scenario with petroleum tax regime.

Table 7-23 – Expected FCF; petroleum tax regime; mean scenario (6,100 USD/t).

Year	2016	2017	2018	2019	2020	2021	2022
Adjusted Revenue			406.67	175.17			
Adjusted OPEX	(1.50)	(1.50)	(227.01)	(97.78)			
Selling of Prod. System				233.05			
EBITDA	(1.50)	(1.50)	179.66	310.44	0.00	0.00	0.00
Depreciation	(36.88)	(73.76)	(73.76)	(73.76)	(73.76)	(73.76)	(36.88)
General Income Tax Basis (EBIT)	(38.38)	(75.26)	105.90	236.67	(73.76)	(73.76)	(36.88)
Income Tax at 27%	9.60	18.82	(26.47)	(59.17)	18.44	18.44	9.22
Uplift	(24.34)	(24.34)	(24.34)	(24.34)			
Special Tax Basis	(14.04)	(50.92)	130.24	261.02	(73.76)	(73.76)	(36.88)
Resource Rent Tax at 51%	7.44	26.99	(69.03)	(138.34)	39.09	39.09	19.55
Net Income	(28.79)	(56.45)	79.42	177.51	(55.32)	(55.32)	(27.66)
Plus: Depreciation and Uplift	61.22	98.11	98.11	98.11	73.76	73.76	36.88
Less: CAPEX	(221.29)	(221.29)	0.00	0.00	0.00	0.00	
Free Cash Flow (FCF)	(188.85)	(179.63)	177.53	275.61	18.44	18.44	9.22
Disc. FCF	**(188.85)**	**(163.30)**	**146.72**	**207.07**	**12.60**	**11.45**	**5.20**
NPV	**1.63**						

High Price Scenario

The expected FCF for the high scenario with petroleum tax regime is shown in Table 7-24.

Table 7-24 – Expected FCF; petroleum tax regime; high scenario (7,300 USD/t).

Year	2016	2017	2018	2019	2020	2021	2022
Adjusted Revenue			486.70	209.63			
Adjusted OPEX	(1.50)	(1.50)	(227.01)	(97.78)			
Selling of Prod. System				233.05			
EBITDA	(1.50)	(1.50)	259.69	344.90	0.00	0.00	0.00
Depreciation	(36.88)	(73.76)	(73.76)	(73.76)	(73.76)	(73.76)	(36.88)
General Income Tax Basis (EBIT)	(38.38)	(75.26)	185.93	271.14	(73.76)	(73.76)	(36.88)
Income Tax at 27%	9.60	18.82	(46.48)	(67.78)	18.44	18.44	9.22
Uplift	(24.34)	(24.34)	(24.34)	(24.34)			
Special Tax Basis	(14.04)	(50.92)	210.27	295.48	(73.76)	(73.76)	(36.88)
Resource Rent Tax at 51%	7.44	26.99	(111.44)	(156.61)	39.09	39.09	19.55
Net Income	(28.79)	(56.45)	139.45	203.35	(55.32)	(55.32)	(27.66)
Plus: Depreciation and Uplift	61.22	98.11	98.11	98.11	73.76	73.76	36.88
Less: CAPEX	(221.29)	(221.29)	0.00	0.00	0.00	0.00	
Free Cash Flow (FCF)	(188.85)	(179.63)	237.55	301.46	18.44	18.44	9.22
Disc. FCF	**(188.85)**	**(163.30)**	**196.32**	**226.49**	**12.60**	**11.45**	**5.20**
NPV	**70.66**						

CHAPTER 8
Discussion

8.1 Concept Realism and Limitations for Loki's Castle Concept

8.1.1 Production System Design

Due to likely issues with respect to structural integrity of the rigid riser system when exposed to the harsh environment along the AMOR, the production system proposed (and under development) by Nautilus Minerals not is regarded as ideal for an operation at Loki's Castle. Furthermore, a significant power consumption (and associated operational cost) is required for heave compensation of such as system. Also, an operational limitation at a significant wave height H_S of about 4-5 m drives downtime from waiting-on-weather and decreasing operational efficiency, as discussed in Chapter 5.3 and Chapter 6.3, and calculated in Chapter 7.1.3. However, the overall system is easily adaptable to using flexible riser; one of various concepts with flexible risers for sites with harsh environments, as sugested by Technip in Chapter 3.5.3. Current solutions tackle H_S up to 10 m, but further development aims at a maximum sea state of 12 m. The deposit size at Loki's Castle, along with most other SMS deposits, take about two years to exploit. Hence, the lifetime of flexible risers should be at least two years. Currently, the erosion (wear) rate is too high for the materials and configurations that are available todays, which is proven by the full-scale experiments described in Chapter **Error! Reference source not found.**. Despite the dynamic load issues of the rigid riser, the remaining system is regarded feasible due to most of the components constituting the various subsystems are proven under demanding operational conditions, and adopted from various offshore or subsea activities. As stated in Chapter 3.6.3, the detail design of the individual system components are limited to a water depth of 2,500 m. Thus, the seafloor production system is not suited for some known hydrothermal vent sites along the Mohns Ridge (e.g., Mohn's Treasure at 2,600 m), as well as those situated along the Knipovich Ridge, for which water depths are increasing when going northwest towards Svalbard. This reduces the possibilities of relocate the production system when Loki's Castle is fully exploited.

8.1.2 Operations

Chapter 5 outlines a scenario for deep-sea mining operation at Loki's Castle. *"The Barents Sea area can still be defined as a frontier area, with very limited infrastructure"*, as stated by Samuelsen (2011, p. 9) The remoteness of the ridge and limited infrastructure in the area challenge the operation both with respect to safety and supply. Its large distances to mainland Norway with about 30-h sailing to the established heliport and logistics hub in Hammerfest for offshore O&G operations in the Barents Sea

(see Chapter 5.4) makes a concept with only one supply vessel vulnerable and may cause production halts if it the bulk/supply vessel is delayed in port or offshore loading is delayed due to environmental conditions. With continuous production at the maximum production rate, the PSV is required to offload and empty is cargo holds every 8.2 days. Furthermore, fuel supply is required (depending on the average effect over the period, thus the season and weather). A mainland logistics hub is reasonable since the ore needs to be taken to an onshore refinery, as outlined in Chapter 5.4. Moreover, arctic conditions introduce additional challenges, such as ice edge extent, seasonal darkness, and freezing surface temperatures. However, this is not likely a showstopper when comparing to various ongoing O&G activities at same latitudes, such as Eni's Goliat field. However, winterization may be required for parts of a surface vessel, and the potential for icebergs most be considered in design. Following the discussion in Chapter 5.5, emergency preparedness in case of life threatening conditions of personnel onboard that require immediate evacuation to land would likely be required by an exploitation permit issued by the government, and can only be provided by helicopter. Also, search-and-rescue (SAR) missions in the surrounding area, as well as mobilization of time critical crew is preferable by helicopter. The entire AMOR is at the absolute maximum range of commercially available helicopters (e.g., Super Puma H225), even with additional fuel tanks fitted. Even the commercial helicopters with the longest available range (e.g., Super Puma) is the best option. However, the AW609 TiltRotor can carry 6-9 passengers and two crew members a range of 700-1,000 nm, respectively. This helicopter will be an operational enabler for an AMOR deep-sea mining operation when delivery beings in 2018.

8.2 Production Volume and Gross Profit

The gross profit (revenue) generated by the deep-sea mining operation is essentially the product of tonnage of pure metals and production rate of the overall production system.

8.2.1 Resource Estimates

The recoverable resource diagram for copper equivalent in Figure 7-9 is remarkably similar to the sum of the recoverable resources of each metal Figure 7-12. The latter shows how the deposit contains large tonnage of zinc and copper, as very small volumes of silver and gold (all in descending metal grade). From Figure 7-11 and Figure 7-14, it is seen that the main variation in recoverable resources originate from the distribution of ore tonnage, and that the significance of metal grade distributions is directly proportional with the degree of metal presence (i.e., grade of the metal in question).

8.2.2 Production Profile and System Operability

Currently, the only experience from commercial subsea mining operations is that of De Beers' diamond mining offshore South Africa and Namibia, as briefly presented in Chapter 3.4.2. It is from significantly shallower and calmer waters than that encountered at Loki's Castle. The production rate of the overall system results from a range of factors, from which only a few have been regarded when estimating the production profile and rate as part of this thesis. Factors that affects the estimated production rate of the overall production chain are as follows:

- **Seafloor operation of SPTs** – The production rates of the AC and the BC depend on their net operating times. In addition to the scheduled maintenance, there will be downtime due to unexpected breakdown. Both the working progress of the crushers and the forces acting on the

tools (thus the wear rates) are dependent on the mechanical properties of the ore. Also, it is expected that the efficiency of the seafloor operation is significantly lower in the first months after commencing production. Even with simulation training of the operators prior to start-up, it is reasonable to assume that the crew will require take some time to get used to the equipment and gain experience with both the behavior of the tools and the properties of the seafloor deposit. Furthermore, an optimal communication and coordination routine between the crews of each SPT will take some time to establish. As the maintenance and operations crews are responsible for optimization of excavator availability and utilization, respectively, and excavator performance is a joint responsibility of the two, coordination and communication between the teams are essential. Using key performance indicators (KPIs) is powerful when evaluating the current capacity and cost in operation, as described by Lewis & Steinberg (2001).

- **SSLP shutdown criteria** – Various assumptions regarding the system are listed in Chapter 5.2, and parallels to similar operations in other offshore activities are found in Chapter 5.3. the system The assumed weather criteria for shutting down the operation is set to an H_s of 5 m, which probably is significantly higher than the real case. The baseline assumption is that the DP pumps needs to be shut down when the active heave compensation in the derrick is not capable of holding the SSLP stationary (with respect to its vertical position). Thus, it is assumed that the production is stopped for a 5 m sea state.

Other situations – and associated delay in operation, thus reduced production rate and operability – are not covered in the analyses and calculations of net operating time for any of the sub-system, which are likely to affect the resulting annual average daily production rate, as stated in Chapter 5.2:

- **Connection time after emergency disconnect of RTP** – The time required for ROVs to reconnect the RTP after an emergency disconnect is disregarded.
- **Operating window for loading operation** – Based on the restrictions in Chapter 5.3.4, the loading operations between the PSV and the bulk/supply vessel (i.e., offloading bulk and returns from the PSV, and loading of supplies in containers and baskets, as well as fuel supplies through hoses) requires a sufficient operating window (and corresponding calm period). However, the risks associated with side-by-side loading of both bulk and supplies is smaller than for O&G operations. Generally, there is a lowered environmental risk when not dealing with hydrocarbons and not being "connected" to a reservoir. Thus, the probability of drift-off and/or collision between the vessels is the same, but the consequence is lower. Also, the situation of bulk accidently being disposed to sea has a quite low environmental impact.
- **Operating window for launch and recovery of SPTs and ROVs** – The harsh environment along the AMOR will introduce challenges with respect to sufficient calm periods for launch and recovery of the SPTs and ROVs, especially for the SPTs, taking into account the location of the A-frames on deck, as well as the large and complex geometries. Being situated at the outermost corners of the deck, they are exposed accelerations from heave and pitch motions of the vessel.
- **Operating window for taking SSLP through the splash zone** – The SSLP is launched through a moonpool in the middle of the ship. Thus, it is likely not to be of much concern.

8.2.3 Metal Market and Price Forecasts

Based on historical data and an market overview in Chapter 3.1, the volatilities seen even in the short term in the metal market is of concern for estimating expected revenues in a project decision-making process. The economic scenarios defined in Chapter 6.7 are show a relatively large spread in values. However, when considering the short length in time over which the project is planned (and evaluated)

8.3 Uncertainties in Cost

8.3.1 Development Costs

As seen from Chapter 6.2.3 and Chapter 7.2.1, the development costs are to a great extent based on the pre-contingency and pre-allowance values of Nautilus Minerals (SRK Consulting, 2010), which are mostly confirmed by their annual reports dating back to 2006. The upper bound is found from the average of historical cost overruns in O&G megaprojects. However, with the current market situation, in which both rates affecting for operational costs, as well as the investment cost level are decreasing as a result of the high focus on cost cutting from the entire O&G industry. Thus, it is reasonable to assume that the general cost level will decrease, especially with respect to equipment/system purchase and facilities construction. As seen from the overall CAPEX distribution in Figure 7-5, the acquisition cost related to SPTs and RALS constitute about one-third of the total CAPEX each. Figure 7-6 shows the distribution of "General" CAPEX items, which also constitute about one-third of the total CAPEX, with most significant part being "Integration and Testing"; constituting more than 15 % of the total project CAPEX. Figure 7-18 (a) and (b) shows that the uncertainty in CAPEX is of a similar level as the CAPEX, which correspond to the practice in industry, where the same deterministic approach for establishing a mean value and corresponding interval is used both for CAPEX and OPEX with the same level of uncertainty.

8.3.2 Operating Costs

Chapter 6.2.4 and Chapter 7.2.2 show the estimated operating costs. Figure 7-7 shows the distribution of OPEX, in which PSV OPEX and PSV TC make up 39.5 % and 45.6 %, respectively. Most of the other costs are variable OPEX per volume produced by each of the sub-systems. Bulk/supply vessel rate is taken as ranging from expensive handymax bulk carriers to supply vessel, while PSV rate is to a great extent based on that of drilling rig – which is way too high, at least when considering historical rates for the late 2000s and early 2010s. A long sailing distance for the supply/bulk vessels than for ordinary platform support vessel. Comments to the PSV OPEX calculations are seen in Table 7-14. As the vessel charters are based on historical rates for the last 10-15 years, and are assumed to stay within the intervals defined by these data, the main uncertainty and error affecting the total OPEX is the PSV OPEX, which is essentially calculated in a deterministic manner. Fuel consumption and related cost are uncertain, as the power calculations are done for a ship, and various input values are based on those used for a semi-submersible, in addition to the various consumers and operational profiles are taken from various sources. Assuming that marine diesel oil (MDO) is chosen over heavy fuel oil (HFO) as part of a company's social responsibility and environmental profile, station-keeping only by DP is an expensive option in such harsh environments. POSMOOR, as used in De Beers' subsea diamond mining operation, which requires an anchor spread to be laid out in advance. When one site is depleted and the PSV is relocated, a new spread mush be laid down.

8.4 Cash Flow and Tax Regime

A drawback of deep-sea mining projects is them generally being capital intensive with respect to initial investments. To compensate for the CAPEX-heavy first years of cash flows and that the production system has a design lifetime spanning 5-15 years (thus enables exploitation of numerous hydrothermal vent sites when assuming a production length of about two years), a resale of the production system is included as a positive cash flow (considering a reduction in asset value, as described in Chapter 6.8.4) at the end of the production period, as seen in Table 7-19 through Table 7-24. Hence, the production system is purchased by the "next project", i.e., the next SMS deposit to be exploited by the company. As such, the project does not carry the entire investment in equipment.

A sensitivity study is performed with respect to tax regime. The effect of applying a petroleum tax scheme is apparent, seen from Table 8-1 and Table 8-2. Positive net present value (NPV) is only reached for the mean and high price scenarios when applying petroleum tax regime. Also listed is the internal rate of return (IRR), which is the discount rate that gives zero NPV (for an initial positive NPV project).

Table 8-1 – Evaluation parameters for Norwegian corporate tax scheme.

Scenario	NPV [M USD]	IRR
Lo	-182.1	–
Mean	-118.8	–
Hi	-49.8	3.6 %

Table 8-2 – Evaluation parameters for Norwegian petroleum tax regime.

Scenario	NPV [M USD]	IRR
Lo	-61.6	–
Mean	1.6	10.2 %
Hi	70.7	20.1 %

8.5 Modelling Capabilities in GeoX

Despite being custom-made for the oil and gas industry, GeoX is highly flexible and provides a range of modelling capabilities that are applicable to subsea mining. The software is useful for subsea mining purposes as it has both a geotechnical analysis tool, as well as an economic analysis. The "Segment Analysis" and resulting resource diagram is very useful (and seems to give reasonable results), and is user-friendly to work with. Also, modelling the production and establishing the cash flow overview in the "Full Cycle Analysis" is effective, but somewhat less user-friendly with input parameters in a lot of different windows. However, the main challenge lies in getting the production profile correct; i.e., without a tail production (long decline).

Various issues were encountered along the path of the work with this thesis, as summarized below, which make modelling of subsea mining projects in GeoX challenging:

- The production system capacity most be modelled in "pure metal flow", thus a daily production rate of ore [t/day] must be multiplied with the Cu_{eq} grade
- It is not possible to run a gas well simulation for such low flow rates as for "pure metal flow"
- Low resolution with respect to time (i.e., only years), and difficult to see whether values are taken as annual averages or not (e.g., daily production rate)
- Not possible to add a model/function for forecast in commodity prices
- Both gas phases must be modelled with the same price under "Economic Scenario", which makes the "Multi-Phase" case less accurate
- When boosting up the resource diagram, suddenly a tail appeared on the production profile. It is also noticeable as the very small volumes present in the production profile in this work.

CHAPTER 9
Conclusion and Further Work

9.1 Concluding Remarks

Loki's Castle is one of the most promising hydrothermal vent site along the Arctic Mid-Ocean Ridge (AMOR) with respect to associated seafloor massive sulfide (SMS) deposits. It has a 20-30 m thick hydrothermal mound, measuring 200 m across, and is located within Norwegian jurisdiction at a water depth of 2,400 m. Based on analysis in GeoX, which is custom-made for geotechnical and economic analysis of early-phase field developments in oil and gas (O&G), 95,900 t of copper equivalent is recoverable. Copper equivalent represents a weighted sum of the individual metals present in a deposit, when converted to copper value. Modelling the metal grade distributions separately in GeoX yields recoverable of 51,100 t copper, 55,600 t zinc, 1.72 t gold, and 86 t silver.

The concept defined for a deep-sea mining operation at Loki's Castle is based on the production system developed for Nautilus Minerals' Solwara 1 project for exploitation of SMS deposits in calm waters offshore Papua New Guinea. A combined bulk carrier and supply vessel handles transportation of ore, supplies and personnel (walk-to-work via an active heave-compensated gangway). The long-range helicopter model AW609 TiltRotor, currently under certification and final-stage development, enables emergency preparedness and mobilization of time-critical personnel. The production system design consists of: three remotely operated mining crawlers (seafloor production tools, SPTs); a rigid riser system (riser and lifting system, RALS) with a positive displacement pump (subsea slurry lift pump, SSLP); and a surface vessel (production support vessel, PSV) at which the ore is dewatered and stored before being shipped to shore for further processing at a refining plant (e.g., shipped to Boliden Odda, or shipped to Narvik with further transportation by train to Boliden refineries along the Baltic Sea). The rigid riser is limited to 4-5 m H_s due to heave compensation. However, Technip has suggested a similar concept with flexible risers that can operate up to 10-12 m. Despite issues with respect to structural integrity of the rigid riser in the harsh environment, the concept defined above is regarded feasible.

With respect to flow restrictions, the production capacity is limited by the SSLP at 8,202 t/day (for 3.3 SG ore, 12 % ore-water slurry). Based on the net operating time, accounting for maintenance schedules and waiting-on-weather time calculated from hindcast data, an annual average production rate of 3,591 t/day and annual production volume of 1,309,917 t are found. Significant downtime is excepted in January and July due to periodic maintenance of the SSLP, which is a critical for the production system performance. Due to the criticality of SSLP and Collecting Machine (CM); downtime on these hauls the entire production. A full production rate, the cargo hold capacity (dependent on volumetric ratio of slurry) of the PSV has a capacity of 8.2 days (for 12 %). Thus, a round-trip including loading times and

contingencies of maximum 8.2 days for the bulk/supply vessel. At 50 % thrust utilization, the average fuel consumption is 103.6 m^3/day, corresponding to 852 m^3 of 8.2 days of operation.

The mean development costs (CAPEX) sum up to 444.754 M USD, with one-third being SPTs and RALS. Operating costs (OPEX) at 643,049 USD/day (234.713 M USD/year) are mainly driven by bareboat 5-year time charter rate and operating costs of the PSV (39.5 % of total OPEX). Uncertainties are mainly related to fuel and repair costs, in addition to ROV charter rates.

The project cash flow is only modelled for the recoverable copper equivalent. After adjusting the production profile that is generated in GeoX (i.e., accumulating all tail production in the second year of production), a mean production period of 1.3 years is found. A typical SMS deposit is exploited in about 2-3 years. Three price scenarios for copper are defined based on forecasts towards 2025: low – 5,000 USD/t; mean – 6,100 USD/t; and high – 7,300 USD/t. When evaluating the expected free cash flow for both Norwegian ordinary corporate tax and the Norwegian petroleum tax scheme, positive net present value (NPV) is only reached for the mean and high price scenarios. To compensate for the CAPEX-heavy first years of cash flows and that the production system has a design lifetime spanning 5-15 years (thus enables exploitation of numerous hydrothermal vent sites when assuming a production length of about two years), a resale of the production system is included as a positive cash flow (considering a reduction in asset value) at the end of the production period. It is concluded that discounted cash flow of the project is strongly affected by both the discount rate and the fiscal (tax) regime that are applied. As the there are no subsea mining operations on the NCS and taxation and licensing regimes do not yet exist, it is up to further assessments (o establish whether or not the concept is economically viable. However, assuming that the reselling of assets makes up for the unfavorable high investment costs, it can be concluded that such an operational concept is not economically viable under the ordinary corporate tax regime.

GeoX is suitable for subsea mining purposes – especially the geotechnical analysis in the "Segment Analysis". The "Full Cycle Analysis" introduces more challenges, both with respect to user-friendliness and logical build-up, but more importantly with respect to modelling low flow rates and short production period (due to low resolution with respect to displayed time).

9.2 Further Work

As seen from the negative NPVs and the conculsion above, a too high initial investment is carried by the first project alone, even when including resale of equipment. Thus, a real option simulation (call option using Black-Scholes) should be performed to grasp this effect. Alternatively, by running a "Full Cycle Analysis" on prospects (i.e., a collection of segments). Modelling the commencement date of development and production for each individual segment, the discounted cash flow of one project might be carried forward to the next, thus getting a resulting NPV for the entire sequence of subsequent SMS deposits to be exploited by the same production system.

Furthermore, multiplying the various input parameters in GeoX by orders of ten should enable running a "Full Cycle Analysis" on a "Multi-Phase Case", in which all the individual metal distributions are modelled together with both an oil well and a gas well.

Sub-field can be modelled as separate segments, and lateral differences (part of the vent area that have different geological characteristics) can be included by using multiple wells in the model. Also, using the same production system for various hydrothermal vent sites can be modelled in this way.

References

Aas, B., Halskau Sr, Ø. & Wallace, S. W., 2009. The role of supply vessels in offshore logistics. *Marine Economics & Logistics,* 11(3), pp. 302-325.

Adamchak, F. & Adede, A., 2013. *Poten & Partners - LNG As Marine Fuel.* [Online]
Available at: http://www.gastechnology.org/Training/Documents/LNG17-proceedings/7-1-Frederick_Adamchak.pdf
[Accessed 16 May 2016].

Ådnanes, A. K., 2003. *Maritime Electrical Installations,* Oslo: ABB Marine.

AgustaWestland, 2014. *AW609 TiltRotor.* [Online]
Available at:
http://www.leonardocompany.com/documents/63265270/68151678/body_AW609.pdf
[Accessed 4 June 2016].

Airbus Helicopters, 2016. *H225.* [Online]
Available at: https://www.airbushelicopters.com/website/docs_wsw/RUB_40/tile_2688/H225-2016.pdf
[Accessed 4 June 2016].

Aker Kværner, 2006. *Aker H-6e - Riggen for ekstreme forhold.* [Online]
Available at: http://www.ktf.no/fileadmin/Dokumenter/Kursdokumenter/2006/2-ankerhandtering-og-forflytting-av-innretninger/13-Aker_H-6e-riggen.pdf
[Accessed 1 February 2016].

Aker Solutions, 2010. *Aker Drilling Riser Brazil.* [Online]
Available at: http://iadc.org/backup/chapters/brazil/Aker.pdf
[Accessed 11 May 2016].

Akins, W. M., Abell, M. P. & Diggins, E. M., 2005. *Enhancing Drilling Risk & Performance Management Through the Use of Probibalistic Time & Cost Estimatin.* Amsterdam, SPE/IADC.

Albright, S. C. & Winston, W. L., 2015. *Business Analytics: Data Analysis and Decision Making.* 5th ed. Stamford: Cengage Learning.

Alvarez Grima, A. et al., 2011. *Into the Deep: A Risk-Based Approach for Research to Deepsea Mining.* Rotterdam, CEDA Dredging Days.

Alvarez Grima, M. et al., 2011. *Into the Deep: A Risk Based Approach for Reseach to Deepsea Mining.* Rotterdam, CEDA Dredging Days.

Amdahl, J. et al., 2014. *Havromsteknologi - Et hav av muligheter.* 1st ed. Bergen: Fagbokforlaget.

American Bureau of Shipping (ABS), 2013. *Guide for Dynamic Positioning Systems.* [Online]
Available at:
https://www.eagle.org/eagleExternalPortalWEB/ShowProperty/BEA%20Repository/Rules&Guides

/Current/191_DPSguide/Guide
[Accessed 3 May 2016].

American Bureau of Shipping (ABS), 2014. *Guide for Passenger Comfort on Ships.* [Online]
Available at: http://ww2.eagle.org/content/dam/eagle/rules-and-guides/current/other/103_passengercomfortonships/COMF_Guide_e-Jan15.pdf
[Accessed 5 May 2016].

Arteaga, F., Nehring, M., Knights, P. & Camus, J., 2014. Schiemes of Exploitation in Open Pit Mining. In: C. Drebenstedt & R. Singhal, eds. *Mine Planning and Equipment Selection.* s.l.:Springer, pp. 1307-1323.

Bailey, W. et al., 2000. Taking a Calculated Risk. *Oilfield Review,* 12(3), pp. 20-35.

Bai, Y. & Bai, Q., 2012. *Subsea Engineering Handbook.* 1st ed. Waltham: Gulf Professional Publishing.

Batker, D. & Schmidt, R., 2015. *Environmental and Social Benchmarking Analysis of Nautilus Minerals Inc. Solwara 1 Project,* Tacoma: Earth Economics.

Beauchesne, C., Parenteau, T., Septseault, C. & Béal, P.-A., 2015. *Development & Large Scale Validation of a Transient Flow Assurence Model for the Design & Monitoring of Large Particles Transportation in Two Phase (Liquid-Solid) Riser Systems.* Houston, Offshore Technology Conference.

Beauchesne, C., Tzotzi, C. & Parenteau, T., 2015. *State Of The Art Of 1D Steady State Flow Assurance Models For Deepsea Mining Production System Using Air-Lift Pumping.* Houston, OTC.

Berk, J. & DeMarzo, P., 2014. *Corporate Finance - Global Edition.* 3rd ed. Harlow: Pearson Education Limited.

Boliden Group, 2016. *Operations.* [Online]
Available at: http://www.boliden.com/Operations/
[Accessed 1 June 2016].

Branch, A. E., 1998. *Marine Economics - Management and Marketing.* 3rd ed. Cheltenham: Stanley Thornes (Publishers) Ltd.

Bristow Group, 2015. *AgustaWestland and Bristow Sign Exclusive Agreement for the AW609 TiltRotor Programme.* [Online]
Available at: http://bristowgroup.com/bristow-news/latest-news/2015/agustawestland-and-bristow-sign-exclusive-platform/
[Accessed 4 June 2016].

Chamanski, A. A., 2002. *Uncertainty in Petroleum Field Development Prokjects: A study of decision-making uncertainty and evaluation methodologies,* Stavanger: Stavanger University College.

Chen, X., Miedema, S. A. & van Rhee, C., 2014. *Numerical Methods for Modeling the Rock Cutting Process in Deep Sea Mining.* San Francisco, OMAE.

Chopra, G. S., 2016. *World's First Subsea Mining Vessel - Design Challanges.* Houston, OTC.

Coffey Natural Systems, 2008. *Environmental Impact Statement - Solwara 1 Project,* Brisbane: Coffey Natural Systems.

Covert, R. P., 2013. *Analytic Method for Probabilistic Cost and Schedule Risk Analysis - Final Report.* [Online]
Available at:
http://www.nasa.gov/pdf/741989main_Analytic%20Method%20for%20Risk%20Analysis%20-%20Final%20Report.pdf
[Accessed 25 April 2016].

Cronan, D. S., 1992. *Marine Minerals in Exclusive Economic Zones.* 1st ed. London: Chapman & Hall.

De Beers Group, 2014. *The Diamond Insight Report,* London: De Beers Group.

De Beers Marine Namibia, 2006. *De Beers Marine Namibia - The Journey Continues.* s.l.:De Beers Marine Namibia.

Deloitte Advokatfirma, 2014. *Oil and Gas Taxation in Norway.* [Online]
Available at: http://www2.deloitte.com/content/dam/Deloitte/global/Documents/Energy-and-Resources/gx-er-oil-and-gas-taxguide-norway.pdf
[Accessed 13 November 2015].

Do, A.-T. & Lambert, A., 2012. *Qualification of Unbounded Dynamic Flexible Riser with Carbon Fibre Composite Armours.* Houston, OTC.

Dredging Supply Company, 2010. *Maximizing Profits by Understanding Hydraulic Dredge Efficiency.* [Online]
Available at: http://www.dscdredge.com/docs/papers/Johnson-AGG1-Maximizing-Profits.pdf
[Accessed 20 11 2015].

Drewry Maritime Research, 2015. *Ship Operating Costs - Annual Review and Forecast - Annual Report 2014/15,* London: Drewry Maritime Research.

Earney, F. C., 1990. *Marine MIneral Resources.* 1st ed. New York: Routledge.

ECORYS, 2014. *Study to Investigate State of Knowledge of Deep Sea Mining - Final report Annex 5 Ongoing and planned activity,* Rotterdam: ECORYS.

ECORYS, 2014. *Study to Investigate the State of Knowledge of Deep-Sea Mining,* Rotterdam: ECORYS.

Eklund, T. & Paulsen, G., 2007. *Ormen Lange Offshore Project - Subsea Development Strategy and Execution.* Lisbon, International Offshore and Polar Engineering Conference.

Ellefmo, S. L. & Frimanslund, E. K., 2015. *Mineralutvinning på havbunnen - utopi eller virkelighet?.* Oslo, Fjellsprengningsdagen.

Environmental Protection Authority, 2014. *Statement of Evidence in Cheif of Kevin Richardson on Behalf of Trans-Tasman Resources Ltd,* Wellington: Environmental Protection Authority.

ERICON, 2012. *Deliverable 4.1 - Verifi ed estimates on future running cost escalation, crewing and support of the vessel.* [Online]
Available at: http://www.esf.org/fileadmin/Public_documents/Publications/ericon_del_4-1.pdf
[Accessed 24 May 2016].

Espinasse, P., 2010. *Deepsea Pilot SMS Mining Systems for Harsh Environment.* Shanghai, OMAE.

EY, 2014. *Business Risks Facing Mining and Metals 2014-2015,* s.l.: EY.

EY, 2014. *Spotlight on oil and gas megaprojects,* s.l.: EY.

EY, 2015. *Global oil and gas tax guide.* [Online]
Available at: http://www.ey.com/Publication/vwLUAssets/EY-2015-Global-oil-and-gas-tax-guide/$FILE/EY-2015-Global-oil-and-gas-tax-guide.pdf
[Accessed 13 November 2015].

EY, 2016. *The Norwegian oilfield services analysis 2015,* Oslo: EY.

Fearnley Offshore Supply, 2013. *The Subsea Report - November 2013,* Oslo: Fearnley Offshore Supply.

Figoni, M. & Chand, S., 2014. *A Classificiation Society's Experience with Subsea Mining.* s.l., ISOPE.

FMC Technologies, 2010. *Offshore LNG Transfer - IBC FLNG Conference.* Houston: FMC Technologies.

Fouquet, Y. & Lacroix, D., 2014. *Deep Marine Mineral Resources.* 1st ed. Versailles: Quæ.

Galar, D. et al., 2014. Fusio of Operations, Event-Log and Maintenance Data: A Case Study for Optimizing Availability of Mining Shovels. In: C. Drebenstedt & R. Singhal, eds. *Mine Planning and Equipment Selection.* s.l.:Springer, pp. 1173-1194.

Garnett, R. H., 1996. *Mineral Recovery Performance in Marine Mining.* Houston, OTC.

Garvey, P. R., 2000. *Proabilistic Methods for Cost Uncertainty Analysis.* 1st ed. New York: Marcel Dekker.

GE Oil & Gas, 2011. *"Crossing the chasm" with the GE MudLift pump.* [Online]
Available at: http://site.ge-energy.com/businesses/ge_oilandgas/en/newsletter/geog_viewsandnews_060911/pdf/GEOG_TI2011_CrossingTheChasmWithTheGEMudLiftPump.pdf
[Accessed 9 December 2015].

GeoKnowledge, 2003. *Doing Resource and Risk.* [Online]
Available at: http://www.ccop.or.th/ppm/document/CAWS1/GeoKnowledge.pdf
[Accessed 2 February 2016].

GeoKnowledge, 2003. *Doing Resource and Risk Assessment with GeoX.* [Online]
Available at: http://www.ccop.or.th/ppm/document/CAWS1/GeoKnowledge.pdf
[Accessed 12 02 2016].

GMC, 2016. *Subsea Mining Riser.* [Online]
Available at: http://gmcdeepwater.com/wp-content/uploads/2016/04/gmc-flyer-mining-riser-2016.pdf
[Accessed 3 June 2016].

Golder Associates, 2012. *Mineral Resource Estimate - Solwara Project, Bismarck Sea, PNG,* Milton: Golder Associates.

Grima, M. A., Boomsma, W., Hofstra, F. & Lotman, R., 2012. *A Linear Rock Cutting Test Set-Up for 3 Dimensional Tests Under Hyperbaric Pressure.* Houston, Offshore Technology Conference.

Gudmestad, O. T., Zolotukhin, A. & Jarlsby, E. T., 2010. *Petroleum Resources with Emphasis on Offshore Fields.* 1st ed. Southampton: WIT Press.

Gu, M. & Gudmestad, O. T., 2012. *Treatment of Uncertainties, Risks and Opportunities in Cost and Schedule Estimates in the Early Phases of Offshore Projects.* Rhodes, ISOPE.

Hall, N. A. & Delille, S., 2011. *EST-491 Cost Estimation Challenges and Uncertainties Confronting Oil and Gas Companies.* Anaheim, California, AACE.

Hallset, J. O., 2006. *Aritic Subsea Systems - IMR Tasks (WP1),* Stavanger: Poseidon Group.

Haug, N., Engebretsen, K. B., Lindstad, P. & Nygård, M., 2008. *Aker H-6e built for harsh environments, ultra deepwater.* Perth, PennWell.

Haver, S., 2014. *OFF600 and OFF605 - Lecture Notes - Description of Metocean Characteristics for Planning of Marine Operations.* 1st ed. Stavanger: University of Stavanger (UiS).

Haver, S. K., 2011. *Prediction of Characteristc Response for Design Purposes,* s.l.: Statoil.

Heeren, J., van de Bosch, J., Munts, E. & Lotman, R., 2013. *New Developments in the Simulation of Slurry Behaviour in Spooled Hoses for Offshore Mining Applications.* Houston , Offshore Technology Conference.

Helmons, R. L., Miedema, S. A. & van Rhee, C., 2014. *A New Approach to Model Hyperbaric Rock Cutting Processes.* San Francisco, OMAE.

Hembre, M., 2009. *Risikostyring – Et bilde av forståelse og prioritering i projektet.* [Online]
Available at:
http://www.nsp.ntnu.no/prosjekt2009/files/pages/20/prosjekt2009_strom3_hembre.pdf
[Accessed 5 May 2016].

Herbich, J. B., 1978. *Development of Offshore Mining.* Houston, OTC.

Honeywell, 2009. *Draft Onondaga Lake Dredging, Sediment Management, & Water Treatment Initial Design Submittal – Section 4 – Engineering Analysis and Design.* [Online]
Available at: http://www.dec.ny.gov/docs/regions_pdf/olids66138.pdf
[Accessed 20 11 2015].

International Seabed Authority, 2002. *Polymetallic Massive Sulphides and Cobalt-Rich Ferromanganese Crusts: Status and Prospects ,* Kingston: International Seabed Authority.

Jackson, E. & Clarke, D., 2007. *Subsea Excavation of Seafloor Massive Sulphides.* Aberdeen, IEEE Oceans.

Jackson, E. & Hunter, J., 2007. *Subsea Massive Sulphide Mining - Technology Test Program.* Denver, SME Annual Meeting and CMA 109th National Western Conference.

Jahn, F., Cook, M. & Graham, M., 2008. *Hydrocarbon Exploration and Production.* 2nd ed. Amsterdam: Elsevier.

Jansen, J. B. & Bjerke, J. M., 2012. *Norwegian Petroleum Taxation - An Introduction.* [Online]
Available at: http://www.bahr.no/en/about-bahr/news/_attachment/2869?_download=true&_ts=13543a13c48
[Accessed 7 June 2016].

Jones, G. R. et al., 2014. *Patent Application Publication - Apparatus and Method for Seafloor Stockpiling.* [Online]
Available at:
https://docs.google.com/viewer?url=patentimages.storage.googleapis.com/pdfs/US20140137443.pdf
[Accessed 4 May 2016].

Judge, R. A. & Yu, A., 2010. *Subsea Slurry Lift Pump for Deepsea Mining.* Shanghai, OMAE.

Kaiser, M. J., 2014. Modeling market valuation of offshore drilling contractors. *WMU Journal of Maritime Affairs,* 13(2), pp. 299-330.

Kaiser, M. J., 2015. *Offshore Service Industry and Logistics Modeling in the Gulf of Mexico.* 1st ed. Cham: Springer International Publishing.

Kitchel, B. G., Moore, S. O., Banks, W. H. & Borland, B. M., 1997. Probibalistic Drilling-Cost Estimating. *SPE Computer Applications,* 9(4), pp. 121-125.

Knodt, S. et al., 2016. *Development and Engineering of Offshore Mining Systems - State of the Art and Future Perspectives.* Houston, OTC.

KPMG International, 2014. *Taxation of Cross-Border Mergers and Acquisitions - Norway.* [Online]
Available at: https://home.kpmg.com/content/dam/kpmg/pdf/2014/05/norway-2014.pdf
[Accessed 9 June 2016].

KPMG International, 2015. *Norway: Budget 2016, petroleum tax proposals, interest deduction rules.* [Online]
Available at: https://home.kpmg.com/xx/en/home/insights/2015/10/tnf-norway-budget-2016-petroleum-tax-proposals-interest-deduction-rules.html
[Accessed 9 June 2016].

Laugesen, J. et al., 2014. *Seabed Mining - Guest Lecture at NTNU - TBA4145 Port and Coastal Facilities.* Trondheim: DNV GL.

Leach, S., Smith, G. & Berndt, R., 2012. *SME Special Session: Subsea Slurry Lift Pump Technology - SMS Development.* Houston, Offshore Technology Conference.

Leonardo-Finmeccanica, 2015. *New Milestones for the AW609.* [Online]
Available at: http://www.leonardocompany.com/en/-/aw609-bristow
[Accessed 4 June 2016].

Lewis, M. W. & Steinberg, L., 2001. Maintenace of mobile mine equipment in the information age. *Journal of Quality in Maintenance Engineering,* 7(4), pp. 264-274.

Markussen, J. M., 2000. *Utnyttelsen av dypvannsmineralene: Norges muligheter, status og perspektiver,* Oslo: Fritjof Nansens Institutt.

McKinsey Global Institute, 2013. *Resource Revolution: Tracking Global Commodity Markets,* s.l.: McKinsey & Company.

MDM Group, 2011. *MDM Sizers.* s.l.:MDM Group.

MineSight, 2014. *MineSight at Work Beneath the Waves.* [Online]
Available at: http://www.minesight.com/en-us/company/newsletters/aug2014/minesightatworkbeneaththewaves.aspx
[Accessed 17 12 2015].

Ministry of Finance, 2016. *Direkte skatter.* [Online]
Available at: https://www.regjeringen.no/no/tema/okonomi-og-budsjett/skatter-og-avgifter/direkte-skatter/id2353512/
[Accessed 9 June 2016].

Murtha, J. A., 1997. Monte Carlo Simulation: Its Status and Future. *SPE Distinguished Author Series,* 49(4), pp. 361-373.

Murtha, J. A. & Janusz, G. J., 1995. *Oil & Gas Journal - Spreadsheets Generate Reservoir Uncertainty Distributions.* [Online]
Available at: http://www.ogj.com/articles/print/volume-93/issue-11/in-this-issue/general-interest/spreadsheets-generate-reservoir-uncertainty-distributions.html
[Accessed 4 May 2016].

Myrhaug, D. & Lian, W., 2014. *TMR4182 - Marine Dynamics - Lecture Notes - Irregular Waves.* Trondheim: Kompendieforlaget.

National Oilwell Varco, 2013. *Comprehensive Floating Production Solutions.* [Online]
Available at: http://www.nov.com/fps_landing/pdfs/comprehensive-floating-production-solutions-brochure.pdf
[Accessed 18 April 2016].

Nautilus Minerals, 2014. *Annual Report 2014,* Toronto: Nautilus Minerals.

Nautilus Minerals, 2015. *Annual Report 2015,* Toronto: Nautilus Minerals.

Nautilus Minerals, 2015. *The Solwara 1 Deepwater Mining Project - Third International Future Mining Conference.* [Online]
Available at:
http://www.futuremining2015.ausimm.com.au/Media/FM2015/presentations/1620%20The%20Solwara.pdf
[Accessed 4 February 2016].

Nautilus Minerals, 2016. *Annual Information Form.* [Online]
Available at: http://www.sedar.com/
[Accessed 3 June 2016].

Nautilus Minerals, 2016. *GCE Subsea - Susbea Innovation Day - Deep-sea Mining - General Update.* [Online]
Available at: http://www.gcesubsea.no/download/572714664359e.pdf
[Accessed 30 May 2016].

Nielsen, F. G., 2007. *Lecture Notes in Marine Operations.* 4th ed. Trondheim: Norwegian University of Science and Technology (NTNU).

Norsk olje og gass, 2015. *064 - Norsk olje og gass - Anbefalte retningslinjer for Etablering av områdeberedskap.* [Online]
Available at:
https://www.norskoljeoggass.no/Global/Retningslinjer/HMS/Beredskap/064%20Etablering%20av%20omr%C3%A5deberedskap.pdf
[Accessed 5 June 2016].

Ocean Rig, 2013. *1st Quarter Ended March 31, 2013 - Earnings Presentation.* [Online]
Available at: http://ocean-rig.irwebpage.com/files/ORIG_2013_Q1_presentation.pdf
[Accessed 16 March 2016].

Ocean Rig, 2015. *4th Quarter Ended December 31, 2014 - Earnings Presentation.* [Online]
Available at: http://cdn.capitallink.com/files/docs/companies/ocean_rig/presentations/2014/ORIG-Q4-2014-Presentation.pdf
[Accessed 26 May 2016].

Oceaneering, 2010. *Remotely Operated Vehicle (ROV) - Rate Schedule,* Houston: Oceaneering.

Oceaneering, 2015. *Investor Presentation – Jefferies Energy Conference.* [Online]
Available at: http://www.oceaneering.com/wp-content/uploads/2015/11/2015-Jefferies-FINAL-website.pdf
[Accessed 20 11 2015].

Odfjell Invest, 2006. *Investor Presentation.* [Online]
Available at: http://otc.nfmf.no/public/news/4382.pdf
[Accessed 1 February 2016].

Odland, J., 1999. *81063 Development of Offshore Oil and Gas Fields - Part 6: Costs, Economics and Decision Criteria.* 1st ed. Trondheim, Norway: Norwegian University of Science and Technology (NTNU).

Økland, I. & Pedersen, R. B., 2015. *GCE Subsea - Subseadag Sogn of Fjordande 2015 - Subsea mining og ressursutnytting.* [Online]
Available at: http://www.gcesubsea.no/download/560bd1bbb85aa.pdf
[Accessed 30 May 2016].

Ottervik, A. O. & Skogdalen, J. E., 2013. *Levetidsforlengelse for halvt nedsenkbare installasjoner - Gjesteforelesning, NTNU, 24 okt. 2013.* Trondheim: Statoil.

Paik, J. K. & Thayamballi, A. K., 2007. *Ship-Shaped Offshore Installations - Design, Building, and Operation.* 1st ed. New York: Cambridge University Press.

Parenteau, T., 2010. *Flow Assurance for Deepwater Mining.* Shanhai, OMAE.

Parenteau, T., 2012. *Flow Assurance for Deep Ocean Mining - Large Scale Experiment for Flow Correlation Validation and Abrasion Testing.* Houston, Offshore Technology Conference.

Parenteau, T., Espinasse, P., Benba, A. & Ngim, B., 2013. *Subsea mining field development concept using a subsea crusher and feeding unit.* Houston, Offshore Technology Conference.

Pedersen, R. B. et al., 2013. Hydrothermal Activity at the Arctic Mid-Ocean Ridges. In: A. G. Union, ed. *Diversity Of Hydrothermal Systems On Slow Spreading Ocean Ridges.* s.l.:John Wiley & Sons, Ltd, pp. 67-89.

PricewaterhouseCoopers, 2015. *Mine 2015 - The Gloves Are Off - Review of the Global Trends in the Mining Industry,* s.l.: PricewaterhouseCoopers.

Remery, J., Silva, C. & Mesnage, O., 2008. *The Free Standing Flexible Riser: A Novel Riser System for an Optimised Installation Process.* Houston, OTC.

Reuters, 2014. *De Beers' big green machine sucks up Namibian diamonds - Reuters.* [Online]
Available at: http://www.reuters.com/article/namibia-diamonds-idUSL6N0OZ1QA20140618#hlPfUSSRedGUeppV.97
[Accessed 06 12 2015].

Richardson, K., 2007. A Perspective of Marine Mining Within De Beers. *The Journal of The Southern African Institute of Mining and Metallurgy,* 107(June), pp. 393-402.

Ridley, N., Graham, S. & Kapusniak, S., 2011. *Seafloor Production Tools for the Resources of the Future.* Houston, Offshore Technology Conference.

Rowan Companies, 2015. *Investor Presentation - December 2015.* [Online]
Available at: http://www.oilandgas360.com/analytics/RDC1215.pdf
[Accessed 24 May 2016].

Royal Dutch Shell, 2013. *Play Based Exploration - A Guide for AAPG's Imperial Barrel Award Participants.* [Online]
Available at: http://iba.aapg.org/Portals/0/docs/iba/Play_Based_ExplorationGuide.pdf
[Accessed 23 February 2016].

RS Plateau, 2015. *The Plateau Report 2015.* [Online]
Available at: http://securities.clarksons.com/~/media/Files/PlatouReport14/ThePlatouReport2015_web_FINAL.pdf
[Accessed 24 May 2016].

Rudenno, V., 2012. *The Mining Valuation Handbook - Mining and Energy Valuation for Investors and Management.* 4th ed. Milton: John Wiley & Sons Australia, Ltd.

Samuelsen, J., 2011. *A Guide to Norwegian Petroleum Taxation.* Oslo: KPMG Law Advokatfirma.

Sangesland, S., 2008. *Drilling and Completion of Subsea Wells.* 1st ed. Trondheim: Norwegian University of Science and Technology (NTNU).

Schlumberger, 2012. *Schlumberger Acquires GeoKnowledge AS.* [Online]
Available at: https://www.slb.com/news/press_releases/2012/2012_1213_geoknowledge_pr.aspx
[Accessed 12 February 2016].

Schoemaker, P. J., 1995. Scenario Planning: A Tool for Strategic Thinking. *Sloan Management Review,* 36(2), pp. 25-40.

Searle, S. G. & Smit, H. D., 2011. *The Challenges of Developing and Operating an Underwater Mine.* Houston, OTC.

Sevan Drilling, 2013. *Company presentation and update in connection with new proposed financing.* [Online]
Available at: http://www.sevandrilling.com/_gfx/Sevan_drilling_presentation.pdf
[Accessed 24 May 2016].

Ship & Offshore, 2010. Sub-sea Diamond Mining. *Ship & Offshore,* Issue 2, pp. 24-25.

Sinding-Larsen, R., 2015. *TGB4160 - Lecture Slides - GeoX Modelling of Hydrocarbon Resources.* Trondheim: Norwegian University of Science and Technology (NTNU).

Smith, G., 2011. *Deepwater Seafloor Resource Production - The Bismarck Sea Development Prosject.* Houston, Offshore Technology Conference.

Soil Machine Dynamics, 2013. *Submerged Mining.* [Online]
Available at:
http://smd.co.uk/download.php?file=/download/SMD_2719_Mining_2013_Brochure_pps_low_res.pdf
[Accessed 1 February 2016].

Songa Offshore, 2016. *Annual Report 2015.* [Online]
Available at: http://www.songaoffshore.com/Reports/Annual%20Report%202015.pdf
[Accessed 25 May 2016].

Spagnoli, G. et al., 2016. *A Novel Mining Approach for Seafloor Massive Sulfide Deposits.* Houston, OTC.

SPC, 2013. Deep Sea Minerals and the Green Economy. In: E. Baker & Y. Beaudoin, eds. *Deep Sea Minerals.* Arendal: Secreteriat of the Pacific Community, p. Vol. 2.

SPC, 2013. Sea-Floor Massive Sulphides, a physical, biological, environmental, and technical review. In: E. Baker & Y. Beaudoin, eds. *Deep Sea Minerals.* s.l.:s.n.

SRK Consulting, 2010. *Offshore Production System Definition and Cost Study,* Perth: SRK Consulting.

SRK Consulting, 2012. *NI 43-101 Technical Report 2011 PNG, Tonga, Fiji, Solomon Islands, New Zealand, Vanuatu and the ISA,* Perth: SRK Consulting.

Statoil, 2013. *Statoil Base Florø.* [Online]
Available at: http://kph.no/uploads/media/Presentasjon_Statoil_-_Logistikksenter_OCTG.pdf
[Accessed 4 June 2016].

Steube, C., 2000. *Offshore Operating Costs for Marginal Fields - Selecting the Best Operating Strategy.* Abuja, Nigeria, SPE.

Stopford, M., 1997. *Maritime Economics.* 2nd ed. London: Routledge.

Stopford, M., 2009. *Maritime Economics.* 3rd ed. Abingdon, Oxon: Routledge.

Surovtsev, D., Hole, P. A. & Meulengracht, C., 2012. *Exploration Assets Evaluation: A Practical Way of Confirming Deterministic to Stocastic Mindsets.* Calgary, SPE.

SUT, 2015. Subsea Mining. *UT3,* 4, 10(2), pp. 38-41.

Technip, 2008. *Nautilus Minerals RALS Project presentation to AFTP.* [Online]
Available at: http://jdp.ecritel.net/Presentations/documents/Atelier_8/5_J-M.Cholley.pdf
[Accessed 1 February 2016].

Technip, 2011. *Flexible System Definitions - Flexi France.* [Online]
Available at:
http://www.technip.com/sites/default/files/technip/page/attachments/flexible_system_definitions.pdf
[Accessed 19 October 2015].

The Naval Architect, 2016. Nautilus Set Out Its Deep Sea Mining Stall. *The Naval Architect,* pp. 20-25.

The World Bank Group, 2016. *World Bank Commodity Price Data (The Pink Sheet) - Annual Prices - 1960 to present, real 2010 US dollars.* [Online]
Available at:
http://pubdocs.worldbank.org/pubdocs/publicdoc/2015/12/547711449679682156/CMO-Historical-Data-Annual.xlsx
[Accessed 20 April 2016].

The World Bank, 2016. *Commodity Markets Outlook - April 2016 - Price Forecasts.* [Online]
Available at:
http://pubdocs.worldbank.org/pubdocs/publicdoc/2016/4/173911461677539927/CMO-April-2016-Historical-Forecasts.pdf
[Accessed 25 April 2016].

Trujillo, A. P. & Thurman, H. V., 2014. *Essentials of Oceanography.* 11th ed. Upper Saddle River: Pearson.

U.S. Energy Information Administration, 2010. *Oil and Gas Lease Equipment and Operating Costs 1994 Through 2009.* [Online]
Available at:
http://www.eia.gov/pub/oil_gas/natural_gas/data_publications/cost_indices_equipment_production/current/coststudy.html
[Accessed 22 May 2016].

UNEP/GRID-Arendal, 2011. *Continental Shelf: The Last Maritime Zone,* s.l.: UNEP/GRID-Arendal.

Utne, I. B. & Rasmussen, M., 2013. *TMR4310 Marine Technology 4 - Reliability, Availability, Maintenance, and Safety (RAMS) in Design and Operation of Marine Systems.* 4th ed. Trondheim: Norwegian University of Science and Technology (NTNU).

van der Vet, P., Rasmussen, M. & Utne, I. B., 2015. *Logistics engineering and managment - Logistic analysis of subsea operations,* Trondheim: Department of Marine Technology, NTNU.

van Wijk, J. M., 2016. *Vertical Hydraulic Transport for Deep Sea Mining - A Study Into Flow Assurance,* 2016: Delft University of Technology.

Vandiver, J. K. et al., 2009. *An Experimental Evaulation of Vortex-Induced Vibration of a Riser Bundle with Gaps.* Honolulu, ASME.

Vinnem, J.-E., 2014. *Offshore Risk Assessment vol 2 - Principles, Modelling and Applications of QRA Studies.* 3rd ed. London: Springer-Verlag London.

Wack, P., 1985. Scenarios: Uncharted Waters Ahead. *Harward Business Review*, September.

Walpole, R. E., Myers, R. H., Myers, S. L. & Ye, K., 2012. *Probability & Statistics for Engineers & Scientists.* 9th ed. Boston: Pearson Education, Inc..

Waquet, B., Faulds, D. & Benbia, A., 2011. *Understanding the Effects of Deep-Sea Conditions on Seafloor Massive Sulfide Deposits Crushing Process.* Houston, Offshore Technology Conference.

Waquet, B., Faulds, D. & Benbia, A., 2011. *Understanding the Effects of Deep-Sea Conditons on Seafloor Massive Sulfide Deposits Crushing Process.* Houston, Offshore Technology Conference.

Waquet, B. & Fouquet, Y., 2010. *Evolution of Geotechnical Properties in Hydrothermal Sulfide Mounds, the Reveal of a Maturation Threshold.* Gelendzhik, Underwater Mining Institute.

Wikborg Rein, 2015. *Update March 2015 Shipping Offshore,* Oslo: Wikborg Rein.

Williamson, H. S., Sawaryn, S. J. & Morrison, J. W., 2006. Monte Carlo Techniques Applied to Well Forwcasting: Some Pitfalls. *SPE Drilling & Completion,* 21(3), pp. 216-227.

World Bank Group, 2015. *Commodity Market Outlook,* Washington, DC: World Bank.

World Economic Forum, 2015. *Mining & Metals in a Sustainable World 2050.* [Online]
Available at: http://www3.weforum.org/docs/WEF_MM_Sustainable_World_2050_report_2015.pdf
[Accessed 1 June 216].

Yu, A. & Espinasse, P., 2009. *Extending Deepwater Technology to Seafloor Mining.* Houston, Offshore Tecnhology Conference.

Zierenberg, R. A. et al., 1998. The deep structure of a sea-floor hydrothermal deposit. *Nature,* Volume 392, pp. 485-488.

Appendices

APPENDIX A BATHYMETRIC MAP OF SOLWARA 1

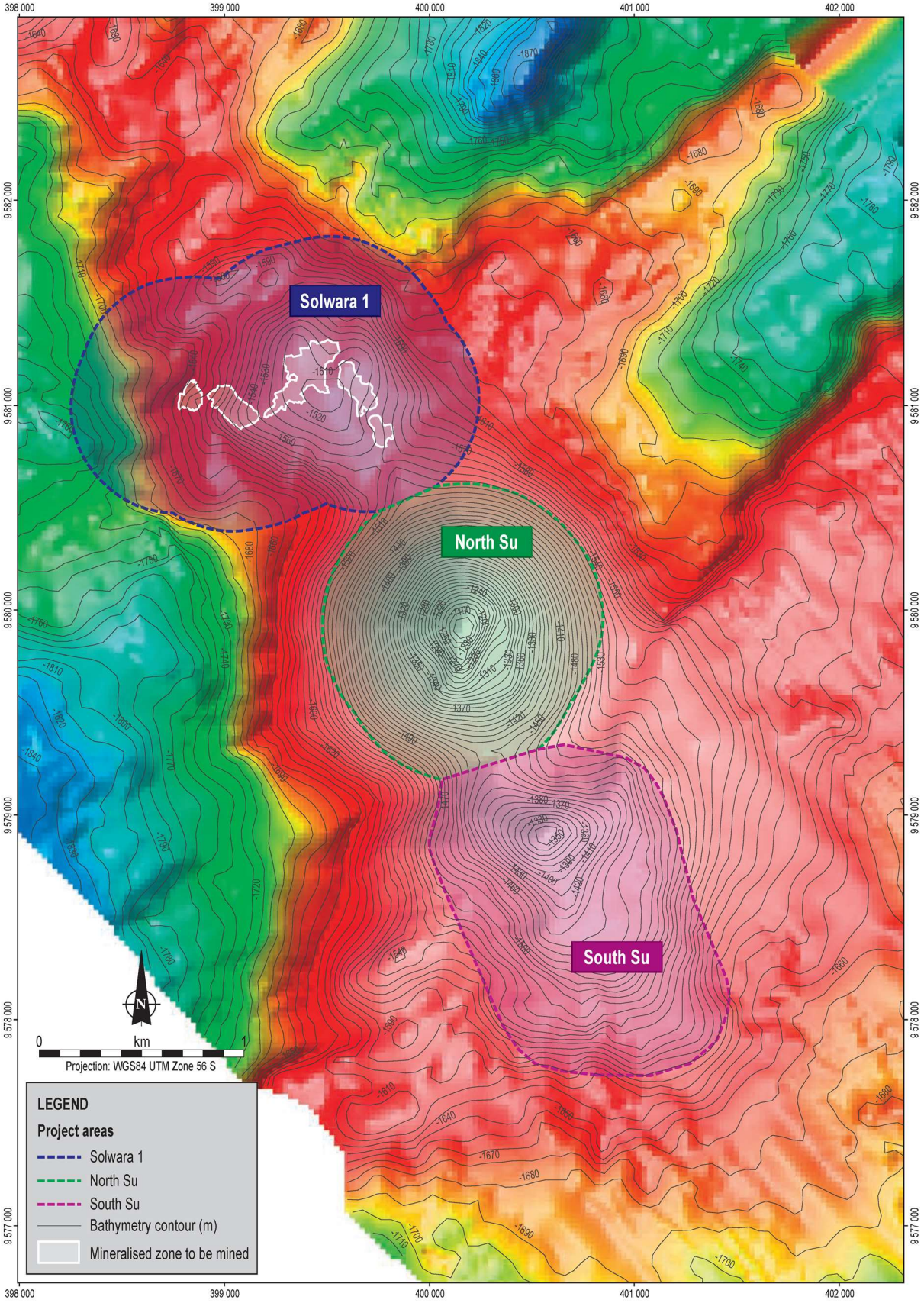

Source: (Coffey Natural Systems, 2008)

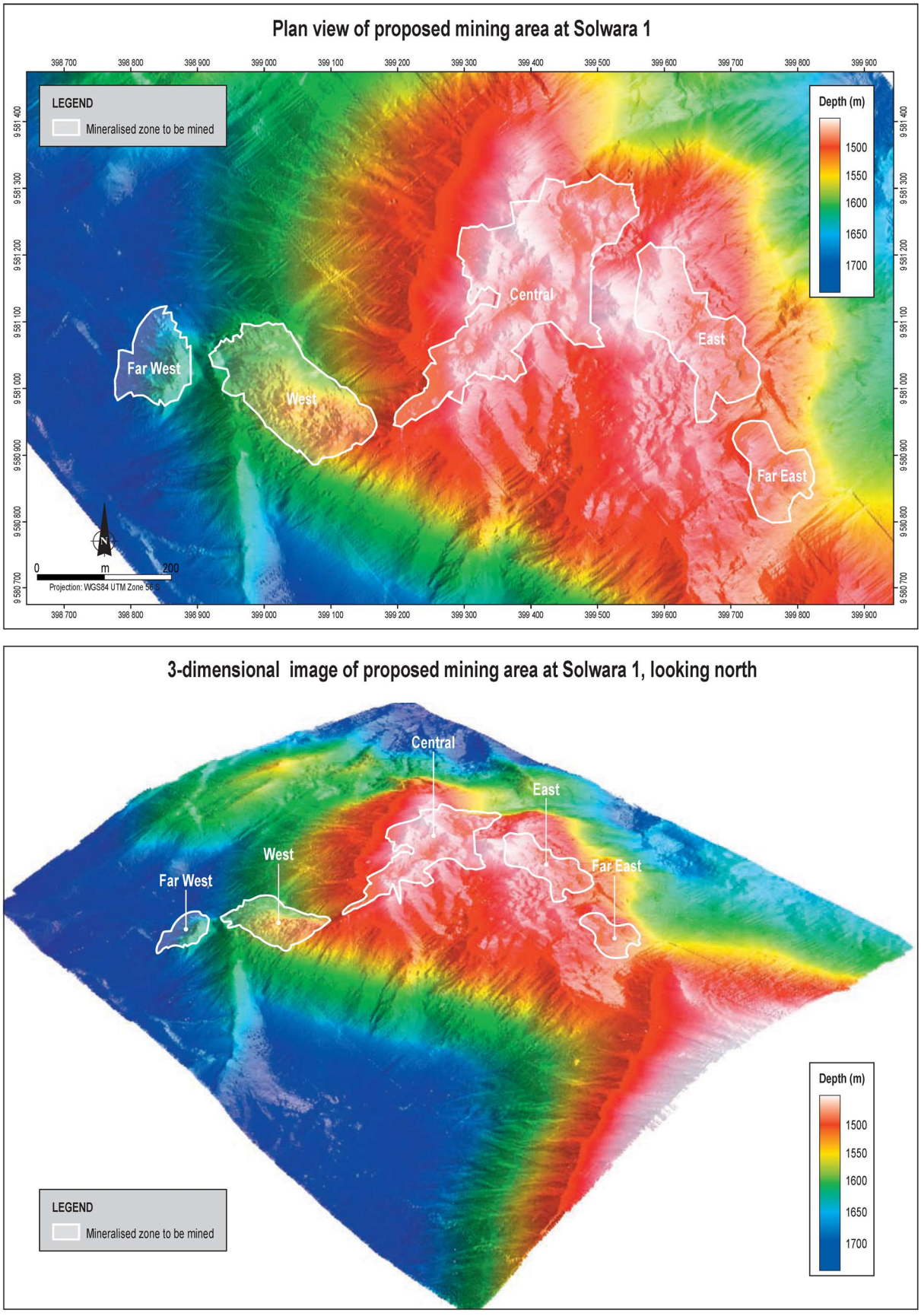

Source: (Coffey Natural Systems, 2008)

APPENDIX B PROCESS FLOW DIAGRAM FOR SOLWARA 1 PROJECT

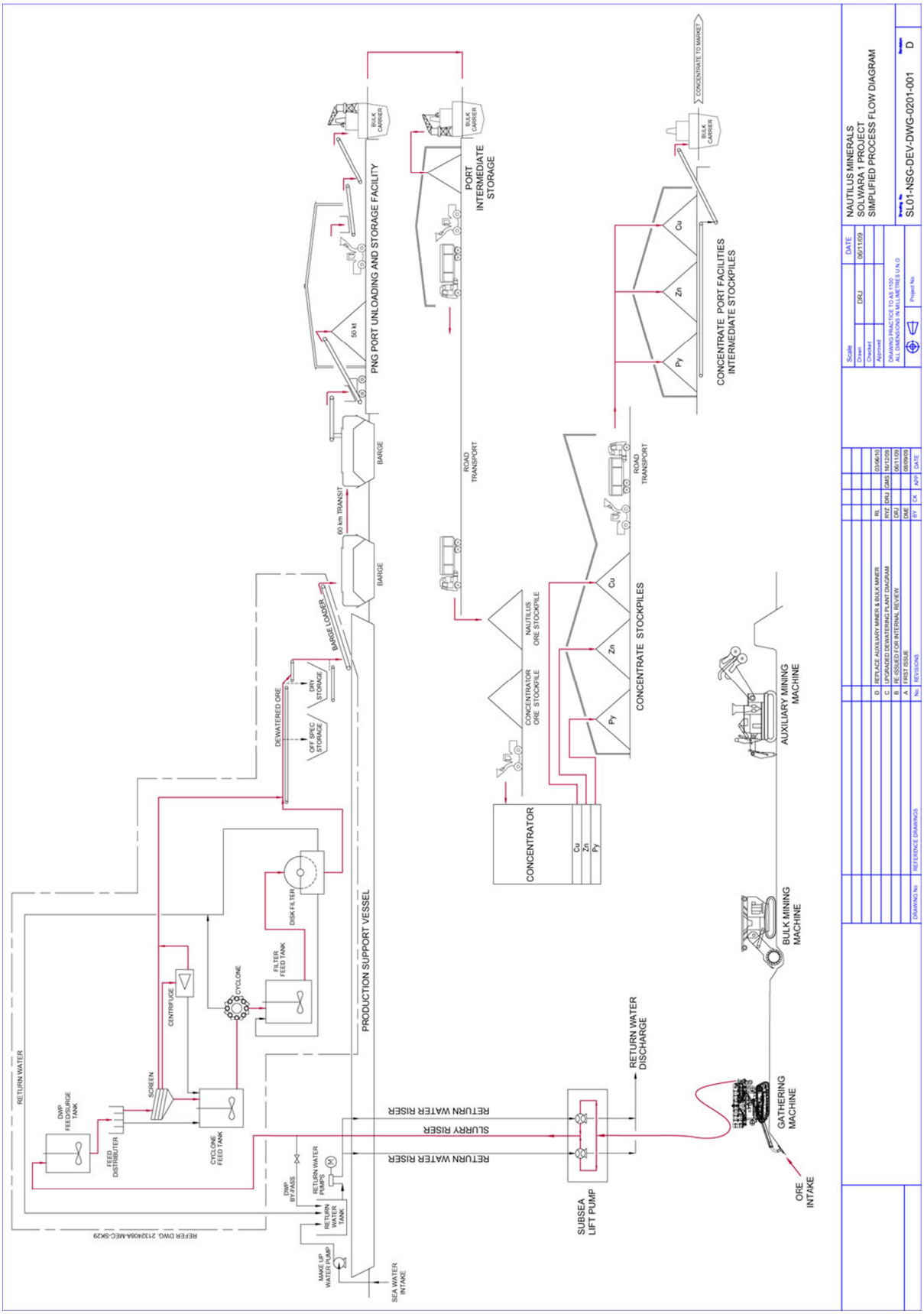

Source: (SRK Consulting, 2010, p. 138)

APPENDIX C TECHNICAL DRAWING OF RISER AND LIFTING SYSTEM (RALS)

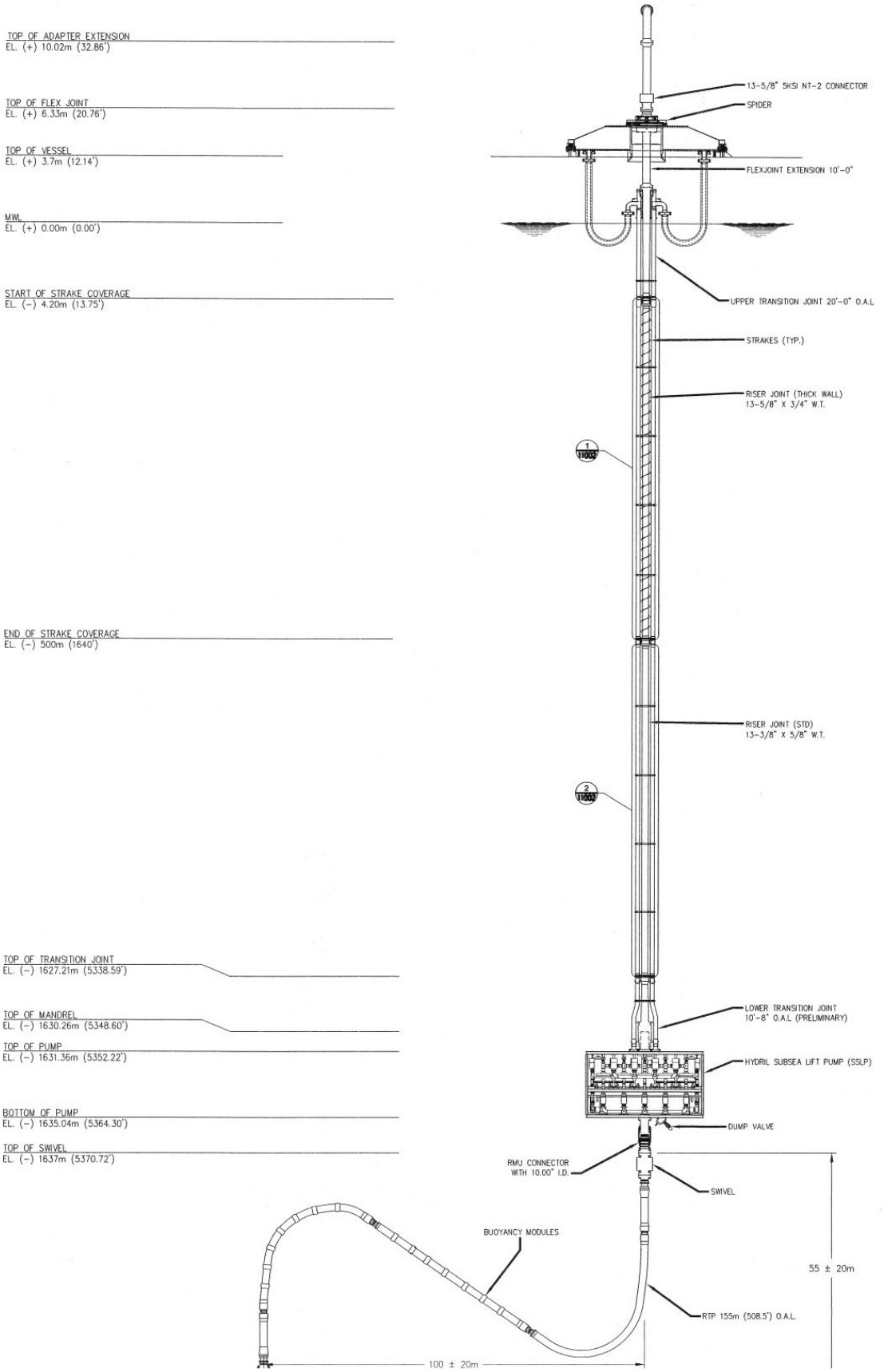

Source: (SRK Consulting, 2010, p. 165)

Cross sections showing the riser connector, which are welded onto the ends of each riser joint are seen in Figure C-1. Components that make up the riser string and the quantity of each are listed in Table C-1.

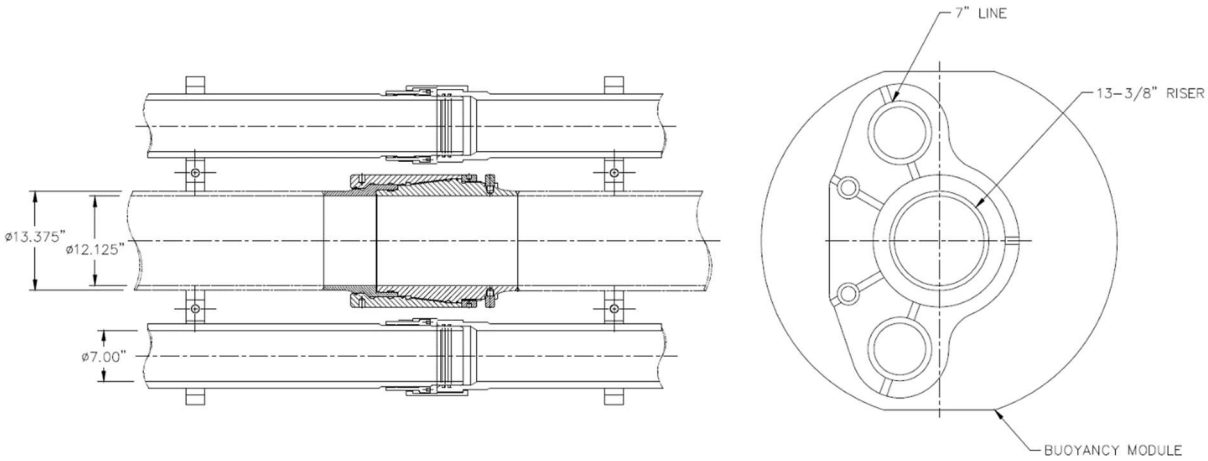

Figure C-1 – Riser connector, showing main vertical riser and water injection lines (Technip, 2008).

Table C-1 – Riser string components (Technip, 2008).

Description	Quantity
External Tieback Connector / Transition Mandrel	1
Transition Joint	1
Water Injection Line Adapters (set of 2)	1
Standard Riser Joint (62 ft)	68
Thick Wall Riser Joint (optional for 2,500 m case)	40
Buoyancy Joints (62 ft)	16
Straked Joints (62 ft)	24
Pup Joint (20 ft)	4
Pup Joint (10 ft)	2
Flex Joint Assembly	1
Flex Joint Receptacle	1
Flex Joint Handling and Running Tool	1
Riser Spider	1
Gimbaled Table	1
Riser Handling and Running Tool	1

APPENDIX D GENERAL ARRANGEMENT FOR PRODUCTION SUPPORT VESSEL

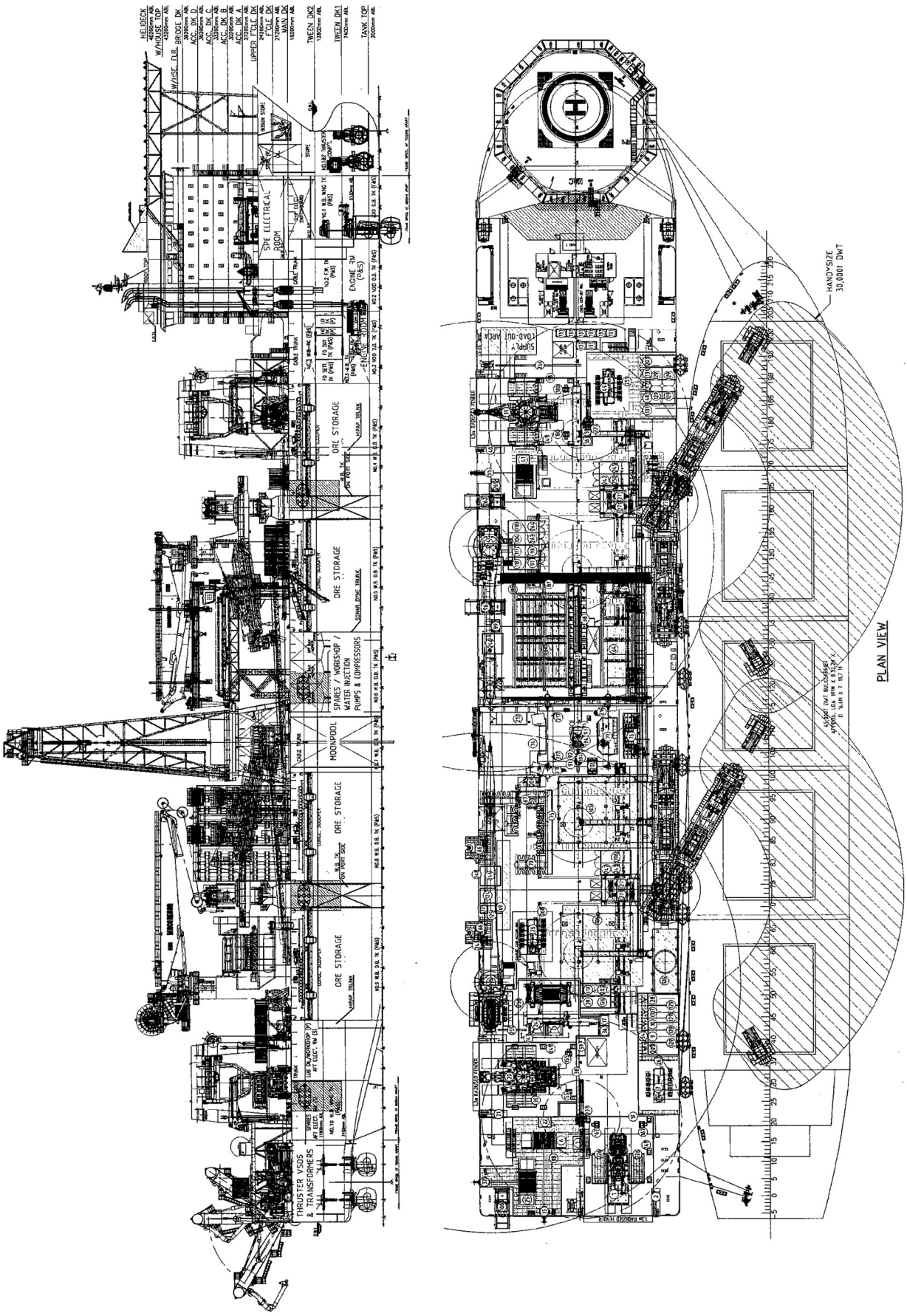

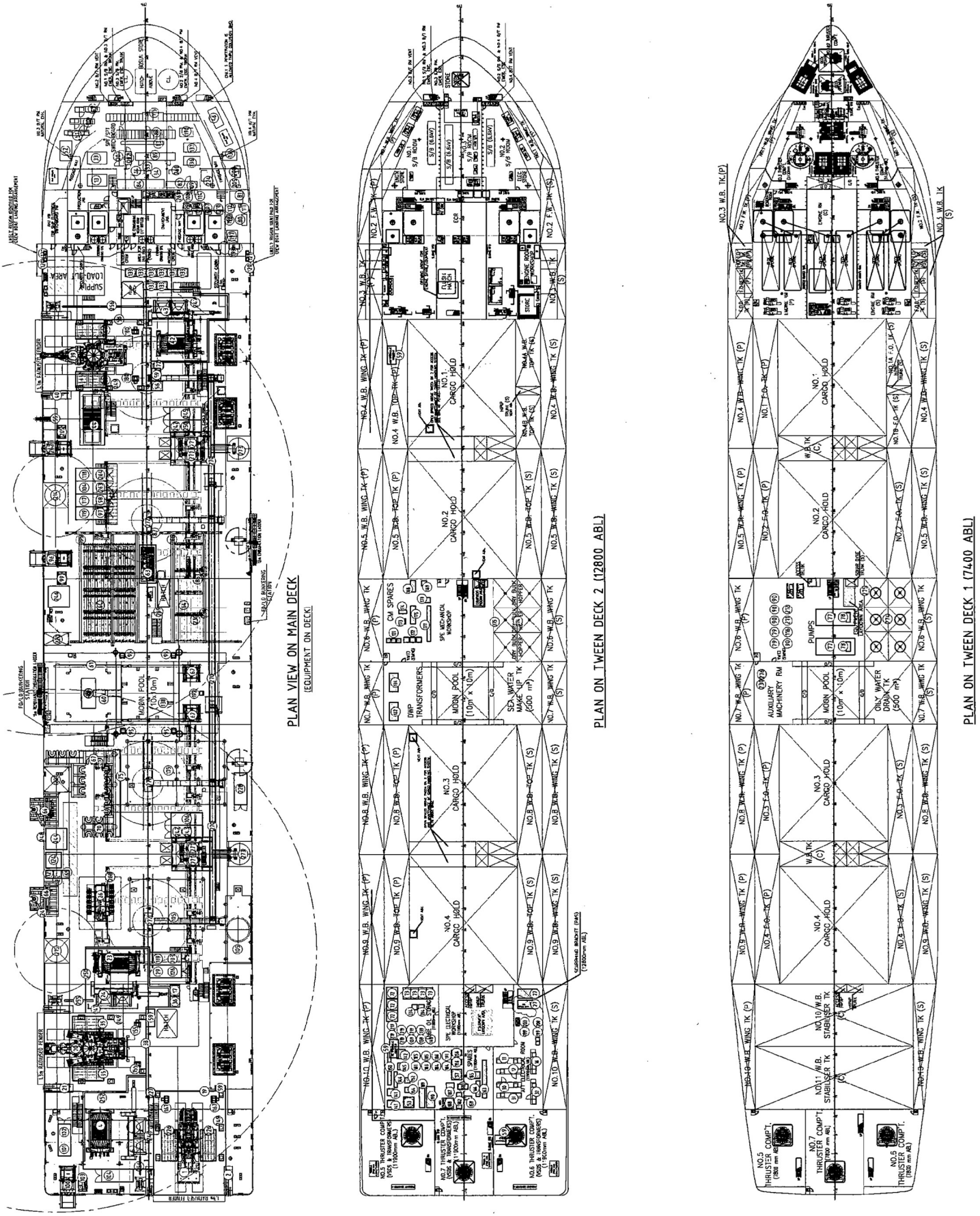

Source: The Naval Architect (2016)

APPENDIX E FINANCING OPTIONS IN MEGAPROJECTS FROM A SHIPPING PERSPECTIVE

Getting a deep-sea mining project off the ground requires a substantial amount of investment capital. Branch (1998, pp. 68-76) discusses different financing options for the construction of a vessel, and serves as the basis for the following overview of financing options for megaprojects. An overview of the different mechanisms is found in Figure E-1. Generally, the main sources of financing are the capital markets and leased-based transactions.

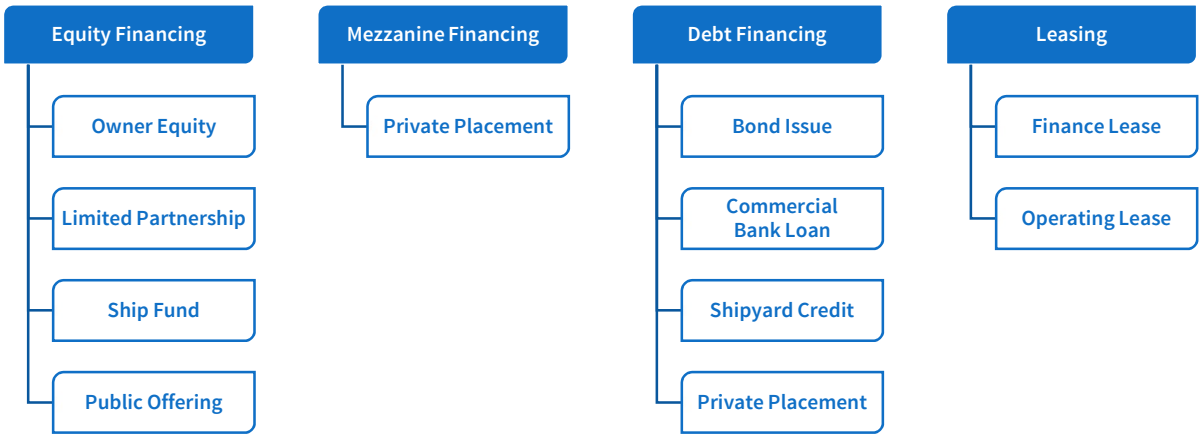

Figure E-1 – Financing options in shipping (Stopford, 1997, p. 206) .

Equity Financing

Through equity finance, the risks and rewards of the company are shared with any investors willing to buy shares in the company. This option consists of four elements:

- **Owner equity** provided by the ship owner's funds and retained earnings.
- **Fund** provided by partners (on a limited partnership basis).
- **Ship fund** through shares bought privately by individuals or publically listed (on stock exchanges)
- **Public offering** through shares sold by subscription on a public stock exchange.

Mezzanine Financing

Mezzanine finance is an intermediate type of financial structure based on debt capital, and involves both debt and equity elements. If the loan is not paid back both in time and in full, the lender has the rights to convert to an ownership or equity interest in the company. Such financing is often quickly mobilized, hence highly priced due to lack of due diligence (on the lender's side) and collateral (on the borrower's side).

Debt Financing

With debt finance, the company sells bonds, bills, or notes to individual and/or institutional investors, and receives interest at predetermined intervals through a legally enforceable loan agreement. Repayments of principal takes place after a specified period. According to Branch (1998, p. 70), there are five principal financial markets; private debt, public equity, public debt, banks, and shipyard credits, with the two last-mentioned being the largest sources. Loan payments (Branch, 1998, p. 70) are affected by the following variables, which all depend on the creditworthiness of the company (i.e., borrower): (i) down payment; (ii) interest rate; (iii) loan repayment period; and (iv) grace periods on interest and capital repayment.

Leasing

Leasing (i.e., a finance lease or an operating lease) provides long-term tax-effective financing, and is based on selling the ship to a company, taking advantage of depreciation. This method also offers leverage.

There are two types of leases:

- Finance lease
- Operating lease

A *finance lease* is normally a long-term lease with an option to purchase, and the lease payments can be regarded as payment for the cost of the equipment agreed upon (e.g., a ship). The leaseholder cannot cancel the contract. Such a lease is usually fully amortized because the lease hire is calculated to cover the cost of purchase of the leased equipment, as well as additional expenses incurred and part of the profit earned by the lessor (i.e., owner).

Generally, a financial lease has the following features Branch (1998, pp. 69-70):

- Equipment is for business or professional purposes
- Specification and selection of equipment are performed by leaseholder
- Equipment supplier (from which lessor acquires equipment) is selected by user or leaseholder
- Equipment is owned by lessor
- Risks associated with operating equipment, such as employment, destruction, and impairment, are transferred to user
- Remedies arising from equipment defects are assigned to user or leaseholder
- Claims made by user or leaseholder against lessor are excluded by contract

Typically, the parties agree on one of the following arrangements upon the end of the lease period:

- Purchase option for leaseholder
- Share proceedings of sale of leased equipment
- Extension of lease on renegotiated terms

An *operating lease* is typically on a short-term basis, and the leaseholder acts as if the vessel was owned. Lease payments do not involve amortization of the leased equipment. Unlike for a finance lease, either parties of an operating lease are entitled to cancel the contract, and the equipment is not purchased by the lessor according to the leaseholder's specifications.

APPENDIX F PRINCIPLES OF STATISTICS

Correlation

Correlation determines the degree of linear relationship between variables. Correlation is measured by Pearson's correlation coefficient, found from (19) and (20), which takes on a value between -1 and $+1$. A value of -1 corresponds to perfectly negative correlation and describes to two variables moving perfectly opposite of one another, while $+1$ is perfectly positive correlation (i.e., the variables move symmetrically together).

$$COV(X,Y) = \frac{\sum_{i=1}^{n}(X_i - \bar{X})\,(Y_i - \bar{Y})}{n-1} \tag{19}$$

$$CORR(X,Y) = \frac{COV(X,Y)}{\sigma_X \sigma_Y} \tag{20}$$

Probability Distributions for Input Variables

Generally, the probability distribution for the input variables indicates the possible values a variable can take and the probability associated to each value within that interval. The following section will describe general characteristics of probability distributions, as wells as different types of distributions and their range of appliance. The main challenge is to choose an appropriate distribution for the specific problem, as the distribution (and its parameters) strongly affect the results.

Key Statistical Parameters

The following parameters are describing random variables:

- **Percentiles** divide the range of outcomes into 100 intervals each containing 1 % of the outcomes. The nth percentile P_n is the value of which n % of the outcomes fall below.
- **Mode** (or *most likely value*) is the value that appears most often in a data set.
- **Mean** (or *expected value*) is the arithmetic average value of all the outcomes, and the sample mean is calculated as in (21).
- **Median** is the middle observation when the data set is sorted[17], and is of most interest for discrete variables. It corresponds to P_{50}, i.e., the value that divides the area under the pdf curve in half .
- **Standard deviation** has the same unit at the underlying variable which it describes, and is the root of the variance (or the average of the squared deviations from the mean). The sample standard deviation s is calculated from (22).

$$\bar{X} = \frac{\sum_{i=1}^{n} X_i}{n} \tag{21}$$

$$s = \sqrt{\frac{\sum_{i=1}^{n}(X_i - \bar{X})^2}{n-1}} \tag{22}$$

[17] For a sorted vector of data points, the median is literally the middle observation for an odd-numbered vector, or the average of the two middle ones for an even-numbered vector.

General Characteristics

The following terminology describe general characteristics of probability distributions:

- **Discrete** distributions have a finite number of possible values with a corresponding probability of occurrence (Walpole, et al., 2012, p. 84), which gives a distribution similar to a bar chart. The bar heights reflect the probability.
- **Continuous** distributions take on all values of random variables. Such distributions are characterized by probability density functions (PDFs) whose height above a given value indicates its relative likelihood of occurrence. As each exact value has a probability of 0, the corresponding probability is found by integrating the curve over an interval (Albright & Winston, 2015, p. 817). The total area underneath the curve sums to 1 (Walpole, et al., 2012, pp. 87-90).
- **Symmetric** distributions have identical values for mode, mean and median (see "Key Statistical Parameters". Thus, $\text{Mode} = \text{Median} = \text{Mean}$.
- **Skewed** distributions are non-symmetric about their mode value (i.e., the two sides are not mirror images). A left-skewed (or negatively skewed) distribution has its tail on the left-hand side, while a right-skewed (or positively skewed) has its tail on the right-hand side, see Figure F-1. The mean is shifted towards the right and left, respectively, to better model the real case. Data that have a lower bound are often skewed right, while data that have an upper bound are often skewed left.
    - Positively skewed: $\text{Mode} < \text{Median} < \text{Mean}$
    - Negatively skewed: $\text{Mode} > \text{Median} > \text{Mean}$
- **Bounded** distributions have a lower bound (i.e., minimum value for the random variable) and/or an upper bound (i.e., maximum value). A *non-negative* distribution has a lower bound equal to or greater than 0, like in the case of modelling a cost variable.

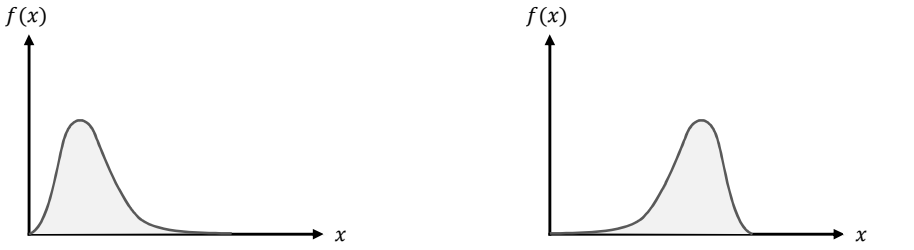

(a) Positively or right-skewed (b) Negatively or left-skewed

Figure F-1 – Skewed probability distributions.

Types of Distributions and Appliance

Figure F-2 shows different probability distributions, and especially the following continuous probability distributions are used in probabilistic modelling and relevant for the purpose of this thesis:

- **Uniform distribution** is square-shaped, thus all values between the lower and upper bounds have the same probability of occurrence. It is typically used for variables with little knowledge associated to them. Input variables: Minimum value and maximum value.
- **Triangular distribution** is triangle-shaped, and has a density function that risers to a point and then falls (similar to the normal distribution). The most likely value can be skewed to either bounds. Using a triangular distribution, the extreme values (i.e., values towards the bounds) are

believed more probable than when the normal distribution. Input variables: Minimum value, maximum value, and a most likely value.

- **Normal distribution** is bell-shaped and symmetric. A normally distributed random variable is within two standard deviations of its mean with a probability of 95 %, and 68 % and 99.7 % are within one and three standard deviations of the mean, respectively. Hence, its applicable when the variable is expected to lie around the mean value. The normal distribution is inapplicable for some cases due to it being symmetric and allowing negative values. Input variables: Mean value and standard deviation.
- **Lognormal distribution** is based on the assumption that the natural logarithm of the random variable is normally distributed.

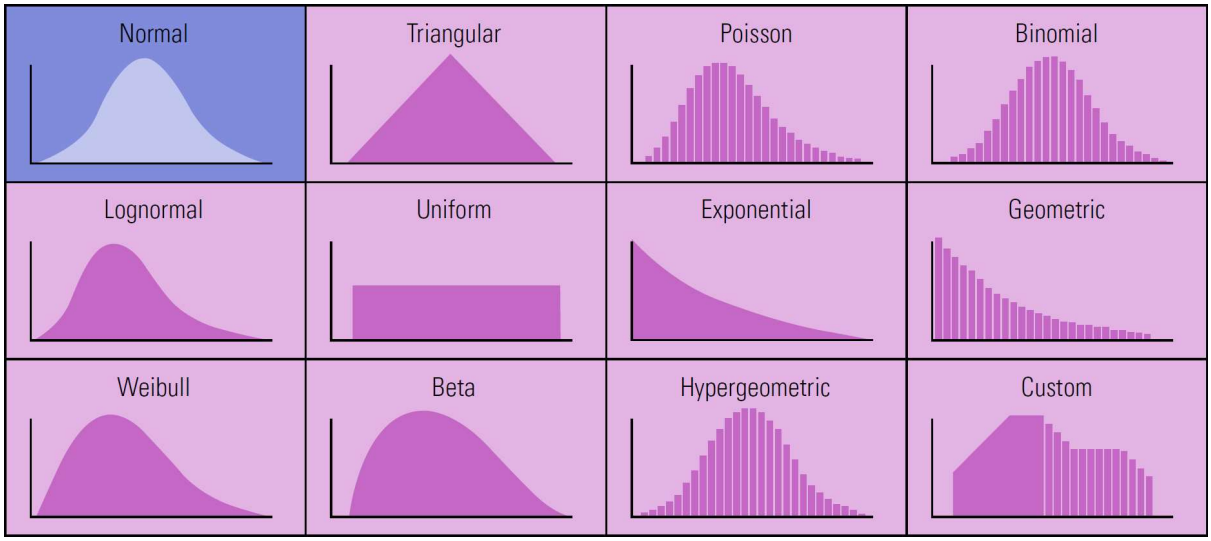

Figure F-2 – Probability distributions (Bailey, et al., 2000).

The characteristic of the particular distribution is established in the following manner (Sinding-Larsen, 2015, p. 32), see Figure F-3, which allows all potential values (and their relative probabilities) to be defined using a minimal number of inputs:

1. Define range by establishing the extremities (i.e., the lowest and highest possible values)
2. Select "mode-likely" value and its relative probability (i.e., height of peak point above horizontal x-axis)
3. Select a distribution to connect the points.

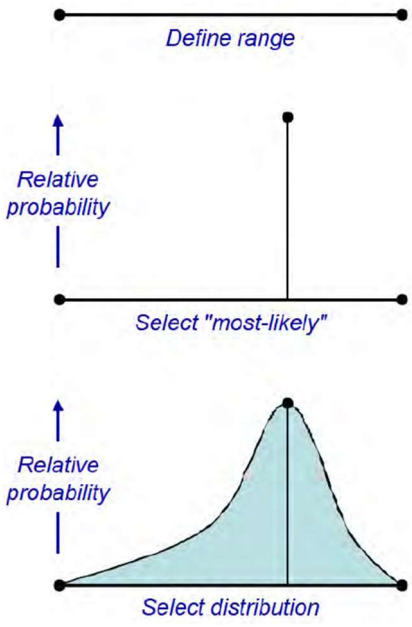

Figure F-3 – Defining distribution for a parameter (Sinding-Larsen, 2015, p. 32).

Graphical Presentation of Random Variables

Box-whisker plots and histograms are complementary ways of displaying a random variables distribution, and both are described in greater detail in the following.

Histogram

A histogram shows the shape of the distribution of a random variable by dividing the variable into bins (or discrete categories) with a constant bin width. The frequency of random variables within the respective bins are summarized in a frequency table, which corresponds to each of the bars in the histogram. Various parameters of the distribution are indicated by a histogram, like its center, variability, and skewness (Albright & Winston, 2015, p. 45). The plot is easily generated by using the "Histogram" tool under "Data" and "Data Analysis" in Excel.

Box-Whisker Plots

Box-whisker plots are typically used to compare distributions of variables. For a probability p, the pth percentile is the value having a probability of p of all values being lower than that value (Albright & Winston, 2015, p. 34). The first, second, and third quartile corresponds to a p of 0.25, 0.5, and 0.75, respectively. Hence, the second quartile is equal the median. The interquartile range (IQR) is defined as the third quartile minus the first quartile (i.e., the range of the middle 50 % of the data points).

The box, as seen in Figure F-4, extends from the first quartile to the left, to the third quartile to the right, covering the IQR. The line across the center of the box is the median, and the $*$ indicates the mean. The whiskers extend to the furthest observations that are no more than 1.5 IQR from the box. Mild outliers (hollow square) are data points within 1.5-3 IQR from the box, while extreme outliers (solid square) are more than 3 IQR from the box. The box height can be varied to show another feature of the distribution.

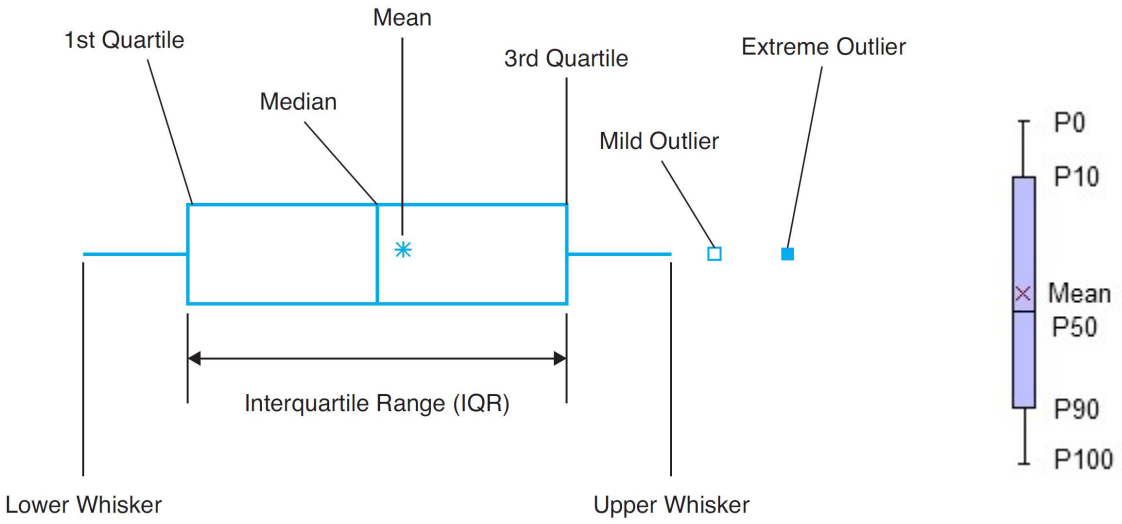

(a) Traditional plot (Albright & Winston, 2015, p. 51) (b) GeoX plot.

Figure F-4 – Box-whisker plots.

APPENDIX G ESSENTIALS OF ECONOMIC EVLAUATION

Cash and Non-Cash Items in Financial Statements and Capital Budgeting

The various financial statements are described by Berk & DeMarzo (2014, pp. 22-48). A company's *income statement* measures its profit over a period. The gross profit net of operating expenses makes up the operating income; adding income/expenses from non-core activates of the company (e.g., financial investments) gives the earnings before interest and taxes (EBIT). *Depreciation and amortization*, one of the operating expenses, represents an estimate of costs associated with wear and tear or obsolescence of assets, and is not an actual cash expense. Depreciation expenses are deducted over time.

However, due to non-cash entries (e.g., depreciation and amortization) and unreported cash usage (e.g., building purchases and inventory expenditures) on the income statement, the net income does not correspond to cash earned. The *statement of cash flows* determines the amount and allocation of cash generated during a period, and is based on both the income statement and the *balance sheet* (i.e., the *statement of financial position*, which lists the firm's assets and liabilities).

The statement of cash flows consists of three sections: Operating activities, investment activities, and financing activities. Under operating activities, depreciation and other non-cash items related to operations are deducted from the net income. Thus, these non-cash expenses (e.g., depreciation and deferred taxes) are added back to net income when determining a firm's cash flow. Under investment activities, purchased properties, plants, and equipment are listed under capital expenditures, which is a cash expense.

Evaluation Criteria

In the following, commonly used economic evaluation criteria for decision making (i.e., investment decision rules) are defined based on Gu & Gudmestad (2012, p. 642).

Net Present Value

The net present value (NPV) is the present value (PV) of the total cash flow discounted at a specific discount rate, and measures the value-adding potential of the investment or project to the company. In GeoX, given as a monetary value, it is the distribution of the NPV of the net after-tax cash flows for the Monte Carlo estimation.

Internal Rate of Return

The internal rate of return (IRR) is the maximum discount rate that is charged for the investment capital (i.e., liabilities) to produce a break-even venture, hence the discount rate which gives a NPV equal to zero. In GeoX, given as a decimal number or percentage, it is the distribution of the IRR for the net after-tax cash flows for the Monte Carlo estimation.

APPENDIX H EVALUATING RESONABLE VESSEL DAY RATES

PSV Time Charter Assumptions

As stated by Nautilus Minerals (2015, p. 9), Marine Assets Corporation (MAC) will charter the Production Support Vessel (PSV) to Nautilus Minerals "*[...] for a minimum period of five years at a rate of 199,910 USD/day, with options to either extend the charter or purchase the PSV at the end of the five year period*". Further, SRK Consulting (2010, p. 218) states that "*the vessel charter costs include the provision of a vessel and basic marine crew to operate the vessel*". Drawing parallels to the Ukpokiti field development by Conoco off the coast of Nigeria in the late 1990s, the FPSO was converted from Conoco's fleet of trading tankers and chartered from Conoco Marine on a bareboat charter (Steube, 2000). The OPEX of the project were divided into three categories: (i) Operations; (ii) Accruals; and (iii) FPSO costs. The FPSO costs included, in addition to the bareboat charter, *"[...] the annual temporary import permit costs for the FPSO, and the associated Nigerian taxes*". Thus, the day rate stated above is assumed to include only bareboat charter and the essential marine crew.

Day Rates of PSV

From the technical outfitting of the PSV (e.g., derrick, installed effect, and vessel size), day rates for mobile offshore drilling units (MODUs) are a reasonable comparison. Day rates include the use of the rig and its crew, but do not include most of the other costs associated with drilling a well (e.g., casing, cementing, evaluation, etc.). Both short and long-term contracts are used among all market players. As discussed by Kaiser (2014), deepwater, high-specification, international rigs are generally more costly to operate than shallow water, low-specification, domestic rigs. Further, rig size and age, port infrastructure, scale economies with respect to a contractor's regional presence, market competition, and the availability of goods and services also impact operating cost. Difference in risk level, as discussed under "Insurance", is also differentiating the cost level of domestic and international contractors. Both Figure H-2 and Figure H-1 show world averages over time for different types of MODUs. Geographic differences in day rates are shown for jack-ups and drillships in Figure H-3.

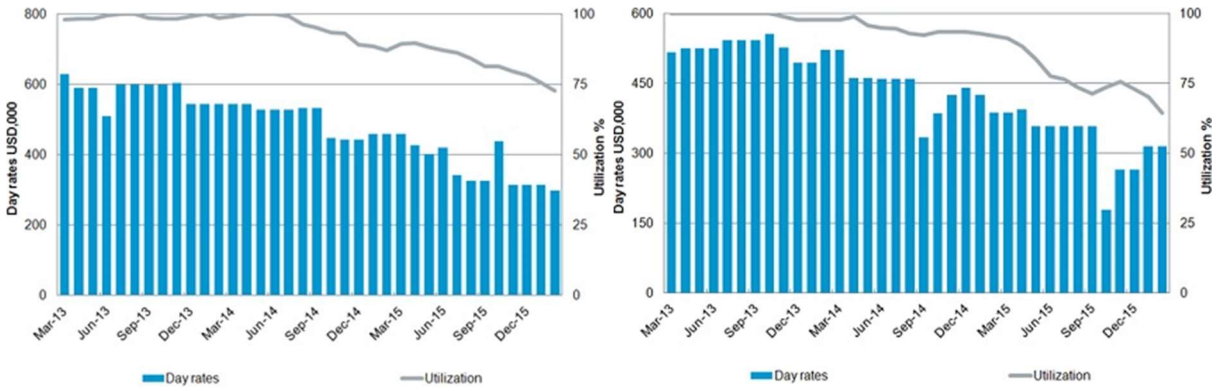

(a) Drillships (b) Semi-submersible

Figure H-1 – Worldwide avg. day rate and total contracted utilization, water depth > 7,500 ft (2,300 m). Modified from IHS (2016)[18].

[18] https://www.ihs.com/products/oil-gas-drilling-rigs-offshore-day-rates.html, accessed Mars 19, 2016.

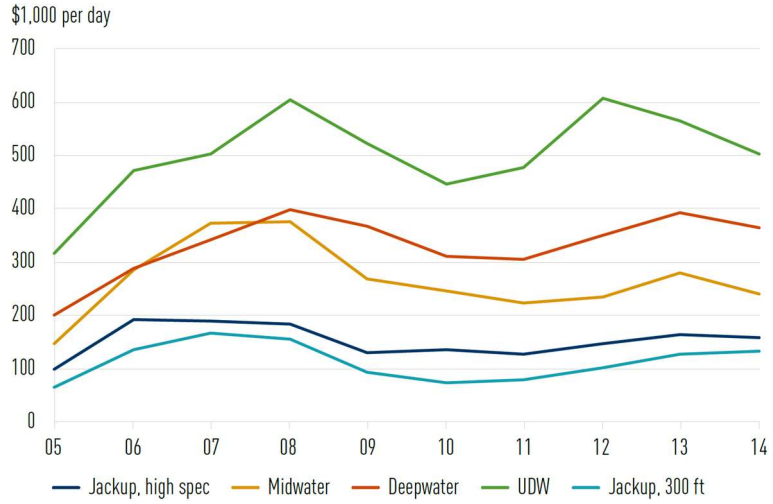

Figure H-2 – Global average day rates for MODUs, 2005-2014 (RS Plateau, 2015, p. 35).

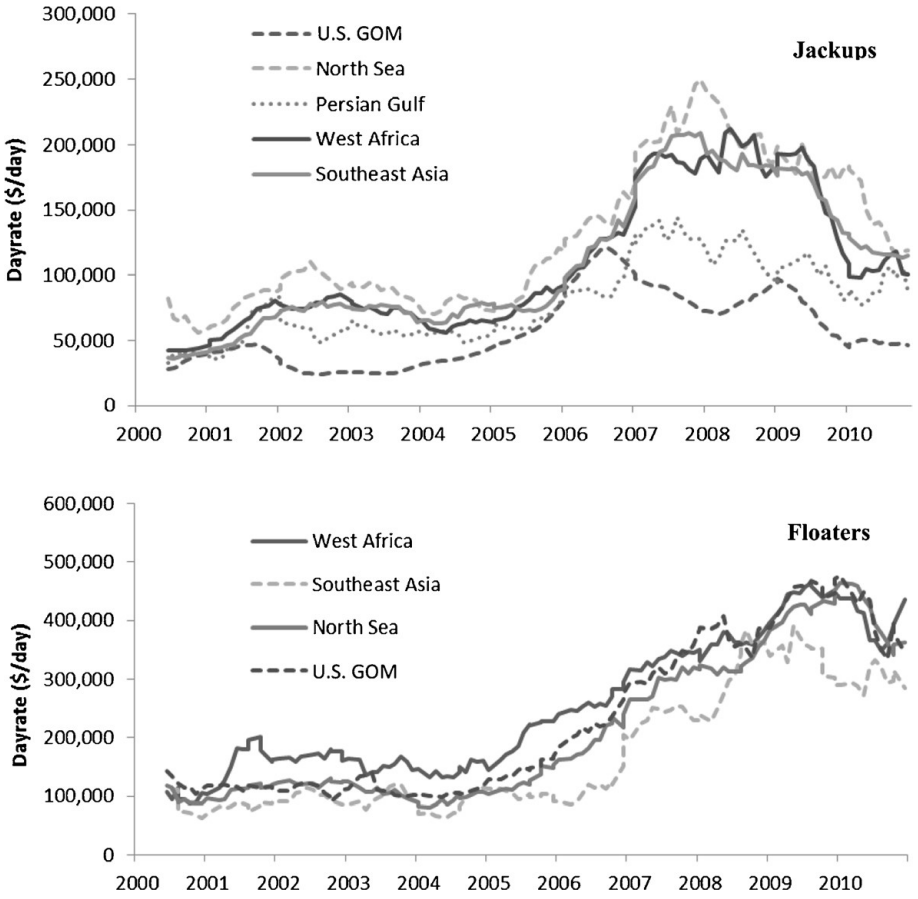

Figure H-3 – Jack-up and floater 6-month average day rates, 2000–2011 (Kaiser, 2014).

Another comparison is the subsea vessel fleet. Following the methodology of Fearnley Offshore Supply (2013, p. 37), the various vessel types are categorized according to the specifications listed in Table H-1. Day rates for these vessel types are seen in Figure H-4 (a)-(c), and are based on long-term time charter (TC) contracts (i.e., 3-5 years) direct from vessel owner to first-tier charterer. The rates exclude ROVs and special topside equipment. In 2010, larger OCVs (with LOA greater than 150 m) entered the market, and as such a larger span between the low and high rates is seen in Figure H-4.

Table H-1 - Subsea vessel categorization.

Type	Short Name	LOA [m]	Subsea Crane Capacity [t]	Accommodation [PAX]
Construction Vessel	CON	120-200	250-400	100+
Light Construction Vessel	LCV	90-120	140-240	50+
MSV/ROV Support Vessel	Multi-Purpose	70-110	0-130	50-100

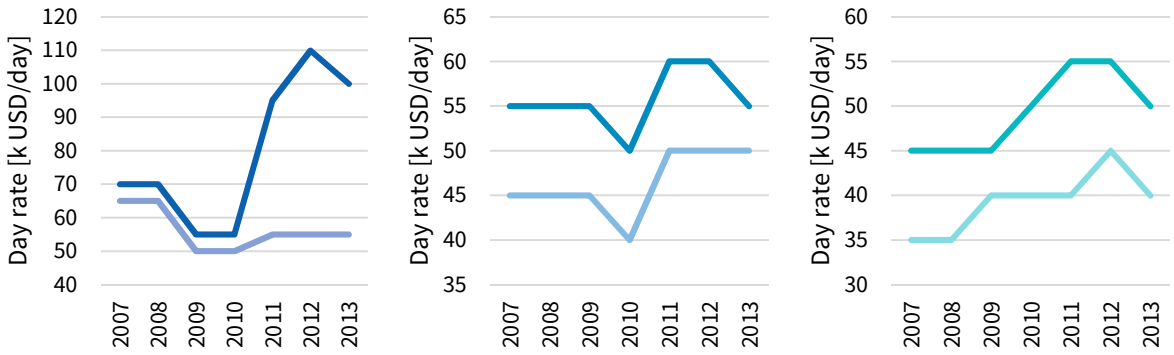

(a) CON (b) LCV (c) Multi-purpose

Figure H-4 – Historic day rates of subsea vessels, ref. Table H-1 (Fearnley Offshore Supply, 2013, p. 29).

Combined Bulk Carrier and Supply Vessel

Figure H-5 and Figure H-6 show historical time charter (TC) rates back to June 2008 for bulk carriers and platform supply vessels (PSVs), respectively. As seen from Figure H-5, the worldwide bulk carrier rates fell together with the financial markets under the financial crises in 2008. Similiarly, the rates on offshore vessels have fallen together with the reduced activity level in the global O&G industry after the falling oil price since 2014. The PSV rates are for the North Sea, and two of the data sets are for the spot market. Furthermore, TC rates of anchor handling tug supply (AHTS) vessels and PSV for the North Sea are shown in Figure H-7 (a)-(d), correspondingly.

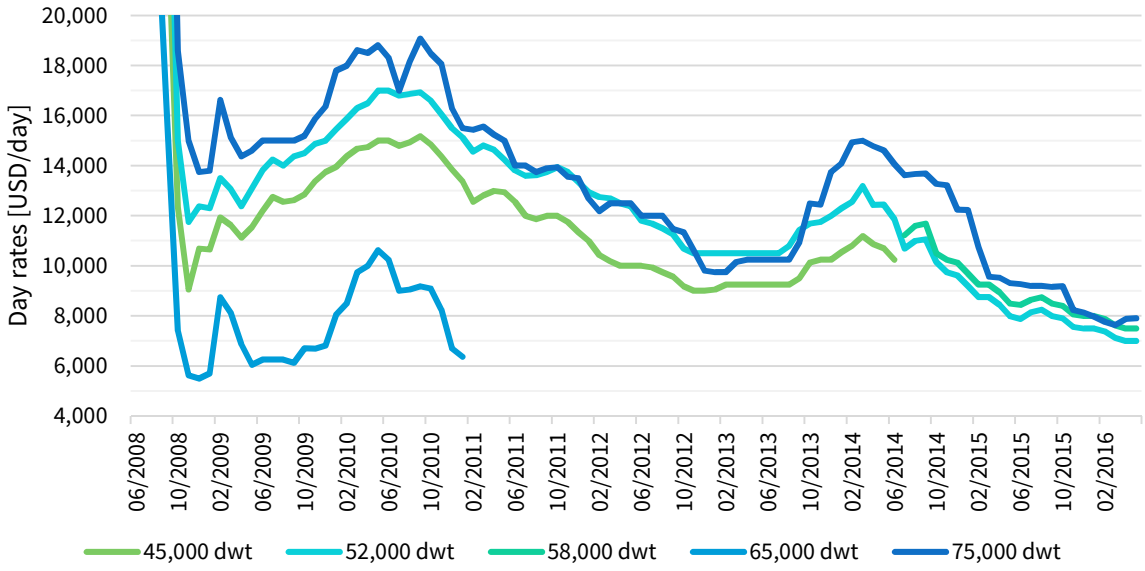

Figure H-5 – Historic 5-year time charter (TC) rates for handymax, nominal values (Clarksons Research).

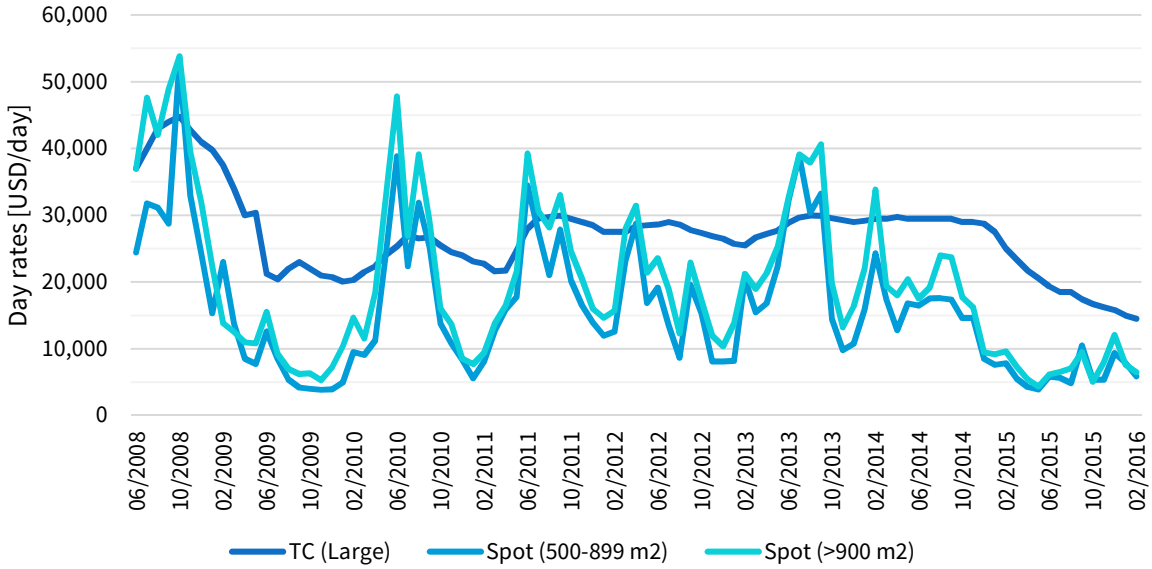

Figure H-6 – Historic rates for North Sea PSVs, nominal values (Clarksons Research).

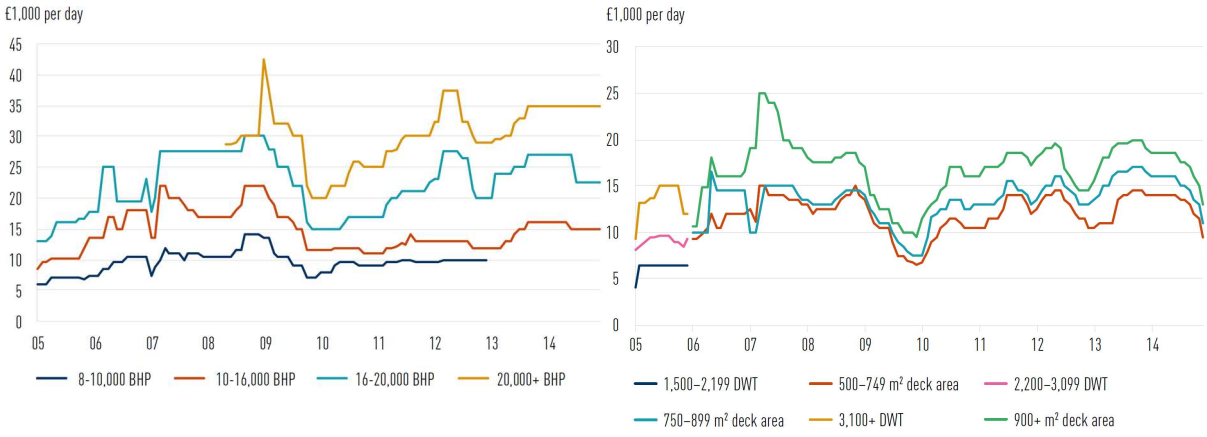

(a) AHTS (b) PSV

Figure H-7 – Average time charter (TC) rates on North Sea tonnage, 2005-2014 (RS Plateau, 2015, p. 38)

APPENDIX I OPEX ITEMS FOR PRODUCTION SUPPORT VESSEL

Cost of ROV Services

According to SRK Consulting (2010, p. 194), two heavy work class remotely operated vehicles (ROVs) will support the subsea production activities. However, The Naval Architect (2016) states that the ship is equipped with three large work class ROVs. A normal ROV package at continuous (24-h) operation consists of a total of one ROV, two supervisors, and four pilots/technicians (Oceaneering, 2010). It is assumed that three ROVs are used, and that one ROV supervisor per shift is sufficient. Based on the day rates for ROV and crews from Oceaneering (2010) for the Asia market, an estimated total cost of ROV services for the project are shown in Table I-1 (at USD/day). Oceaneering maximum crew rotation is every 28 days, and overtime comes at 300 USD/h (Oceaneering, 2010).

Table I-1 – Day rate for three ROV packages, two 12-h shifts with one supervisor (Oceaneering, 2010).

Cost Item	Unit Price [USD/day]	Number	Cost [USD/day]
Heavy work class ROV (Hydra MAGNUM PLUS)	5,340	3	16,020
ROV supervisors	2,880	2	5,760
ROV pilots/technicians	2,590	12	31,080
Total			**52,860**

Crew Size and Direct Manning Costs

The everyday crew onboard the initial PSV design is shown in Table I-2, which corresponds to the required number of personnel to perform 24-hour operation (i.e., two shifts) with a crew working rotation of four weeks on/off (SRK Consulting, 2010, p. 208). Table I-3 shows the final manning profile of the PSV, as published by The Naval Architect (2016). Based on a report on the ERICON[19] Aurora Borealis project (ERICON, 2012, pp. 34-44), directs manning cost for the "Seabed Production" and "Mining Maintenance" crews are taken as the average of a European drilling crew and a Norwegian ship crew, as seen in Table I-4. An estimated crew overview and total direct manning costs are found in Table I-5.

Table I-2 – Personnel summary (SRK Consulting, 2010, p. 208).

Area	PAX
Vessel Marine Operations	30
Mining Operations	54
Mining Maintenance	31
Medical and HSE	2
Vendor Representatives	4
Total	**121**

Table I-3 – Final manning overview (The Naval Architect, 2016).

Area	PAX

[19] ERICON – European Research Icebreaker Consortium.

Ship Crew	30
Seabed Production Crew	69
Others	100
Total Manning	**199**

Table I-4 – Direct manning costs

Crew	Avg. [USD/month]
European Drilling Crew	10,796
Norwegian Ship Crew	4,596
Average	**7,696**

Table I-5 – Crew overview and total direct manning costs.

Category	Position	PAX	Unit Cost [USD/month]	Total Cost [USD/month]	Comments
Marine Crew	All	30	0	0	The Naval Architect (2016), (Nautilus Minerals (2015). Included in bareboat charter.
Seabed Production Crew	All	69	7,696	531,033	The Naval Architect (2016), and ERICON (2012, pp. 34-44)
Mining Maintenance Crew	All	31	7,696	238,580	SRK Consulting (2010, pp. 206-210), and ERICON (2012, pp. 34-44)
Medical / HSE	QHSE Advisor	1	5,228	5,228	SRK Consulting (2010, pp. 206-210)
Medical / HSE	Medic	1	5,228	5,228	SRK Consulting (2010, pp. 206-210)
Vendor Representatives	All	4	0	0	Representatives of SPTs (SMD) and RALS (Technip and/or GE Hydril). SRK Consulting (2010, pp. 206-210). Included in fixed OPEX for SPTs/RALS.
ROV Crew	ROV supervisors	2	0	0	Oceaneering (2010). Included in ROV Charter.
ROV Crew	ROV pilots/ technicians	12	0	0	Oceaneering (2010). Included in ROV Charter.
Other Marine	Chief cook	1	5,037	5,037	ERICON (2012, pp. 34-44)
Other Marine	Second cook	2	5,037	10,073	ERICON (2012, pp. 34-44)
Other Marine	Leading steward	1	5,037	5,037	ERICON (2012, pp. 34-44)
Other Marine	Steward's staff	2	4,058	8,117	ERICON (2012, pp. 34-44)
Total		**156**		**808,333**	

Indirect Manning Costs

Indirects, which include training and catering, as well as crew transportation to the site from which they are mobilized, are taken as 60 % of the direct manning costs (based on OPEX distribution of Rowan's MODUs in Appendix J.

Financing Cost

Assumed financing costs (based on basic annuity calculations) are found in Table I-6.

Table I-6 - Financing cost parameters.

Equity	30 %
Debt	70 %
CAPEX, mean [M USD]	444.754
Annual percentage rate (APR)	5.0000 %
Loan length [years]	25
Compounding periods per year, k	12
Effective annual rate (EAR)	5.1162 %
One-month discount rate	0.4167 %
Periods w/ monthly payments	300
Monthly payment, C [M USD]	1.820
Monthly interest expense	0.337478
Daily average financing cost [USD]	11,095

Insurance

The insurance costs of a vessel are associated with its general risk level, which is elaborated on by Kaiser (2014). Drilling contractors involved in international operations are subject to additional risks to that of domestic contractors. Risk factors are: terrorist acts; war and civil disturbance; expropriation or nationalization of assets; renegotiation or nullification of contracts; changes in law or interpretation of existing law; assaults on property or personnel; foreign and domestic monetary policies; and travel limitations or operational problems caused by public health threats. The general risk level of a deep-sea mining vessel is lower than that of a MODU, as it is not exposed to the risks associated with hydrocarbons (e.g., blowouts, fire, and oil spills). However, with respect to the daily operation and the routine work tasks performed by the personnel onboard, the risks are regarded more or less the same. Thus, the insurance costs for a deep-sea mining vessel is assumed to be somewhat lower due to an overall lower risk level for a worst-case scenario – defining risk as the product of consequence and probability of occurrence. The insurance cost is taken at 75 % of that of Rowan for a drillship operating in Norwegian waters in the North Sea (estimated costs scaled from jack-up data) – equaling 9,374 USD/day. See background data and estimates in Appendix J.

APPENDIX J INDUSTRY COMPARABLES FOR OPEX NUMBERS

Contractors of Mobile Offshore Drilling Units

Ocean Rig

Earning reports in Ocean Rig (2013) and (2015) give the combined direct and onshore OPEX for Ocean Rig fleet, as shown in Figure J-1 and Table J-1. The numbers exclude maintenance CAPEX that are treated as OPEX for accounting purposes.

Table J-1 – Direct and onshore OPEX for Ocean Rig's fleet, Q1 2013 (Ocean Rig, 2013, p. 10).

Vessel	Type	OPEX [USD/day]
Eirik Raude	Semi-submersible	258,600
OCR Corcovado	Drillship	219,900
OCR Olympia	Drillship	198,200
OCR Poseidon	Drillship	181,400
OCR Mykonos	Drillship	201,400

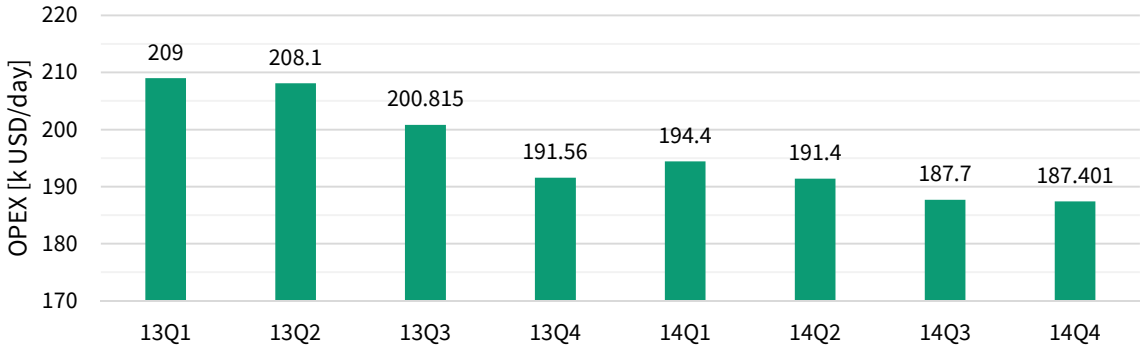

Figure J-1 – Average OPEX (direct and onshore) for Ocean Rig's fleet (Ocean Rig, 2015, p. 5).

Rowan

Based on rough data ranges in Rowan Companies (2015, pp. 33-34), and assuming that mid, lo, and hi thousands correspond to $500, $167 and $833, respectively, an average regional OPEX for Rowan's MODUs are estimated (for the market situation of November 2015), see Figure J-2. The ranges exclude mobilization, amortization, and rebills. Rowan Companies (2015) elaborate that the daily OPEX vary by rig class and region, and that rigs with higher specifications generally earn higher day rates, thus typically have higher OPEX. Furthermore, during shipyard stays, crew and other personnel-related costs are usually capitalized rather than expensed. The distribution of Rowan's MODU OPEX is seen in Figure J-3, in which "Employee-related" costs include training, catering, and crew transportation, and correspond to 60 % of "Labor and fringes" (which equals direct manning costs). "Other" includes rentals, medics, agent commissions, satellite communications, and other miscellaneous drilling costs.

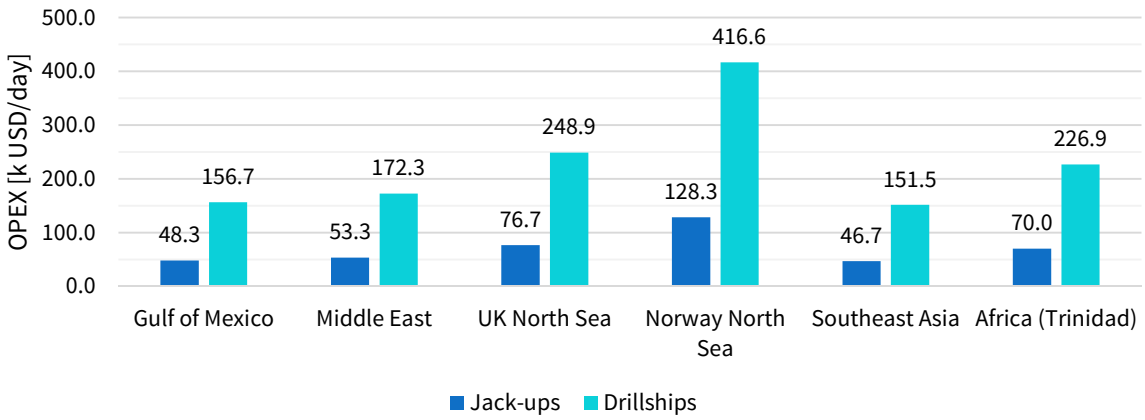

Figure J-2 – Average regional OPEX for Rowan's fleet. Data from Rowan Companies (2015, p. 33)

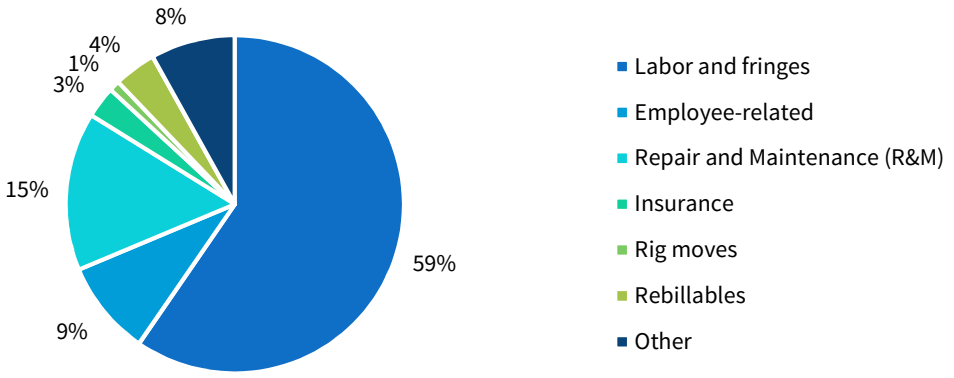

Figure J-3 – Distribution of total OPEX for Rowan (Rowan Companies, 2015, p. 34).

Sevan Drilling

Figure J-4 shows the average OPEX for Sevan Drilling's fleet offshore Brazil (i.e., the bucket-shaped MODUs Sevan Driller and Sevan Brazil). Disregarding Q4 2011 due to abnormalities, the average OPEX is 163,500 USD/day, of which "Offshore Crew Costs", "Operation and Maintenance Costs", and "Other Operating Costs" constitute 53 %, 24 %, and 23 %, respectively. The difference in OPEX due to the geographical location where the rig is set to operate is illustrated by the assumption in OPEX for four rigs of the exact same design, as stated in Sevan Drilling (2013, p. 7). An average of 150,000 USD/day is assumed for the above rigs in Brazil compared to 150,000 USD/day for the units Seven Lousiana and "Rig 4", which at the time were under construction and planned for contracts in the Gulf of Mexico (GOM).

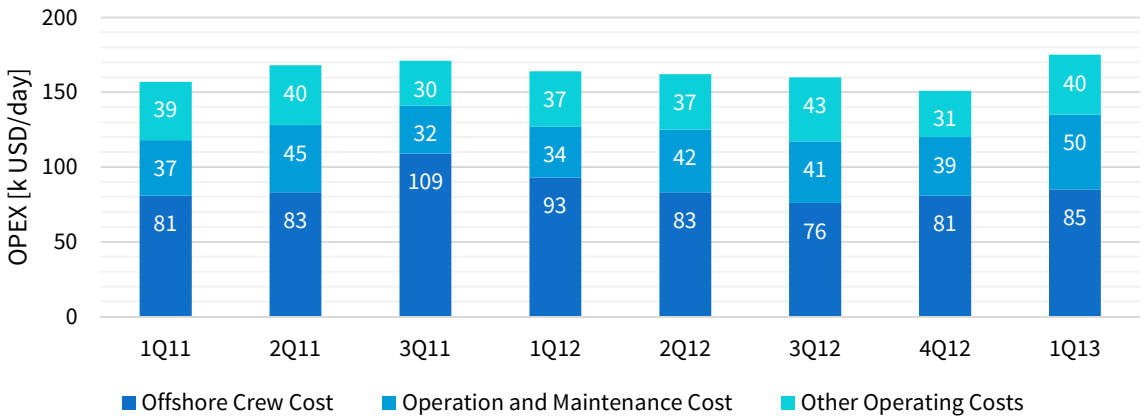

Figure J-4 – Fleet avg. OPEX for Sevan Drilling: 1Q11-2Q12, only Sevan Driller; 3Q12-1Q13, mean of Sevan Driller and Sevan Brazil (Sevan Drilling, 2013, p. 18)

Others

Based on Kaiser (2014), OPEX for contractors in the GOM are listed in Table J-2 and Table J-3. Both Transocean and Diamond define ultra-deepwater as $>$ 7,500 ft. However, Transocean defines deepwater as $>$ 4,500 ft, and midwater as $<$ 4,500 ft, while Diamond defines ultra-deepwater as deepwater as $>$ 5,000 ft, and midwater as $<$ 5,000 ft. Furthermore, data from 2014 of Songa Offshore (2016) in Figure J-5 supports the OPEX distribution of Rowan in Figure J-3.

Table J-2 – Transocean and Diamond OPEX statistics in 2011 (Kaiser, 2014).

Firm	Rig Class	OPEX [k USD/day]
Transocean	Ultra-deepwater	199
Transocean	Deepwater	135
Transocean	Harsh floaters	171
Transocean	Midwater floaters	91
Transocean	High-specification jack-ups	81
Transocean	Jackups	29
Diamond	Ultra-deepwater	169
Diamond	Deepwater	119
Diamond	Midwater floaters	86
Diamond	Jack-ups	36

Table J-3 – OPEX for MODUs by contractor in 2011 (Kaiser, 2014).

Rig Class	Firm	Rig type	OPEX [USD/day]
Jack-ups	Transocean	High-specification	87,000
Jack-ups	Transocean	Standard	46,000
Jack-ups	Hercules	Domestic	32,000
Jack-ups	Hercules	International	47,000

Jack-ups	Atwood	High-specification	64,000
Jack-ups	Atwood	Standard	44,000
Jack-ups	Diamond	High-specification	55,000
Jack-ups	Diamond	Standard	52,000
Floaters	Transocean	Ultra-deepwater	150,000
Floaters	Transocean	Deepwater	137,000
Floaters	Transocean	Midwater	104,000
Floaters	Atwood	Ultra-deepwater	191,000
Floaters	Atwood	Deepwater	119,000

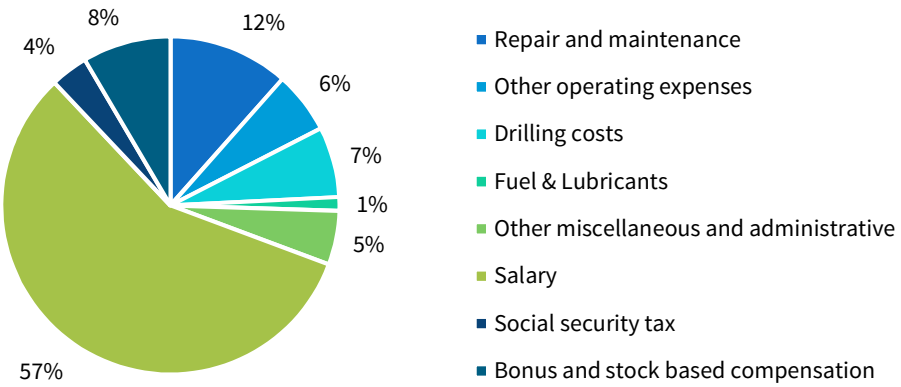

Figure J-5 – OPEX distribution for Songa Offshore for 2014. Data from (Songa Offshore, 2016, p. 65).

OPEX in Offshore Oil & Gas Projects

As a first indication, annual OPEX is often assumed to 5-10 % of CAPEX (Odland, 1999, p. 24). Estimated operating costs for the offshore Gulf of Mexico (GOM) by U.S. Energy Information Administration (2010) for fixed structure platforms in 600 ft (183 m) and 120 miles offshore (104 nmi) are shown in Table J-4. Meals, platform maintenance, helicopter and boat transportation of personnel and supplies, communication costs, insurance costs for platform and production equipment, and administrative expenses are included in normal production expenses. Crude oil and natural gas transportation costs to shore were excluded, as were water disposal costs.

Table J-4 – Average daily OPEX for 18-slot fixed platform in the GOM (600 ft water depth, 125 miles offshore) (U.S. Energy Information Administration, 2010).

Cost Items [USD/day]	2006	2007	2008	2009
Labor	3,209	3,370	3,538	3,715
Supervision	481	505	531	557
Payroll Overhead	1,476	1,550	1,627	1,709
Food Expense	297	384	384	384
Labor Transportation	6,687	7,535	8,699	9,874
Surface Equipment	560	591	629	629
Operating Supplies	112	118	126	126
Workover	12,487	10,750	10,968	8,092
Communications	214	214	214	214
Administrative	1,552	1,631	1,717	1,788
Insurance	3,073	2,842	2,842	2,842

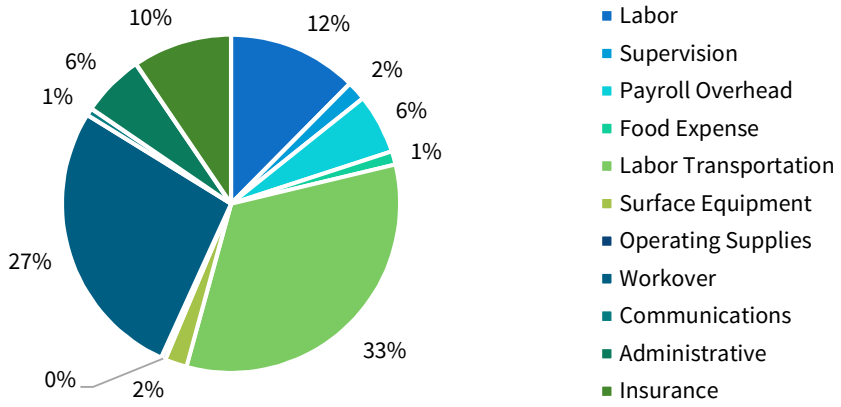

Figure J-6 – Distribution of average daily OPEX for 2009, ref. Table J-4.

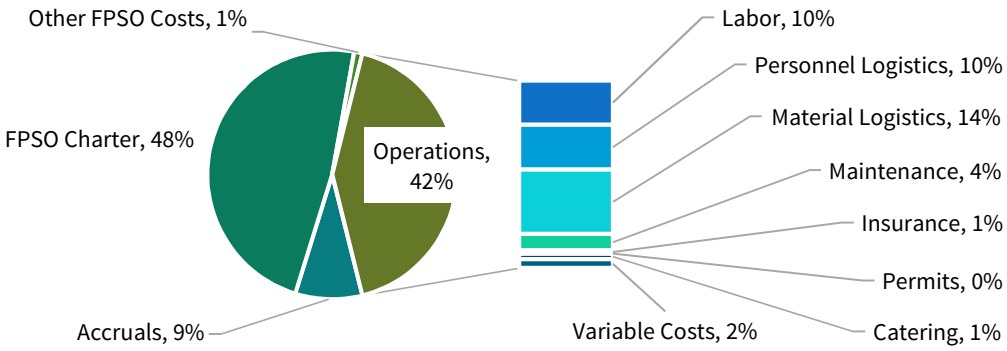

Figure J-7 – Total field OPEX distribution for Conoco's Ukpokiti project (Steube, 2000).

As a comparison to the cost level on the NCS, vessel costs for the Gulf of Mexico (GOM) are summarized in Table J-5. OPEX include crew and maintenance costs, and show great variation between vessel sizes, ages, and specifications. According to Kaiser (2015, p. 70), fuel costs are typically paid by the E&P firm.

Table J-5 - Vessel costs for GOM, 2013-2015 (Kaiser, 2015, p. 70).

Vessel	CAPEX [M USD]	OPEX [k USD/day]	Day Rate [k USD/day]
PSV	20-40	5-10	20-40
Crewboat	5-15	3-5	5-10
MSV	10-30	3-5	5-10
AHTS	40-100	10-20	40-60
Lifeboat	20-40	5-15	10-40
Pipelay Barge	40-200	10-60	10-150
MPSV	40-150	15-60	60-120
Derrick Barge	10-200	5-50	5-500
Well Intervension	50-120	30-75	50-200
DSV	5-50	3-50	5-75

OPEX Distributions in Shipping

Table J-6 and Table J-7 show OPEX distributions for bulk carriers. For the latter, Table J-8 gives an overview of the features of the "Operating costs". The basic manning cost is given by Table J-9, and covers direct wages and employment related costs. These sum to 544,000 USD/year for a 5-year-old ship. According to Stopford (2009, p. 228), an additional 119,000 USD/year (73,000 USD/year for travel, insurance, etc.; 46,000 USD/year for victualling) is required to cover the following cost items, which constitute 16 % of the total crew costs for a 5-year-old ship of 743,000 USD/year:

- Travel
- Manning and support
- Medical insurance and victualling
- Basic management costs that apply to crew (i.e., crew selection, rotation, making travel arrangements, purchase of victuals, and ship supplies)

Table J-6 – Panamax bulk carrier operation cost (Branch, 1998, p. 126).

Onshore Cost	10 %
Stores and Supplies	15 %
Bulker Fuel and Water	15 %
Dry Dock and Maintenance	10 %
Insurance	25 %
Crewing	25 %

Table J-7 – Costs of running 10-year-old capesize bulk carrier (Stopford, 2009, p. 225).

Operating Costs	14 %
Periodic Maintenance	4 %
Voyage Costs	40 %
Cargo-Handling Costs	0 %
Capital Costs	42 %

Table J-8 – Operating cost for 5- and 10-year-old capesize bulk carriers (Stopford, 2009, p. 227).

Vessel Age [years]	**5**	**10**
Crew Cost	32 %	31 %
Stores and Consumables	12 %	11 %
Maintenance and Repair	9 %	15 %
Insurance	32 %	32 %
General Costs	14 %	11 %

Table J-9 – Crew costs on 160,000 dwt bulk carrier, 2007 [USD/month] (Stopford, 2009, p. 228).

Rank	**Basic**	**Consolidated Allowances**	**Bonus**	**Provided Funds, Incl. Social Costs**	**Subtotal**	**Crew Number**	**Total**
Master	1,967	3,933	300	35	6,235	1	6,235
Chief officer	1,294	3,206	200	35	4,735	1	4,735
2nd officer	1,077	1,773		35	2,885	1	2,885
3rd officer	1,030	1,320		35	2,385	1	2,385
Chief engineer	1,760	3,990	300	35	6,085	1	6,085
1st assistant engineer	1,294	3,206	200	35	4,735	1	4,735
2nd assistant engineer	1,077	1,773		35	2,885	1	2,885
Bosun	670	649		182	1,501	1	1,501
AB (Able Seaman)	558	542		171	1,271	5	6,355
Motorman/Oiler	558	542		171	1,271	3	3,813
Cook/Steward	670	649		182	1,501	1	1,501
Steward	558	542		171	1,271	1	1,271
Messman	426	378		158	962	1	962
Total						**19**	**45,348**

APPENDIX K ESTIMATING POWER REQUIREMENT AND FUEL CONSUMPTION

Aker H-6e Semi-Submersible Drilling Unit

Screening various sources for estimates on fuel consumption for offshore vessels, the best available ones are those for the Aker H-6e. As described by Haug, et al. (2008), the semi-submersible rig design is designed for extreme environmental conditions based on DNV's recommendations for world-wide operations, including the North Atlantic. Particulars and technical features are listed in Figure K-1

Aker H-6e hull particulars

Pontoon Length	120 m
Breadth Pontoons	77 m
Pontoon Width	19,5 m
Pontoon Height	10 m
Main Deck Length	90 m
Main Deck Width	70 m
Columns	12,5 x 12,5 m
Displacement	
- transit	44,580 tonnes
- survival	60,240 tonnes
- operating	65,300 tonnes
Draft	
- transit	9.7 m
- survival	19.0 m
- operating	23.0 m
Air-gap	18.5 m

Aker H-6e key technical features

Design	DP Drilling Vessel, Aker Solutions
Registration	Bahamas
Classification	+DNV 1A1, Column Stabilized Drilling Unit (N), DRILL (N), HELDK, CRANE, E0, DYNPOS AUTRO, POSMOOR ATA
Water Depth	3,000 m (10,000 ft)
Drilling depth	10,000 m (33,000 ft)
Variable Drilling Load	7,000 tonnes in transit
Operation and survival	10,000 tonnes
Diesel Generators	8 x 5 300 kW, 720 rpm
Thrusters	8 x 4 500 kW, 800 kN bollard pull, variable speed, fixed pitch
Mooring system (optional)	8 point anchor line system, 84 mm Stud Chain, 15 tonnes anchors Stevpris Mk5.
Windlasses (optional)	4 double winches
Living Quarters	140 single bed cabins, extendable to 160
Helicopter Deck	Sikorsky S92 and S-61N, Superpuma AS332L2, EC225 and EH-101.
Lifeboats	Free fall type, 4 x 80 men
Deck cranes	2 ea, max capacity: 85 tonnes at 17 m, max reach 51 m

Figure K-1 – Specifications for Aker H-6e (Haug, et al., 2008).

Figure K-2 – Transocean Barents (Transocean).

According to Haug, et al. (2008), the Aker H-6e rig is designed as DP-3, with the option for thruster assisted mooring in water depths of 100-500 m, or alternatively a pre-set system in deeper water. The DP system is capable of keeping the rig on location in all operational conditions. The Aker H-6e design provides station-keeping by eight thrusters and eight mooring lines (Aker Kværner, 2006). Estimated fuel consumption for normal average thrust utilization for the given operating modes are shown in Table K-1, and corresponding power load diagram in Figure K-3.

Table K-1 – Estimated Fuel Consumption. Modified from Aker Kværner (2006, p. 24).

Operating Mode	Only DP	Anchor	Transit
Drilling [MW]	8.5	8.5	0.0
Utility [MW]	6.0	6.0	4.0
Thrust [MW]	14.8	3.6	27.0
% of Total Trust Effect	*41 %*	*10 %*	*75 %*
Power Consumed	29.3	18.1	31.0
% of Installed Total Effect	*69 %*	*43 %*	*73 %*
Daily Fuel Consumption [t/Day]	128.5	79.5	136.2
Daily Fuel Consumption [m^3/day]	146.0	90.3	154.7

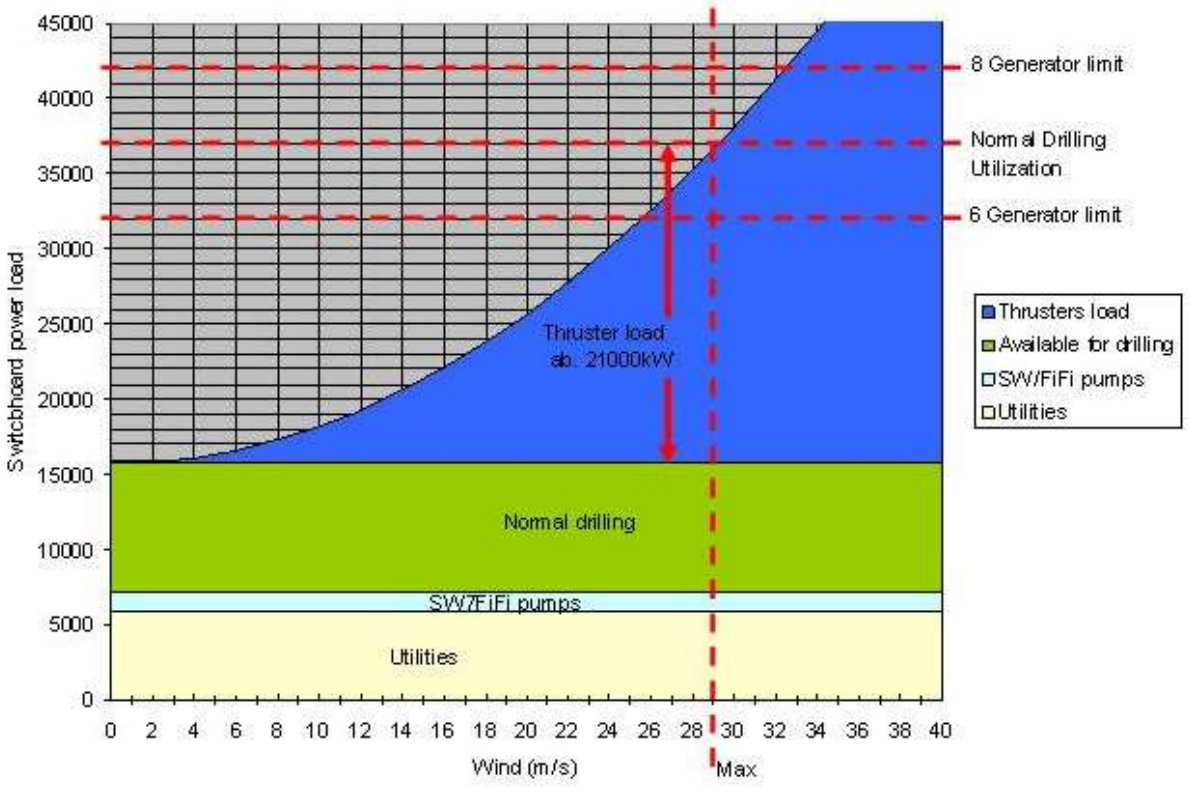

Figure K-3 – Typical electrical load scenario for normal operation (Aker Kværner, 2006, p. 18).

Power Consumption

The estimates for power and fuel consumption for the surface vessel are based on the numbers and methodology applied in the same estimates for the semi-submersible drilling rig design Aker H-6e (Aker Kværner, 2006, p. 24). The bulk carrier is not regarded in the following.

Chopra (2016) and Nautilus Minerals (2015, p. 11) give a total power of for the Production Support Vessel (PSV) at about 30 MW and 31 MW, respectively. In Yu & Espinasse (2009), the required operating power of the SSLP at a water depth of 2,500 m is 6 MW. Further, SRK Consulting (2010, p. 158) states the power consumption of mining equipment to be 13.8 MW, which is assumed to include both the SSLP and the three SPTs (that are equipped with a slurry pump each). The installed thruster power is found in Chopra (2016), and is given in Chapter 3.6.3. For the semi-submersible design above, ship services account for 6 MW. However, ship serives make up only 1.1 MW for the preliminary surface vessel in SRK Consulting (2010, p. 158). When adding all the above bits and pieces together, and assuming that the total power of 30-31 MW is somewhat low.

Table K-2 – Pump flow and corresponding power consumption (Technip, 2008).

Scenario	Ct [-]	SG [-]	D [in]	Qm [gpm]	TP [psi]	Total Power [MW]	Power Change [%]
Design case	0.12	3.0	1.0	3,058	1,287	3.2	0.0
Minimum pressure	0.072	3.0	1.0	5,096	999	5.1	59.0
1,700 m depth	0.12	3.0	1.0	3,058	875	2.4	-25.0
Increased SGs	0.12	3.6	1.0	2,548	1,785	3.4	6.0
Reduced ore size	0.12	3.0	0.3	3,058	1,116	2.9	-9.4
Increased Ct	0.17	3.0	1.0	2,158	1,847	3.0	-7.2
Both 5 & 6	0.17	3.0	0.3	2,158	1,510	2.6	-20.0

Table K-3 – Electrical power demand of initial PSV design (SRK Consulting, 2010, p. 158).

		Average Condition		Return Period			
				1 year		10 years	
Consumer	Max. Load [kW]	DF [-]	Power [kW]	DF [-]	Power [kW]	DF [-]	Power [kW]
Mining Equipment	13,800	1	13,800	1	13,800	0	0
Thruster #1-8 (1.5 MW each)	12,000	0.3	3,600	0.6	7,200	1	12,000
Ship Services	1,100	1	1,100	1	1,100	1	1,100
Total Power Demand			**18,500**		**22,100**		**13,100**

As discussed by Ådnanes (2003), drilling semi-submersible rigs and ships operates most of their lifetime in stationary positioning. DP rigs and ships utilize thruster devices for station keeping and for transit between locations. Using fixed pitch, speed controlled propellers will significantly improve fuel savings and operation economy. The power system configuration depends much on the environmental requirements for the vessel. A two, three, or four-split power system is typical. The drilling plant also requires a substantial power, typically 5-10 MW. As an alternative to fixed pitch mechanical azimuth

thrusters are podded thrusters, which are characterized by higher efficiency, reduced space requirements, and higher reliability due to the simpler and more robust mechanical construction. Further, nearly all floating production vessels are kept on location by using a mooring system. Some of them, especially in harsh environment, utilize azimuth thrusters and/or shaft line propellers and tunnel thrusters to obtain heading control and reduce the strain of the mooring lines.

Table K-4 – Installed thruster effect (Chopra, 2016).

Consumer	Amount	Unit [kW]	Total [kW]
Azimuth thruster (aft)	3	3,000	9,000
Azimuth thruster (fore)	2	3,500	7,000
Bow tunnel thruster (fore peak)	2	2,000	4,000
Total			**20,000**

Table K-5 – Other power consumers for PSV.

Consumer	Amount	Unit [kW]	Total [kW]
Auxiliary Cutter (AC) (Nautilus Minerals, 2016)	1	2,000	2,000
Bulk Cutter (BC) (Nautilus Minerals, 2016)	1	2,500	2,500
Collecting Machine (CM) (Nautilus Minerals, 2016)	1	1,800	1,800
SSLP @ 2,500 m (Yu & Espinasse, 2009)	1	6,000	6,000
Mining system, other (SRK Consulting, 2010, p. 158)	1	1,500	1,500
Utility	1	6,000	6,000

Fuel Types and Fuel Price History

With respect to choosing marine diesel oil (MDO) or heavy fuel oil (HFO) as bunker for the PSV, MDO is not required for the AMOR, see Figure K-4. However, in a corporate conversance perspective, MDO is a preferred choice. It is also the conservative option with respect to cost calculations, being at almost twice the price of HFO. Hence, HFO is used for the lower bound and MDO for the upper bound in the below fuel cost calculations.

Figure K-4 – Existing and possible future emission control areas (ECAs) and major bunker ports (Adamchak & Adede, 2013).

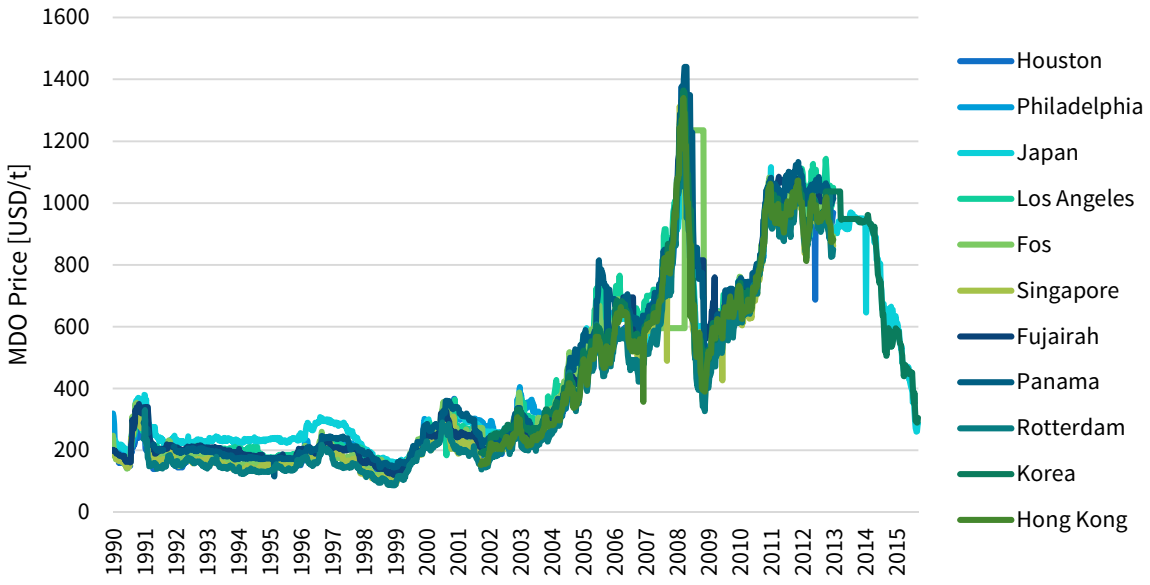

Fuel Consumption Calculations

When calculating the fuel consumption, an average value (for 50-100 % load for Aker H-6 semi-submersibles) of 183 g/kWh is applied (Aker Kværner, 2006, p. 24). Using the same approach as in Aker Kværner (2006, p. 24), a specific fuel consumption b_e of 183 g/kWh is applied, which is an average value for 50-100% load (or maximum continuous rating, MCR). Medium speed four-stroke diesel engines typically have a b_e ranging 170-210 g/kWh (Amdahl, et al., 2014, p. 7.11), so the value used in the below calculation seems reasonable being within the range.

Table K-6 – Fuel calculation parameters.

Parameter	Unit	Value
Installed Power	MW	31.0
Installed Thruster Effect	MW	20.0
Mining System Consumption	MW	13.8
Utilities, Avg. Consumption	MW	3.0
Specific fuel consumption, b_e	g/kWh	183
Marine Diesel Oil (MDO) density, SG	-	0.88
MDO price	USD/t	440

Table K-7 – Fuel consumption.

Parameter	Unit	Lower @ 10%	Upper @ 50%	Mean @ 40%
Thrust Usage	-	0.1	0.5	0.45
Effective thrust	MW	2	10	9
Total power consumption	MW	18.8	26.8	25.8
% of total installed		*61%*	*86%*	*83%*
Daily fuel consumption	t/day	82.6	117.7	113.3
Daily fuel consumption	m3/day	72.7	103.6	99.7
Daily fuel cost for MDO*	USD/day	36,331	51,790	49,858
Annual fuel cost (MDO)	M USD/year	13.261	18.904	18.198

APPENDIX L COST ESTIMATES FOR SEAFLOOR PRODUCTION SYSTEM OF SOLWARA 1

CAPEX Overview

The total CAPEX for the Solwara 1 project is 382.78 million USD, including a contingency of 17.5 % to account for varying levels of maturity for the cost items (SRK Consulting, 2010), see Table L-1. Background numbers on these costs are presented in Appendix M presents the items that constitute the total CAPEX for the subsea mining equipment, which sums up to 84.1 million USD, or 26 % of the total project CAPEX. This is based on the fixed-price contract between Nautilus Minerals and the vendor SMD, and included an allowance to go from a system design with three instead of two SPTs. However, the overall cost estimates are assumed to be significantly underestimated, and the real numbers are most likely close to 1 billion USD. This is based on, e.g., that the government of Papua New Guinea's acquisition of equity in Nautilus Minerals, valuing a 15 % share to 120 million USD (ECORYS, 2014).

Table L-1 – CAPEX overview for Solwara 1 (SRK Consulting, 2010, p. 214).

Project part	Description	Sum [M USD]
Mining	SPT	84.10
Mining	RALS	101.10
Mining	DWP	23.97
Mining	PSV Mobilization	6.50
Mining	Integration and Testing	59.70
Mining	Port	10.80
Other	Project Services	32.20
Other	Owner's Costs	7.40
Other	CAPEX Sub-Total	325.77
Other	Contingency (17.5 %)	57.01
Total		**382.78**

An FPSO has many similarities both in design and construction to the PSV, and a sample cost breakdown for an FPSO project is shown in Table L-2.

Table L-2 – Breakdown of FPSO project costs (Paik & Thayamballi, 2007, p. 34).

Engineering and management	10 %
Vessel hull and system	40-50 %
Process topsides	20-30 %
Moorings and installation	4-5 %
FPSO installation and commissioning	2-3 %

OPEX

The daily total OPEX of the seafloor mining equipment is calculated to be 20,130 USD (SRK Consulting, 2010), and the project's total OPEX is in Table L-3. Included in the OPEX are yearly contract costs, such as a service contract with the vendor of the seafloor mining equipment to have two or more technical specialists constantly present at the PSV to support and assist the operation.

Table L-3 – Daily OPEX overview (SRK Consulting, 2010, p. 218).

Description	Daily Cost [$]
PSV	144,796
SPT	20,130
ROV	20,910
RALS	23,184
Support Services	15,235
Barging	12,694
Sub-Total OPEX	236,949
Contingency (10 %)	23,695
Total	**260,644**

Table_App L-4 – Project lifetime OPEX.

Project Lifetime OPEX Cost Items	Cost [$/day]
Vessel charter*	75,000
ROV charter	9,200
Labor**	30,622
Fuel***	21,854
Spares, consumables and miscellaneous	100,273
Total	**236,949**

* Vessel provisions, marine crew. DP, long-term.
** Wages, food, flights, accommodation, transport, etc. Higher first 6 months (expats).
*** HFO @ 523USD/t

Table L-5 – Adjusted daily OPEX.

Daily OPEX Cost Items	Cost [$/day]	Unit cost [$/t]	Adjusted cost [$/day]	Adjusted unit cost [$/t]
PSV	144,796.00	39.15	138449.22	37.43
SPT	20,130.00	5.44	20130.00	5.44
ROV	20,910.00	5.65	20910.00	5.65
RALS	23,184.00	6.27	23184.00	6.27
Support services	15,235.00	4.12	15235.00	4.12
Barging	12,694.00	3.43	12694.00	3.43
DWP			6346.78	1.72
Total	**236,949.00**		**236949.00**	

APPENDIX M DETAILED CAPEX ESTIMATES FOR SOLWARA 1 PRODUCTION SYSTEM

All amounts in mill. USD

COST ITEM	ESTIMATE FOR SOLWARA 1	% of sub-system total	% of system total	% of total
SYSTEM COMPONENTS				
Seafloor Production Tools (SPTs)				
Subsea mining tool and handling system	76.2		91%	23%
Initial spares	6.6		8%	2%
Freight and insurance	1.3		2%	0%
Total	**84.1**			**26%**
Riser and Lifting System (RALS)				
Riser Transfer Pipe (STP)	3.9		4%	1%
Subsea Slurry Lift Pump (SSLP)	30.8		30%	9%
Riser	14.8		15%	5%
Lifiting and hoisting system	16.7		17%	5%
Indirects	34.9		35%	11%
Total	**101.1**			**31%**
Dewatering Plant (DWP)				
Equipment costs				
Screen	*1.9*	*16%*	*8%*	*1%*
Centrifuge	*0.56*	*5%*	*2%*	*0%*
Cyclone circuit	*2.6*	*22%*	*11%*	*1%*
Filtration	*2.7*	*23%*	*11%*	*1%*
Barge loading	*1.3*	*11%*	*5%*	*0%*
Controls	*1.7*	*14%*	*7%*	*1%*
General services	*0.62*	*5%*	*3%*	*0%*
Tankage	*0.59*	*5%*	*2%*	*0%*
Sub-total	***11.97***		***50%***	***4%***
Fabrication and assembly costs				
Structural steel	*1.5*	*13%*	*6%*	*0%*
Assembly and installation	*6.3*	*53%*	*26%*	*2%*
Indirects	*4.2*	*35%*	*18%*	*1%*
Sub-total	***12***		***50%***	***4%***
Total	**23.97**			**7%**
Port				
Barges, procurement and upgrade	8.8		81%	3%
Material and handling equipment	2		19%	1%
Total	**10.8**			**3%**
MOBILIZATION AND INSTALLATION				
PSV mobilization				
Total	**6.5**			**2%**
Integration and testing				
Vessel cost, incl. modification	8.7		15%	3%
Additional eq., steel work and materials	30.5		51%	9%
Assembley, installation and testing	4.5		8%	1%
Indirects, incl. EPCM mgmt. and feight	16		27%	5%
Total	**59.7**			**18%**

PROJECT RUNNING COSTS				
Project services				
Total	**32.2**			**10%**
Owner's costs				
Total	**7.4**			**2%**
Total CAPEX	**325.77**			
Contingency (17.5 %)	57.0			
Total CAPEX, incl. contingency	**382.8**			

Source: (SRK Consulting, 2010, pp. 211-220)

APPENDIX N CALCULATIONS OF COPPER EQUIVALENT

Historic Prices

Based on the historical price data in Chapter 3.1.2, a large span values for the specific price ratios are found, as seen from Table N-1.

Table N-1 – Statistical properties of historical metal price ratios.

	Zn/Cu	Au/Cu	Ag/Cu
Min.	0.184	737.559	27.147
Max.	0.684	8957.218	306.564
Mean	0.419	4521.946	91.101
Median	0.441	4760.570	74.171

Capturing Metal Price Correlations in Price Ratios

As described by Covert (2013, p. 42), there is much literature on generating correlated random numbers for use in statistical simulation, but few families of joint PDFs specified in terms of their Pearson product-moment correlation. However, Garvey (2000) discussed correlated joint normal, joint normal-lognormal, and joint lognormal distributions. Other collections of joint distributions are formed through the use of copulas, which is a transformation technique used to create joint probability distribution.

The correlating behavior of the annual commodity price data in Figure 3-4 and Figure 3-5 is confirmed by the correlation factors in Table N-2, which are 0.605 and 0.84 for Cu-Zn and Au-Ag, respectively. Thus, it important to capture this correlation effect when calculating the copper equivalent.

Table N-2 – Correlation matrix for historical metal prices.

	Cu	Zn	Au	Ag
Cu	1	0.605	0.412	0.459
Zn	0.605	1	0.331	0.284
Au	0.412	0.331	1	0.840
Ag	0.459	0.284	0.840	1

Assuming that the respective metal prices fluctuate with the overall commodity market, linear regression lines are fitted for both copper (Cu) price versus zinc (Zn) price, and gold (Au) price versus silver (Ag) price. The expression for the linear regression lines seen in Figure N-1 (a) and (b) are (23) and (24), respectively. Both are found using the "Trendline" option under "Chart Tools" in Excel.

$$y_{\mathrm{Zn}} = 0.1844 x_{\mathrm{Cu}} + 791.51, \quad R^2 = 0.3656 \tag{23}$$

$$y_{\mathrm{Ag}} = 0.0162 x_{\mathrm{Au}} + 71215, \quad R^2 = 0.7063 \tag{24}$$

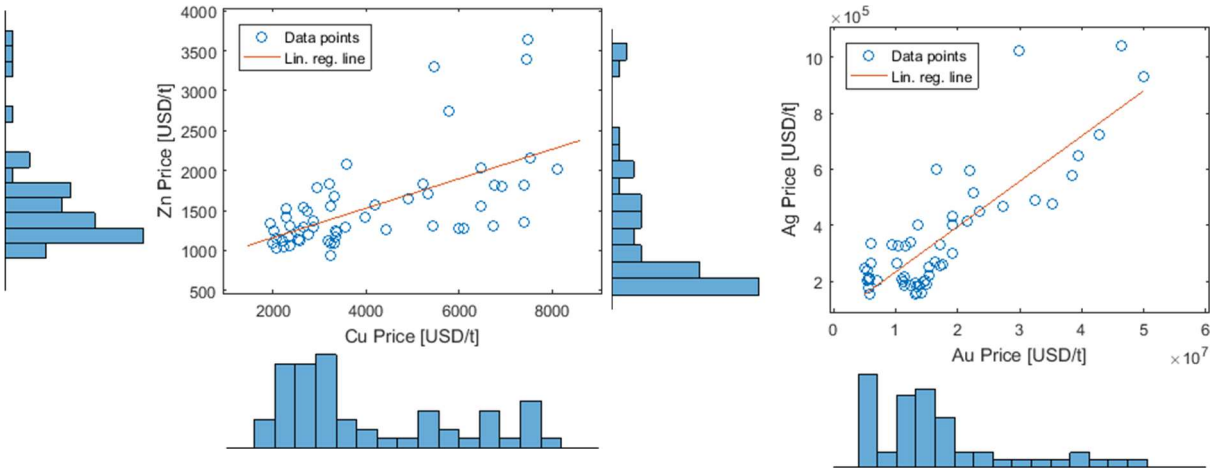

(a) Copper (Cu) and zinc (Zn) (b) Gold (Au) and silver (Ag)

Figure N-1 – Histogram and scatter plot of corresponding historic prices, real 2010 USD.

To be able to use the built-in inverse cumulative distribution function "icdf" in MATLAB, lognormal distributions were fitted to the Cu and Au historic, and was found as the most appropriate distribution for both the data sets by use of the "Distribution Fitting" application. Distribution parameters were evaluated with the built-in function "lognfit", and corresponds to the distributions in Figure N-2.

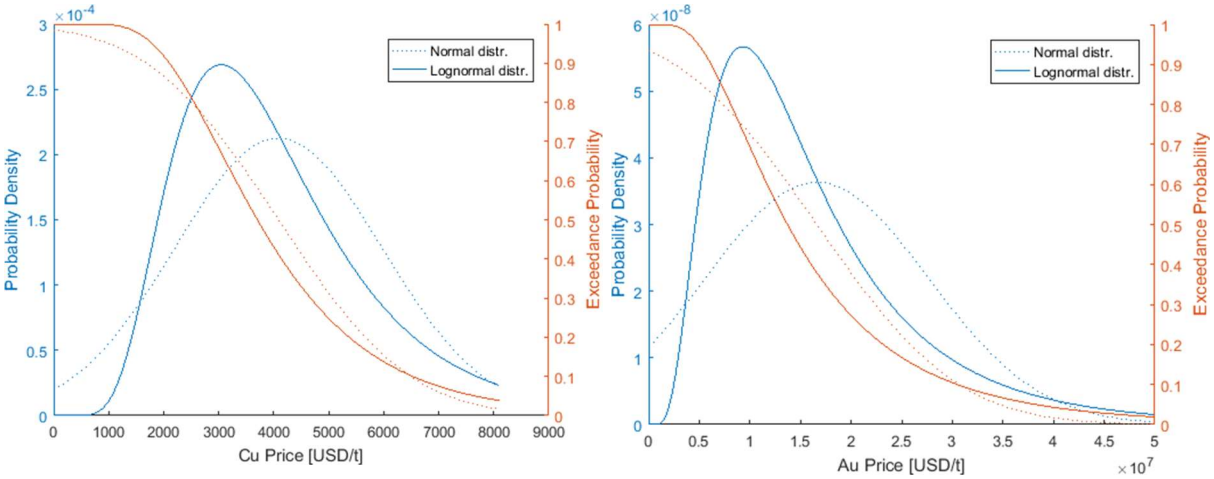

(a) Copper (b) Gold

Figure N-2 – Probability distributions fitted to histograms of historic prices.

Walpole, et al. (2012, pp. 389-402) elaborate on the *simple linear regression (SLR) model* in (25),

$$Y = \beta_0 + \beta_1 x + \epsilon \tag{25}$$

in which β_0 and β_1 are unknown intercept and slope parameters, and ϵ a random error with constant variance (i.e., the homogeneous variance assumption). At a specific x, the y-values are distributed around the *true regression line* $y = \mu_{Y|x} = E(Y) = \beta_0 + \beta_1 x$, see Figure N-3, in which the points plotted are actual (x, y) points scattered around the line. Each point is on its own normal distribution with its center (i.e., the mean of y) falling on the line and variance σ^2. Thus, the true regression line goes through the means of the response, for which the *fitted regression line* $\hat{y} = b_0 + b_1 x$ is an estimate, and the actual observations are on the distribution around the means.

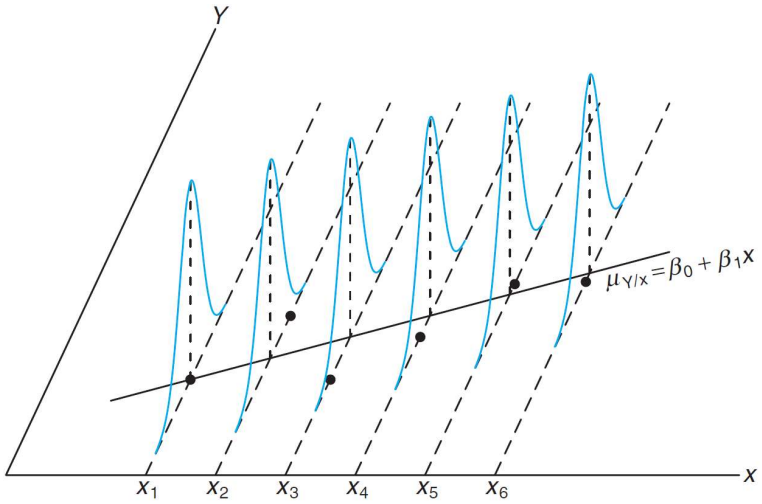

Figure N-3 – Normal distr. around true regression line of data set (Walpole, et al., 2012, p. 394).

By the *method of least squares*, b_0 and b_1 (estimates for β_0 and β_1) are found so that the sum of the squares of the residuals $e_i = y_i - \hat{y}_i$, also known as the *sum of squares of the errors* about the regression line SSE, is minimized. The least squares procedure gives a fitted line that minimizes the sum of squares of vertical deviation (from the points to the line). The model error variance σ^2 reflects random variance around the regression line of which s^2 in (31) is an unbiased estimator. Thus, the *mean squared error* s^2 measures the squared deviation between Y and y, and is found by evaluating (26) through (30) for the given data set (i.e., observations). Table N-3 shows the estimated standard deviations s (for the normal distributions) around the regression lines found above for the zinc and silver prices.

$$S_{xx} = \sum_{i=1}^{n} (x_i - \bar{x})^2 \tag{26}$$

$$S_{yy} = \sum_{i=1}^{n} (y_i - \bar{y})^2 \tag{27}$$

$$S_{xy} = \sum_{i=1}^{n} (x_i - \bar{x})(y_i - \bar{y}) \tag{28}$$

$$b_1 = \frac{S_{xy}}{S_{xx}} \tag{29}$$

$$SSE = S_{yy} - b_1 S_{xy} \tag{30}$$

$$s^2 = \frac{SSE}{n-2} \tag{31}$$

Table N-3 – Estimated std. dev. of normal distr. around regression lines.

$\boldsymbol{s(\mathbf{Zn}\vert\mathbf{Cu})}$	460.4010
$\boldsymbol{s(\mathbf{Ag}\vert\mathbf{Au})}$	116046.2021

APPENDIX O MATLAB SCRIPT: CUMMULATIVE PROBABILITY OF SIGNIFICANT WAVE HEIGHT

```
% Weather Window Estimation for Subsea Mining Operation at Loki's Castle
% Part of MSc in Marine Technology - Underwater Engineering


%% Import hindcast data

clear all
close all
clc

% Importing hindcast data for Loki's Castle
raw_data = importdata('Mohn_5.txt',' ',6);

% Allocate imported array to column variable names
month = raw_data.data(:,2);
Hs = raw_data.data(:,7);
Tp = raw_data.data(:,8);

% Find max. values
Hs_max = ceil(max(Hs)/0.5)*0.5;
Tp_max = ceil(max(Tp));

%% Generate scatter diagram
% One scatter diagram generated for each month

% Establishing scatter diagram matrices
[scat_jan scat_feb scat_mar scat_apr scat_may scat_jun scat_jul scat_aug...
    scat_sep scat_oct scat_nov scat_dec] = deal(zeros(Hs_max*2,Tp_max));

% Finding frequence for each (Hs, Tp) class
for i=0.5:0.5:Hs_max
    r=i/0.5;
    for j=1:Tp_max
        for k=1:size(Hs)
            if (Hs(k)<= i && Hs(k)>(i-0.5) && Tp(k)<= j && Tp(k)>(j-1))
                switch month(k)
                    case 1      % January
                        scat_jan(r,j) = scat_jan(r,j) + 1;
                    case 2      % February
                        scat_feb(r,j) = scat_feb(r,j) + 1;
                    case 3      % Mars
                        scat_mar(r,j) = scat_mar(r,j) + 1;
                    case 4      % April
                        scat_apr(r,j) = scat_apr(r,j) + 1;
                    case 5      % May
                        scat_may(r,j) = scat_may(r,j) + 1;
                    case 6      % June
                        scat_jun(r,j) = scat_jun(r,j) + 1;
                    case 7      % July
                        scat_jul(r,j) = scat_jul(r,j) + 1;
                    case 8      % August
                        scat_aug(r,j) = scat_aug(r,j) + 1;
                    case 9      % September
                        scat_sep(r,j) = scat_sep(r,j) + 1;
                    case 10     % October
                        scat_oct(r,j) = scat_oct(r,j) + 1;
```

```
                    case 11     % November
                        scat_nov(r,j) = scat_nov(r,j) + 1;
                    case 12     % December
                        scat_dec(r,j) = scat_dec(r,j) + 1;
                end
            end
        end
    end
end

%% Sum of each Hs and Tp class
scat_jan(:,Tp_max+1) = sum(scat_jan,2);
scat_jan(Hs_max*2+1,:) = sum(scat_jan,1);

scat_feb(:,Tp_max+1) = sum(scat_feb,2);
scat_feb(Hs_max*2+1,:) = sum(scat_feb,1);

scat_mar(:,Tp_max+1) = sum(scat_mar,2);
scat_mar(Hs_max*2+1,:) = sum(scat_mar,1);

scat_apr(:,Tp_max+1) = sum(scat_apr,2);
scat_apr(Hs_max*2+1,:) = sum(scat_apr,1);

scat_may(:,Tp_max+1) = sum(scat_may,2);
scat_may(Hs_max*2+1,:) = sum(scat_may,1);

scat_jun(:,Tp_max+1) = sum(scat_jun,2);
scat_jun(Hs_max*2+1,:) = sum(scat_jun,1);

scat_jul(:,Tp_max+1) = sum(scat_jul,2);
scat_jul(Hs_max*2+1,:) = sum(scat_jul,1);

scat_aug(:,Tp_max+1) = sum(scat_aug,2);
scat_aug(Hs_max*2+1,:) = sum(scat_aug,1);

scat_sep(:,Tp_max+1) = sum(scat_sep,2);
scat_sep(Hs_max*2+1,:) = sum(scat_sep,1);

scat_oct(:,Tp_max+1) = sum(scat_oct,2);
scat_oct(Hs_max*2+1,:) = sum(scat_oct,1);

scat_nov(:,Tp_max+1) = sum(scat_nov,2);
scat_nov(Hs_max*2+1,:) = sum(scat_nov,1);

scat_dec(:,Tp_max+1) = sum(scat_dec,2);
scat_dec(Hs_max*2+1,:) = sum(scat_dec,1);

%% Adding column of cummulative sum and probability of each Hs class
% Find size of scatter diagrams
[m,n] = size(scat_jan);

% Cummulative sum - First row
scat_jan(1,n+1) = scat_jan(1,n);
scat_feb(1,n+1) = scat_feb(1,n);
scat_mar(1,n+1) = scat_mar(1,n);
scat_apr(1,n+1) = scat_apr(1,n);
scat_may(1,n+1) = scat_may(1,n);
scat_jun(1,n+1) = scat_jun(1,n);
```

```
115  scat_jul(1,n+1) = scat_jul(1,n);
116  scat_aug(1,n+1) = scat_aug(1,n);
117  scat_sep(1,n+1) = scat_sep(1,n);
118  scat_oct(1,n+1) = scat_oct(1,n);
119  scat_nov(1,n+1) = scat_nov(1,n);
120  scat_dec(1,n+1) = scat_dec(1,n);
121
122  for i=2:m-1
123      % Cummulative sum - Remaining rows
124      scat_jan(i,n+1) = scat_jan(i-1,n+1) + scat_jan(i,n);
125      scat_feb(i,n+1) = scat_feb(i-1,n+1) + scat_feb(i,n);
126      scat_mar(i,n+1) = scat_mar(i-1,n+1) + scat_mar(i,n);
127      scat_apr(i,n+1) = scat_apr(i-1,n+1) + scat_apr(i,n);
128      scat_may(i,n+1) = scat_may(i-1,n+1) + scat_may(i,n);
129      scat_jun(i,n+1) = scat_jun(i-1,n+1) + scat_jun(i,n);
130      scat_jul(i,n+1) = scat_jul(i-1,n+1) + scat_jul(i,n);
131      scat_aug(i,n+1) = scat_aug(i-1,n+1) + scat_aug(i,n);
132      scat_sep(i,n+1) = scat_sep(i-1,n+1) + scat_sep(i,n);
133      scat_oct(i,n+1) = scat_oct(i-1,n+1) + scat_oct(i,n);
134      scat_nov(i,n+1) = scat_nov(i-1,n+1) + scat_nov(i,n);
135      scat_dec(i,n+1) = scat_dec(i-1,n+1) + scat_dec(i,n);
136  end
137
138  for i=2:m-1
139      % Cummulative probability
140      scat_jan(i,n+2) = scat_jan(i,n+1)/(scat_jan(m-1,n+1)+1);
141      scat_feb(i,n+2) = scat_feb(i,n+1)/(scat_feb(m-1,n+1)+1);
142      scat_mar(i,n+2) = scat_mar(i,n+1)/(scat_mar(m-1,n+1)+1);
143      scat_apr(i,n+2) = scat_apr(i,n+1)/(scat_apr(m-1,n+1)+1);
144      scat_may(i,n+2) = scat_may(i,n+1)/(scat_may(m-1,n+1)+1);
145      scat_jun(i,n+2) = scat_jun(i,n+1)/(scat_jun(m-1,n+1)+1);
146      scat_jul(i,n+2) = scat_jul(i,n+1)/(scat_jul(m-1,n+1)+1);
147      scat_aug(i,n+2) = scat_aug(i,n+1)/(scat_aug(m-1,n+1)+1);
148      scat_sep(i,n+2) = scat_sep(i,n+1)/(scat_sep(m-1,n+1)+1);
149      scat_oct(i,n+2) = scat_oct(i,n+1)/(scat_oct(m-1,n+1)+1);
150      scat_nov(i,n+2) = scat_nov(i,n+1)/(scat_nov(m-1,n+1)+1);
151      scat_dec(i,n+2) = scat_dec(i,n+1)/(scat_dec(m-1,n+1)+1);
152  end
153
154  % Find new size of scatter diagrams
155  [m,n] = size(scat_jan);
156
157  % Upper bound of each Hs class
158  Hs_values = 0.5:0.5:Hs_max;
159
160  %% Generate mean and variance of Hs
161  %
162  %for iter = 1:12
163
164  %    temp_1 = 0;
165  %    temp_2 = 0;
166
167  %    for i=1:(m-1)
168  %        % Mean of Hs
169  %        temp_1 = temp_1 + scat_jan(i,n-1)*Hs_values(i);
170  %    end
171
172  %    Hs_mean(iter) = temp_1/scat_jan(m,n-1);
173
```

```
174 %     for i=1:(m-1)
175 %         % Variance of Hs
176 %         temp_2 = temp_2 + scat_jan(i,n-1)*((i/2-0.25)- Hs_mean)^2;
177 %     end
178 
179 %     Hs_var(iter) = temp_2/(scat_jan(m,n-1)-1);
180 
181 %end
182 
183 %clearvars temp_1 temp_2
184 
185 %% Export to Excel file
186 
187 filename = 'lokis_castle_scatter_diagram_export.xlsx';
188 scat_vector = {scat_jan scat_feb scat_mar scat_apr scat_may scat_jun...
189     scat_jul scat_aug scat_sep scat_oct scat_nov scat_dec};
190 
191 warning('off','MATLAB:xlswrite:AddSheet')
192 for iter = 1:12
193         xlswrite(filename,scat_vector{iter},iter,'A1:Y38')
194 end
```

APPENDIX P MATLAB SCRIPT: MONTE CARLO SIMULATION OF COPPER EQUIVALENT

```
clear all
close all
clc

% Seeds the random number generator using the nonnegative integer
% Easier to compare changes in runs
rng(33564)

% Import
raw_data = importdata('Commodity_Price_Real.xlsx');

% Year vector
year = raw_data.data(:,1);

% Historical metal prices in real USD
prices = raw_data.data(:,2:5);
% Col: 1 = Au, 2 = Zn, 3 = Au, and 4 = Ag

% troy oz in t
conversion_factor = 3.11E-5;

% Adjusted prices (i.e., all in $/t)
prices(:,3:4) = prices(:,3:4)/conversion_factor;

% Correlation matrix for historic metal prices
corr_coef = corrcoef(prices);

% Price ratios
for i = 1:4
    price_ratios(:,i) = prices(:,i)./prices(:,1);
end

% Bounds
prices_max = ceil(max(prices));
prices_min = floor(min(prices));

%% Linear regression line

% ********************************** %
%  Historic prices, real 2010 USD     %
%  x_1 = Cu, y_1 = Zn                 %
%  x_2 = Au, y_2 = Ag                 %
%                                     %
%  Using Excel linear trendline:      %
%  y_1 = 0.1844*x_1 + 791.51          %
%  R^2 = 0.3656                       %
%                                     %
%  y_2 = 0.0162*x_2 + 71215           %
%  R^2 = 0.7063                       %
% ********************************** %

% Linear regression line for Zn price given Cu price
Zn_reg = @(x) 0.1844*x + 791.51;
x_1 = [prices_min(1)-500:prices_max(1)+500];
y_1 = Zn_reg(x_1);
```

```
56
57  % Linear regression line for Ag price given Au price
58  Ag_reg = @(x) 0.0162*x + 71215;
59  x_2 = [prices_min(3):1000:prices_max(3)];
60  y_2 = Ag_reg(x_2);
61
62  % Plotting prices
63  figure(1)
64  scatterhist(prices(:,1),prices(:,2),'NBins',[15,15])
65  xlabel('Cu Price [USD/t]')
66  ylabel('Zn Price [USD/t]')
67  hold on
68  plot(x_1,y_1)
69  legend('Data points','Lin. reg. line','Location','northwest')
70
71  figure(2)
72  scatterhist(prices(:,3),prices(:,4),'NBins',[15,15])
73  xlabel('Au Price [USD/t]')
74  ylabel('Ag Price [USD/t]')
75  hold on
76  plot(x_2,y_2)
77  legend('Data points','Lin. reg. line','Location','northwest')
78
79  %% Fitting probability distributions for historic metal prices
80  % Col 1 = mu (expected value or mean), Col 2 = sigma (std.dev.)
81
82  for i = 1:4
83      % Lognormal distr.
84      lognorm_distr(i,:) = lognfit(prices(:,i)) ;
85      % Normal distr.
86      [norm_distr(i,1), norm_distr(i,2)] = normfit(prices(:,i));
87  end
88
89  %% PDFs & CDFs
90
91  % Probability Density Functions (PDFs)
92  % 1 = Cu, 2 = Zn, 3 = Au, 4 = Ag
93
94  Cu_reg = [0:prices_max(1)];
95  Au_reg = [0:5000:prices_max(3)];
96
97  % PDFs
98  Cu_pdf_n = pdf('Normal',Cu_reg,norm_distr(1,1),norm_distr(1,2));
99  Cu_pdf_ln = pdf('Lognormal',Cu_reg,lognorm_distr(1,1),lognorm_distr(1,2));
100
101 Au_pdf_n = pdf('Normal',Au_reg,norm_distr(3,1),norm_distr(3,2));
102 Au_pdf_ln = pdf('Lognormal',Au_reg,lognorm_distr(3,1),lognorm_distr(3,2));
103
104 % Exeedance Probability (1 - CDFs)
105 Cu_cdf_n = 1 - cdf('Normal',Cu_reg,norm_distr(1,1),norm_distr(1,2));
106 Cu_cdf_ln = 1 - ...
107     cdf('Lognormal',Cu_reg,lognorm_distr(1,1),lognorm_distr(1,2));
108
109 Au_cdf_n = 1 - cdf('Normal',Au_reg,norm_distr(3,1),norm_distr(3,2));
110 Au_cdf_ln = 1 - ...
111     cdf('Lognormal',Au_reg,lognorm_distr(3,1),lognorm_distr(3,2));
112
113 figure(3)
114 hold on
```

```
yyaxis left
plot(Cu_reg,Cu_pdf_n,':')
plot(Cu_reg,Cu_pdf_ln,'-')
xlabel('Cu Price [USD/t]')
ylabel('Probability Density')
yyaxis right
plot(Cu_reg,Cu_cdf_n,':')
plot(Cu_reg,Cu_cdf_ln,'-')
ylabel('Exceedance Probability')
legend('Normal distr.','Lognormal distr.','Location','northeast')

figure(4)
hold on
yyaxis left
plot(Au_reg,Au_pdf_n,':')
plot(Au_reg,Au_pdf_ln,'-')
xlabel('Au Price [USD/t]')
ylabel('Probability Density')
yyaxis right
plot(Au_reg,Au_cdf_n,':')
plot(Au_reg,Au_cdf_ln,'-')
ylabel('Exceedance Probability')
legend('Normal distr.','Lognormal distr.','Location','northeast')


%% Monte Carlo Simulation - Copper Equivalent
% Equation: Metal Grade Distr. * Price Ratio Distr. * Ore Texture Distr.

% Normal distr. std.dev. around real linear regression lines
% Based on estimates in Excel sheet
Zn_price_sigma = 460.4010037;
Ag_price_sigma = 116046.2021;


for mc_iter = 1:5000

% -------------------- METAL GRADE DISTRIBUITONS --------------------
% Linear interpolation of cum. distr. curve of metal grades

prob_vector = [1 0.75 0.5 0.25 0];
Cu_grade = [5.90 1.35 3.00 5.04 5.78 6.62 10.90]/1E2;
Zn_grade = [6.08 1.82 2.66 4.88 5.84 6.94 13.34]/1E2;
Au_grade = [1.58 1.91 0.07 0.61 1.06 1.82 12.80]/1E6;
Ag_grade = [90.90 44.10 19.20 62.30 82.90 109.00 284.00]/1E6;
grade = [Cu_grade; Zn_grade; Au_grade; Ag_grade];

for j = 1:4
    rand_prob_1 = rand;
    for i = 2:5
        if rand_prob_1 > prob_vector(i)
            metal_grade_lower = grade(j,i);
            metal_grade_upper = grade(j,i-1);
            prob_vector_lower = prob_vector(i);
            prob_vector_upper = prob_vector(i-1);
            metal_grade_distr(j) = metal_grade_lower + ...
                (metal_grade_upper - metal_grade_lower)/...
                (prob_vector_upper - prob_vector_lower)*...
                (rand_prob_1 - prob_vector_lower);
            break
```

```
        end
    end
end

% -------------------- PRICE RATIO DISTRIBUITONS --------------------

% (1)   Cu/Cu Ratio
price_ratio_distr(1) = 1;

% (2)   Zn/Cu Ratio
% Cu price - Randomly drawn from distr.
Cu_price = icdf('Lognormal',1-rand,lognorm_distr(1,1),lognorm_distr(1,2));
if Cu_price < prices_min(1)
    Cu_price = prices_min(1);
elseif Cu_price > prices_max(1)
    Cu_price = prices_max(1);
end

% Zn price - Found from normal distr. around lin. reg. line
Zn_price_mu = Zn_reg(Cu_price);
Zn_price = icdf('Normal',rand,Zn_price_mu,Zn_price_sigma);
if Zn_price < prices_min(2)
    Zn_price = prices_min(2);
elseif Zn_price > prices_max(2)
    Zn_price = prices_max(2);
end

price_ratio_distr(2) = Zn_price/Cu_price;

% (3)   Au/Cu Ratio
% Au price - Randomly drawn from distr.
Au_price = icdf('Lognormal',1-rand,lognorm_distr(3,1),lognorm_distr(3,2));
if Au_price < prices_min(3)
    Au_price = prices_min(3);
elseif Au_price > prices_max(3)
    Au_price = prices_max(3);
end

price_ratio_distr(3) = Au_price/Cu_price;

% (4)   Ag/Cu Ratio
% Ag price - Found from normal distr. around lin. reg. line
Ag_price_mu = Ag_reg(Au_price);
Ag_price = icdf('Normal',rand,Ag_price_mu,Ag_price_sigma);
if Ag_price < prices_min(4)
    Ag_price = prices_min(4);
elseif Ag_price > prices_max(4)
    Ag_price = prices_max(4);
end

price_ratio_distr(4) = Ag_price/Cu_price;

% -------------------- ORE TEXTURE DISTRIBUITONS --------------------
% Mill recoveries for Cu, Zn, Au, and Ag, ref. Rudenno (2012, pp. 434-492)
    ore_texture_lower = [0.85 0.695 0.85 0.367];
    ore_texture_upper = [0.95 0.891 0.98 0.706];

for i = 1:4
    ore_texture_distr(i) = ore_texture_lower(i) + ...
```

```
233             rand*(ore_texture_upper(i)-ore_texture_lower(i));
234     end
235
236     % -------------------- PRODUCT OF DISTRIBUITONS --------------------
237
238     % Establish iteration value
239     temp = 0;
240
241     for i = 1:4
242         temp = temp + ...
243             metal_grade_distr(i)*price_ratio_distr(i)*ore_texture_distr(i);
244     end
245
246     % Store iteration value
247     Cu_eq(mc_iter) = temp;
248
249     end
250
251     % --------------- DISTRIBUTION FOR COPPER EQUIVALENT ---------------
252
253     % Establish bin range and bin count
254     [Cu_eq_count,Cu_eq_bins] = histcounts(Cu_eq,20);
255
256     % Cummulative prob.
257     for i = 1:length(Cu_eq_count)
258         if i == 1
259             Cu_eq_cum_prob(i) = Cu_eq_count(i)/length(Cu_eq);
260         else
261             Cu_eq_cum_prob(i) = Cu_eq_cum_prob(i-1) + ...
262                 Cu_eq_count(i)/length(Cu_eq);
263         end
264     end
265
266     % Exceedance prob.
267     Cu_eq_ex_prob = 1 - Cu_eq_cum_prob;
268
269     figure(5)
270     yyaxis left
271     histogram(Cu_eq*100)
272     xlabel('Cu_{eq} Grade [%]')
273     ylabel('Frequency')
274     hold on
275     yyaxis right
276     plot(Cu_eq_bins(2:end)*100,Cu_eq_ex_prob)
277     ylabel('Exceedance Probability')
278
279     % Distr. parameters
280     Cu_eq_mean = mean(Cu_eq);
281     Cu_eq_std = std(Cu_eq);
282
283     % Find F99.5
284     for i = 1:length(Cu_eq_ex_prob)
285         if Cu_eq_ex_prob(i) < 0.995
286             Cu_eq_lower = Cu_eq_bins(i);
287             Cu_eq_upper = Cu_eq_bins(i+1);
288             Cu_eq_ex_prob_lower = Cu_eq_ex_prob(i-1);
289             Cu_eq_ex_prob_upper = Cu_eq_ex_prob(i);
290             Cu_eq_F995 = Cu_eq_lower + ...
```

```
            (Cu_eq_upper-Cu_eq_lower)/(Cu_eq_ex_prob_upper-
Cu_eq_ex_prob_lower)*(0.995-Cu_eq_ex_prob_lower);
        break
    end
end

% Find F90
for i = 1:length(Cu_eq_ex_prob)
    if Cu_eq_ex_prob(i) < 0.9
        Cu_eq_lower = Cu_eq_bins(i);
        Cu_eq_upper = Cu_eq_bins(i+1);
        Cu_eq_ex_prob_lower = Cu_eq_ex_prob(i-1);
        Cu_eq_ex_prob_upper = Cu_eq_ex_prob(i);
        Cu_eq_F90 = Cu_eq_lower + ...
            (Cu_eq_upper-Cu_eq_lower)/(Cu_eq_ex_prob_upper-
Cu_eq_ex_prob_lower)*(0.9-Cu_eq_ex_prob_lower);
        break
    end
end

% Find F50(Cu_eq) or Mode(Cu_eq)
for i = 1:length(Cu_eq_ex_prob)
    if Cu_eq_ex_prob(i) < 0.5
        Cu_eq_lower = Cu_eq_bins(i);
        Cu_eq_upper = Cu_eq_bins(i+1);
        Cu_eq_ex_prob_lower = Cu_eq_ex_prob(i-1);
        Cu_eq_ex_prob_upper = Cu_eq_ex_prob(i);
        Cu_eq_mode = Cu_eq_lower + ...
            (Cu_eq_upper-Cu_eq_lower)/(Cu_eq_ex_prob_upper-
Cu_eq_ex_prob_lower)*(0.5-Cu_eq_ex_prob_lower);
        break
    end
end

% Find F10
for i = 1:length(Cu_eq_ex_prob)
    if Cu_eq_ex_prob(i) < 0.1
        Cu_eq_lower = Cu_eq_bins(i);
        Cu_eq_upper = Cu_eq_bins(i+1);
        Cu_eq_ex_prob_lower = Cu_eq_ex_prob(i-1);
        Cu_eq_ex_prob_upper = Cu_eq_ex_prob(i);
        Cu_eq_F10 = Cu_eq_lower + ...
            (Cu_eq_upper-Cu_eq_lower)/(Cu_eq_ex_prob_upper-
Cu_eq_ex_prob_lower)*(0.1-Cu_eq_ex_prob_lower);
        break
    end
end

% Find F0.5
for i = 1:length(Cu_eq_ex_prob)
    if Cu_eq_ex_prob(i) < 0.005
        Cu_eq_lower = Cu_eq_bins(i);
        Cu_eq_upper = Cu_eq_bins(i+1);
        Cu_eq_ex_prob_lower = Cu_eq_ex_prob(i-1);
        Cu_eq_ex_prob_upper = Cu_eq_ex_prob(i);
        Cu_eq_F05 = Cu_eq_lower + ...
            (Cu_eq_upper-Cu_eq_lower)/(Cu_eq_ex_prob_upper-
Cu_eq_ex_prob_lower)*(0.005-Cu_eq_ex_prob_lower);
        break
    end
```

```
351 end
352
353 %% Print results
354 fprintf('-----------------------\n')
355 fprintf('   Copper eq. distr.   \n')
356 fprintf('-----------------------\n')
357 fprintf('Mean\t\t\t%.5f\n',Cu_eq_mean)
358 fprintf('Median (P50)\t\t%.5f\n',Cu_eq_mode)
359 fprintf('Std.dev.\t\t%.5f\n',Cu_eq_std)
360 fprintf('P99.5\t\t\t%.5f\n',Cu_eq_F995)
361 fprintf('P90\t\t\t\t%.5f\n',Cu_eq_F90)
362 fprintf('P10\t\t\t\t%.5f\n',Cu_eq_F10)
363 fprintf('P0.5\t\t\t%.5f\n',Cu_eq_F05)
364 fprintf('-----------------------\n')
```

APPENDIX Q MAP OF THE NORWEGIAN CONTINENTAL SHELF

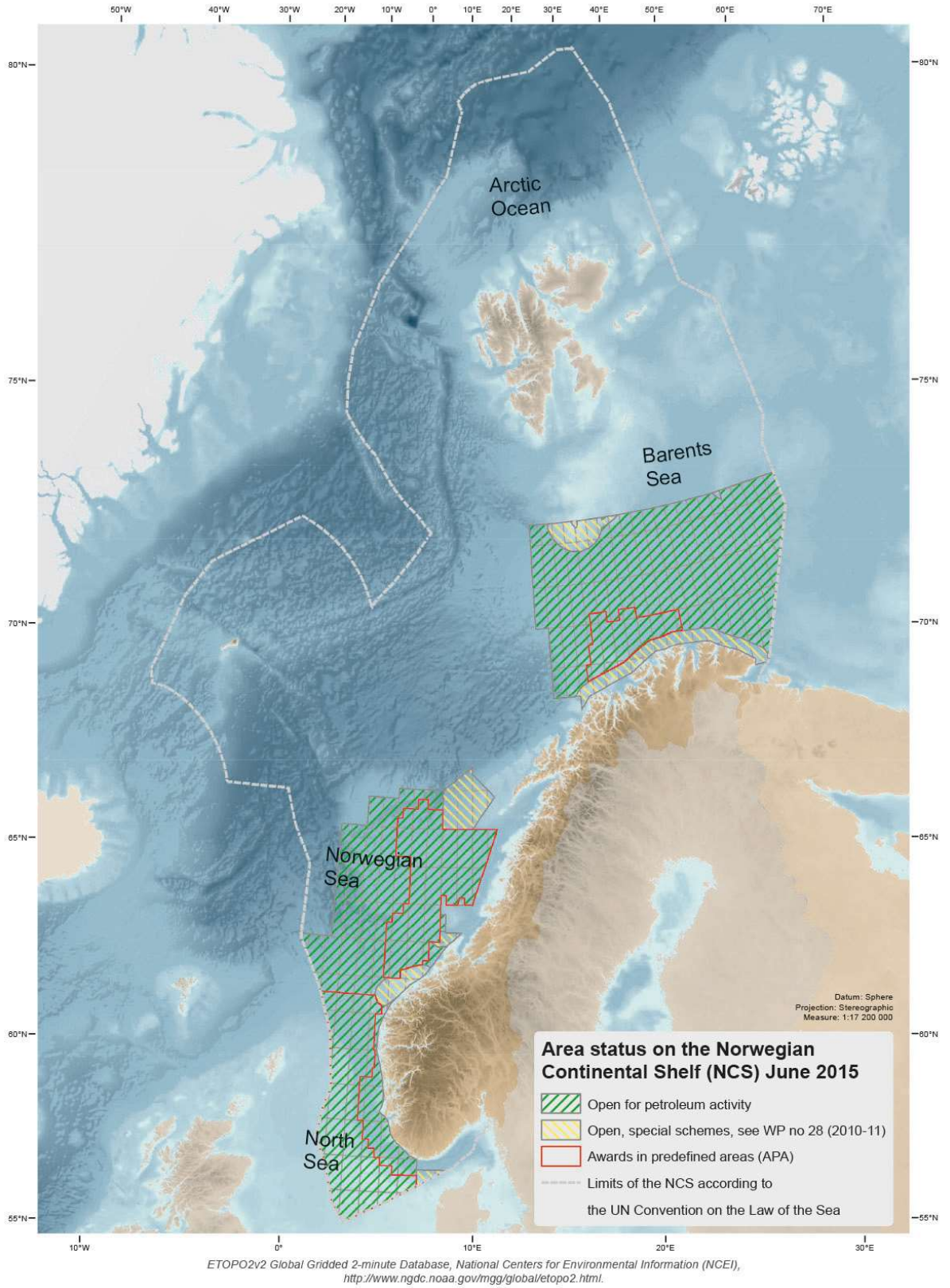

(Norwegian Petroleum Directorate[20])

[20] http://www.npd.no/Global/Norsk/4-Kart/Sokkelkart2015/Kontsok15-Arealstatus.jpg, accessed May 30, 2016.

APPENDIX R OUTPUT FROM "SEGMENT ANALYSIS" IN GEOX

Case I: Copper Equivalent

Table R-1 – Resources.

Resource Type	Mode	Mean	Std. dev.	F90	F50	F10
Total Recoverable Resources [1E6 t]						
Oil [1e6 t]	1.51	1.72	0.544	1.09	1.64	2.46
Assoc. Gas [1e9 t]	0	0	0	0	0	0
Non Assoc. Gas [1e9 t]	0	0	0	0	0	0
Total Resources [1e6 t]	**1.51**	**1.72**	**0.544**	**1.09**	**1.64**	**2.46**
HC liquid [1e6 t]	*1.51*	*1.72*	*0.544*	*1.09*	*1.64*	*2.46*
Gas [1e9 t]	*0*	*0*	*0*	*0*	*0*	*0*
Recoverable						
Oil [1e6 Sm3]	0.0745	0.0959	0.0405	0.0516	0.0889	0.15
Non Assoc. Gas [1e9 t]	0	0	0	0	0	0
Assoc. Gas [1e9 t]	0	0	0	0	0	0
Condensate [1e6 t]	0	0	0	0	0	0
Total Resources [1e6 t]	**0.0745**	**0.0959**	**0.0405**	**0.0516**	**0.0889**	**0.15**
HC liquid [1e6 t]	*0.0745*	*0.0959*	*0.0405*	*0.0516*	*0.0889*	*0.15*
Gas [1e9 t]	*0*	*0*	*0*	*0*	*0*	*0*
Marketable Gross						
Gross Total Resources [1e6 t]	0.0745	0.0959	0.0405	0.0516	0.0889	0.15
Risked gross Total Resources [1e6 t]		0.0432	0.0549	0	0	0.123

Case II – Individual Metal Grade Distributions

Resource Type	Mode	Mean	Std. dev.	F90	F50	F10
Inplace						
Oil [1e6 t]	0.817	0.858	0.274	0.546	0.818	1.22
Assoc. Gas [1e9 t]	0.817	0.858	0.274	0.546	0.818	1.22
Non Assoc. Gas [1e9 t]	0.817	0.858	0.274	0.546	0.818	1.22
Total Resources [1e6 t]	**3.27**	**3.43**	**1.1**	**2.18**	**3.27**	**4.9**
HC liquid [1e6 t]	*1.63*	*1.72*	*0.548*	*1.09*	*1.64*	*2.45*
Gas [1e9 t]	*1.63*	*1.72*	*0.548*	*1.09*	*1.64*	*2.45*
Recoverable						
Oil [1e6 t]	0.0392	0.0511	0.0207	0.0287	0.0474	0.0786
Assoc. Gas [1e9 t]	0.0382	0.0556	0.0249	0.0288	0.0508	0.0896
Non Assoc. Gas [1e9 t]	4.96E-07	1.72E-06	1.77E-06	3.31E-07	1.17E-06	3.74E-06
Condensate [1e6 t]	4.86E-05	0.000086	5.04E-05	3.48E-05	7.49E-05	0.00015
Total Resources [1e6 t]	**0.0848**	**0.107**	**0.0434**	**0.0599**	**0.0986**	**0.164**
HC liquid [1e6 t]	*0.041*	*0.0512*	*0.0207*	*0.0287*	*0.0475*	*0.0786*
Gas [1e9 t]	*0.0382*	*0.0556*	*0.0249*	*0.0288*	*0.0508*	*0.0896*
Marketable Gross						
Gross Total Resources [1e6 t]	0.0848	0.107	0.0434	0.0599	0.0986	0.164
Risked gross Total Resources [1e6 t]		0.048	0.0606	0	0	0.134